REGULATION OF THE PROGESTERONE RECEPTOR IN THE MOUSE MAMMARY GLAND: CHARACTERIZATION OF THE TRANSCRIPTION UNIT, THE ROLE OF ACTIVATING PROTEIN-1 (AP-1), AND THE INFLUENCE OF OVARIAN HORMONES

By

Emily Elizabeth Flynn

A DISSERTATION

Submitted to
Michigan State University
in partial fulfillment of the requirements
for the degree of

DOCTOR OF PHILOSOPHY

Genetics

2011

ABSTRACT

REGULATION OF THE PROGESTERONE RECEPTOR IN THE MOUSE MAMMARY GLAND: CHARACTERISATION OF THE TRASCRIPTION UNIT, THE ROLE OF ACTIVATING PROTEIN-1 (AP-1), AND THE INFLUENCE OF OVARIAN HORMONES

By

Emily Elizabeth Flynn

The mouse progesterone receptor (Pgr) gene contains tandem promoter regions that control expression of the two receptor isoforms, PRB and PRA. This locus also forms a *cis*-sense/antisense pair with a naturally occurring non-coding antisense transcript ($PR^{antisense}$) whose expression is controlled by its own promoter. All three promoters respond to activating protein-1 (AP-1), but the sense PRA and PRB promoters were more responsive to c-Jun, while the antisense promoter was preferentially responsive to JunD or JunB. In cultured cells, as well as in tissues *in vivo*, the $PR^{antisense}$ transcript co-localized with the sense mRNA and with PRA protein. Both transcripts showed co-regulation, rather than anti-regulation, and were co-expressed across mouse mammary gland development.

Expression of the mouse Pgr gene during mammary gland development is regulated by complex interplay between hormones and growth factors that affect growth and differentiation, many of which influence the activity of AP-1 family members and other transcription factors. We therefore examined the effect of steroid hormones and co-expression of Jun and Fos subunits on the activity of the mouse PR promoters, hypothesizing that differential regulation of PR isoform expression occurs at a transcriptional level. Although the hormonal milieu of pregnancy supports increased

PBR expression in the mouse, these studies did not support a prominent role of estrogen receptor (ER) or AP-1 in this regulation.

Additional experiments utilized an immunofluorescence approach with isoform-specific antibodies to examine the relationship between AP-1 and PR expression across development or following ovariectomy. The underlying hypothesis for these studies is that a change in the composition of AP-1 subunits may contribute to a shift from PRA to PRB expression during alveologenesis due to preferential effects of different AP-1 isoforms on the two promoters. These experiments establish that AP-1 alone cannot account for the appearance of PRB during pregnancy. However, the composition of AP-1 undergoes significant changes across development and, as noted above, AP-1 promotes transcription from both PR promoters. cJun correlated most highly with overall expression of PRA, and PRA expression invariably accompanied the expression of one Jun isoform or another. In ovariectomized mice expression of c-Fos disappeared entirely, while ovariectomy affected only the intensity of PRA staining.

In summary, these studies characterized the effects of hormone and phorbol ester treatment along with ER and AP-1 in transcriptional regulation of the mouse Pgr gene. Expression of AP-1 and $PR^{antisense}$ mRNA correlated positively with PRA expression across development in the mouse mammary gland. These correlations persisted in the pregnant mammary gland, failing to explain the appearance of PRB, but accounting for a subset of $c\text{-}Jun^{+}/PRB^{+}$ cells that maintained their expression of PRA. Additionally, experiments in ovariectomized mice supported the interesting finding that progesterone and well as estradiol can stimulate mammary gland expression of both c-Fos and c-Jun.

TABLE OF CONTENTS

LIST OF TABLES

CHAPTER 2

LIST OF FIGURES

CHAPTER 1

CHAPTER 2

CHAPTER 3

APPENDIX

CHAPTER 4

Note: Images in this dissertation are presented in color.

CHAPTER 1

LITERATURE REVIEW

LITERATURE REVIEW

Progesterone receptor (PR) exists in two major isoforms, PRA and PRB that are encoded by the Pgr gene on mouse chromosome 9. The human and rat progesterone receptor (PGR) genes contain a tandem arrangement of two promoters giving rise to transcripts encoding the separate PR isoforms, PRA and PRB, which are believed to have different functions in the mammary gland. This is also believed to be true for the mouse Pgr gene however, evidence of two promoters and two classes of mRNA transcripts have not been defined. During mammary gland development in the mouse, expression of the PRA and PRB proteins is temporally and spatially dissociated, allowing study of the functional role of the separate isoforms. This differential expression of the PR proteins led to the hypothesis that differential regulation of the mouse PRB and PRA promoters is, at least in part, responsible for the switch in PR isoform expression seen during mouse development. Of particular interest are the two main changes in PR isoform expression that are coincident with maturation of the mammary gland during puberty and as a result of lobulo-alveolar development that occurs during pregnancy. The first developmental transition is characterized by a decrease in the number of PRA^+ epithelial cells and the second switch shows a further decrease in the number of PRA^+ cells with a marked increase in the number of PRB^+ cells. At a transcriptional level, this differential promoter regulation may be accomplished by transcription factors binding to conserved DNA motifs in the PRB and PRA promoters and subsequent coactivator or corepressor recruitment.

As alluded to above, PR is an important transcription factor involved in key stages of mammary gland development and breast cancer. During the course of these studies, we discovered that the mouse Pgr locus contains an antisense mRNA transcript ($PR^{antisense}$ mRNA)

which overlaps with the beginning of the Pgr gene. This unusual arrangement may be important because antisense RNA has the potential to modulate gene expression through a variety of novel mechanisms including transcriptional interference, mRNA stability, and translational efficiency. Since $PR^{antisense}$ mRNA overlaps with the promoters that are believed to control PRA and PRB expression through separate $PR^{(A)}$ and $PR^{(B)}$ mRNA transcripts, antisense transcription may influence the balance between these two PR isoforms. Superimposed on hormonal effects on mammary gland development and gene expression are important growth factor pathways, many of which converge on the Activating Protein-1 (AP-1) family of transcription factors, consisting of homologous or heterologous dimers between several jun and fos family members. The 5'-flanking region of the mouse Pgr gene contains several predicted AP-1 binding sites, suggesting that its expression may be regulated not just by steroid hormones (estrogen and progesterone), but also by growth regulatory pathways that signal through AP-1 and other transcription factors. Our hypothesis, therefore, is that a change in the composition of AP-1 subunits is, at least in part, responsible for the shift from PRA to PRB expression during pregnancy. Additionally, we hypothesize that $PR^{antisense}$ RNA can modulate production or translational activity of PR^{sense} transcripts, and that AP-1 might exert important regulatory effects through both the sense and antisense transcription units.

This project aims to characterize the transcriptional regulation of the Pgr gene in the mouse with a focus on potential mechanisms of differential regulation of the PRA and PRB promoters. AP-1 and other transcription factors are hypothesized to be required for the differential switches between PRA and PRB protein observed in mouse mammary gland development. Differential Jun/Fos isoform usage at the AP-1 sites overlapping the PR mRNA

start sites may lead to activation/repression of PRA or PRB transcription with or without hormone treatment.

1. Role of Progesterone and Progesterone Receptor (PR) in Breast Cancer

In the normal human mammary gland, the expression of PR isoforms has only been determined for adult premenopausal women between 21 and 50 years of age (Mote PA 2002). Between 10 and 20% of the mammary epithelial cells are PR^+ with each duct or lobular structure ranging greatly from 0 to 90% PR^+ cells (Williams G 1991); (Mote PA 2002); (Aupperlee M 2005b). Human PRA and PRB protein isoforms show uniform colocalization in the same cells at a ratio of 1:1 in the normal mammary gland (Graham JD 1995); (Mote PA 2002). The estrogen receptor $(ER)^+/PR^+$ cells are usually non-dividing cells that act via a paracrine signaling mechanism to promote proliferation of the adjacent ER-negative/PR-negative cells (Lange C 2008). Early events in breast cancer are thought to alter the paracrine signaling to an autocrine mechanism in ER^+/PR^+ tumor cells to promote proliferation (Lange C 2008). ER^+/PR^+ cells in the normal mammary gland are capable of proliferation, but are usually growth arrested due to expression of growth-inhibitory molecules (Lange C 2008).

Studies using immunoblot analysis have found that the ratio of PR isoforms in PR-positive mammary tumors is altered due to a low level of PRB expression and resultant high PRA:B ratio (Graham JD 1995); (Hopp TA 2004). This is clinically significant because a high PRA:B ratio is associated with the progression to a malignant phenotype, invasiveness and a higher likelihood of relapse following treatment of the primary tumor (Hopp TA 2004). Another study of mammary carcinomas showed that 94% of examined tumors had a PRA level greater than or equal to that of PRB protein, as well as a significant correlation between a high PRA:B

ratio and a more undifferentiated phenotype (Bamberger AM 2000). High PRA:B ratio tumors are also associated with more rapid tumor recurrence after being treated with tamoxifen due to either increased aggressiveness or increased resistance to hormones (Jacobsen BM 2005). In a tumor containing high levels of PRA or expressing exclusively PRA, unliganded PRA can increase cell adhesion to the extracellular matrix (ECM), which is thought to prime cells for stromal invasion as well as metastasis (Jacobsen BM 2005). Human breast tumors that are ER^+/PR^+ account for about 70% of newly diagnosed tumors and are much more likely to be responsive to hormone therapies than a tumor lacking ER or PR (Lange C 2008); (Jacobsen BM 2003). ER-negative/PR-negative tumors are generally hormone resistant and predictably do not respond to therapies such as tamoxifen or aromatase inhibitors (Jacobsen BM 2003). While they represent only a small fraction of all breast cancers, tumors that are ER-negative/PR^+ typically show aggressive growth and a less favorable prognosis for patient survival (Jacobsen BM 2005). Conversely, tumors with high levels of PRB significantly correlate with a lack of ErbB2/neu overexpression as well as a more differentiated phenotype, which are both indicative of a good prognosis (Bamberger AM 2000).

In humans, it has been assumed based on studies in rodents and various cell lines that in the normal mammary gland progesterone (P) acts to stimulate both proliferation and the formation and expansion of terminal ductal lobular units (TDLU) during puberty and pregnancy (Anderson E 2004). However, this has never been examined in detail due to the limited availability of healthy human mammary gland tissues, specifically during puberty (Anderson E 2004). Rather, studies on postmenopausal breast cancer risk for women taking hormone replacement therapy (HRT) have shown a role for progesterone in tumorigenesis (Anderson E 2004). Combined estradiol (E_2) plus P HRT has a strong association with an increased risk of

breast cancer, with the risk factor ranging from 1.2 to 2.43 between different studies (Lund E 2007); (Kumle M 2002). A recent large cohort study on postmenopausal breast cancer risk showed that there was no increased risk for ductal or lobular breast cancer with less than two years of hormone use (RR= 0.72 and 0.79, respectively) (Calle EE 2009). But after 2 years, the risk increased proportional to the longer duration of E_2+P use for both ductal (RR=1.91) and lobular (RR=1.95) mammary carcinomas (Calle EE 2009).

In addition to HRT therapy, the use of exogenous ovarian hormones in the form of the oral contraceptive pill (OCP) increases the risk of breast cancer (Anderson E 2004). There is also a slightly increased risk of breast cancer in women using progesterone only oral contraceptives (OC), which correlates with increased mammary cell proliferation (Lund E 2007); (Kumle M 2002). It has long been known that the age of onset for menarche and menopause has an impact on the incidence of breast cancer, as well as that early menarche and late menopause are associated with increased breast cancer risk (Anderson E 2004). This is due to higher cumulative exposure of the breast to estrogen and progesterone and their accompanying proliferative effects on mammary tissue (Anderson E 2004). After an initial carcinogenic event, an increase in the amount or duration of proliferation combined with a lack of differentiation in the breast is thought to be how malignant tumors in the breast epithelium arise (Anderson E 2004).

2. Overview of PR Function and Structure, and its Role in Mammary Gland Development

a. PR Function

The progesterone receptor is a member of the nuclear steroid receptor superfamily which, in the classical mechanism, regulates steroid-dependent gene expression by interacting with ligand-responsive elements. As a transcription factor, PR mediates the physiological effects of P

including proliferation and differentiation in the normal human and murine mammary gland (Sutherland RL 1998); (Pestell RG 1999). Upon ligand binding, PR is able to dissociate from heat shock proteins, dimerize, translocate to the nucleus and bind to the progesterone response elements (PREs) in target genes (Gao X 2002). PR regulates the transcriptional response by coregulator recruitment to its target genes, which is referred to as a genomic action of PR to distinguish this from a variety of non-transcriptional (non-genomic) effects (Li X 2004). There are two principal PR isoforms, the full length PRB protein and the N-terminally truncated PRA isoform, both of which are present in human, mouse and rat reproductive tissues (Jacobsen BM 2003). The PRA and PRB isoforms have very different physiological functions based on promoter context and cell type (Li X 2004). Additionally, both homo- and hetero-dimers can form between the PRB and PRA subunits, presumably with distinct functions due to differential recruitment of coregulators to the promoter regions of target genes (Jacobsen BM 2003). Liganded PRB is a stronger transactivator than PRA and in gene-expression profiling studies, liganded PRB regulates more genes than does PRA (Jacobsen BM 2005); (Tung L 2006). Alternatively, PR can also be activated in a ligand-independent manner by cross-talk with growth factor pathways activated by signaling molecules such as phorbol myristate acetate (PMA), cyclic adenosine monophosphate (cAMP), and epidermal growth factor (EGF) (Jacobsen BM 2005). Without ligand, PRA is a stronger transcriptional activator compared with unliganded PRB and also regulates more genes through a ligand-independent mechanism than does PRB (Jacobsen BM 2005). Whether liganded or unliganded, PRA and PRB regulate distinct sets of genes which are not overlapping in their functions (Tung L 2006).

The gene which encodes the various isoforms of PR has been given the designation PGR. As shown in Figure 1.1, the human PGR gene uses two tandem promoters and translational start

sites to produce two classes of mRNAs which are translated into the PRB and PRA proteins, respectively (Kastner P 1990). The human PRB protein is 120 kDa, while the N-terminally truncated PRA isoform is 94 kDa, 165 amino acids shorter. The mouse PRB protein is 119 kDa, while the PRA protein is reported to be 91 kDa (Aupperlee M 2005a). In addition to the predominant PRB and PRB isoforms, there is also expression evidence of PRC, PRM, and other minor isoforms (Wei LL 1990); (Samalecos A 2008). The PRC message encodes a small 45 to 50 kDa protein that retains the second DNA-binding finger, the hinge (H) region as well as the ligand binding domain (LBD) (Wei LL 1990). The PRM message encodes a 38 kDa protein which contains a novel 16 amino acid signal peptide spliced onto the hinge region and ligand binding domain (Samalecos A 2008).

b. PR Structure

The human and mouse PR protein contains three activation function (AF) domains, a zinc-finger DNA-binding domain (DBD), a hinge region, and a LBD (Figure 1.1) (Gao X 2002). AF1 is located in the central region upstream of the DBD and is ligand-independent, conversely AF2 is located in the LBD and its activity depends on the presence of an activating ligand (Gao X 2002). Lastly, AF3 is located in the N-terminal B-upstream sequence (BUS) region unique to PRB. The AF3 domain in PRB allows binding of a subset of coactivators that are not recruited effectively by PRA (Li X 2004), through the two LXXLL motifs (nuclear receptor boxes) and tryptophan 140 (Tung L 2006)*;* (Takimoto GS 2003)*;* (Gao X 2002). AF3 is able to synergize with AF1 and AF2 but only on promoters containing multiple PREs (Tung L 2006). This AF3-dependent synergism is due to the intermolecular protein interactions of multiple PR dimmers bound to adjacent PREs (Tung L 2006). The BUS region regulates PRB-dependent transcription

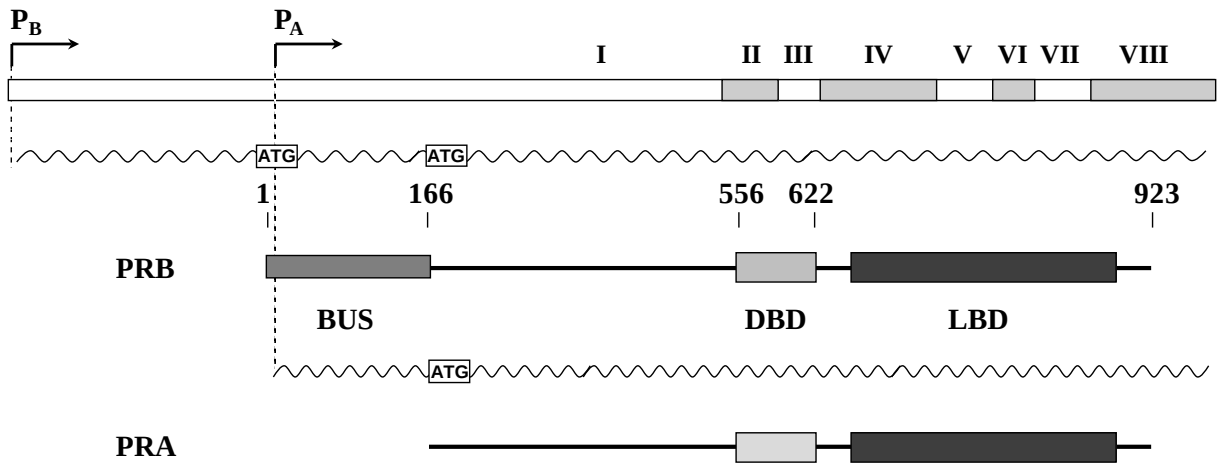

Figure 1.1: Human progesterone receptor transcription unit structure. PR transcription start sites and structure of the eight exon human PGR gene (top). The PRB promoter (P_B) and PRA promoter (P_A) drive transcription of the PRB and PRA proteins (below), respectively. The PRB protein contains the B-upstream sequence (BUS), while the PRA form is N-terminally truncated and 165 amino acids shorter. In the lower half, the translation start sites along with the structure of the human PR proteins are depicted including the DNA binding domain (DBD) and ligand binding domain (LBD). Numbering is relative to the PRB ATG (amino acid 1), while the PRA ATG is located at amino acid 166.

by limiting the number of possible PRB conformations to a few configurations with high transcriptional activity (Tung L 2006). The BUS is believed to control PRB through direct binding or allosteric interactions with N-terminal sequences common to both PRB and PRA (Tung L 2006). These interactions stabilize active conformations and optimize binding with co-regulatory proteins (Tung L 2006); (Takimoto GS 2003). Using a hormone-responsive transfection system, PRB has been shown to act primarily as a potent transcriptional activator of target genes (Gao X 2002). In some cell lines, PRA predominantly acts as a dominant repressor of PRB transcription as well as a few other nuclear receptors including ER (Gao X 2002); (Li X 2004). The transrepressor properties of PRA are entirely dependent upon the presence of the inhibitory domain (ID) and bound ligand (Takimoto GS 2003). The ID is located in the N-terminal domain of both PRA and PRB (Huse B 1998). Deletion of the N-terminal 140 amino acids in PRA (i.e. the entire ID and its flanking sequences) yields ΔID-PRA which acts as a transcriptional activator of genes normally activated only by PRB (Giangrande PH 1997). The ID can inhibit the activating activity of AF1 and AF2 (present in PRA and PRB) but not AF3 (present only in PRB), providing a possible explanation of why PRB functions primarily as an activator of transcription (Gao X 2002).

In addition to the sumoylation state of PRB (Takimoto GS 2003), the promoter structure of a target gene also plays a large role in determining PR's ability to synergize (Tung L 2006). Mutation of key BUS amino acids lead to complete inactivation of autonomous AF-3 activity as well as inactivation of AF-3's ability to control downstream AFs (Tung L 2006). These AF-3 functions are only observed using promoters that contain a minimum of two palindromic PREs (Tung L 2006). Although there is synergism between AF-3 and AF-1/AF-2 within one PR molecule, the stronger interaction is actually between the AF-3 of one PR dimer and the AF-3 of

another PR dimer bound to an adjacent PRE (Tung L 2006). This is evident in transfection experiments using different numbers of PRE DNA binding sequences, where on a single PRE the transcriptional activity of PRA and PRB are similar (Tung L 2006). But on a PRE_2- or PRE_3-driven promoter, the PRB transcriptional activity is 5-10 fold higher than that of PRA (Tung L 2006).

Although historically PRB is usually thought of as an activator of transcription based on transfection studies, there are a few genes that PRB down-regulates when measured using microarray analysis. RNA expression profiling using gene chips was carried out using T47D-YA and T47-YB cell lines, which express only PRA or PRB, respectively (Tung L 2006); (Jacobsen BM 2003). As expected, PRB up-regulated the highest percentage of genes, but surprising there was also a small group of genes uniquely up-regulated by PRA (Tung L 2006); (Jacobsen BM 2003). Some genes are down-regulated by both PRA and PRB, but there is a small subset of genes that are uniquely down-regulated only by PRB (Tung L 2006); (Jacobsen BM 2003).

c. Importance of PR for Normal Mammary Gland Development

Studies in transgenic mice confirm that overexpression of PRA leads to an abnormal mammary gland phenotype consisting of excessive ductal branching, epithelial cell hyperplasia, multilayered cells and a disorganized basement membrane (Shyamala G 1998). Whereas overexpression of PRB leads to reduced ductal elongation and branching as well as precocious alveologenesis (Shyamala G 2000). In the C57/Bl6 background, PRA knockout (PRAKO) mice failed to show a mammary phenotype but had uterine and ovarian abnormalities that led to infertility (Mulac-Jericevic B 2000). The PRB knockout (PRBKO) mouse had decreased

proliferation of the ductal and alveolar epithelial cells which lead to reduced side branching and reduced lobuloalveolar development (Mulac-Jericevic B 2003). The PRBKO mouse also showed a decrease in the survival of alveolar epithelium (Mulac-Jericevic B 2003). The PR null adult mouse ($PR^{-/-}$) in which both isoforms of PR have been knocked out, had normal ductal elongation, but impaired ductal branching as well as impaired lobuloalveolar development (Lydon JP 1995).

d. Regulation of Mouse Mammary Gland Development

Although both ERα and ERβ are expressed in the mouse mammary gland (Haslam SZ 1992), the mammary glands of ERβ-/- knock out mice develop normally (Krege JH 1998), implying that ERβ does not serve a critical function in the mammary gland. Total ER knock out mice (ERαβ-/-) and ERα knock out mice (ERα-/-) mice fail to develop beyond a rudimentary tree, indicating a requirement for ERα in ductal outgrowth (Lubahn DB 1993); (Couse JF 1999). Although ductal elongation in the mouse mammary gland requires ERα and E_2 (Lubahn DB 1993); (Couse JF 1999), it also requires growth hormone (GH) from the pituitary (Flux DS 1954). Insulin-like growth factor-1 (IGF-1) acts as a local effector of GH function, which is potentiated by E_2 (Feldman M 1999). It is believed that stroma-derived IGF-1 binds to the IGF-1 receptors located on mammary epithelial cells and stimulates their proliferation in cooperation with E_2 (Wood TL 2000); (Feldman M 1999).

Another important growth factor is epidermal growth factor (EGF), which has been shown to be a mitogen in mammary epithelial cells (DiAugustine RP 1997). In ovariectomized mice, local release of EGF leads to stimulated ductal development (Haslam SZ 1993). EGF

binds to its receptor EGFR and is present in both mammary epithelial and stromal cells (Troyer KL 2001). EGFR knock out mice (EGFR-/-) fail to undergo mammary gland ductal elongation due to a lack of stromal EGFR (Wiesen JF 1999). Lastly, hepatocyte growth factor/scatter factor (HGF/SF) is a stroma-derived paracrine factor which regulates ductal morphogenesis and is also a mitogen for mammary epithelial cells (Soriano JV 1998). These growth factors produced locally in the mammary gland all represent possible effectors of steroid hormone action (Hovey RC 2002) through non-genomic actions of PR and estrogen receptor (ER) (Lange C 2008). Alternatively, ER and PR may act genomically but still alter GF signaling through the production of a factor that can alter signaling (i.e. receptor activator of nuclear factor-κB ligand (RANKL), which colocalizes with PRA in mammary epithelial cells of adult mice (Aupperlee MD 2009)).

Growth factors acting through their cognate receptors and the Ras pathway can lead to mitogen-activated protein kinase (MAPK) activation (Lange CA 2004). The P/PRB/c-Src/ER complex independently activates the MAPK pathway, which may result in positive regulation of PR via direct PR phosphorylation (Lange CA 2004). Additionally, MAPK activation ultimately leads to increased c-Jun N-terminal kinase (JNK), extracellular-signal-regulated kinase (ERK) and p38 kinase activity and phosphorylation can lead to changes in the amount, activity, or stability of AP-1 dimers in multiple ways (Hess J 2004). First, the AP-1 isoforms themselves can be phosphorylated: c-Jun (JNK and ERK), JunB (JNK), JunD (JNK and ERK) (Mechta-Grigoriou F 2001), c-Fos (ERK) (Gutzman JH 2005), and Fra1 (ERK) (Verde P). Secondly, transcription factors involved in up-regulating an AP-1 family member gene can be phosphorylated, thus increasing transcription of that particular AP-1 gene (Mechta-Grigoriou F 2001). Third, phosphorylation alters the stability of the AP-1 isoforms dramatically, for

example, when Fra1 is phosphorylated in its C-terminal destabilizer element this prevents proteasome-dependent degradation (Verde P) .

e. Role of Activating Protein 1 (AP-1) in Normal Mammary Gland Development and Breast Cancer

AP-1 is a family of dimeric basic region leucine zipper (bZIP) transcription factors that contain the subfamilies of Jun, Fos, Maf, and activating transcription factor (ATF) (Shaulian E 2002). Jun proteins can homo- or heterodimerize, while Fos family members can only heterodimerize with Jun to form a stable complex that binds to a DNA sequence motif that serves as PMA or AP-1 binding sites (Shaulian E 2002). The Jun family has three members, c-Jun, JunB and JunD, of which c-Jun is the strongest activator (Shaulian E 2002) and is the only member capable of efficiently activating promoters containing a single AP-1 site (Passegue E 2002). JunB has lower homodimerization affinity as well as weaker AP-1 site binding activity (Passegue E 2002). This requires JunB to form synergistic interactions with other homodimers bound to nearby sites (Passegue E 2002). Therefore, JunB can only strongly activate promoters containing multiple AP-1 sites and can actually antagonize c-Jun transactivation of a promoter containing a single AP-1 site (Passegue E 2002); (Shaulian E 2002). JunD is the most broadly expressed member of the Jun family, but lacks a well defined function (Shaulian E 2002). The Fos family contains four members of which only c-Fos and FosB contain transcriptional activation domains (Shaulian E 2002). Induction of c-Fos is seen in tissue remodeling, such as during mammary gland involution following lactation (Shaulian E 2002) when PRA levels are reduced (Aupperlee M 2005a). Additionally, members of the Jun family show tissue specificity as well as differential expression during development (Marti A 1994). Therefore, differential usage of AP-1 isoforms may lead to changes in transcriptional activity of AP-1 responsive

promoters. Changes in the expression of individual AP-1 family members have not been systematically studied during mammary gland development.

AP-1 is known to regulate many physiological functions including proliferation, apoptosis, survival and differentiation (Shaulian E 2002). In the normal mammary gland, AP-1 controls the postnatal regulation of epithelial cell proliferation (Shen Q 2006). Studies utilized a dominant negative inducible AP-1 inhibitor, Tam 67, which lacks the transactivation domain of c-Jun, but still retains the DNA-binding domain and dimerization domain (Shen Q 2006). Using this dominant negative c-Jun in pre-pubertal, pubertal, adult and hormone-treated mice resulted in significantly decreased mammary cell proliferation (Shen Q 2006). Additionally, the pre-pubertal and pubertal mammary glands showed reduced overall gland size, reduced branching and budding (Shen Q 2006).

Using human mammary carcinomas, one study examined PR and AP-1 isoform expression. By western blot, Fra1 showed an inverse correlation with PRB, while FosB expression correlated with both PRA and PRB (Bamberger AM 2000). They also confirmed earlier findings that most of the tumors had an altered PR ratio, expressing more PRA than PRB protein (Bamberger AM 2000). Using immunohistochemistry (IHC), another group correlated Fra1 expression with ER and PR expression levels (Song Y 2006). All of the neoplastic breast tissue tested was positive for nuclear Fra1, regardless of whether it was benign or malignant tissue (Song Y 2006). Whereas adjacent normal tissue had much weaker nuclear staining in only a subset of the epithelial cells (Song Y 2006). In 90% of breast carcinomas studied, there was a shift from exclusively nuclear Fra1 staining to the simultaneous expression of Fra1 in the nucleus and cytoplasm (Song Y 2006). Fra1 has been shown to be important for cell motility, invasion, and invasiveness in ER^+ MCF-7 cells and ER-negative MDA-MB231 cells (Belguise K 2005).

Combined with data showing that high Fra1 expression is associated with a more malignant phenotype, this establishes Fra1 as an important player in breast cancer progression (Belguise K 2005).

Expression of the other AP-1 isoforms was determined for human mammary tumors, where c-Jun showed weak protein expression levels, while JunB expression was moderate and Fra2 levels were moderate to strong (Bamberger AM 1999). The protein levels of JunD varied greatly between specimens, with no clear pattern (Bamberger AM 1999). Since c-Jun is often the predominant Jun isoform in normal tissues, over-expression of c-Jun was tested in MCF-7 cells and lead to a tumorigenic, invasive, hormone resistant phenotype that is associated with an increase in Fra1 expression and a loss of ER (Smith LM 1999).

3. Regulation of PGR Gene Expression
a. Transcription Factors That Influence PR Expression

In addition to AP-1 as described above, other important transcription factors that influence Pgr gene expression are estrogen receptor α (ERα), specificity protein 1 (Sp1) and CCAAT/Enhancer-Binding Protein β (C/EBPβ).

i. Estrogen Receptor α (ERα)

ERα is a member of the steroid nuclear receptor superfamily and is a transcription factor that binds in dimeric form to target sequences known as estrogen response elements (EREs). There are two isoforms of the ER encoded by separate genes, α and β, which show high relatively homology to each other (Flototto T 2004). ERα and β have overlapping transcriptional activity, ligand binding properties, and are capable of forming both homo- and hetero-dimers (Saville B 2000). The effects of the ER on transcription are dependent on the ligand, cell type,

and the promoter of the target gene (Saville B 2000). Upon ligand binding, ER is able to dissociate from heat shock proteins, dimerize, translocate to the nucleus and bind to an ERE in a target gene (Gruber CJ 2004). ER regulates the transcriptional response by coactivator recruitment to its target genes, which is referred to as a genomic action of ER (Gruber CJ 2004). The ER is also capable of regulating gene expression without directly binding to DNA by acting through protein-protein interactions with other DNA-binding transcription factors in the nucleus (Gruber CJ 2004). Examples of ERE-independent genomic actions of ER include interactions with the AP-1 proteins, Sp1 and C/EBPβ (Bjornstrom L 2005). As described with PR above, ER is also able to exert effects outside of the nucleus that are independent of transcription, which are therefore referred to as non-genomic actions of ER (Bjornstrom L 2005).

ii. Specificity Protein 1 (Sp1)

Sp1 is a transcription factor that binds to GC-rich binding sites present in the promoters of many genes to regulate their expression (Safe S 2005). Sp1 directly interacts with the TATA-binding protein associated factors (TAFs) as well as nuclear cofactors that make up the basal transcriptional machinery allowing Sp1 to substitute for TATA-binding factor (TBF) to promote transcription initiation within genes that contain GC-rich motifs, but lack recognizable TATA-boxes (Safe S 2005); (Naar AM 1998). Sp1 is also able to bind via protein-protein interactions to transcription factors like c-Jun as well as the nuclear receptors ER and PR (Safe S 2005); (Saville B 2000). Since differential Sp1-dependent transactivation depends on the interaction between Sp1 and other proteins like PR, this creates an opportunity for both promoter- and cell type-specific regulation of transcription (Safe S 2005). Although there are over 12,000 predicted GC-rich motifs in the human genome, only 22% of these are regions are located at the 5'-end of

a known protein coding gene and therefore likely that the genes are dependent on Sp1 for their expression (Cawley S 2004). Furthermore, only a small subset of these genes are actually regulated by any one hormone (Cawley S 2004), in particular estrogen or progesterone.

iii. CCAAT/Enhancer-Binding Protein β (C/EBPβ)

C/EBPβ is a member of the bZIP transcription factor family containing both a basic DBD and a protein-protein interaction motif (Grimm SL 2003). C/EBPβ is also an important mammary gland regulatory protein essential for ductal morphogenesis, lobuloalveolar proliferation and differentiation in the mouse mammary gland (Christian M 2002). There are three C/EBPβ isoforms produced through a leaky ribosome scanning mechanism that uses alternate in-frame initiation start sites for translation (Grimm SL 2003). The largest of the isoforms is LAP (full length activator liver-enriched inhibitory protein), followed by LAP* and by LIP (truncated inhibitor liver-enriched inhibitory protein) (Grimm SL 2003). In the mouse, LAP* is an N-terminally truncated form of LAP, while LIP lacks the N-terminal transactivation domains explaining why LIP typically acts as a dominant negative isoform of C/EBPβ (Grimm SL 2003).

Throughout development of the mouse mammary gland, the balance of LAP to LIP ratio controls both proliferation and differentiation of epithelial cells (Grimm SL 2003). The ratios of PR and C/EBPβ isoforms are also important for determining the biological response to P in the reproductive tract (Christian M 2002). A predominance of PRB and LIP activate PRE-driven promoters, whereas PRA and LAP activate C/EBPβ-dependent genes in endometrial stromal cells (Christian M 2002). In the virgin adult mouse, C/EBPβ is increased in myoepithelial cells whereas PRA is increased in luminal epithelial cells, but C/EBPβ and PRA rarely if ever

colocalize (SZ Haslam, personal communication). This suggests that C/EPBβ may be acting on PRA through an indirect mechanism or that C/EPBβ and PRA are regulated by parallel mechanisms in different cells. In the pregnant mouse mammary gland, PRA is decreased both in intensity and percentage of cells whereas C/EBPβ expression is increased in luminal epithelial cells that are PRA-negative (Haslam SZ, personal communication). Affymetrix GeneChip showed 6.4 fold induction of C/EBPβ following P treatment of PRB expressing T47-D cells (Richer JK 2002). C/EBPβ binding sites present in the PR promoter may be involved in a positive regulatory loop. Liganded PRB protein may upregulate C/EBPβ transcription, allowing more C/EBPβ protein to bind to the PR promoter and to further upregulate PRB transcription. PR expression may be regulated downstream of C/EBPβ or alternatively, a common factor may upregulate PRB and C/EBPβ in parallel due to coregulation of these genes (Seagroves TN 2000).

b. Interactions between AP-1, ERα, and Sp1 on the PR Promoter

The human PGR locus contains two distinct promoters, defined by Kastner *et al*. to correspond to -711 to +31 bp for PRB and at +464 and + 1105 bp for PRA (Kastner P 1990). These promoters each drive expression of separate classes of mRNA, the full length $PR^{(B)}$ transcripts, which initiate at +1 bp, and the 5'-end truncated $PR^{(A)}$ transcripts, which initiate at +737 bp (Kastner P 1990). In addition to these major start sites, there are also minor start sites for both PRB and PRA located just downstream of the major initiation sites (Kastner P 1990). Translation initiates at AUG1 (+744 bp) for PRB and at AUG2 (+1236 bp) for PRA (Kastner P 1990).

Near the PRB mRNA start site of the human PR promoter is an AP-1 site flanked by an imperfect half ERE, which is referred to as the +90 AP-1 site (Figure 1.2) (Petz LN 2002). ERα

binding to this half ERE in gel mobility shift assays enhances binding of c-Jun and c-Fos to the adjacent AP-1 site (Petz LN 2002). In this context, ERα, c-Jun and c-Fos all act as transcriptional activators and are bound to their respective binding sites in the PRB promoter of MCF-7 cells as visualized by chromatin immunoprecipitation (ChIP), but binding is observed only in the presence of E_2 (Petz LN 2002).

The human PRB promoter contains a distal and a proximal Sp1 site which is referred to as the -61 Sp1 region (Figure 1.2) (Schultz JR 2003). The proximal Sp1 site is a stronger transcriptional enhancer than the distal Sp1 site in the presence of E_2 and ERα, assessed in transient transfections. Sp1 interacts with the proximal Sp1 site first and then interacts with the distal Sp1 site. Both Sp1 sites confer E_2-responsiveness, but ERα does not appear to bind directly to DNA in the -61 bp region (Sp1 sites) in gel mobility shift assays. However, tethered ERα can still enhance Sp1 protein binding to the Sp1 sites. Mutation of the flanking CCAAT box does not change protein-DNA complex formation in gel mobility shift assays, nor transactivation in the presence of ERα and E_2 in transient transfections (Schultz JR 2003). Therefore, the CCAAT box appears not to be involved in E_2-mediated activation of the PGR gene. This means that PRB promoter activity must rely on the ability of ERα to enhance binding of Sp1 to the -61 Sp1 site to achieve E_2-mediated transactivation.

The human PRA promoter (which lies downstream of the PRB promoter) also contains an AP-1 site flanked by an imperfect ERE, referred to as the +745 AP-1 site (Figure 1.2) (Petz LN 2004a). ERα binding to the adjacent imperfect half ERE enhances c-Jun and c-Fos binding to the AP-1 site (Petz LN 2004a). Based on ChIP analysis in MCF-7 cells, c-Fos and ERα are associated only in the presence of E_2 (Petz LN 2004a). In contrast, c-Jun is associated with its

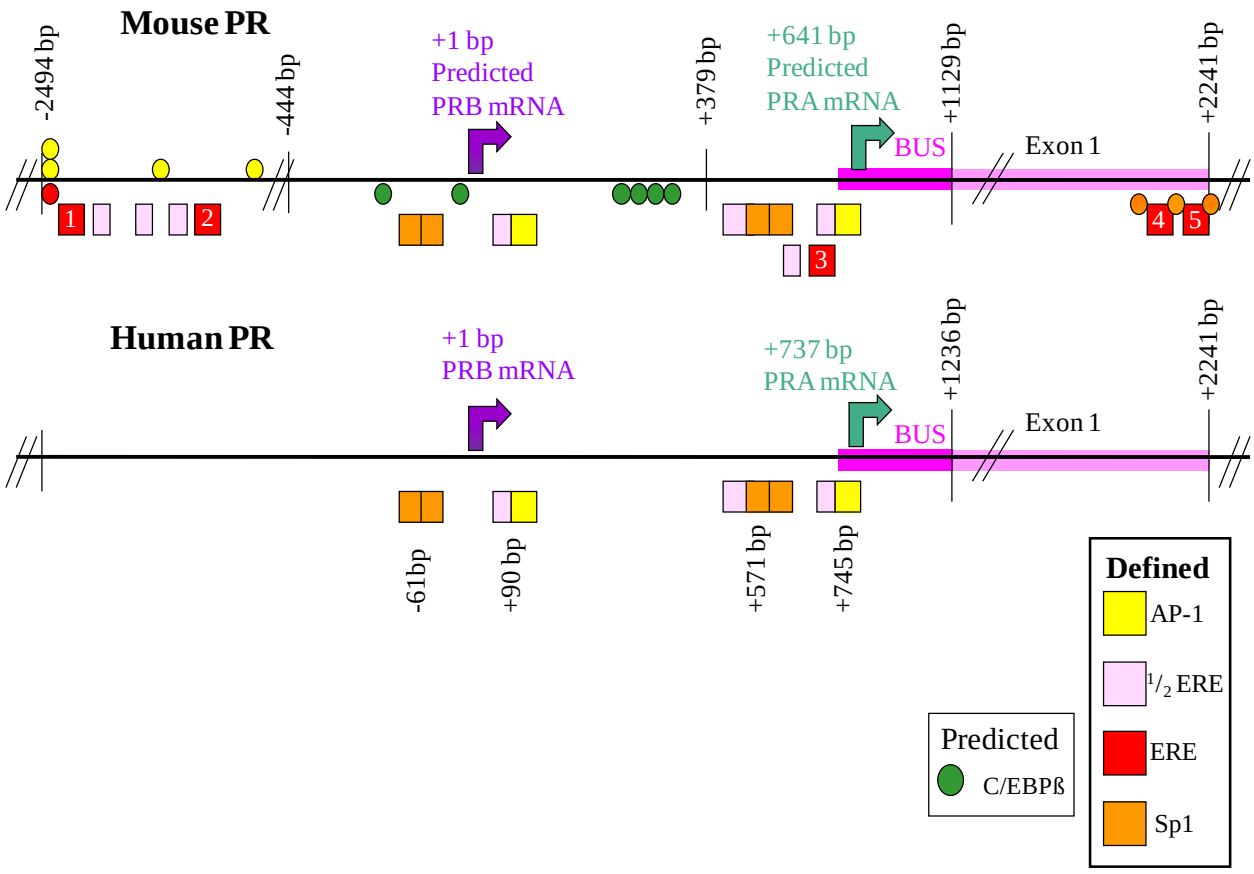

Figure 1.2: Comparison of transcription factor binding sites in the mouse and human progesterone receptor genes. In the human PGR gene, transcription factor binding sites that have been experimentally confirmed are shown as squares (Petz LN 2002); (Petz LN 2004a); (Petz LN 2004b); (Schultz JR 2003); (Schultz JR 2005). Using sequence comparisons, the location of the analogous sites are shown as squares for the mouse Pgr locus as well (top). Also using sequence comparisons, the location of the 5 main EREs mapped for the rat Pgr gene (Kraus WL 1994) are indicated as squares in the mouse PR sequence. For mouse PR, predicted transcription factor binding sites are shown as circles based on Transfac MatInspector transcription factor analysis (MatInspector 2005). For interpretation of the references to color in this and all other figures, the reader is referred to the electronic version of this dissertation.

binding site both in the presence and absence of E_2 (Petz LN 2004a). Cotransfection of a construct containing the +745 AP-1 site, together with ERα and increasing amounts of c-Jun/ c-Fos into U2-OS (osteosarcoma) cells demonstrated that c-Jun/c-Fos can cause E_2-dependent repression of transcriptional activity through its AP-1 site (Petz LN 2004a). This suggests that differential Jun/Fos isoform usage at the +745 AP-1 site may lead to activation or repression of PR transcription in a hormone-dependent manner. Conversely, the +90 AP-1 site overlapping with the PRB mRNA start site appears to only be involved in activation of PR transcription, presumably causing a preferential increase in the level of PRB mRNA.

The human PRA promoter contains a pair of Sp1 sites in this case flanked by a half ERE, which is referred to as the +571 ERE/Sp1 site (Figure 1.2) (Petz LN 2004b). Using gel mobility shift assays, in the presence of E_2, ERα is bound directly to the flanking ERE half site enhancing Sp1 binding to the Sp1 sites (Petz LN 2004b). Sp1 binds first to the proximal Sp1 site, then to the distal Sp1 site showing additive, rather than cooperative binding. In MCF-7 cells, however, Sp1 is associated with the endogenous +571 ERE/Sp1 site both in the presence and absence of E_2 as shown by ChIP (Petz LN 2004b). Unlike Sp1, ERα is only associated with the half ERE in the presence of E_2. However, the +571 ERE half site may have an important role in limiting PR expression since mutating the half ERE increased transcriptional activity in a hormone-independent manner approximately 3 fold in a transient transfection assay using U2-OS cells (Petz LN 2004b).

The studies summarized above demonstrate that ERα plays an important role in mediating E_2-responsiveness of the human PGR gene (Schultz JR 2003); (Petz LN 2004b); (Petz LN 2002); (Petz LN 2004a). ER is absolutely required for complete mammary gland

development since the mammary gland is unable to develop beyond a rudimentary ductal tree in knockout mice lacking ERα (Lubahn DB 1993). Using IHC, ERα and PRA usually colocalize in mammary epithelial cells during mouse development (Aupperlee MD 2007) suggesting a functional interaction between ERα and PRA. Multiple EREs are present in the mouse PR promoter (Figure 1.2), most of which have been shown to be functional in the context of either the rat or human PGR genes (Kraus WL 1994); (Schultz JR 2005), therefore if ERα has a direct effect, then it may be through binding one or more of these EREs to alter PR transcription.

Nardulli *et al.* characterized the hormonal responsiveness of the four PR regulatory sites described above by cotransfecting them with ERα into the ER negative U2-OS, HEC-1 and SK-BR-3 cell lines (human osteosarcoma, endometrial adenocarcinoma and breast adenocarcinoma cells, respectively) (Schultz JR 2005). Transactivation of each individual site was compared to a 1.5 kb tandem PR promoter construct (-711/+817), which contains all four AP-1/Sp1 sites in their native context (Schultz JR 2005). In all three cell lines, strongest transactivation by cotransfected ERα was seen with the tandem 1.5 kb construct, followed by the -61 Sp1 site, the +571 ERE/Sp1 site, and the AP-1 sites (Schultz JR 2005). It is important to note that the transfections in these studies were performed in cells that have lost expression of the endogenous ERα gene and that all of the constructs were based on a PR fragment placed upstream of a minimal TATA-chloramphenicol acetyltransferase (CAT) reporter cassette. This represents an artificial situation since the human and murine PGR genes are in fact TATA-less (Kraus WL 1993); (Kraus WL 1994); (Hagihara K 1994), therefore addition of a TATA box may create an artificially favorable context in which these hormone-responsive cassettes may function.

In U2-OS cells, the -61 bp Sp1 site in the distal PRB promoter showed the greatest stimulatory response to E_2 (Schultz JR 2003). It is probable that this site preferentially activates

the nearby PRB transcriptional start sites and combined with other transcription factors, such as Stat5a and C/EBPβ, up-regulated during pregnancy, may be responsible for the surge in PRB levels observed during this stage of mammary gland development (Grimm SL 2003); (Christian M 2002); (Aupperlee M 2005a); (Aupperlee M 2005b). Since Sp1 is bound to the +571 ERE/Sp1 site in MCF-7 cells both in the presence and absence of E_2 (Petz LN 2004b), Sp1 may contribute to basal expression of the nearby PRA transcription start sites even in the absence of E_2.

4. Mouse Progesterone Receptor
a. PR in Mouse Development

At birth, the mammary gland is present as a rudimentary tree with terminal end buds (TEBs) present at the end of ducts (Hovey RC 2002); (Brisken C 2010). Although ER and PR are present before the onset of puberty (Haslam SZ 1992); (Aupperlee M 2005a), peripubertal development of the mouse mammary gland is thought to be steroid hormone-independent (Atwood CS 2000); (Hovey RC 2002); (Brisken C 2010).

The ductal network within the mouse mammary gland is established prior to pregnancy at the start of ovarian function (Brisken C 2002). During puberty, the mammary gland develops through E_2-dependent ductal elongation (Haslam SZ 1989); (Brisken C 2002), along with PRA-dependent secondary and tertiary ductal branching (Atwood CS 2000); (Aupperlee M 2005a). Ductal growth continues until the ductal tree reaches the boundary of the stromal fat pad and then the gland enters a relatively quiescent state of proliferation until pregnancy (Hovey RC 2002). The architecture of the non-pregnant mouse mammary gland is considered primarily ductal (Hovey RC 2002). Increased E_2 and P levels during pregnancy trigger proliferation

which leads to ductal sidebranching, alveologenesis and lobuloalveolar growth (Brisken C 1998); (Aupperlee M 2005a). P acting specifically through PRB is required for alveologenesis as well as for lobule formation (Aupperlee M 2005a); (Mulac-Jericevic B 2000); (Mulac-Jericevic B 2003). Once the suckling stimulus is removed, the mammary gland undergoes involution and reorganizes into an architecture reminiscent of the pre-pregnant state (Neville MC 2002). However, the involuted gland contains a larger amount of regressed alveoli than the nulliparous mammary gland (Aupperlee M 2005a).

In situ localization experiments showed that in the mouse mammary gland, PR protein was found only in the epithelial compartment and that the stromal compartment was completely PR-negative (Shyamala G 1999). At both the protein and mRNA levels, the ducts contained both PR-positive and negative cells located adjacent to each other within the luminal epithelium (Shyamala G 1999). Studies using IHC have shown that PRA protein is detected at 3 weeks of age in the BALB/c mouse, prior to the onset of ovarian cycles, when the mammary gland has not developed beyond a rudimentary tree (Aupperlee M 2005a). Aupperlee *et al.* demonstrated two distinct switches in PR protein expression patterns that occur during the course of normal mouse mammary gland development. In the 6 week old pubertal mouse mammary gland, 58% of epithelial cells were PRA^+ (Aupperlee M 2005a). The PRA^+ cells were located in both ducts and end buds, with the internal cell layer of the end bud containing the PRA^+ cells (Aupperlee M 2005a). At this stage, PRA infrequently colocalizes with the proliferation marker bromodeoxyuridine (BrdU), indicating that the majority of PRA^+ cells are not proliferating (Aupperlee M 2005a). Most of the $BrdU^+$ cells in the immature virgin gland are found in the cap cell layer of the end buds where PRA^+ cells are absent (Aupperlee M 2005a). During ductal

development in the pubertal mammary gland, P acting through PR leads to the formation of secondary and tertiary ductal branches (Aupperlee M 2005b). At this developmental stage only PRA is detectable, so P must be acting through the non-proliferative PRA^+ cells via a paracrine mechanism to induce branching.

In the 10 to 12 week old virgin adult mice, about 50% of ductal epithelial cells were PRA^+ and PRB was still undetectable (Aupperlee M 2005a). In the 17 to 20 week old virgin adult mouse which no longer contains end buds, the number of PRA^+ cells is reduced significantly to 28% (Aupperlee M 2005a). Upon transition from virgin adult to 14 day pregnant mouse, the number of PRA^+ cells is further reduced to 11% in ductal cells and 6% in alveolar cells whereas the number of PRB^+ cells increases to 48% (Aupperlee M 2005a). At pregnancy, most of the PR^+ cells are PRB^+ and colocalization of PRA with PRB is only seen in a few epithelial cells (Aupperlee M 2005b). However, PRB does frequently colocalize with BrdU in the pregnant mammary gland, indicating that the majority of PRB^+ cells are proliferating (Aupperlee M 2005a). Unlike PRB, BrdU and PRA do not colocalize in the mid-pregnant gland indicating that the PRA^+ cells are in a non-proliferative state during pregnancy just as they are in the non-pregnant gland (Aupperlee M 2005b). Based on these findings plus knockout mouse studies described above, PRB has been shown to be required for alveologenesis as well as in the formation of lobules during pregnancy (Mulac-Jericevic B 2003).

During lactation, both PRB and PRA proteins are undetectable (Aupperlee M 2005a). After involution, the PR levels return to similar but lower levels than virgin adult mice of the same age. In the regressed gland, PRB is detected in less than 1% of ductal cells and 6% of

alveolar cells (Aupperlee M 2005a). In comparison, 12% of the ductal cells were PRA^+ while 10% of regressed alveolar cells were PRA^+ (Aupperlee M 2005a).

Using Northern blot analysis, PR mRNA levels were examined in the BALB/c mammary gland by Shyamala *et al.* across developmental stages and with E_2 treatment. In the intact nulliparous mammary gland (2 to 5 months old), there were abundant 6.9 and 8.7 kb PR mRNAs present (Shyamala G 1990). These transcript levels were greatly reduced upon ovariectomy, but returned to control levels following E_2 treatment (Shyamala G 1990). Similarly, involuting mammary gland (45 days postpartum) from ovary-intact mice contained the 6.9 and 8.7 kb transcripts, but at a slightly lower level of expression (Shyamala G 1990). Ovary intact mice which were pregnant (12-15 dpc), had very low levels of the 6.9 and 8.7 kb PR mRNAs, detectable only after over-exposure of the autoradiograph (Shyamala G 1990). After ovariectomy, PR mRNA was undetectable in the pregnant mammary gland, but increased dramatically after E_2 treatment (Shyamala G 1990). For the lactating mammary gland (7-10 days postpartum), these samples did not have any detectable PR mRNA regardless of whether the mice were ovary-intact, ovariectomized (ovx) or ovx and treated with E_2 (Shyamala G 1990). In contrast, expression data from the FANTOM project mapped three PR RIKEN cDNAs in the 10 day adult lactating mammary gland library (FANTOM2 2002); (Kiyosawa H 2003). This may reflect mouse strain differences, differences in the timing or levels of PR expression, or may be due to greater sensitivity to detect rare messages in the RIKEN sequencing project. Therefore, it remains unclear if there is PR RNA expressed during lactation and if so, which PR isoform is being expressed at this stage.

b. PR in Mouse Mammary Cancer and Mouse Mammary Tumor Cell Lines

One method to induce tumors in the mouse mammary gland is through continuous treatment with medroxyprogesterone acetate (MPA). The resulting tumors are ductal carcinomas that are similar to those ductal carcinomas seen in humans (Lanari C 2001). A model that utilizes this approach was developed by Lanari *et al*. who obtained progestin-dependent tumors (C4-HD) in BALB/c female mice that are highly ER^+ and PR^+ (Lanari C 2001). After serial transplantation, progestin-independent tumors (C7-H1) were also obtained that retained high ER and PR expression. From primary culture of these two MPA-induced tumors, multiple new cell lines were then established that also retain expression of ER and PR in culture (Lanari C 2001). The C4-HD tumors, which are progestin-dependent for growth *in vivo*, gave rise to four cell lines: the MC4-L1, MC4-L3, MC4-L5 (Lanari C 2001) and MC4-L4 cells (Lamb CA 2005a). After passage 7 of the MC4-L1 cells, a subpopulation of cells, designated MC4-L2, was isolated that differed from the parental cells (Lanari C 2001). MC4-L2 cells are spindle-shaped epithelial cells that when injected into syngeneic mice give rise to biphasic spindle cell/tubular carcinomas that are metastatic (Lanari C 2001). MC4-L1, MC4-L3 and MC4-L5 are polygonal-shaped epithelial cells that produce metastatic carcinomas in syngeneic mice with varying degrees of differentiation (Lanari C 2001). C7-HI tumors are progestin-independent for growth *in vivo* and after 3-4 months in primary culture, gave rise to the MC7-L1 cell line (Lanari C 2001). MC7-L1 cells are spindle-shaped epithelial cells that produce very aggressive anaplastic carcinomas that are metastatic when injected into syngeneic mice (Lanari C 2001). These C7-H1 and C4-HD derived cell lines are the first non-transgenic mouse mammary carcinoma cell lines that express both ER and PR. These cell lines therefore represent good cell culture models for steroid receptor-positive mouse mammary carcinomas.

After 15 passages of homogeneous MC4-L4 cells, two different populations of cells emerged, MC4-L4E and MC4-L4F, which were subsequently isolated (Lamb CA 2005a). MC4-L4E is a cuboidal-shaped epithelial cell line that was cloned by limit dilution and is tumorigenic in syngeneic mice (Lamb CA 2005a). MC4-L4F is a spindle-shaped fibroblastic cell line that was separated by detachment and attachment selection and is nontumorigenic in syngeneic mice (Lamb CA 2005a). Both MC4-L4E and MC4-L4F cells are $ER\alpha^{+}$ by western blot and hormone binding assays (Lamb CA 2005a). ERα protein was down-regulated in both cell lines in response to E_2 treatment (Lamb CA 2005a). When grown in isolation, both cell lines were PR-negative by western blot and hormone binding assays even though MC4-L4E tumors in syngeneic mice are PR^{+} (Lamb CA 2005a). When MC4-L4E and MC4-L4F cells were cultured together, both PRB and PRA proteins were detected by western blot and E_2 increased their levels of expression (Lamb CA 2005a).

Mouse mammary cell lines from normal mice are often used as experimental controls. For instance, the normal mammary epithelial cell line Comma-1D was derived from mid-pregnant BALB/c mice (Danielson KG 1984). Comma-1D cells are nontumorigenic and exhibit normal mammary duct morphology when injected into cleared fat pads of syngeneic mice (Danielson KG 1984). Comma-1D cells are hormone-responsive to both E_2 and P, and express both ER and PR, as detected using semi-quantitative PCR (Miksicek RJ, data not shown). NMuMG cells were established from a female adult NARMU mouse mammary gland and are epithelial in nature (Danielson KG 1984). *In vitro*, NMuMG cells exhibit normal morphology, but produce benign cystadenomas when injected into syngeneic mice (Danielson KG 1984).

NMuMG cells were non-responsive to hormones, either E_2 or P, in a cell culture model using transient transfections (data not shown).

5. Sense Versus Antisense Transcription at the Pgr Locus in Rodents
a. Overview of Antisense Transcription and its Potential Relation to Mouse PR Expression

In genome-wide transcriptional (transcriptome) analysis, full-length mouse cDNAs are clustered into transcriptional units (TU) and then mapped to the genome (Katayama S 2005); (Lapidot M 2006). Previous studies on the mammalian transcriptome have concluded that about 20% of transcripts have a corresponding antisense transcript, but the FANTOM3 project showed that antisense transcription is much more prevalent (Katayama S 2005). This is especially true in mouse, where 72% of all transcripts are part of a TU that shows an overlapping cDNA, a cap analysis of gene expression (CAGE) tag or a CAGE tag pair (Katayama S 2005). Using more stringent criteria, almost 29% of the TUs overlapped a cDNA in the opposite strand, forming a sense-antisense pair (Katayama S 2005). For the human transcriptome, naturally occurring antisense transcripts (NATs) are present for 20% of transcripts (Faghihi MA 2006). The majority of NATs are *cis*-encoded antisense RNAs, which are transcribed from the same locus as their sense complement but in the opposite direction (Lapidot M 2006). Conversely, *trans*-NATs that contain imperfect sequence complementarity, are transcribed from different loci, and can act on multiple sense targets (Lapidot M 2006). More than 70% of *cis*-NATs have a tail-to-tail orientation (3' overlap) (Figure 1.3) (Faghihi MA 2006). The 5' overlap (head-to-head) orientation accounts for only 15% of *cis*-NATs (Faghihi MA 2006). In both the human and mouse genomes, the 5' overlap arrangement is present at a lower frequency than convergent antisense pairs (3' overlap) (Numata K 2007). It has been hypothesized that transcripts with

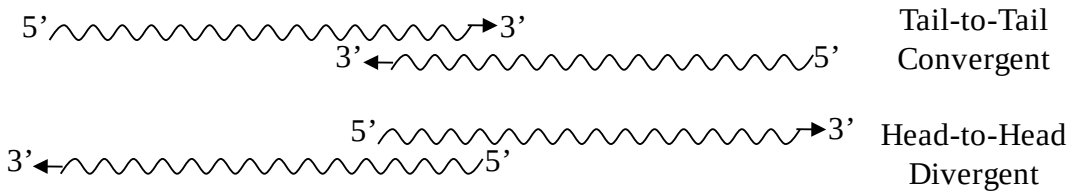

Figure 1.3: Predominant orientations of natural *cis* antisense transcripts. Schematic of genetic loci that contain natural *cis* antisense transcripts that overlap their corresponding sense transcript. The two predominant orientations are tail-to-tail (convergent) and head-to-head (divergent).

heterogeneous start sites may tend to form 5' overlaps, while other transcripts that overlap in their 3'-UTRs show alternative polyadenylation (Lapidot M 2006). In mouse full length cDNA libraries, about half of the representative cloned sequences do not appear to contain a protein coding sequence (Yazgan O 2007). However, experimental analysis of these mouse cDNAs showed that they were derived from genuine transcripts of an unknown function and that they show regulated expression (Yazgan O 2007). For sense/antisense pairs containing unspliced non-coding RNAs (ncRNAs) in the FANTOM2 database, divergent (5' overlaps) pairs are the predominant arrangement (Munroe SH 2006). In both human and mouse, many ncRNAs are transcribed by RNA Polymerase II, contain a capped 5'-end and are polyadenlyated (Munroe SH 2006).

Munroe, *et al.* proposed 5 models to explain mechanisms for antisense regulation. The first model, "Transcriptional regulation independent of overlapping antisense transcription," suggests that *cis*-antisense transcription could compete for (or share) transcription factors in order to regulate expression (Munroe SH 2006). Sharing of transcription factors could result in co-expression of overlapping transcripts, while competition for overlapping binding sites may result in reciprocal or negative correlation of expression (Munroe SH 2006).

The second model, transcriptional interference (TI), suggests that transcription from both strands at the same time may result in topological constraint on the DNA which would result in repression of transcription (Munroe SH 2006). TI can occur at either the initiation or at the elongation stage of transcription (Beiter T 2008). During initiation, TI can result from competition between two overlapped promoters for binding to regulatory elements as well as binding of RNA Polymerase II (Beiter T 2008). An overlap on the 5'-end (head-to-head) is most likely to inhibit at the transcription initiation step and thus decrease the expression level of the

cis-NAT (Osato N 2007). Whereas a short 3' overlap (tail-to-tail) would not alter the *cis*-NAT expression level significantly (Osato N 2007).

During elongation, the RNA polymerases can actually collide if transcription occurs on the same molecule of DNA, as has been experimentally shown for convergent (3' overlapping) pairs in yeast (Munroe SH 2006). Microscopic observation of *E. coli* RNA polymerase collisions demonstrated that the RNA polymerases actually can not pass or displace one another; rather the polymerases just stall against each other (Osato N 2007). In two yeast genes arranged convergently, transcription initiation was unaffected but as soon as the two transcripts started to overlap, there was a stall in elongation that led to greatly reduced mRNA levels (Lapidot M 2006). If transcription only occurs in one direction, then the mRNA levels are predicted to be inverse for sense and antisense transcripts, while if both transcription units are turned off as in the case of transcriptional arrest, there will be no mRNA from either strand (Lapidot M 2006). Although TI is more common in the convergent orientation, TI is conceivable in divergent (5' overlapping) pairs if there is sufficient overlap, especially overlap of an exon, such that the second transcript interferes with either the initiation or elongation step of transcription.

Using serial analysis of gene expression (SAGE) tagging of mouse and human *cis*-NATs, it has been shown that the expression level of all *cis*-NAT arrangements decreased proportionally as the length of the overlapping sense/antisense region increased (Osato N 2007). In mouse, when the overlapping region was l to 200 bp in length, 47% of the highly expressed *cis*-NATs were detected (Osato N 2007). This proportion of highly expressed *cis*-NATs dropped to almost zero when the overlapping region was greater than 2 kb (Osato N 2007). This data fits with a transcription interference collision model, where the collision frequency of RNA polymerase increases as the length of the overlapping region increases (Osato N 2007). According to the TI

model, overlapping of the sense/antisense pair at the 5'-end would inhibit transcription initiation and thus decrease the expression of the *cis*-NATs.

The third model, "Transcriptional regulation mediated by the antisense RNA transcript itself," suggests that a nascent or mature antisense transcript could directly feed back to the overlapping gene or indirectly recruit factors which will in turn promote or inhibit transcription of the overlapping gene (Munroe SH 2006). If there is duplex formation between the sense and antisense transcripts, this could trigger epigenetic alteration either by DNA methylation or by chromosome remodeling (Munroe SH 2006). In this model, the antisense transcript is thought to silence expression of nearby gene clusters via recruitment of histone-modifying enzymes (Lapidot M 2006). The high level of antisense mRNA is predicted to be inversely proportional to the mRNA level of every sense gene in the cluster (Lapidot M 2006).

The fourth model, RNA masking or "Post-transcriptional regulation mediated by sense/antisense base pairing that directly blocks binding of factors to the target transcript," suggests that sites in the sense sequence which are required for its expression (i.e. RNA binding proteins, splicing factors) can be masked by the antisense transcript (Munroe SH 2006). This could occur during splicing, export, stability or control of translation, but does not trigger downstream signaling events (Munroe SH 2006). In the RNA masking model, the antisense transcript masks one of the splice sites on a pre-mRNA message (Lapidot M 2006). It is more favorable to produce splice variants that do not require the masked site, so the balance between splice variants is shifted (Lapidot M 2006). The mRNA level of the antisense transcript and the preferred splice variant are predicted to correlate, while the masked splice variant mRNA level would be inversely proportional to the antisense transcript level (Lapidot M 2006). Additionally,

in the sense/antisense pair, functional ncRNAs could be titrated out by base-pair complementarity (Munroe SH 2006).

The fifth model, "Post-transcriptional regulation mediated by antisense/sense base-pairing that recruits factors that alter downstream expression," suggests that formation of a dsRNA duplex recruits factors which alter expression (Munroe SH 2006). Formation of a dsRNA duplex can also induce post-transcriptional gene silencing (PTGS) via pathways related to siRNA (Munroe SH 2006). Specifically, an antisense RNA may trigger siRNA production which leads to downstream cleavage of homologous transcripts (Munroe SH 2006). However, formation of siRNA from a natural antisense transcript has only been reported in one study of mammals, but has also been reported in *Arabidopsis thaliana* (Munroe SH 2006) and *Drosophila* (Lapidot M 2006). In mice, recent studies report that the interaction of *cis*-sense/antisense pairs can produce endogenous siRNAs (Beiter T 2008). Formation of dsRNA between a pseudogene/ mRNA pair as well as a bidirectionally transcribed *cis*-sense/antisense pair can result in products that can feed into the miRNA or the siRNA pathway (Sasidharan R 2008). In *Drosophila*, a sense/antisense duplex is formed for the Su (Ste) tandem repeats, which is cleaved into 25-27 nt fragments that specifically silence the Stellate repeats, possibly through a Piwi-interacting RNA mechanism (Lapidot M 2006).

As for the possible RNAi mechanism, it has been shown that overlapping regions of an endogenous sense/antisense sequence can feed into the RNAi or the micro-RNA machinery even if the hybridization occurred in the nucleus (Werner A 2005). Therefore, both pathways must be considered for overlapping sense/antisense pairs. In the case of *Arabidopsis*, 11 siRNAs were mapped to the complementary sequence of overlapping transcripts, which may feed into a RNAi pathway (Lapidot M 2006). Regardless of the mechanism, it has been hypothesized that the high

degree of exon complementarity in sense/antisense pairs allows RNA hybridization, which represents a critical step in the processing of NATs (Werner A 2009).

b. Antisense Oligonucleotides Targeting the Mouse or Rat Progesterone Receptor

A few studies have used antisense RNA or siRNAs against the progesterone receptor in mouse, rat and human. However, all of these studies looked at other end points than just knockdown of PR mRNA or protein, i.e. tumor size, sexual behavior and the downstream effect on COX-2 RNA levels. The mouse and rat studies used a 20 nt antisense transcript against the PRA ATG to reduce the level of PRA RNA and protein. In both studies, PRB RNA/protein was also greatly reduced even though this wasn't the expected result in the original study. The mechanism of total PR knockdown is not discussed in either paper, but is assumed to be siRNA since siRNA target sequences are usually 17-23 nt and a 20 mer was used. miRNAs are usually 20-22 nt in length, but are only partially complementary to one or more mRNAs, binding to the 3'-UTR (Yazgan O 2007). Since the 20 mer oligonucleotide is completely complementary and binds to exon 1, this rules out a miRNA mechanism. In the case of the human PR study, siRNAs targeted to PRB only and total PR were successfully used to reduce PR protein expression (Hardy DB 2006).

In another study, Lamb *et al*. used an antisense RNA (asRNA) to target the mouse PRA ATG (+1115 to +1134 bp mPR) in primary cultures of progestin-independent tumors (Lamb CA 2005b). Primary cultures from MPA-induced mammary ductal carcinomas in BALB/c female mice show progestin-independent growth and regress when treated with E_2, RU486 or ZK299 (Lamb CA 2005b). Using a thymidine assay to measure DNA synthesis, the asRNA treatment inhibited cell proliferation approximately 2 fold at the highest concentration tested (2.5 μg/ml),

compared to the scrambled RNA control (scRNA) (Lamb CA 2005b). An *in vitro* whole cell binding assay in primary cultures showed strong inhibition of [^{3}H]R5020 binding activity in asRNA-treated cells by greater than 3 fold, while the scrambled RNA control showed no effect (Lamb CA 2005b). Primary cultures were grown in the presence of 2.5% charcoal-stripped fetal calf serum (csFCS) with or without asRNA (5 μg/ml) and then cell extracts were western blotted using hPRa7 (Neomarkers) (Lamb CA 2005b). Immunoblotting showed that both PRB and PRA proteins were expressed at decreased levels in asRNA-treated cells compared to the positive uterus and negative NMuMG controls (Lamb CA 2005b).

An *in vivo* study compared the effects of asRNA, scRNA and RU486 treatment on tumor size. When tumors in BALB/c mice were about 25 mm^2, either saline solution, antisense RNA or scrambled RNA were administered intraperitoneally twice daily (1 mg/dose) for 5 days (Lamb CA 2005b). RU486 was administered as a 5 mg pellet subcutaneously (6.5 mg/kg body weight) (Lamb CA 2005b). On day 5, change in tumor size was determined by dividing the final tumor area by the tumor area at the start of the experiment (100%) (Lamb CA 2005b). Treatment with the asRNA resulted in an approximately 2 fold decrease in tumor size while the scRNA treatment was not significantly different than the saline control (Lamb CA 2005b). The most dramatic decrease in size resulted from RU486 treatment, which showed an approximate 8 fold decrease in tumor size after only 5 days of treatment (Lamb CA 2005b). Treatment with antisense RNA for 10 days showed a significant decrease in tumor growth for the first 5 days, after which tumor growth resumed at a slower rate (Lamb CA 2005b).

In a separate study, both sense and antisense RNAs targeting the rat PRA ATG (+1115 to +1134 bp mouse PR) were given intracerebroventricularly into the third cerebral ventricle of ovariectomized E_2-primed female rats (Mani SK 1994). Cytosolic PR levels in the

hypothalamus, assayed by [^{3}H] R5020 binding increased 161% in the E_2-primed rat compared to vehicle control (Mani SK 1994). E_2-priming plus antisense RNA (4 nmol) resulted in a 52.2% decrease in cytosolic PR, while E_2 plus sense RNA (4 nmol) was not significantly different than E_2 alone (Mani SK 1994). The antisense RNA used in this study is the same as the siRNA used by Lamb *et al.* for mouse PR correcting for a one basepair difference between the rat and mouse sequences.

6. Sense versus Antisense Transcription at the Human PGR Locus
a. Human PR Sense Transcription

The human PR transcription unit is comprised of two promoters, a distal and a proximal promoter, that drive expression of the two predominant isoforms, PRB and PRA, respectively (Kastner P 1990). The $PR^{(A)}$ and $PR^{(B)}$ mRNAs are composed of 8 exons, the largest of which is the 1.6 kb exon 1 (GenBank (NCBI) 2005). Similar to mouse PR, human PR messages contain a large degree of 5'-termini heterogeneity (Wei LL 1990). Using Northern blots of human T47-D mammary carcinoma cells, there were 3 classes of PR RNAs identified (Wei LL 1990). The class A transcripts are 2.5 and 5.2 kb in size and lack the ATG_B region, but retain the ATG_A and therefore can only encode PRA protein (Wei LL 1990). Class B transcripts are 3.2, 4.5, and 6.1 kb in size, and also consist of bands I and II of a 11.4 kb complex (Wei LL 1990). The class B transcripts contain both the ATG_B and ATG_A initiation codons and could encode PRB or PRA protein (Wei LL 1990). There is also a class C of PR transcripts that consists of bands III and IV of the 11.4 kb complex, but lacks both ATG_B and ATG_A and therefore cannot encode PRB or PRA protein (Wei LL 1990). The 5'-truncated PRC transcripts are homologous to the

DBDs and LBDs and believed to initiate at codon 595 within exon 2 (Wei LL 1990). There is evidence of additional promoter activity within intron 3, where a leader exon with an in-frame initiator codon is located (Samalecos A 2008). This leader exon codes for a novel 16 amino acid exon that is a potential signal peptide and is spliced to exons 4-8 forming class M transcripts (PRM) (Samalecos A 2008).

b. Human PR Antisense Transcription

The human PGR locus gives rise to three different types of antisense transcripts in breast cancer cells (Figure 1.4) which are presumably controlled by uncharacterized upstream promoters (Schwartz JC 2008). The farthest upstream transcript, antisense transcript-1 (AT-1) represents an intronless RNA that initiates at +1431 bp (Schwartz JC 2008), downstream relative to the PRB mRNA start location of +1 bp. This 2155 bp transcript is found in both MCF-7 and T47-D cells, but is the least abundant of the three antisense transcripts (Schwartz JC 2008). AT-1 is polyadenylated and terminates within the PRB promoter region (Schwartz JC 2008). The AT2-MCF7 transcript is only found in MCF-7 cells and initiates at +738 bp, relative to the PRB transcription start site (Schwartz JC 2008). The AT2-MCF7 transcript contains 7 exons, is polyadenylated and spans 70,000 bp of genomic sequence (Schwartz JC 2008). This transcript contains long interspersed sequences (LINES), short interspersed sequences (SINES), and long terminal repeat (LTR) elements (Schwartz JC 2008). T47-D cells contain a 5'-end truncated version of AT-2 which initiates at +536 bp, but is otherwise identical in sequence to AT2-MCF7 (Schwartz JC 2008). AT2-MCF7 and ATF2-T47D were the most abundant transcript forms and each had RNA levels approximately 10 fold below the level of sense PR mRNA, as detected by quantitative (Q)-PCR (Schwartz JC 2008).

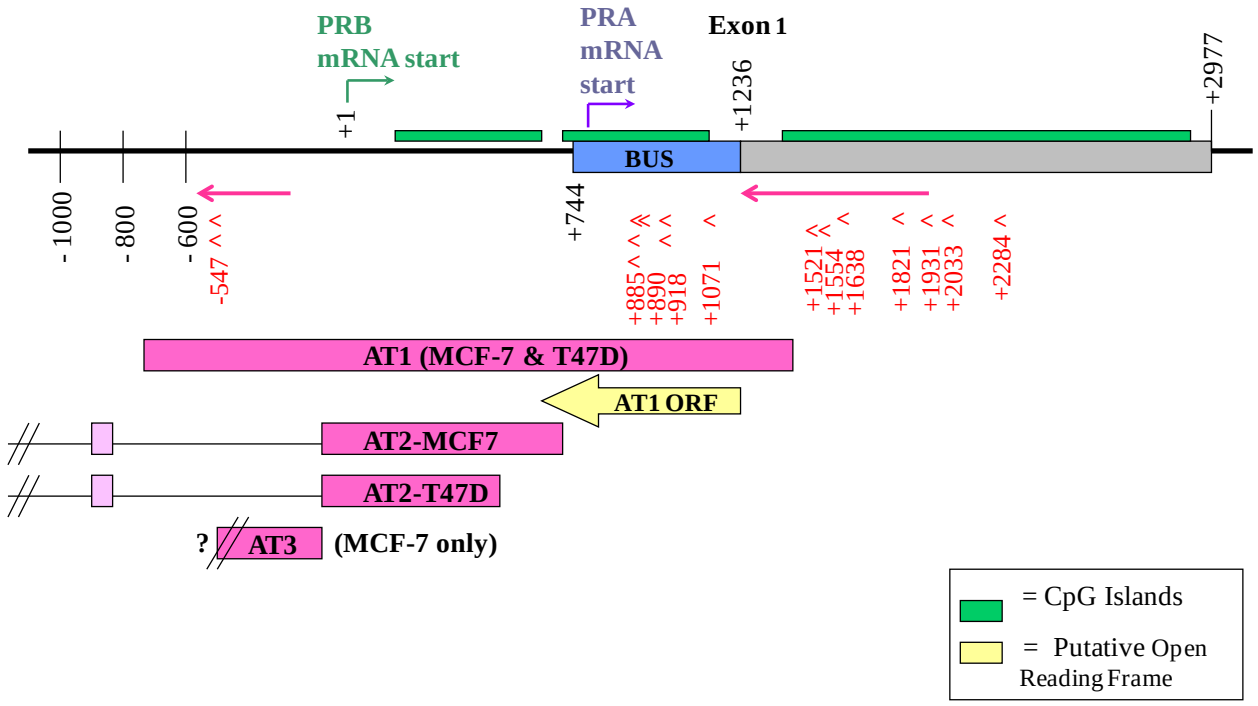

Figure 1.4: Location of known antisense transcripts in the human progesterone receptor gene. The antisense cap analysis of gene expression (CAGE) tags (red carrots), antisense expressed sequence tags (ESTs) (pink arrows) and $PR^{antisense}$ transcripts (pink boxes) of the human progesterone receptor gene. Numbering is relative to the PRB mRNA start site at +1 bp, while the PRA mRNA start site is located at +751 bp. The location of the three CpG islands is indicated in green. The B-upstream region (BUS), unique to the PRB transcript, is indicted in blue. The PRB ATG is located at +744 bp and the PRA ATG at +1236 bp. In yellow (boxed arrow) is a putative open reading frame (ORF) for antisense transcript 1 (AT-1).

The shortest transcript in the antisense strand is AT-3, which is located at -114 bp, upstream of the PRB mRNA start site (Schwartz JC 2008). AT-3 is a moderately abundant transcript, but was only partially sequenced, leaving the exon structure and polyadenylation status unknown (Schwartz JC 2008). The exon structures of AT-1 and AT-2 were confirmed using the Spidey alignment tool (Spidey [NCBI] 2008). Transcripts AT-1, AT-2 and AT-3 do not contain homology to any known gene or protein other than the portion that overlaps with sense PR exon 1.

Experiments using antigene RNAs (agRNAs) directed against the human PR promoter have helped to define a role for these $PR^{antisense}$ transcripts in MCF-7 and T47-D cells. Antigene RNAs are synthetic 19- to 21-basepair duplex RNAs that are being tested as potential therapeutic agents to positively or negatively modulate PR expression for use in breast cancer treatment (Janowski BA 2007). Human $PR^{antisense}$ transcripts are thought to be noncoding RNAs that act as the targets for agRNAs since expression of antisense PR RNA is required for agRNA activity (Schwartz JC 2008). However, the mechanism doesn't involve transcript cleavage (Schwartz JC 2008). This suggests that the antisense promoter is not controlled by an RNAi mechanism. When the level of the $PR^{antisense}$ transcript was reduced, this reversed the function of the activating agRNAs, suggesting that there is a threshold level of antisense transcript required to achieve activation with the agRNAs (Younger ST 2009). Although it wasn't tested extensively, preliminary data suggests that inhibiting the expression of $PR^{antisense}$ transcripts alone is not sufficient to activate or repress expression of the endogenous PR in human breast cancer cells (Schwartz JC 2008). Criticisms of the assay include that overexpression of antisense transcripts was not tested and the assay only measured fold changes of total PR mRNA, rather than

separately measuring PRB and total PR RNA levels. Changing the level of $PR^{antisense}$ transcript may impact the regulation of the PRB and PRA promoters as well as the spatial or temporal expression of the transcripts.

The agRNAs recruit argonaute proteins to the $PR^{antisense}$ transcript and form a complex with RNA polymerase II and other proteins (Schwartz JC 2008). This agRNA complex shifts the localization of heterogeneous nuclear riboprotein k (hnRNP-k) from the chromosomes to the antisense AT-2 transcript (Schwartz JC 2008). HnRNP-k is known to interact with RNA, DNA as well as proteins and is a candidate gene for agRNA complexes (Schwartz JC 2008). Under conditions of PGR gene activation, treatment with agRNA allows cells to recruit RNA polymerase II to the PRB promoter (Schwartz JC 2008). Whereas under conditions of PGR gene silencing, treatment with agRNA causes RNA Polymerase II to dissociate from the PRB promoter (Schwartz JC 2008).

In T47-D cells, growth conditions leading to high PR expression allow agRNAs to repress PRB gene expression, while low PR expression conditions allow agRNAs to activate PRB gene expression (Schwartz JC 2008). Therefore, PRB gene expression is dependent on basal PR expression levels as well as the promoter state when the agRNA-argonaute complex is recruited to the PR promoter. Since the PRA promoter was not analyzed, it is unknown if PRA is regulated in a similar manner. It is not known if a similar feedback loop is utilized *in vivo* to control when PR expression is activated or repressed, but it is possible that the $PR^{antisense}$ transcript could act as a target for natural miRNAs that serve as the endogenous counterpart of PR agRNA.

The inhibition of PR expression by agRNA is not due to changes in methylation of the DNA, as was previously suggested by other studies (Janowski BA 2005). Using both bisulfite

sequencing and methylation specific PCR, there was no methylation detected at the human PRB promoter (Janowski BA 2005). When DNA Methyltransferase (DNMT1) was silenced, there was no effect on agRNA inhibition of hPRB expression (Janowski BA 2005). Treatment of cells with 5-aza-2'-deoxycytidine (5-aza-dc), a DNA methylation inhibitor, also did not affect agRNA inhibition of hPRB expression (Janowski BA 2005). The proposed mechanism is a RNA-RNA-protein complex that interacts with the promoter DNA to form a "blockade" that prevents transcription from initiating at the major start sites (Janowski BA 2005). Since only the human PRB promoter was analyzed, it would be interesting to know if this "blockade" occurs at the PRA promoter as well or whether this phenomenon is PRB promoter specific. If only the PRB promoter is subject to a "blockade", this would represent a possible mechanism to selectively silence the PRB promoter and allow only PRA transcription. In this model, in order to achieve PRB expression, the "blockade" must be released by interfering with the RNA-RNA-protein interaction or perhaps by simply down-regulating the antisense transcript so that the complex cannot form. Strong transcriptional initiation at the PRB promoter could lead to occlusion of the PRA promoter, selectively decreasing the level of PRA transcription.

c. Antisense Oligonucleotides Targeting the Human Progesterone Receptor

In T47-D human mammary carcinoma cells (ER^+/PR^+) , two siRNAs directed against PRB only (+176 to +194 bp; +160 to +178 bp) and one against PRB plus PRA (+652 to +670 bp) were used to knockdown PR levels (Hardy DB 2006). T47-D cell lysates were analyzed by western blot using a rabbit PR antibody that detects both PRB and PRA (Hardy DB 2006). For the PRB only siRNA, the level of PRB was decreased $\geq$ 3 fold, while the level of PRA protein appeared unchanged (Hardy DB 2006). The combined $PR^{(B+A)}$ siRNA completely knocked

down protein levels of both PR isoforms below the level of detection by western blot (Hardy DB 2006). Control treatments with transfection reagent without siRNA or a mismatched siRNA did not significantly alter the protein level of either PR isoform (Hardy DB 2006).

Summary and Overview

Immunohistochemical analysis in the human mammary gland revealed that the progesterone receptor isoforms PRA and PRB are usually expressed at an equal ratio and show uniform colocalization (Graham JD 1995); (Mote PA 2002). Therefore, studies of PR function in human cell lines would have to address three species of protein dimers: AA, BB and AB. The mouse represents a unique situation in which the PRA and PRB isoforms rarely colocalize, so that the majority of endogenous PR forms only homodimers (Aupperlee M 2005a). PRA protein levels are high in the pubertal mouse, lower in the virgin adult and lowest in the pregnant mouse, while PRB protein is undetectable in the pubertal and virgin adult mouse, but high in the pregnant mouse (Aupperlee M 2005a). Since the PR proteins are both spatially and temporally separated (Aupperlee M 2005a), the mouse is an ideal model system to study the isolated PR isoforms during mammary gland development. Experiments conducted on rodents point toward progesterone and its signaling pathways as important factors in the development of the normal mammary gland as well as the induction, progression and maintenance of mammary tumors (Lanari C 2002). In both the normal mouse mammary gland and the human breast, studies show that progestins increase cell proliferation (Aupperlee M 2005b); (Anderson E 2004). In humans, E_2+P HRT increases the risk of postmenopausal breast cancer more than E_2 replacement alone (Anderson E 2002); (Calle EE 2009). Therefore, it is important to understand what controls PR isoform expression as well as the downstream target genes and PR signaling pathways that

mediate PR function. In addition to hormonal regulation of the PR sense strand, there is also the question of what function the $PR^{antisense}$ transcript plays in regulation of the mouse Pgr locus. Since $PR^{antisense}$ mRNA overlaps with the promoters that are believed to control PRA and PRB expression through separate $PR^{(A)}$ and $PR^{(B)}$ mRNA transcripts, it is possible that antisense transcription may influence the balance between these two PR isoforms.

Superimposed on these hormonal influences are important growth factor pathways, many of which ultimately converge on the AP-1 family, shown to be important for transcriptional regulation of human PRA and PRB. Since expression of the mouse Pgr gene is regulated not just by E_2 and P, but also by growth regulatory pathways that signal through AP-1 and other transcription factors, we decided to examine the effect of steroid hormones and co-expression of jun and fos subunits on the activity of both the sense and antisense promoters, and on their respective mRNA transcripts. Our underlying hypothesis is that a change in the composition of AP-1 subunits is, at least in part, responsible for the shift from PRA to PRB expression during alveologenesis, perhaps due to their ability to regulate the activity of the $PR^{antisense}$ promoter.

REFERENCES

REFERENCES

Anderson E. "The Role of Oestrogen and Progesterone Receptors in Human Mammary Development and Tumorigenesis ." Breast Cancer Research 4 (2002): 197-201 .

Anderson E, Clarke RB. "Steroid Receptors and Cell Cycle in Normal Mammary Epithelium." Journal of Mammary Gland Biology and Neoplasia 9.1 (2004): 3-13.

Atwood CS, Hovey RC, Glover JP, Chepko G, Ginsburg E, Robinson Jr WG, Vonderhaar BK. "Progesterone Induces Side-Branching of the Ductal Epithelium in the Mammary Glands of Peripubertal Mice." Journal of Endocrinology 167 (2000): 39-52.

Aupperlee M, Smith KT, Kariagina A, Haslam SZ. "Progesterone Receptor Isoforms A and B: Temporal and Spatial Differences in Expression during Murine Mammary Gland Development." Endocrinology 146.8 (2005a): 3577-3588.

Aupperlee M, Kariagina A, Osuch J, Haslam SZ. "Progestins and Breast Cancer." Breast Disease 24 (2005b): 37-57.

Aupperlee MD, Haslam SZ. "Differential Hormonal Regulation and Function of Progesterone Receptor Isoforms in Normal Adult Mouse Mammary Gland." Endocrinology 148.5 (2007): 2290-2300.

Aupperlee MD, Drolet AA, Durairaj S, Wang W, Schwartz RC, Haslam SZ. "Strain-Specific Differences in the Mechanisms of Progesterone Regulation of Murine Mammary Gland Development." Endocrinology 150.3 (2009): 1485-1494.

Bamberger AM, Methner C, Lisboa BW, Stadtler C, Schulte HM, Loning T, Milde-Langosch K. "Expression Pattern of the AP-1 Family in Breast Cancer: Association of fosB Expression with a Well-Differentiated Receptor-Positive Tumor Phenotype." International Journal of Cancer 84 (1999): 533-538.

Bamberger AM, Milde-Langosch K, Schulte HM. "Progesterone Receptor Isoforms, PRB and PRA, in Breast Cancer: Correlations with Clinicopathologic Tumor Parameters and Expression of AP-1 factors." Hormone Research 54 (2000): 32-37.

Beiter T, Reich E, Williams RW, Simon P. "Antisense Transcription: A Critical Look in Both Directions." Cellular and Molecular Life Sciences 66 (2008): 94-112.

Belguise K, Kersual N, Galtier F, Chalbos D. "FRA-1 Expression Level Regulates Proliferation and Invasiveness of Breast Cancer Cells." Oncogene 24 (2005): 1434-1444.

Bjornstrom L, Sjoberg M. "Mechanisms of Estrogen Receptor Signaling: Convergence of Genomic and Nongenomic Actions on Target Genes." Molecular Endocrinology 19 (2005): 833-842.

Brisken C, Park S, Vass T, Lydon JP, O'Malley BW, Weinberg RA. "A Paracrine Role for the Epithelial Progesterone Receptor in Mammary Gland Development." Proceedings of the National Academy of Sciences U.S.A 95 (1998): 5076-5081.

Brisken C. "Hormonal Control of Alveolar Deveopment and Its Implications for Breast Carcinogenesis." Journal of Mammary Gland Biology and Neoplasia 7.1 (2002): 39-48.

Brisken C, O'Malley B. "Hormone Action in the Mammary Gland." Cold Spring Harbor Prespectives in Biology 2.12 (2010): 1-15.

Calle EE, Feigelson HS, Hildebrand JS,. "Postmenopausal Hormone Use and Breast Cancer Associations Differ by Hormone Regimen and Histologic Subtype." Cancer 115 (2009): 936-945.

Cawley S, Berkiranov S, Ng HH, Kapranov P, Sekinger EA, Kampa D, Piccolboni A, Sementchenko V, Cheng J, Williams AJ, Wheeler R, Wong B, Drenkow J, Yamanaka M, Patel S, Brubaker S, Tammana H, Helt G, Struhl K, Gingeras TR. "Unbiased Mapping of Transcription Factor Binding Sites along Human Chromosomes 21 and 22 Points to Widespread Regulation of Noncoding RNAs." Cell 116 (2004): 499-509.

Christian M, Pohnke Y, Kempf R, Gellersen B, Brosens JJ. "Functional Association of PR and CCAAT/Enhancer Binding Protein Beta Isoforms: Promoter-dependent Cooperation Between PR-B and Liver-Enriched Inhibitory Protein, or Liver-Enriched Activatory Protein and PR-A in Human Endometrial Stromal Cells." Molecular Endocrinology 16.1 (2002): 141-154.

Couse JF, Korach KS. "Estrogen Receptor Null Mice: What Have We Learned and Where Will They Lead Us?" Endocrinology Reviews 20 (1999): 358-417.

Danielson KG, Oborn CJ, Durban EM, Butel JS, Medina D. "Epithelial Mouse Mammary Cell Line Exhibiting Normal Morphogenesis in Vivo and Functional Differentiation in Vitro." PNAS 81 (1984): 3756-3760.

DiAugustine RP, Richards RG, Sebastian J. "EGF-related Peptides and Their Receptors in Mammary Gland Development." Journal of Mammary Gland Biology and Neoplasia 2 (1997): 109-117.

Faghihi MA, Wahlestedt C. "RNA Interference is not Involved in Natural Antisense Mediated Regulation of Gene Expression in Mammals." Genome Biology 7 (2006): R38-R38.9.
FANTOM2 2002, Functional Annotation of Mouse Consortium and the Riken Group. "<http://fantom2.gsc.riken.go.jp/db/annotate/main.cgi?masterid=9930019P03>." (2002 October 4).

Feldman M, Ruan W, Tappin I, Wieczorek R, Kleinberg DL. "The Effect of GH on Estrogen Receptor Expression in the Rat Mammary Gland." The Journal of Endocrinology 163 (1999): 515-522.

Flototto T, Niederacher D, Hohmann, Heimerzheim T, Dall P, Djahansouzi S, Bender HG, Hanstein B. "Molecular Mechanism of Estrogen Receptor(ER)alpha-specific, Estradiol-dependent Expression of the Progesterone Receptor (PR) B-isoform." Steroid Biochemistry & Molecular Biology 88 (2004): 131-142.

Flux DS. "Growth of the Mammary Duct System in Intact and Ovariectomized Mice of the Chi Strain." Journal of Endocrinology 11 (1954): 223-237.

Gao X, Nawaz Z. "Progesterone Receptors-Animal Models and Cell Signaling in Breast Cancer: Role of Steroid Receptor Coactivators and Corepressors of Progesterone Receptor in Breast Cancer." Breast Cancer Research 4.5 (2002): 182-186.

GenBank (NCBI) 2005. GenBank. <http://www.ncbi.nlm.nih.gov/Genbank/>.

Giangrande PH, Pollio G, McDonnell DP. "Mapping and Characterization of the Functional Domains Responsible for the Differential Activity of the A and B Isoforms of the Human Progesterone Receptor." The Journal of Biological Chemistry 272.52 (1997): 32889-32900.

Graham JD, Yeates C, Balleine RL, Harvey SS, Milliken JS, Bilous AM, Clarke CL. "Characterization of Progesterone Receptor A and B Protein Expression in Human Breast Cancer." Cancer Research 55 (1995): 5063-5068.

Grimm SL, Rosen JM. "The Role of C/EBPBeta in Mammary Gland Development and Breast Cancer." Journal of Mammary Gland Biology and Neoplasia 8.2 (2003): 191-204.

Gruber CJ, Gruber DM, Gruber IML, Wieser F, Huber JC. "Anatomy of the Estrogen Response Element." TRENDS in Endocrinology and Metabolism 15.2 (2004): 73-78.

Gutzman JH, Nikolai SE, Rugowski DE, Watters JJ, Schuler LA. "Prolactin and Estrogen Enhance the Activity of Activating Protein 1 in Breast Cancer Cells: Role of Extracellularly Regulated Kinase 1/2-Mediated Signals to c-fos ." Molecular Endocinology 19.7 (2005): 1765-1778.

Hagihara K, Wu-Peng XS, Funabashi T, Kato J, Pfaff DW. "Nucleic Acid Sequence and DNase Hypersensitive Sites of the 5’ Region of the Mouse Progesterone Receptor." Biochemical and Biophysical Research Communications 205.2 (1994): 1093-1101.

Hardy DB, Janowski BA, Corey DR, Mendelson CR. "Progesterone Receptor Plays a Major Antiinflammatory Role in Human Myometrial Cells by Antagonism of Nuclear Factor-KappaB Activation of Cyclooxygenase 2 Expression." Molecular Endocrinology 20.11 (2006): 2724-2733.

Haslam SZ. "The Ontogeny of Mouse Mammary Gland Responsiveness to Ovarian Steroid Hormones." Endocrinology 125 (1989): 2766-2772.

Haslam SZ, Nummy KA. "The Ontogeny and Cellular Distribution of Estrogen Receptors in Normal Mouse Mammary Gland." Journal of Steroid Biochemistry and Molecular Biology 42 (1992): 589-595.

Haslam SZ, Counterman LJ, Nummy KA. "Effects of Epidermal Growth Factor, Estrogen, and Progestin on DNA Synthesis in Mammary Cells in vivo are Determined by the Developmental State of the Gland." Journal of Cellular Physiology 155 (1993): 72-78.

Hess J, Angel P, Schorpp-Kistner M. "AP-1 Subunits: Quarrel and Harmony Among Siblings." Journal of Cell Science 117 (2004): 5965-5973.

Hopp TA, Weiss HL, Hilsenbeck SG, Cui Y, Allred DC, Horwitz KB, Fuqua SA. "Breast Cancer Patients with Progesterone Receptor PR-A-Rich Tumors Have Poorer Disease-Free Survival Rates." Clinical Cancer Research 10 (2004): 2751-2760.

Hovey RC, Trott JF, Vonderhaar BK. "Establishing a Framework for the Functional Mammary Gland: From Endocrinology to Morphology." Journal of Mammary Gland Biology and Neoplasia 7.1 (2002): 17-38.

Huse B, Verca SB, Matthey P, Rusconi S. "Definition of a Negative Modulation Domain in the Human Progesterone Receptor." Molecular Endocrinology 12 (1998): 1334-1342.

Jacobsen BM, Richer JK, Sartorius CA, Horwitz KB. "Expression Profiling of Human Breast Cancers and Gene Regulation by Progesterone Receptors." Journal of Mammary Gland Biology and Neoplasia 8.3 (2003): 257-268.

Jacobsen BM, Schittone SA, Richer JK, Horwitz KB. "Progesterone-Independent Effects of Human Progesterone Receptors (PRs) in Estrogen Receptor-Positive Breast Cancer: PR Isoform-Specific Gene Regulation and Tumor Biology." Molecular Endocrinology 19.3 (2005): 574-587.

Janowski BA, Huffman KE, Schwartz JC, Ram R, Hardy D, Shames DS, Minna JD, Corey DR. "Inhibiting Gene Expression at Transcription Start Sites in Chromosomal DNA with Antigene RNAs." Nature Chemical Biology 1.4 (2005): 216-222.

Janowski BA, Younger ST, Hardy DB, Ram R, Huffman KE, Corey DR. "Activating Gene Expression in Mammalian Cells With Promoter-targeted Duplex RNAs." Nature Chemical Biology 3.3 (2007): 166-173.

Kastner P, Krust A, Turcotte B, Stropp U, Tora L, Gronemeyer H, Chambon P. "Two Distinct Estrogen-Regulated Promoters Generate Transcripts Encoding the Two Functionally Different Human Progesterone Receptor Forms A and B." The EMBO Journal 9.5 (1990): 1603-1614.

Katayama S, Tomaru Y, Kasukawa T, Wak Ki, Nakanish M, Nakamura M, Nishida H, Yap CC, Suzuki M, Kawai J, Suzuki H (RIKEN Genome Exploration Research Group and Genome Science Group (Genome Network Project Core Group) and the FANTOM Consortium). "Antisense Transcription in the Mammalian Transcriptome." Science 309 (2005): 1564-1566.

Kiyosawa H, Yamanaka I, Osato N, Kondo S, RIKEN GER Group & GSL Members, Hayashizaki Y. "Antisense Transcripts With FANTOM2 Clone Set and Their Implications for Gene Regulation." Genome Research 13 (2003): 1324-1334.

Kraus WL, Montano MM, Katzenellenbogen BS. "Cloning of the Rat Progesterone Receptor Gene 5' Region and Identification of Two Functionally Distinct Promoters." Molecular Endocrinology 7 (1993): 1603-1616.

Kraus WL, Montano MM, Katzenellenbogen BS. " Identification of Multiple, Widely Spaced Estrogen-Responsive Regions in the Rat Progesterone Receptor Gene." Molecular Endocrinology 8 (1994): 952-969.

Krege JH, Hodgin JB, Couse JF, Enmark E, Warner M, Mahler JF, Sar M, Korach KS, Gustafssonh JA, Smithies O. "Generation and Reproductive Phenotypes of Mice Lacking Estrogen Receptor Beta." Proceedings of the National Academy of Sciences U.S.A. 95 (1998): 15677-15682.

Kumle M, Weiderpass E, Braaten T, Persson I, Adami HO, Lund E. "Use of Oral Contraceptives and Breast Cancer Risk: The Norwegian-Swedish Women's Lifestyle and Health Cohort Study." Cancer Epidemiology Biomarkers and Prevention 11 (2002): 1375-1381.

Lamb CA, Fabris V, Gorostiaga MA, Helguero LA, Efeyan A, Bottino MC, Simian M, Soldati R, Sanjuan N, Molinolo A, Lanari C. "Isolation of a Stromal Cell Line From an Early Passage of a Mouse Mammary Tumor Line: A Model for Stromal Parenchymal Interactions." Journal of Cellular Physiology 202 (2005a): 672-682.

Lamb CA, Helguero LA, Giulianelli S, Soldati R, Vanzulli SI, Molinolo A, Lanari C. "Antisense Oligonucleotides Targeting the Progesterone Receptor Inhibit Hormone-independent Breast Cancer Growth in Mice." Breast Cancer Research 7.6 (2005b): R1111-R1121.

Lanari C, Luthy I, Lamb CA, Fabris V, Pagano E, Helguero LA, Sanjuan N, Merani S, Molinolo AA. "Five Novel Hormone-responsive Cell Lines Derived from Murine Mammary Ductal Carcinomas: In Vivo and in Vitro Effects if Estrogens and Progestins." Cancer Research 61 (2001): 293-302.

Lanari C, Molinolo AA. "Diverse Activation Pathways for the Progesterone Receptor: Possible Implications for Breast Cancer Biology." Breast Cancer Research 4.6 (2002): 240-243 .

Lange C. "Challenges to Defining a Role for Progesterone Receptor in Breast Cancer." Steroids 73 (2008): 914-921.

Lange CA. "Making Sense of Cross-Talk between Steroid Hormone Receptors and Intracellular Signaling Pathways: Who Will Have the Last Word?" Molecular Endocrinology 18.2 (2004): 269-278.

Lapidot M, Pilpel Y. "Genome-wide Natural Antisense Transcription: Coupling its Regulation to its Different Regulatory Mechanisms." EMBO Reports (2006): 1216-1222.

Li X, Lonard DM, O'Malley BW. "A Contemporary Understanding of Progesterone Receptor Function." Mechanisms of Ageing and Development 125 (2004): 669-678.

Lubahn DB, Moyer JS, Golding TS, Couse JF, Korach KS, Smithies O. "Alteration of Reproductive Function But Not Prenatal Sexual Development After Insertional Disruption of the Mouse Estrogen Receptor Gene." Proceedings of the National Academy of Sciences U.S.A 90 (1993): 11162-11166.

Lund E, Bakken K, Dumeaux V, Andersen V, Kumle M. "Hormone replacement therapy and breast cancer in former users of oral contraceptives—The Norwegian women and cancer study." International Journal of Cancer 121 (2007): 645-648.

Lydon JP, MeMayo FJ, Funk CR, Mani SK, Hughes AR, Montgomery Jr. CA, Shyamala G, Conneely OM, O'Malley BW. "Mice Lacking Progesterone Receptor Exhibit Pleotropic Reproductive Abnormalities." Genes & Development 9 (1995): 2266-2278.

Mani SK, Blaustein JD, Allen JMC, Law SW, O'Malley BW, Clark JH. "Inhibition of Rat Sexual Behavior by Antisense Oligonucleotides to the Progesterone Receptor." Endocrinology 135.4 (1994): 1409-1414.

Marti A, Jehn B, Costello E, Keon N, Ke N, Martin F, Jaggi R. "Protein Kinase A and AP-1 (c-Jun/FosD) are Induced During Apoptosis of Mouse Mammary Epithelial Cells." Oncogene 9 (1994): 1213-1223.

MatInspector 2005. Genomatix MatInspector. 2005. <http://www.genomatix.de/cgi-bin/sessions/login.pl?s=5fea7747b00c3b1638b142a04b37e562>.

Mechta-Grigoriou F, Gerald D, Yaniv M. "The Mammalian Jun Proteins: Redundancy and Specificity." Oncogene 20 (2001): 2378-2389.

Mote PA, Bartow S, Tran N, Clarke CL. "Loss of Co-ordinate Expression of Progesterone Receptors A and B is an Early Event in Breast Carcinogenesis." Breast Cancer Research and Treatment 72 (2002): 163-172.

Mulac-Jericevic B, Mullinax RA, DeMayo FJ, Lydon JP, Conneely OM. "Subgroup of Reproductive Functions of Progesterone Mediated by Progesterone Receptor-B Isoform." Science 289 (2000): 1751-1754.

Mulac-Jericevic B, Lydon JP, DeMayo FJ, Conneely OM. "Defective Mammary Gland Morphogenesis in Mice Lacking the Progesterone Receptor B Isoform." PNAS 100.17 (2003): 9744-9749.

Munroe SH, Zhu J. "Review: Overlapping Transcripts, Double-stranded RNA and antisense Regulation: a Genomic Perspective." Cellular and Molecular Life Sciences 63 (2006): 2102-2118.

Naar AM, Ryu S, Tjian R. "Cofactor Requirements for Transcriptional Activation by Sp1." Cold Spring Harbor Symposia on Quantitative Biology. Vol. 63. Cold Spring Harbor Laboratory Press, 1998. 189-200.

Neville MC, McFadden TB, Forsyth I. "Hormonal Regulation of Mammary Differentiation." Journal of Mammary Gland Biology and Neoplasia 7.1 (2002): 49-66.

Numata K, Okada Y, Saito R, Kiyosawa H, Kanai A, Tomita M. "Comparative Analysis of cis-encoded Antisense RNAs in Eukaryotes." Gene 392 (2007): 134-141.

Osato N, Suzuki Y, Ikeo K, Gojobori T. "Transcriptional Interferences in cis Natural antisense Transcripts of Human and Mice." Genetics 176 (2007): 1299-1306.

Passegue E, Jochum W, Behrens A, Ricci R, Wagner EF. "JunB Can Substitute for Jun in Mouse Development and Cell Proliferation." Nature Genetics 30.2 (2002): 158-166.

Pestell RG, Albanese C, Reutens AT, Segall JE, Lee RJ, Arnold A. "The Cyclins and Cyclin-Dependent Kinase Inhibitors in Hormonal Regulation of Proliferation and Differentiation." Endocrine Reviews 20.4 (1999): 501-534.

Petz LN, Ziegler YS, Loven MA, Nardulli AM. " Estrogen Receptor α and Activating Protein-1 Mediate Estrogen Responsiveness of the Progesterone Receptor Gene in MCF-7 Breast Cancer Cells." Endocrinology 143.12 (2002): 4583-4591.

Petz LN, Ziegler YS, Schultz JR, Nardulli AM. "Fos and Jun Inhibit Estrogen-Induced Transcription of the Human Progesterone Receptor Gene Through an Activator Protein-1 Site." Molecular Endocrinology 18.3 (2004a): 521-532.

Petz LN, Ziegler YS, Schultz JR, Kim H, Kemper JK, Nardulli AM. "Differential Regulation of the Human Progesterone Receptor Gene Through an Estrogen Response Element Half Site and Sp1 Sites." The Journal of Steroid Biochemistry and Molecular Biology 88 (2004b): 113-122.

Richer JK, Jacobsen BM, Manning NG, Abel MG, Wolf DM, Horwitz KB. "Differential Gene Regulation by The Two Progesterone Receptor Isoforms in Human Breast Cancer Cells." The Journal of Biological Chemistry 277.7 (2002): 5209-5218.

Safe S, Abdelrahim M. "Sp Transcription Factor Family and its Role in Cancer." European Journal of Cancer 41 (2005): 2438-2448.

Samalecos A, Gellersen B. "Systematic Expression Analysis and Antibody Screening Do Not Support the Existence of Naturally Occuring Progesterone Receptor (PR)-C, PR-M, or Other Truncated PR Isoforms." Endocrinology 149.11 (2008): 5872-5887.

Sasidharan R, Gerstein M. "Protein Fossils Live on as RNA." Genomics 435 (2008): 729-731.

Saville B, Wormke M, Wang F, Nguyen T, Enmark E, Kuiper G, Gustafsson JA, Safe S. "Ligand-, Cell-, and Estrogen Receptor Subtype (alpha/beta)-dependent Activation at GC-rich (Sp1) Promoter Elements." The Journal of Biological Chemistry 275.8 (2000): 5379-5387.

Schultz JR, Petz LN, Nardulli AM. "Estrogen Receptor α and Sp1 Regulate Progesterone Receptor Gene Expression." Molecular and Cellular Endocrinology 201 (2003): 165-175.

Schultz JR, Petz LN, Nardulli AM. "Cell- and Ligand-specific Regulation of Promoters Containing Activator Protein-1 and Sp1 Sites by Estrogen Receptors α and β." The Journal of Biological Chemistry 280.1 (2005): 347-354.

Schwartz JC, Younger ST, Nguyen NB, Hardy DB, Monia BP, Corey DR, Janowski BA. "Antisense Transcripts are Targets for Activating Small RNAs." Nature Structural & Molecular Biology 15.8 (2008): 842-848.

Seagroves TN, Lydon JP, Hovey RC, Vonderhaar BK, Rosen JM. "C/EBPBeta (CCAAT/Enhancer Binding Protein) Controls Cell Fate Determination During Mammary Gland Development." Molecular Endocrinology 14 (2000): 359-368.

Shaulian E, Karin M. "AP-1 as a Regulator of Cell Life and Death." Nature Cell Biology 4 (2002): E131-E136.

Shen Q, Zhang Y, Uray IP, Hill JL, Kim HT, Lu C, Young MR, Gunther EJ, Hilsenbeck SG, Chodosh LA, Colburn NH, Brown PH. "The AP-1 Transcription Factor Regulates Postnatal Mammary Gland Development." 295 (2006): 589-603.

Shyamala G, Schneider W, Schott D. "Developmental Regulation of Murine Mammary Progesterone Receptor Gene Expression." Endocrinology 126.6 (1990): 2882-2889.

Shyamala G, Yang X, Silberstein G, Barcellos-Hoff MH, Dale E. "Transgenic Mice Carrying an Imbalance in the Native Ratio of A to B Forms of Progesterone Receptor Exhibit Developmental Abnormalities in Mammary Glands." PNAS 95 (1998): 696-701.

Shyamala G, Louie SG, Camarillo IG, Talamantes F. "Minireview: The Progesterone Receptor and Its Isoforms in Mammary Development." Molecular Genetics and Metabolism 68 (1999): 182-190.

Shyamala G, Yang X, Cardiff RD, Dale E. "Impact of Progesterone Receptor on Cell-Fate Decisions During Mammary Gland Development." PNAS 97.7 (2000): 3044-3049.

Smith LM, Wise SC, Hendricks DT, Sabichi AL, Bos T, Reddy P, Brown PH, Birrer MJ. "c-Jun Overexpression in MCF-7 Breast Cancer Cells Produces a Tumorigenic, Invasive and Hormone Resistant Phenotype." Oncogene 18.44 (1999): 6063-6070.

Song Y, Song S, Zhang D, Zhang Y, Chen L, Qian L, Shi M, Zhao H, Jiang Z, Guo N. "An Association of a Similtaneous Nuclear and Cytoplasmic Localization of Fra-1 with Breast Malignancy." BMC Cancer 6 (2006): 298-304.

Soriano JV, Pepper MS, Orci L, Montesano R. "Roles of Hepatocyte Growth Factor/Scatter Factor and Transforming Growth Factor Beta in Mammary Gland Ductal Morphogenesis." Journal of Mammary Gland Biology and Neoplasia 3 (1998): 133-150.

Spidey [NCBI] 2008. "<http://www.ncbi.nlm.nih.gov/IEB/Research/Ostell/Spidey/>." (2008).

Sutherland RL, Prall OWJ, Watts CKW, Musgrove EA. "Estrogen and Progestin Regulation of Cell Cycle Progression." Journal of Mammary Gland Biology and Neoplasia 3.1 (1998): 63-72.

Takimoto GS, Tung L, Abdel-Hafiz H, Abel MG, Sartorius CA, Richer JK, Jacobsen BM, Bain DL, Horwitz KB. "Functional Properties of the N-Terminal Region of Progesterone Receptors and Their Mechanistic Relationship to Structure." The Journal of Steroid Biochemistry and Molecular Biology 85 (2003): 209-219.

Troyer KL, Lee DC. "Regulation of Mouse Mammary Gland Development and Tumorigenesis by the ERBB Signaling Network." Journal of Mammary Gland Biology and Neoplasia 6 (2001): 7-21.

Tung L, Abdel-Hafiz H, Shen T, Harvell DME, Nitao LK, Richer JK, Sartorius CA, Takimoto GS, and Horwitz KB. "Progesterone Receptors (PR)-B and -A Regulate Transcription by Different Mechanisms: AF-3 Exerts Regulatory Control over Coactivator Binding." Molecular Endocrinology (2006): 2656-2670.

Verde P, Casalino L, Talotta F, Yaniv M, Weitzman JB. "Deciphering AP-1 Functions in Tumorigenesis: Fra-ternizing on Target Promoters." Cell Cycle 6.21 (2007): 2632-2639.

Wei LL, Gonzalez-Aller C, Wood WM, Miller LA, Horwitz KB. "5'-Heterogeneity in Human Progesterone Receptor Transcripts Predicts a New Amino-Terminal Truncated "C"-Receptor and Unique A-Receptor Messages." Molecular Endocrinology 4 (1990): 1833-1840.

Werner A, Berdal A. "Natural Antisense Transcripts: Sound or Silence." Physiological Genomics 23 (2005): 125-131.

Werner A, Carlile M, SwanD. "What do Natural Antisense Transcripts Regulate?" RNA Biology (2009): 43-48.

Wiesen JF, Young P, Werb Z, Cunha GR. "Signaling Through the Stromal Epidermal Growth Factor Receptor is Nessary for Mammary Gland Development." Development 126 (1999): 335-344.

Williams G, Anderson E, Howell A, Watson R, Coyne J, Roberts SA, Potten CS. "Oral contraceptive (OCP) use increases proliferation and decreases oestrogen receptor content of epithelial cells in the normal human breast." International Journal of Cancer 48 (1991): 206-210.

Wood TL, Richert MM, Stull MA, Allar MA. "The Insulin-Like Growth Factors (IGFs) and IGF Binding Proteins in Postnatal Development of Murine Mammary Glands." Journal of Mammary Gland Biology and Neoplasia 5 (2000): 31-42.

Yazgan O, Krebs JE. "Noncoding But Nonexpendable: Transcriptional Regulation by Large Noncoding RNA in Eukaryotes." Biochemistry and Cell Biology 85 (2007): 484-494.

Younger ST, Corey DR. "The Puzzle of RNAs that Target Gene Promoters." ChemBioChem: A European Journal of Chemical Biology 10 (2009): 1135-1139.

CHAPTER 2

MATERIALS AND METHODS

MATERIALS AND METHODS

In Silico Analysis:

The RIKEN Fantom2/Fantom3 mouse databases were used for *cis*-sense/antisense pair analysis and to find cap analysis of gene expression (CAGE) tags, expressed sequence tags (ESTs) and RIKEN clones at the mouse progesterone receptor (Pgr) locus (Kawaji H); (Kiyosawa H); (Katayama S); (Carninci P). GenBank was also used to determine the mapped ESTs, mRNAs and presence or absence of a poly(A) tail (GenBank (NCBI)). Three of the transcripts contained evidence for polyadenylation in the UniGene entry and also when run through Polyadq, a polyadenlyation prediction program (Tabaska JE). Geneomatix MatInspector, a computer algorithm for predicting transcription factor binding sites, was used for both sense and antisense PR promoter prediction and analysis (MatInspector). The PR^{sense} and $PR^{antisense}$ transcripts were run through Genescanw to determine their coding potential (Burge C). Sequence analysis was based on build mm5 (2005) of the mouse genome and Fantom2/ Fantom 3 databases.

Primer Extension:

Primer extension was performed according to Sambrook and Russell (Sambrook J). Briefly, lower strand primers located at least 100 bp downstream of the predicted PRB and PRA start sites were [γ-32P] 5'-end labeled. Or, for the antisense PR promoter mapping, upper strand primers were located at least 100 bp upstream of the strongest cluster of CAGE tags and ESTs. For each reaction, 40 μg of virgin adult BALB/c mouse uterine total RNA was used from either ovary-intact or ovariectomized mice. RNA was isolated following the standard Trizol protocol

(Invitrogen, TRIZOL® Reagent). Additionally, virgin adult BALB/c mouse mammary gland and liver total RNA were used from ovary-intact and ovariectomized mice. Total RNA from 10 day pregnant BALB/c mammary gland was used for comparison to virgin adult mammary gland. Total yeast RNA was used as a negative control for each primer, 40 μg per reaction. The lower (or upper) strand primer was hybridized to the RNA and extended using reverse transcriptase. The RNA-DNA duplex was denatured and the products were run out on a 6% denaturing polyacrylamide gel. In parallel, a sequencing reaction was carried out using Sequenase™ Version 2.0 DNA sequencing Kit (United States Biochemical, Cleveland, OH) to create a size standard for each primer. Mouse long tandem PR plasmid DNA was used as a template in the sequencing reaction with the same primers as the primer extension reaction. The size of the primer extension products was compared to the sequencing ladder in order to accurately map the 5'-end of the PR message to a specific nucleotide position in the sequence.

Semi-Quantitative PCR:

Strand-specific cDNAs were prepared as follows: for the PRA + PRB cDNA, a lower strand primer in the 3'-untranslated region (UTR) of the progesterone receptor gene was used. For the antisense PR transcript, an upper strand primer located in the PR promoter at -146 bp was used. One primer set used for PCR was the ATG_B set located at +634 bp, the PRB start codon within exon 1 and detects either $PR^{(A)}$* and $PR^{(B)}$ transcripts as well as $PR^{antisense}$ transcripts (Table 2.1). The second primer set was the exon 4/5 primer set which spans intron 4 and is located in the common region of PR in the ligand binding domain. This primer set detects both $PR^{(A)}$ and $PR^{(B)}$, but does not detect $PR^{antisense}$ transcripts. The third primer set used was the

exon 1/2 set, which spans intron 1 and is located in the common region of PR (Table 2.1). This primer set detects detects both $PR^{(A)}$ and $PR^{(B)}$, but does not detect $PR^{antisense}$ transcripts that initiate within exon 1 (most cell lines and tissues examined had $PR^{antisense}$ message capsites within exon 1, but estradiol (E_2) or E_2+ progesterone (P) treated uterus may be an exception). PCR products were analyzed using standard gel electrophoresis of a 1.2% agarose gel. *Only PRA mRNAs with 5'-UTRs that extend upstream to +634 bp will be detected by the ATG_B primer set that spans from +634 to +1004 bp, while all PRB transcripts will be amplified.

a. Tissue Samples:

(i) Tissues were harvested from ovary-intact and ovariectomized female BALB/c virgin adult (18/19 week old) mice. The liver, uterus, and mammary glands were collected from the animals and flash frozen with liquid nitrogen. RNA was extracted using Trizol reagent (Invitrogen, TRIZOL® Reagent) following the standard Trizol protocol. Animal experiments were performed according to the accepted standards of humane animal care and were approved by the All University Committee on Animal Use and Care at Michigan State University.

(ii) BALB/c virgin adult (18-21 week old) mice were ovariectomized, then allowed to recover for 1 week. After recovery, the mice were treated subcutaneously with saline control, E_2, P, or E_2 + P for 5 days (1 µg E_2 per injection per day or 1 mg P per injection per day). Uterine, mammary gland, and liver tissues were extracted and flash frozen in liquid nitrogen. RNA was extracted following the Trizol protocol as explained above.

Primer	Location	Sequence	Strand
Distal 1 (D1): RMK 37 (+63 to +43 bp)	Distal PRB promoter	5’ TAGCAGAATGTCAGAATCCTC 3’	Reverse
D2: RMK 77 (+151 to +132 bp)	Distal PRB promoter	5’CTGCAGCGACAGTCTCTATG 3’	Reverse
D3: RMK 137 (+255 to +235 bp)	Distal PRB promoter	5’ CCGGACTTCTTATGTTTGTTG 3’	Reverse
Proximal 1 (P1): RMK 136 (+728 to +710 bp)	Proximal PRA promoter	5’ AAGCGTGCAAGCAAGGGGG 3’	Reverse
P2: RMK 44 (+769 to +751 bp)	Proximal PRA promoter	5’ ACACGTCCGAGTGCTGGCT 3’	Reverse
P3: RMK 138 (+863 to +845 bp)	Proximal PRA promoter	5’ TCCCCTGTCTTTCCGTCTG 3’	Reverse
Forward 1 (F1): RMK 54 (+1565 to + 1583 bp)	Antisense PR promoter	5’ CTCTGAACCACGCACTCCT 3’	Forward
F2: RMK 145 (+1771 to + 1790 bp)	Antisense PR promoter	5’ CAGACGCCTGGCTTGAAGAT 3’	Forward
F3: RMK 146 (+1861 to + 1881 bp)	Antisense PR promoter	5’ TCCTCCACCTTCCCAGACTTC 3’	Forward

Table 2.1: Primers used in the primer extension reactions to map the distal $PR^{(B)}$, proximal $PR^{(A)}$, and $PR^{antisense}$ transcription start sites.

b. Cell Lines:

The following mouse cell lines were used: MC7-L1, MC4-L2, MC4-L3, NMuMG, and UMD-208 (Table 2.3). The treatments were: 10^{-8} M E_2, 10^{-8} M R5020 (R), 10^{-8} M E_2 and 10^{-8} M R5020 or 10^{-8} M phorbol myristate acetate (PMA). Cells were grown in phenol red free medium with 5% charcoal stripped fetal bovine serum (CSS) (Table 2.3) and hormone treatments were administered for the final 24 hours prior to harvest.

Cell lines and Cell Culture:

Cells were cultured according to their standard growth conditions listed in Table 2.3. For experiments that utilized hormone or PMA treatments, the cells were cultured in the same media but the phenol red free version and were cultured in 5% charcoal stripped fetal bovine serum. Cells were plated in their standard media/serum conditions and then switched to phenol red free media prior to transfection and/or hormone treatments. Cells grown in DMEM for hormone treatments were cultured in phenol red free DMEM/glutamine free medium that was supplemented with 2 mM glutamine.

Plasmids:

The mouse sense PR promoter constructs were generated by PCR amplification of C57/Bl6 genomic mouse DNA using the appropriate primers (Table 2.4) and TA cloning to capture the PCR fragment in pCR2.1 vector (Invitrogen, TA Cloning Kit). The PR promoter fragments were excised using the appropriate restriction enzymes (Table 2.4) and ligated into pGL3Basic (pGL3B).

(a)

cDNA Primers	Location	Sequence	Strand	cDNA Synthesized
RMK 50 (+3432 to +3404 bp)	PR 3' UTR	5'TCACAAAGAAACAAAGAAAAGTCATCACT 3'	Reverse	PR^{sense}
RMK 57 (+2629 to +2610 bp)	Exon 4	5'AGGTGATTCTCTGGCTCAGG 3'	Reverse	PR^{sense}
RMK 76 (-146 to -126 bp)	PRB promoter/ near the 3' end of $PR^{antisense}$	5'AAGCATCTGATATTCCAGGTG 3'	Forward	$PR^{antisense}$
RMK 40 (+381 to +401 bp)	PRB 5' UTR/ near the 3' end of $PR^{antisense}$	5'GCTACTTCTTCCTGTCCTCAC 3'	Forward	$PR^{antisense}$

(b)

PCR Primer Pairs	Location	Sequence	PCR product size	Detects
RMK 64 (+634 to +655 bp)	ATG_B (Exon 1)	5'ATGACTGAGCTGCAGGCAAAGG 3'	369 bp	$PR^{(B)}$, $PR^{(A)}$ (long 5' UTR), $PR^{antisense}$
RMK 65 (+983 to +1004 bp)		5'CGGAGGGAGTCAACAACGAGTC 3'		
RMK 66 (+2560 to +2579 bp)	Exon 4/5	5'CGGTGTTGCTCTCCCCCAGT 3'	335 bp	$PR^{(B)}$, $PR^{(A)}$
RMK 67 (+2876 to +2895 bp)		5'CCCAGGCCAAACACCATCAG 3'		
RMK 56 (+2071 to +2088 bp)	Exon 1/2	5' GCCGCGTCCTGCCTACTA 3'	307 bp	$PR^{(B)}$, $PR^{(A)}$
RMK 87 (+2355 to + 2378 bp)		5'AAGAAGACCTTGCAGCTCCCACAG 3'		

<u>Table 2.2:</u> (a) The location and sequence of primers used for strand-specific cDNA synthesis.
(b) The location, sequence, product size and which PR transcripts are detected with PCR primer pairs using semi-quantitative analysis.

Cell line	Cell Type	Species	Culture Conditions	Source
Comma-D1	Mammary epithelial	Mouse	DMEM + 10% FBS + 1X Penicillin/Streptomycin + 5 mM HEPES + 5 ng/ml EGF + 10 µg/ml insulin	
L	Fibroblast	Mouse	Phenol red free DMEM/F12 (1:1) + 5% fetal bovine serum (FBS) + 1X Penicillin/Streptomycin + 5 mM HEPES	
MCF-7	Mammary epithelial carcinoma	Human	DMEM + 10% FBS + 1X Penicillin/Streptomycin + 5 mM HEPES	
MC7-L1	Mammary epithelial (MPA-induced carcinoma)	Mouse	Phenol red free DMEM/F12 (1:1) + 5% FBS + 1X Penicillin/Streptomycin + 5 mM HEPES	(Lanari C)
MC4-L2	Mammary epithelial (MPA-induced carcinoma)	Mouse	Phenol red free DMEM/F12 (1:1) + 5% FBS + 1X Penicillin/Streptomycin + 5 mM HEPES	(Lanari C)
MC4-L3	Mammary epithelial (MPA-induced carcinoma)	Mouse	Phenol red free DMEM/F12 (1:1) + 10% FBS + 1X Penicillin/Streptomycin + 5 mM HEPES	(Lanari C)
NMuMG	Mammary epithelial	Mouse	DMEM + 10% FBS + 1X Penicillin/Streptomycin + 4.5 g/L glucose + 10 µg/ml insulin	ATCC
UMD-208	Mammary epithelial (tamoxifen induced carcinomas in NRL-TGF-α mice)	Mouse	Phenol red free DMEM/F12 (1:1) + 5% FBS + 1X Penicillin/Streptomycin + 5 mM HEPES	Skildum A; (Rose-Hellekant TA)
U2-OS	Osteosarcoma	Human	McCoy's 5a Medium + 10% FBS + 1X Penicillin/Streptomycin + 1.5 mM glutamine + 2.2 g/L sodium bicarbonate	ATCC

Table 2.3: Cell culture standard growth conditions, species, cell type and source.

To generate the long PR tandem promoter (LTP) with ERE(4/5) cassette (LTP-ERE), the LTP construct was digested with Sal*I* downstream of the luciferase gene. Primers RMK 121 and 122 (Table 2.4) were used to amplify the ERE(4/5) region of PR using the PR cDNA plasmid as a template. These primers had Sal*I* sites on both ends and the PCR product was inserted into pCR2.1 using Topo TA cloning (Invitrogen, TA Cloning Kit). The ERE(4) and ERE(5) subclone was digested with Sal*I*, and the insert ligated into the linearized LTP plasmid. This cloning strategy allowed the ERE(4/5) enhancer cassette to be placed downstream of the PRB and PRA promoters as an enhancer/repressor cassette in approximately its endogenous distance without disrupting the reading frame of the PRB/luciferase region in the construct.

The antisense PR promoter was generated using primers RMK 147 and RMK 149 to PCR amplify the + 2241 bp to + 1909 bp region of mouse Pgr using genomic DNA from virgin adult BALB/c mice. The PCR primers contained flanking Hind*III* and Asp718 sites, respectively. Using TA cloning, the fragment was inserted into pCR2.1 (Invitrogen, TA Cloning Kit). Next, the 332 bp Asp718/Hind*III* fragment that spanned the 3' end of PR sense exon 1 was excised. The Asp718/Hind*III* insert was ligated into pGL3B vector (Figure 2.1).

The $PR^{antisense}$ cDNA was generated by using primers RMK 166 and RMK 167 to PCR amplify the +2144 bp to -981 bp region of mouse PR from genomic BALB/c DNA. Using TA cloning, the fragment was inserted into pCR2.1 (Invitrogen, TA Cloning Kit). Next, a 3125 bp Nhe*I*/Hind*III* fragment was excised that spanned PR sense exon 1 and the promoter region from +2144 bp to -981 bp. The Nhe*I*/Hind*III* insert was cloned into pcDNA3.1(+) expression vector driven by a cytomegalovirus (CMV) promoter (Figure 2.2).

In order to generate the progesterone response element (PRE)-thymidine kinase (TK) vector, the pERE-TK-luc vector was digested with BamH*I* and Hind*III*. This removed the ERE

cassette and linearized the vector. Oligonucleotides RMK 125 and RMK 126 (Table 2.7) were generated with a consensus PRE flanked by BamH*I* and Hind*III* restriction sites. The oligonucleotides were first annealed together and then ligated into the linearized pERE-TK-luc vector. This created the pPRE-TK-luc vector, which just has a single PRE. To generate the empty pGEM-TK-luc vector, the pERE- TK-luc vector was digested with Hind*III*, which cuts once on each side of the ERE cassette. The purified Hind*III* digested vector was ligated back together, eliminating the 21 bp ERE cassette and creating the pGEM-TK-luc vector.

Transient Transfections and Luciferase Assays:
a. Standard Transfection Conditions:

MCF-7 breast cancer cells were transiently transfected with firefly luciferase expression vectors driven by short distal promoter B (short DPB), long distal promoter PRB (long DPB), proximal promoter A (PPA), or long tandem PR promoter (contains both DPB and PPA; LTP) of the mouse progesterone receptor. Additional constructs included short tandem PR promoter (STP), the LTP with an ERE(4/5) enhancer cassette (LTP-ERE) and the antisense PR promoter. Fugene-6 reagent was used for cell transfections at a ratio of 3 parts FuGene-6 to 1 part of DNA.

In all experiments, the PR vectors were cotransfected with a renilla luciferase reporter construct (pRL-TK r- luc) as an internal normalization control. In some experiments, cells were cotransfected with an AP-1 isoform expression vector, Sp1 expression vector, or empty vector control (pCMV-4) (Table 2.6). The standard control vector for normalization between experiments was pGL3Basic (pGL3B), the vector backbone of the PR promoter constructs. Additional control vectors included: pGEM-TK and TK-luc, both of which are thymidine kinase-luciferase plasmids (Table 2.6). A total of 50 ng of AP-1 complex was cotransfected in the form of 50 ng of Jun isoforms (c-Jun, JunB or JunD) or alternatively 25 ng each of a Jun and a Fos

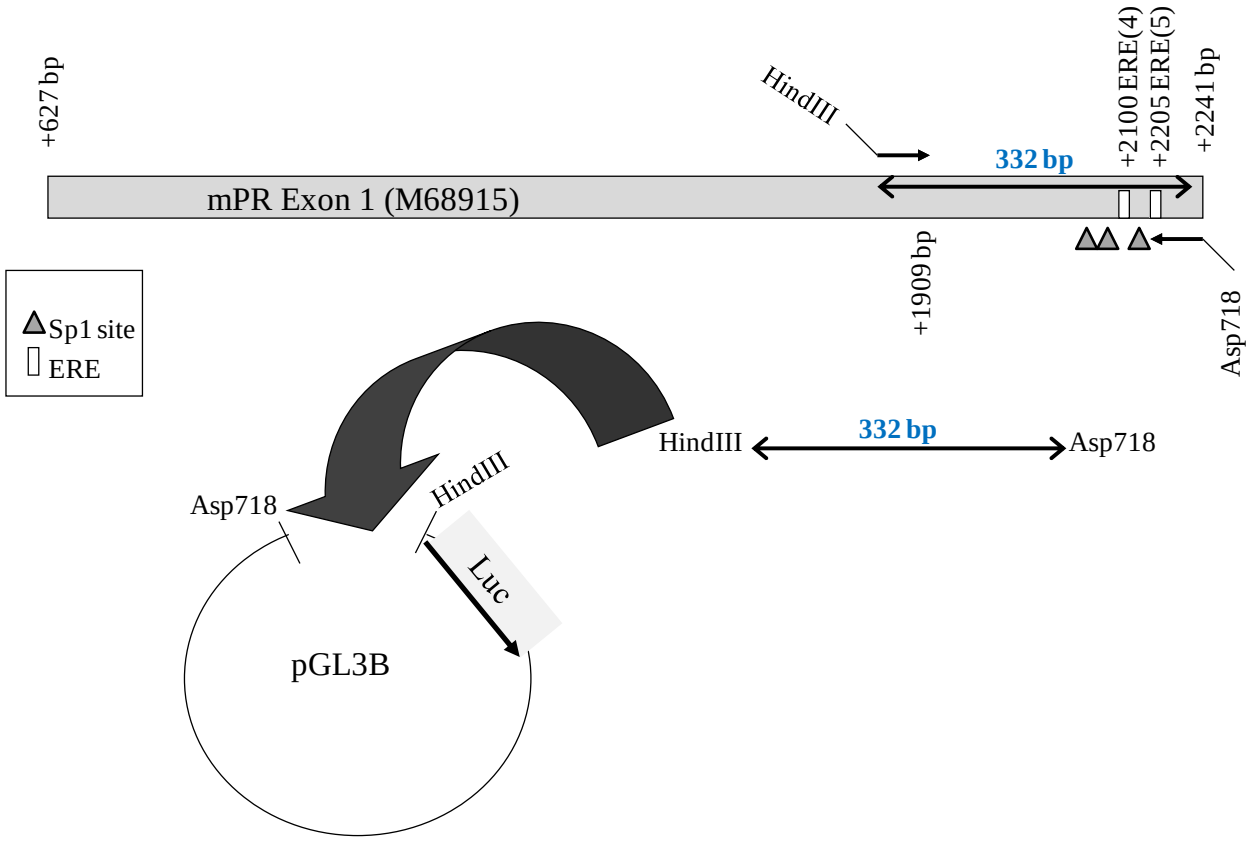

Figure 2.1: Construction of the PR antisense promoter construct. The region of the mouse Pgr gene used for making the antisense promoter insert spans from +2241 to +1909 bp (two-sided arrow) and is 332 bp in length. This insert was cut out of the cloning vector pCR2.1 and was inserted into the promoter-less pGL3B vector. The antisense promoter drives expression of the firefly luciferase gene.

isoform (c-Fos, Fra1, Fra2) (Table 2.6). For Sp1 experiments, 50 ng of the Sp1 expression vector (pcDNA3.1(+).Sp1) was cotransfected with the various PR promoter constructs and pcDNA3.1(+) was used as the matching empty vector control (Table 2.6). If applicable, treatments were: 10^{-8} M E_2, 10^{-8} M R5020, 10^{-8} M E_2+10^{-8} M R5020 or 10^{-8} M PMA. Treatments were given for the final 24 hours prior to harvest. Under hormone treatment conditions, the effect of hormone on the cells was internally monitored using a positive control for E_2 or P treatment. For E_2, control cells were transfected with an estrogen response element (ERE)-containing plasmid (pERE) and for P, control cells were transfected with a progesterone response element (PRE)-containing plasmid (pPRE) (Table 2.7). Similarly, for experiments utilizing PMA treatment, control cells were transfected with a 12-O-tetradecanoylphorbol 13-acetate (TPA)-response element (TRE)-containing plasmid. The two plasmids used were: Col 73-luc (collagenase 73-luciferase), which contains a single TRE and pAP-1-luc, which contains four consensus TREs (Table 2.6). After 48 hours, firefly and renilla luciferase activity was assayed in the cell lysates using the Promega Dual Glo Assay kit (Promega).

b. Antisense cDNA Titration on the Sense PR Promoter Constructs:

MCF-7 cells were transfected with a constant amount of the sense PR promoter reporter plasmids (PPA, short DPB, and LTP). An increasing amount of the $PR^{antisense}$ transcript, driven by a CMV promoter, was titrated into the cells (Table 2.8). One day after transfection, the PR promoter reporter luciferase activity was measured by the Dual Glo Luciferase Assay (see above) (Promega). Transfections were normalized to the renilla luciferase internal control (pRL-TK r-luc) and pGL3B empty vector.

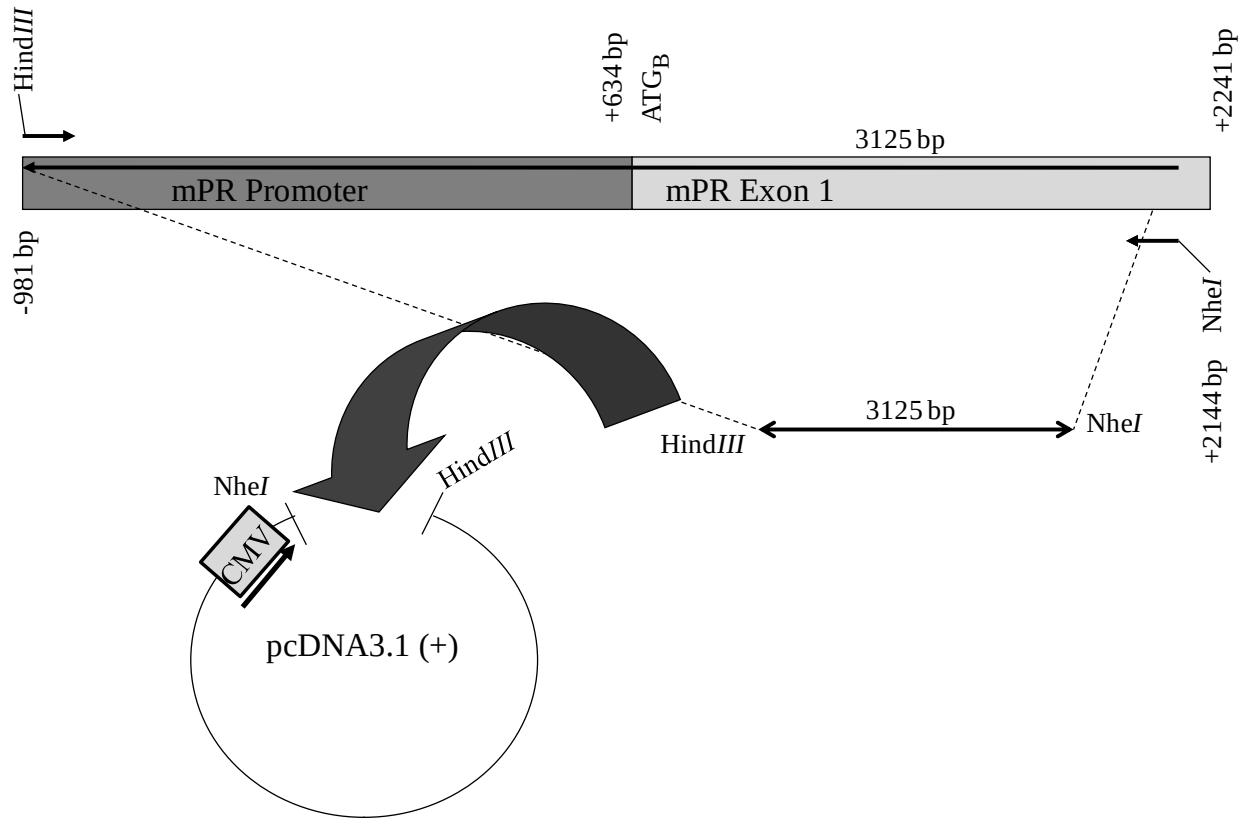

Figure 2.2: Construction of the PR^{antisense} cDNA construct. The region of the mouse Pgr gene used for making the PR^{antisense} cDNA insert spans from +2144 to -981 bp (two-sided arrow) and is 3125 bp in length. This insert was cut out of the cloning vector pCR2.1 and was inserted into pcDNA3.1(+) expression vector. A CMV promoter drives expression of the PR^{antisense} cDNA.

Plasmid	**Location in Pgr Gene**	**PCR primers or restriction sites used; notes**	**Source**
pGL3B.518 Short distal promoter B (Short DPB) 507 bp	-444 bp to +63 bp	**RMK 80** (-444 to -423 bp) 5' AGCACCTGCAACTTCACCTCTG 3' **RMK 37** (+43 to +63 bp) 5' TAGCAGAATGTCAGAATCCTC 3'	Flynn E
pGL3B. Long distal promoter B (Long DPB) 843 bp	-444 bp to +399 bp	**RMK 80** (-444 to -423 bp) 5' AGCACCTGCAACTTCACCTCTG 3' **RMK 111** (+399 to +379 bp) 5'GTGAGGACAGGAAGAAGTAGC 3'	Flynn E

Table 2.4: A list of progesterone receptor plasmids, their location within the Pgr gene, how they were constructed and the source of the plasmid.

Table 2.4 (Cont'd.)

Plasmid	Location in Pgr Gene	PCR primers or restriction sites used; notes	Source
pGL3B. Proximal promoter PRA (PPA)	+379 bp to +769 bp	**RMK 40** (+379 to +399 bp) 5' GCTACTTCTTCCTGTCCTCAC 3' **RMK 88** (+751 to +769 bp) 5'GCACGTCCGAGTGCTGGCT 3'	Flynn E
pGL3B.PR.15 Long Tandem PR promoter (LTP)	-2494 bp to +769 bp	**RMK 19** (-2502 to -2471) 5' ACATGGTACCAGCGTGTCACCTGG CACAGA 3' (with Asp718 site) **RMK 90** (+771 to +753 bp) 5'CTGTCCATGGACACGTCCGAGTG CTGGCT 3'(with Nco*I* site)	Flynn E
pGL3B. Short tandem PR promoter (STP)	-444 bp to +769 bp		Wang W
pGL3B.PR.15.ERE.K Tandem PR promoter + ERE(4/5) (LTP-ERE)	2494 bp to +769 bp and +2093 bp to +2238 bp	Tandem PR + (RMK 121 & RMK 122 cassette) **RMK 121** (+2093 to +2110 bp) 5'ATAGTCGACGGTACCCCGGGACA GCCTGC 3' **RMK 122** (+2238 to 2218 bp) 5'CTAGTCGACAAGGTATGGCGGGT AGACCTG 3'	Flynn E
mPR Antisense promoter	+2241 bp to +1909 bp	**RMK 147** (+1909 to +1927 bp) 5'GATCAAGCTTatcctccaggcccggagaa 3' (with Hind*III* site) **RMK 149** (+2218 to +2241 bp) 5'ACATGGTACCCTCAGGTAGTTGA GGTATGGCGGG 3' (with Asp718 site)	Flynn E
$mPR^{antisense}$ cDNA Expression vector	+2144 bp to -981 bp	**RMK 166** (-981 to -957 bp) 5'TCGTAAGCTTATCATATTACTCTC TCCCCTCCACA3'(with Hind*III* site) **RMK 167** (+2144 to +2126 bp) 5'GGATGCTAGCTGGTAGATGGCGG GTGCTG3'(with Nhe*I* site) Excised the 3125 bp Nhe*I*/Hind*III* fragment spanning PR sense exon 1 and the promoter region. Ligated into the Nhe*I*/Hind*III* MCS of pcDNA3.1(+).	Flynn E

Plasmid	Location in Pgr Gene	PCR primers or restriction sites used; notes	Source
pcDNA3.1(-) .mPRA.3 mPRA Expression vector	+994 bp to +3422 bp	Hinc*II*/EcoR*V* digested M68915 PR cDNA and ligated the fragment into the EcoR*V* site of pcDNA3.1(-). Lacks the PRB ATG B-upstream sequence region.	Durairaj S
pcDNA3.1(+). mPRB.II mPRB Expression vector	+627 bp to +3422 bp	M68915 PR cDNA with the PRA ATG mutated to GCG in pcDNA3. Moved into pcDNA3.1(+) as a Nhe*I*/Not*I* fragment.	Durairaj S; Flynn E
mPR cDNA.2 mPR cDNA Expression vector	+627 bp to +3422 bp	M68915 PR cDNA in pcDNA3.1(+)	(Schott DR)

Table 2.5: A list of progesterone receptor expression plasmids, their location within the Pgr gene, how they were constructed and the source of the plasmid.

Plasmid	Purpose	Source
pGL3B	pGL3Basic; Empty vector control; vector backbone for PR promoters	Promega; cat# E1751
pCR2.1	Cloning vector	Invitrogen; cat# K2020-20
pcDNA3.1(+)	Expression vector backbone; empty vector control	Invitrogen; cat# V790-20
pcDNA3.1(-)	Expression vector backbone; empty vector control	Invitrogen; cat# V795-20
pCMV-4	Cytomegalovirus promoter empty vector control	
pAP1-luc	4X AP-1-firefly luciferase	Clontech, cat# 631911
Col73-luc	Collagenase 73-firefly luciferase	
CMV.c-Jun	c-Jun expression vector	(McCabe LR)
CMV.JunB	JunB expression vector	(McCabe LR)
CMV.JunD	JunD expression vector	(McCabe LR)
CMV.c-Fos	c-Fos expression vector	(McCabe LR)
CMV.Fra-1	Fra-1 expression vector	(McCabe LR)
CMV.Fra-2	Fra-2 expression vector	(McCabe LR)
pcDNA3.1(+).Sp1	Human Sp1 expression vector	McCormick J
pRL-TK- renilla-luc	Thymidine kinase -renilla luciferase; transfection internal control	Promega; cat# E2241
pTK-luc	Herpes simplex virus thymidine kinase promoter driving constitutive luciferase expression (pUC 8 backbone)	
pBluescript II KS(+)	Vector backbone for riboprobes	Stratagene

Table 2.6: A list of miscellaneous plasmids, their purpose and the source of the plasmid.

Plasmid	Purpose	PCR primers or restriction sites used	Source
pGEM-TK-luc	Thymidine kinase- firefly luciferase empty vector control	pERE-TK-luc cut with Hind*III* to remove ERE cassette, then ligated back together	Flynn E
pERE-TK-luc	Estrogen response element-thymidine kinase-firefly luciferase vector	Xenopus vitellogenin A_2 ERE cloned into the Hind*III* site of tk109-luc, both in a pGEM-7Zf(+) vector backbone	(Gehm BD)
pPRE-TK-luc	Progesterone response element-thymidine kinase-firefly luciferase vector	**RMK 125** 5'gatccaagctcagatccaagcttaAGAACACAGTGTTCTta 3' **RMK 126** 5' agcttaAGAACACTGTGTTCTtaagcttggatctgagcttg 3'	Flynn E

Table 2.7: Construction of the pGEM-Thymidine Kinase transfection control vectors, their specific purpose and source.

PR Promoter Reporter (ng)	0	150	150	150	150	150	150
$PR^{antisense}$ cDNA (ng)	0	0	7.5	30	150	300	750
pCDNA3.1+ (ng)	900	750	742.5	720	600	450	0
Ratio (PR sense promoter: Antisense cDNA)	0:0	1:0	20:1	5:1	1:1	1:2	1:5
	pGL3B only	pCDNA3.1+ & promoter reporter					

Table 2.8: Antisense cDNA titration on the sense PR promoter constructs. A constant amount of PR promoter reporter was transfected into MCF-7cells. The $PR^{antisense}$ cDNA was titrated in from a 20:1 to 1:5 ratio (PR promoter reporter to $PR^{antisense}$). Empty vector pcDNA3.1(+) was cotransfected in to normalize the total amount of CMV plasmid at each concentration.

RNA *In Situ* Hybridization (ISH):

Using the mPR cDNA or LTP plasmids as templates, a 648 or 726 bp region of PR was amplified by PCR (Table 2.9) and inserted into pCR2.1 using Topo TA cloning (Invitrogen, TA Cloning Kit). The pCR2.1 subclones were digested with Xba*I* or Hind*III* and the 628 or 623 bp fragments were ligated into pBluescript II KS(+). Riboprobes for $PR^{(A+B)}$ and $PR^{antisense}$ (exon 1) were synthesized from a 628 bp cloned fragment of mouse PR exon 1 (+1130 to +1758 bp) in pBluescript II KS(+) (Figure 2.3). Riboprobes for $PR^{(B)}$ and $PR^{antisense}$ were synthesized from a 623 bp cloned fragment of mouse PR exon 1 (+3 to +626 bp) in pBluescript II KS(+) (Figure 2.4). Probes to detect both sense and antisense transcripts were labeled with digoxigenin (DIG) using *in vitro* transcription from Not*I* or Asp718 digested templates using T3 or T7 polymerase, respectively (Roche, DIG RNA Labeling Kit). Probes were visualized using nitroblue tetrazolium salt and 5-bromo-4-chloro-3-indolyl phosphate (NBT/BCIP) according to (Roche, DIG Nucleic Acid Detection Kit). ISH was performed according to (Silbertstein GB); (Roche, Non-radioactive In Situ Hybridization Application Mannual); (Roche, ISH Protocol for Detection of mRNA with DIG-labeled RNA Probes) with adaptations for adherent mammary cells (Singer Lab). Cells were counter stained with hematoxylin or nuclear fast red (Sigma) and mounted with Permount (Invitrogen) (hematoxylin staining) or Vectamount AQ (Vector Laboratories) (fast red staining). Slides were photographed using brightfield microscopy at 40X magnification. The cell lines used were: mouse L cells, UMD-208 and MC7-L1 cells (Table 2.3). Hormone treatments used were: 10^{-8} M E_2, 10^{-8} M R5020, 10^{-8} M E_2+10^{-8} M R5020 and were given for the final 24 hours prior to cell fixation.

There were three different positive controls used in these experiments. First, cells were transfected 24 hours before fixation using FuGene-6 transfection reagent to over-express the full

PCR Primer Pairs	Location	Sequence	Probe size	Detects
RMK 153 (+1130 to +1152 bp)	PR Exon 1 (+1130 to +1758 bp)	5'GGTCTCTAGAATGAGTCGGCCA GAGATCAAGGT 3' (with Xba*I* site)	628 bp	$PR^{(A+B)}$ $PR^{antisense}$
RMK 154 (+1758 to +1734 bp)		5'TCGTAAGCTTTAAAGAGGGAA CACGTCCTCTTTGG 3' (with Hind*III* site)		
RMK 155 (+607 to +626 bp)	PR promoter (+3 to +626 bp)	5'TCGTAAGCTTCAAGCTCCCCTT TTCTCCT 3' (with Hind*III* site)	623 bp	$PR^{(B)}$ $PR^{antisense}$
RMK 38 (-90 to -69 bp)		5' AGAGATTTAGATCTAGCCAGT G 3' (Cut with Xba*I*)		

Table 2.9: The name, location and sequence of PCR primer pairs used to amplify the *in situ* hybridization probes. The resulting probe size and detection target as listed as well.

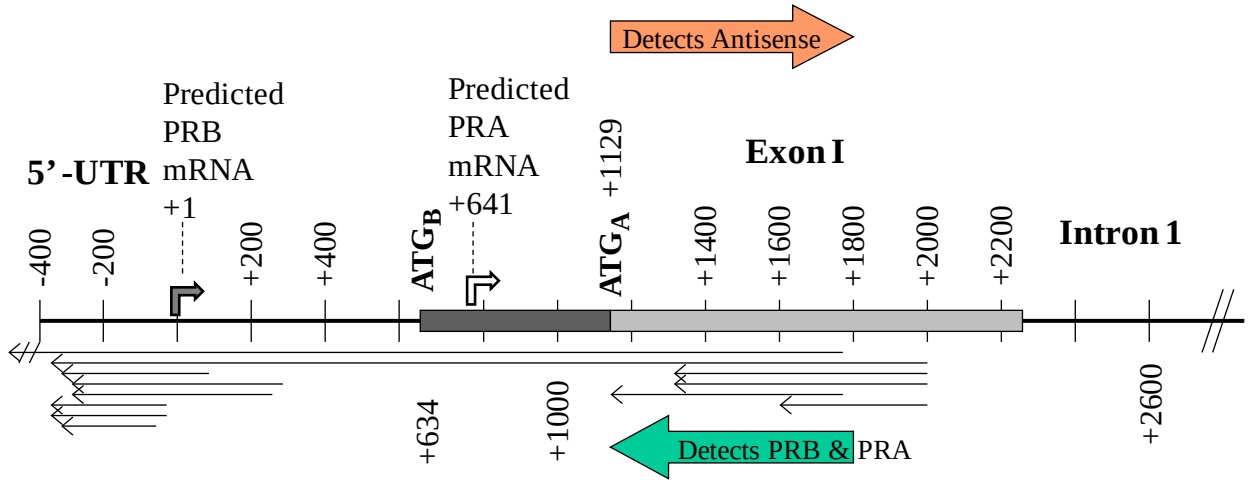

Figure 2.3: *In situ* hybridization probes to detect antisense transcript within exon 1 (salmon) and total PRA+B message (green). In black are the antisense ESTs and cDNAs of the mouse Pgr gene.

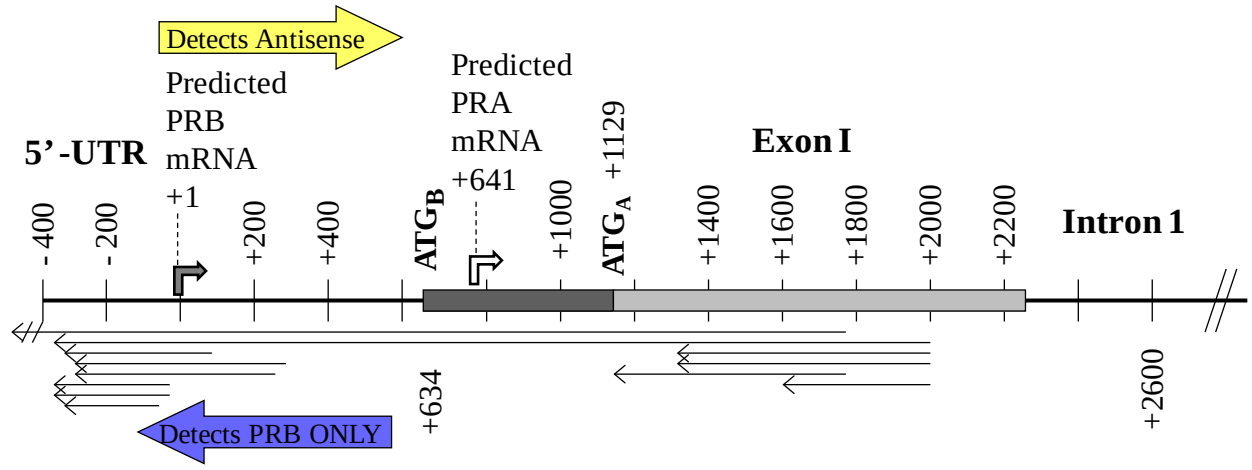

Figure 2.4: ***In situ*** **hybridization probes to detect internal antisense transcript (yellow) and total PR$^{(A+B)}$ message (blue).** In black are the antisense ESTs and cDNAs of the mouse Pgr gene.

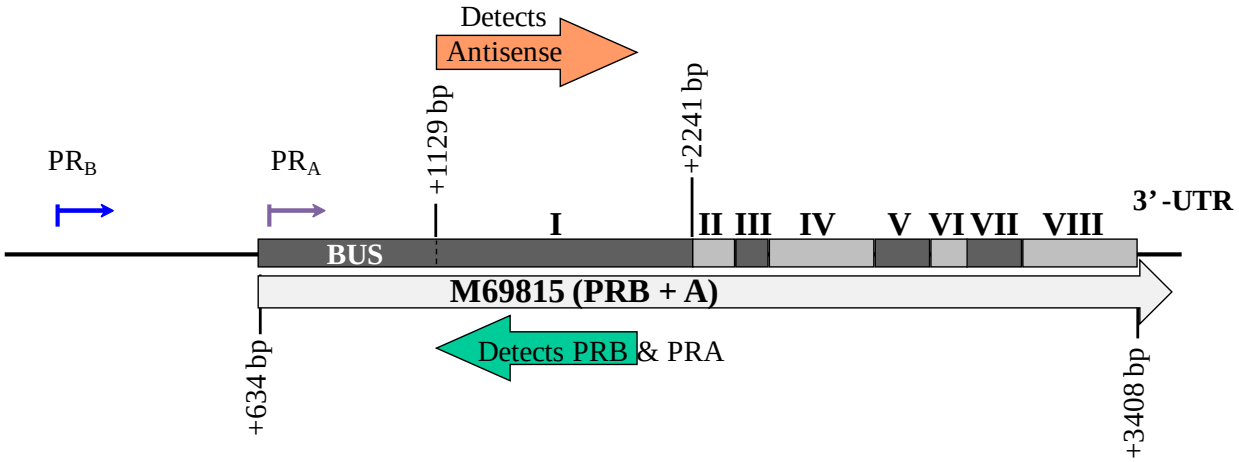

Figure 2.5: ***In situ*** **hybridization probes to detect antisense transcript within exon 1 (salmon) and total PR$^{(A+B)}$ message (green).** The PR cDNA expression vector (M69815) spans all eight exons of the mouse Pgr gene (shown above) and part of the 3'-untranslated region (UTR). The PR cDNA was transfected into cells as a positive control for the PRA+B probe.

length PR cDNA (mPR cDNA). The PR cDNA expression vector expresses both PRB and PRA (Schott DR). The other two positive controls consisted of cells transfected with the PRA or PRB expression vectors (pcDNA3.1(-).mPRA or pcDNA3.1(+).mPRB, respectively). Background staining is given by the negative control coverslips without probe and *in situ* hybridization/ staining of the PR-negative mouse L cell line.

RNA *In Situ* Hybridization Followed by Immunofluorescence (ISH/IF):

Three developmental stages of the female BALB/c mouse mammary gland were studied: pubertal (6 weeks), virgin adult (19 weeks), and pregnancy-like (age-matched 19 week old virgin adult treated for 14 days with E_2+P). The E_2+P treatment was given as a 7 day beeswax pellet implanted on days 1 and 8, containing 20 µg E_2 and 20 mg P. Mammary gland #4 was formalin fixed, paraffin-embedded and sectioned to 5 µm according to Aupperlee, *et* al. (Aupperlee M 2005). The sections were dewaxed in two changes of xylene followed by an ethanol series into water. Next, the sections were microwaved until they just reached boiling in 0.01 M sodium citrate buffer (pH 6) for antigen retrieval. Once cooled, sections were permeabilized with 20 µg/ml proteinase-K for 5 minutes at 37˚C. Sections were post-fixed in 4% paraformaldehyde for 5 minutes at 4˚C prior to hybridization. DIG labeled riboprobes were synthesized as explained above. Hybridization conditions were as listed above with fluorescent modifications to post-hybridization steps according to (Speel EJM); (Baskin DG). DIG probes were detected using a mouse anti-DIG-biotinylated primary antibody (Table 2.10), followed by streptavidin Alexa-488 (Molecular Probes, Eugene, OR) (Table 2.11). After adding the streptavidin, immunofluorescence detection of PRA protein was performed. Briefly, coverslips were washed in Tris-HCl/NaCl and then blocked in 2% PBSA. Tissues were incubated overnight at 4˚C in a

Primary Antibody	Using ICC, IF, ISH detects:	Species	Source	Catalog #	Dilution
α-DIG-AP (alkaline phosphatase)	DIG (digoxigenin)	Mouse monoclonal	Roche	11175041910	1:500
α-DIG-Biotin	DIG	Mouse monoclonal	Novus Biological	NB100-1879	1:500
hPRa7	mPRA	Mouse monoclonal	Neomarkers	MS-197-P	1:100 (fixed cells) 1:50 (tissue sections)
Zymed αPRA	mPRA	Mouse monoclonal	Zymed	18-0172	1:100
DAKO α-humanPR	mPRA, (weakly mPRB)	Rabbit polyclonal	DAKO	A0098	1:100
B15	mPRB	Rabbit polyclonal	(custom) Affinity BioReagents	A232001	1:800
c-Jun	c-Jun	Rabbit polyclonal	Santa Cruz Biotechnology	sc-1694	1:25
JunB	JunB	Rabbit polyclonal	Santa Cruz Biotechnology	sc-46	1:50
JunD	JunD	Rabbit polyclonal	Santa Cruz Biotechnology	sc-74	1:50
c-Fos	c-Fos	Rabbit polyclonal	Santa Cruz Biotechnology	sc-52	1:25
Fra-1	Fra-1	Rabbit polyclonal	Santa Cruz Biotechnology	sc-183	1:25
Total Jun (Pan Jun)	c-Jun, JunB, JunD	Rabbit Polyclonal	Santa Cruz Biotechnology	sc-44	1:50
BrdU	BrdU (5-bromo-2'-deoxyuridine)	Mouse Monoclonal	Amersham GE Healthcare	RPN202	Undiluted

Table 2.10: Primary antibodies used for *in situ* hybridization (ISH), immunofluorescence (IF) or immunocytochemistry (ICC).

rabbit polyclonal primary antibody that detects PRA (DAKO, anti-human PR #A0098; Carpinteria, CA) diluted 1:100 in 2% PBSA. The next day after washing with 1X-PBS/0.5% Triton X-100, coverslips were incubated with a goat anti-rabbit Alexa-546 secondary antibody (Molecular Probes). After a 1X PBS wash, the tissue sections were counterstained with DAPI and mounted using fluorescence mounting media (Aqua Poly/Mount; Polysciences, Inc.). Images were viewed using an inverted epifluorescence microscope. Metamorph software was used to capture and analyze the images.

Immunocytochemistry (ICC):

UMD-208, MC7-L1, and mouse L cells were grown on sterile polylysine coated coverslips in 6-well tissue culture-treated plates. The cells were transfected with pcDNA3.1(+) empty vector, the PR cDNA expression vector, a PRA expression vector, a PRB expression vector, or the $PR^{antisense}$ cDNA expression vector (Table 2.5) using FuGene-6 as above. If applicable, hormone treatments were: 10^{-8} M E_2, 10^{-8} M R5020, 10^{-8} M E_2+10^{-8} M R5020 for 24 hours prior to fixation. Depending on the experiment, the cells were either not treated/untransfected, transfected, hormone treated or both transfected and hormone treated. Prior to fixation, the cells were rinsed with 37˚C 1X PBS. Next, the cells were fixed in ice-cold methanol for 5 minutes, then permeabilized with ice-cold acetone for 1 minute. PRA and B protein expression levels were assayed for using fluorescence immunocytochemistry.

PRA staining was the same as above in the section entitled "Antisense cDNA Titration on PRA Protein". PRB staining was performed first by blocking non-specific binding with 2% PBSA for 30 minutes; no rinse. The cells were incubated overnight at 4˚C with a rabbit polyclonal primary antibody that specifically detects PRB (B15; Affinity BioReagents) diluted

Secondary Antibody/ Secondary Detection Reagent	**Source**	**Catalog #**	**Dilution**
Goat α-mouse Alexa-488	Molecular Probes	A11029	1:100 (ICC)
Goat α-mouse Alexa-546	Molecular Probes	A11030	1:200 (IF)
Goat α-rabbit Alexa-488	Molecular Probes	A11008	1:100 (ICC) 1:400 (IF)
Goat α-rabbit Alexa-546	Molecular Probes	A11035	1:400 (ISH) 1:400 (IF)
Streptavidin* Alexa-488	Molecular Probes	S11223	1:400 (ISH)

Table 2.11: Secondary antibodies or components used for *in situ* hybridization (ISH), immunofluorescence (IF) or immunocytochemistry (ICC). *Streptavidin Alexa-488 is a secondary component that binds to biotin (anti-biotin).

1:800 in 2% PBSA (Kariagina A). The next day, after washing with 2% PBSA, the cells were incubated with a goat anti-rabbit Alexa-488 secondary antibody. After a 1X PBS wash, the cells were counterstained with DAPI and mounted with fluorescence mounting media (Aqua Poly/Mount; Polysciences, Inc.). Slides were viewed using an inverted epifluorescence microscope, while images were captured and analyzed using Metamorph software.

Immunofluorescence (IF):
a. Developmental Mammary Gland Study:

Tissue samples were from three developmental stages of the female BALB/c mouse mammary gland: pubertal (6 weeks), virgin adult (19 weeks), and pregnancy-like (age-matched 19 week old virgin adult mice treated for 14 days with E_2+P). Mammary gland #4 was formalin fixed, paraffin-embedded and sectioned to 5 μm according to Aupperlee, *et* al. (Aupperlee M 2005). The second set of mammary glands #4 and 2/3 were processed as whole mounts as previously described (Banerjee MR). For paraffin blocks, sections were dewaxed in two changes of xylene followed by an ethanol series into ddH_2O. Antigen retrieval was carried out in a standard small autoclave in 0.01 M sodium citrate buffer (pH 6) for 20 minutes. After cooling, sections were washed in 1X PBS and then blocked in goat anti-mouse IgG Fab (diluted 1:100 in 1% PBSA) for 1 hour. Next sections were rinsed in 1X PBS and blocked in normal goat serum (diluted 1:1 in 1X PBS) for 30 minutes. The cells were incubated overnight at 4˚C with a primary antibody that specifically detects PRA (hPRa7; diluted 1:50 in 1X-PBS/0.5% Triton X-100). The next day, after washing with 1X-PBS/0.5% Triton X-100, the sections were incubated with a goat anti-mouse Alexa-546 secondary antibody. Tissue sections were rinsed with 1X PBS and then blocked with 10% goat serum/2% PBSA/0.1% Triton X-100; no rinse. Tissues were

incubated overnight at 4˚C in a primary antibody that specifically detects a single AP-1 isoform (c-Jun, JunB, JunD, c-Fos, Fra-1) or an antibody that detects all three Jun isoforms (total Jun) diluted in 1X PBS/0.5% Triton X-100 (all AP-1 antibodies Santa Cruz Biotechnology, Santa Cruz, CA). The next day after washing with 1X PBS, coverslips were incubated with a goat anti-rabbit Alexa-488 secondary antibody. After a 1X PBS wash, the tissue sections were counterstained with DAPI and mounted using fluorescence mounting media. Images were viewed using an inverted epifluorescence microscope. Metamorph software was used to capture, analyze and quantitate the images. Sections were quantitated for the number of cells that were positive for PRA only, PRA + AP-1, and AP-1 only per DAPI stained nuclei of epithelial cells. A minimum of 1000 luminal epithelial cells per structure-type (small ducts, large ducts, terminal end buds or lobules) were analyzed for each animal. There were 4-6 mice per developmental age group. The results are expressed as the mean ± SEM. Student's *t test* was used to analyze the data and results were significant if $p < 0.05$. Additionally, Fischer's exact test was used to determine the degree of colocalization between the AP-1 isoforms and PRA or PRB with PRA. If the colocalization was greater than expected by chance alone, then $p<0.05$ and the results were significant.

b. Hormone Treated Ovariectomized Virgin Adult Mice:

22 week old female virgin adult BALB/c mice were ovariectomized and allowed to recover for 1 week. Mice were treated subcutaneously with saline control, E_2 (1 µg/injection), P (1 mg/injection), or E_2+P (1 µg and 1 mg, respectively) for 3 days to determine the effect of hormones on the various AP-1 isoforms. Prior to sacrifice, mice were also treated with a 2 hour 5-bromo-2'-deoxyuridine (BrdU) pulse (70 µg/g of body weight). Mammary glands were

double-labeled with antibodies against PRA (hPRa7) and the AP-1 isoforms examined above (c-Jun, JunB, JunD, c-Fos, and Fra1). Additionally, sections were double-labeled with antibodies against BrdU and c-Jun or c-Fos to determine the correlation of c-Jun and c-Fos with proliferation. Staining for the AP-1 isoforms was performed as described above for day 1, followed by BrdU staining on day 2. After incubating in goat anti-rabbit Alexa 488 secondary antibody, sections were washed in 1X PBS and then blocked in goat anti-mouse IgG Fab diluted 1:100 in 1% PBSA for 1 hour. Next sections were rinsed in 1X PBS and blocked in normal goat serum diluted 1:1 in 1X PBS for 30 minutes; no rinse. Sections were incubated for 1 hour with freshly prepared undiluted mouse monoclonal anti-BrdU antibody (Amersham GE Healthcare) at room temperature. After a 1X PBS-0.5% Triton X-100 wash, sections were incubated with goat anti-mouse Alexa-546 secondary antibody (Molecular Probes). Finally, the tissue sections were counterstained with DAPI and mounted using fluorescence mounting media. Image capture and analysis was performed as described above. Sections were quantitated for the number of cells that were positive for PRA only, PRA + AP-1, and AP-1 only per DAPI stained nuclei of luminal epithelial cells. Additionally, sections were quantitated for the number of cells that were positive for BrdU only, AP-1 + BrdU, and AP-1 only for c-Jun and c-Fos staining experiments. A minimum of 500 luminal epithelial cells per structure-type (small and large ducts) were analyzed for each animal. There were 3-4 mice per hormone treatment group. The results are expressed as the mean ± SEM. Student's *t test* was used to analyze the data and results were significant if $p < 0.05$. For bar graphs, results are indicated * if hormone treatment was significantly different compared to control. Additionally, Fischer's exact test was used to determine the degree of colocalization between the AP-1 isoforms and PRA or AP-1 with BrdU. If the colocalization was greater than expected by chance alone, then $p<0.05$ and the results were significant.

REFERENCES

REFERENCES

Aupperlee M 2005, Smith KT, Kariagina A, Haslam SZ. "Progesterone Receptor Isoforms A and B: Temporal and Spatial Differences in Expression during Murine Mammary Gland Development." Endocrinology 146.8 (2005): 3577-3588.

Banerjee MR, Wood BG, Lin FK, Crump LR. "Organ Culture of Whole Mammary Gland of the Mouse." Tissue Culture Association Manual 1976: 457-462.

Baskin DG. "In Situ Hybridization Using Antibody-Based Methods." 2008. 2009.

Burge C. Stanford University GeneScan. 2005. <http://genes.mit.edu/GENSCAN.html>.

Carninci P, et al. (The FANTOM Consortium and RIKEN Genome Exploration Research Group and Genome Science Group [Genome Network Project Core Group]). "The Transcriptional Landscape of the Mammalian Genome." Science 309 (2005): 1559-1563.

Gehm BD, McAndrews JM, Chien PY, Jameson JL. "Resveratrol, a Polyphenolic Compound Found in Grapes and Wine is an Agonist for the Estrogen Receptor." PNAS 94 (1997): 14138-14143.

GenBank (NCBI). GenBank. <http://www.ncbi.nlm.nih.gov/Genbank/>.

Invitrogen. 2004. TA Cloning Kit. <http://tools.invitrogen.com/content/sfs/manuals/ta_man.pdf>.

Invitrogen. "TRIZOL® Reagent." 2005. Invitrogen. <http://tools.invitrogen.com/content/sfs/manuals/15596018%20pps%20Trizol%20Reagent%20061207.pdf>.

Kariagina A, Aupperlee MD, Haslam SZ. "Progesterone Receptor Isoforms and Proliferation in the Rat Mammary Gland during Development." Endocrinology 148.6 (2007): 2723–2736.

Katayama S, Tomaru Y, Kasukawa T, Wak Ki, Nakanish M, Nakamura M, Nishida H, Yap CC, Suzuki M, Kawai J, Suzuki H (RIKEN Genome Exploration Research Group and Genome Science Group (Genome Network Project Core Group) and the FANTOM Consortium). "Antisense Transcription in the Mammalian Transcriptome." Science 309 (2005): 1564-1566.

Kawaji H, Kasukawa T, Fukuda S, Katayama S, Kai C, Kawai J, Carninci P, Hayashizaki Y. "CAGE Basic/Analysis Databases: The CAGE Resourse for Comprehensive Promoter Analysis." Nucleic Acids Research 34 (2006): 632-636.

Kiyosawa H, Yamanaka I, Osato N, Kondo S, RIKEN GER Group and GSL Members, Hayashizaki Y. "Antisense Transcripts With FANTOM2 Clone Set and Their Implications for Gene Regulation." Genome Research 13 (2003): 1324-1334.

Lanari C, Luthy I, Lamb CA, Fabris V, Pagano E, Helguero LA, Sanjuan N, Merani S, Molinolo AA. "Five Novel Hormone-responsive Cell Lines Derived from Murine Mammary Ductal Carcinomas: In Vivo and in Vitro Effects if Estrogens and Progestins." Cancer Research 61 (2001): 293-302.

MatInspector. Genomatix MatInspector. 2005. <http://www.genomatix.de/cgi-bin/sessions/login.pl?s=5fea7747b00c3b1638b142a04b37e562>.

McCabe LR, Banerjee C, Kundu R, Harrison RJ, Dobner PR, Stein JL, Lian JB, Stein GS. "Developmental Expression and Activities of Specific Fos and Jun Proteins are Functionally Related to Osteoblast Maturation: Role of Fra-2 and Jun D During Differentiation." Endocrinology 137.10 (1996): 4398-4408.

Promega. "Dual Glo Luciferase Assay System." 2003. Part# TM058. <http://www.promega.com/tbs/tm058/tm058.pdf>.

Roche. "DIG Nucleic Acid Detection Kit ." 2005. Cat# 11175041910.

Roche. "DIG RNA Labeling Kit." 2005. Cat# 11175025910.

Roche. "ISH Protocol for Detection of mRNA with DIG-labeled RNA Probes ." <https://www.roche-applied-science.com/PROD_INF/MANUALS/InSitu/pdf/ISH_149-163.pdf>.

Roche. "Non-radioactive In Situ Hybridization Application Mannual." 2007 <https://www.roche-applied-science.com/PROD_INF/MANUALS/InSitu/InSi_toc.htm>.

Rose-Hellekant TA, Schroder MD, Brockman JL, Zhdankin O, Bolstad R, Chen KS, Gould MN, Schuler LA, Sangren EP. "Estrogen Receptor-Positive Mammary Tumorigenesis in TGFalpha Transgenic Mice Progresses with Progesterone Receptor Loss." Oncogene 26 (2007): 5238-5246.

Sambrook J, Russell DW. "Molecular Cloning: A Laboratory Manual." 3rd. Vol. 1. Cold Spring Harbor: Cold Spring Harbor Laboratory Press, 2001. 7.75-7.94.

Schott DR, Shyamala G, Schnneider W, Parry G. "Molecular Cloning, Sequence Analyses, and Expression of Complementary DNA Encoding Murine Progesterone Receptor." Biochemistry 30 (1991): 7014-7011.

Silbertstein GB, Van Horn K, Shyamala G, Daniel CW. "Progesterone Receptors in the Mouse Mammary Duct: Distribution and Developmental Regulation." Cell Growth & Differentiation 7 (1996): 945-952.

Singer Lab. "In Situ Hybridization of Mammalian Cells." 1998. 2008 <http://singerlab.aecom.yu.edu/protocols/insitu_mammalian.htm>.

Speel EJM, Hopman AHN, Komminoth P. "Tyramide Signal Amplification for DNA and mRNA In Situ." Methods in Molecular Biology: In Situ Hybridization Protocols. Ed. Hewitson TD Darby IA. 3rd. Vol. 326. Totowa: Humana Press Inc., 2006. 33-60.

Tabaska JE, Zhang MQ. "Detection of Polyadenylation Signals in Human DNA Sequences." Gene 1999: 77 - 86.

Vector Laboratories. Cat# H-5501, n.d.

CHAPTER 3

REGULATION OF THE PROGESTERONE RECEPTOR IN THE MOUSE MAMMARY GLAND

ABSTRACT

The mouse progesterone receptor exists in two isoforms, PRB and PRA, encoded by a single gene and driven by distal and proximal promoters, respectively. PR proteins have differing functions in the mouse mammary gland and show spatial and temporal separation of expression. Since PRA and PRB colocalized only in a subset of cells and respond differently to hormones, this suggests that the proximal and distal promoters may be under independent transcriptional control. Expression of the mouse progesterone receptor (Pgr) gene is regulated not just by estrogen (E_2) and progesterone (P), but also by growth regulatory pathways that signal through activating protein-1 (AP-1) and other transcription factors. We therefore examined the effect of steroid hormones and co-expression of Jun and Fos subunits on the activity of the mouse PR promoters and on their respective mRNA transcripts. Immunofluorescence analysis with isoform-specific antibodies was used to examine the correlation of AP-1 with PR expression across development in ovary-intact mice and after hormone treatment in ovariectomized mice. The underlying hypothesis for this specific aim is that a change in the composition of AP-1 subunits is, at least in part, responsible for the shift from PRA to PRB expression during alveologenesis, perhaps due to differential regulation of the two promoters. Expression of the various AP-1 isoforms was seen to vary across key stages of mouse mammary gland development as did their colocalization with PRA. As expected, c-Jun expression was high across development, but unexpectedly, Fra1, rather than c-Fos, was the predominant Fos isoform expressed. In luminal epithelial cells, PRA colocalizes highly with c-Jun and Fra1 in all structures during development, as well as with JunB and JunD to a lesser extent. The greatest degree of co-correlation was seen in the pregnancy-like mammary gland,

where 9-12% of luminal epithelial cells which co-express PRA with PRB also appear to express c-Jun/Fra1 AP-1. This suggests that c-Jun and Fra1 contribute to the maintenance of PRA expression during pregnancy and that these transcription factors may represent useful lineage markers for a specialized subset of luminal epithelial cells in the pregnant mouse mammary gland. Staining with an antibody to detect all of the Jun isoforms (pan Jun) revealed that PRA-positive cells invariably expressed one or another Jun isoform, suggesting that Jun supports efficient PRA expression. Taken together, these observations indicate that AP-1 is not the sole deciding factor that governs expression of either PRA or PRB, although it is probably a significant contributing factor for both.

In ovariectomized mice, c-Fos was not expressed, but was up-regulated by treatment for 3 days with E_2, P, or E_2+P. c-Jun was moderately expressed in control ovariectomized mice and was slightly up-regulated by E_2, P, or E_2+P treatment, defining a positive regulatory loop involving mutual reinforcement of PRA expression by c-Jun and c-Fos and vice versa, mediated by the ovarian steroids, P and E_2. Colocalization of AP-1 with a proliferation marker (BrdU) showed moderate c-Jun but no c-Fos expression in ovariectomized mice, along with a complete lack of proliferation in luminal epithelial cells. Despite sufficient c-Jun and c-Fos in mice treated for 3 days with E_2 only, BrdU staining indicates that the mammary epithelium remained proliferatively quiescent under these conditions. Luminal epithelial cells in ovariectomized mice do not appear to be capable of proliferating until treatment with P or E_2+P, conditions which are thought to alter the expression or phosphorylation of many cell cycle regulatory proteins including AP-1 itself. Overall, Jun proteins appear important in up-regulating efficient PRA expression, especially in the pregnancy-like gland; however, AP-1 expression is insufficient to

fully account for the large increase in PRB expressing cells after treatment for 14 days with E_2+P. Therefore, a pregnancy-specific transcription factor other than AP-1 must be responsible for promoting PRB expression in the hormonal environment of pregnancy.

INTRODUCTION

We have previously proposed a "two promoter model" to explain how a single Pgr gene gives rise to discrete patterns of PRA and PRB isoform expression that vary as a function of mammary development and hormonal exposure, based on evidence reported for the human and rat PGR genes describing a PRA (proximal) promoter and a separate PRB (distal) promoter (Kastner P 1990); (Kraus WL 1993). In contrast to the human and rat systems where PRA and PRB colocalize in a majority of PR^+ cells, isoform expression in the mouse mammary gland is spatially and temporally separated, with a subset of luminal epithelial cells expressing PRA in the immature and adult glands, followed by reduced expression of PRA and the appearance of PRB in developing lobules (Aupperlee M 2005a); (Aupperlee M 2005b). In brief, we have proposed a model in which the proximal promoter, capable of supporting expression of only the shorter PRA isoform, is active predominantly in the pubertal mammary gland, when the basic architecture of the ductal tree is established by a combination of steroid- and growth factor-driven ductal elongation and side-branching (Aupperlee M 2005a); (Hovey RC 2002). PRB expression, may depend upon *de novo* activation of a second set of transcripts arising within a distal promoter further upstream. Since PRB is restricted to luminal cells of lobules and ducts in mid- to late-pregnancy, its appearance seems to require a developmental program that is initiated by the combined effects of estradiol (E_2) and progesterone (P) in the hormonal environment of pregnancy (Aupperlee M 2005a). Since PRA and PRB protein only colocalize in a subset of cells and respond differently to hormones (Aupperlee M 2005a); (Aupperlee M 2005b), this

further suggests that the proximal and distal promoters of the mouse Pgr gene are, at least to some extent, under independent transcriptional control.

Precedent for this type of organization comes from analysis of the human and rat progesterone receptor (PGR) genes. In humans and rats, the PGR gene contains a tandem arrangement of two promoters, which give rise to transcripts encoding the two major PR isoforms, PRB and PRA (Kastner P 1990); (Schott DR 1991). Immunohistochemical (IHC) analysis in the human mammary gland revealed that the progesterone receptor proteins PRA and PRB are expressed at an equal ratio and show uniform colocalization (Aupperlee M 2005a). Therefore, studies looking at PR function in human mammary gland cells and tissues would have to consider three species of protein dimmers: AA, BB and AB. The mouse represents a unique situation in which the majority of endogenous PR is only involved in homodimers since PRA and PRB colocalize only in a subset of PRB^{+} cells (Aupperlee M 2005a). For these reasons, since PR proteins are both spatially and temporally separated (Aupperlee M 2005a), the mouse is an ideal system to study the isolated PR isoforms during mammary gland development.

We hypothesized that differential regulation of PR isoform expression occurs at a transcriptional level and that there are independent mechanisms to regulate the distal and proximal promoters. Two of the transcription factors thought to be important in regulating PR expression are the estrogen receptor (ER) and activating protein-1 (AP-1). In the rat and human species, PR is regulated by E_2 treatment and several estrogen response elements (EREs) have been characterized in the promoter region of these genes (Kraus WL 1994). Of the five EREs found in the rat Pgr gene, all five EREs are present in the mouse sequence with slight deviations from the optimal consensus sequence (Kraus WL 1994), but analysis of the mouse EREs has not been carried out at a functional level. It has also been shown that AP-1, especially the c-Jun/

c-Fos heterodimer, plays an important role in up-regulating human PR via binding to an AP-1 site (+90 bp) overlapping the PRB transcription start site in the presence of E_2 and ERα (Petz LN 2002). Conversely, c-Jun/c-Fos binding to a similar AP-1 site (+745 bp) overlapping the PRA start site are involved in down-regulating human PR in the presence of E_2 and ERα (Petz LN 2004a). c-Jun is associated with the +745 AP-1 site both in the presence and absence of E_2, which may account for the low basal level of PR seen in MCF-7 cells (Petz LN 2004a). For human PR, therefore, differential Jun/Fos isoform usage at the +745 AP-1 site may lead to activation or repression of PR transcription depending on the hormonal environment. Conversely, the +90 bp AP-1 site appears to only be involved in activating PR transcription, which can then presumably increase the level of $PR^{(B)}$ transcripts. Unfortunately, AP-1 subunits other than c-Jun/c-Fos were not examined in the above studies on human PR.

In this study, transcriptional regulation of the mouse PR by AP-1 isoforms and other transcription factor(s) were examined in an effort to establish spatial and temporal correlations in expression patterns across development, or in response to changes in hormonal exposure. This may allow for a better understanding of the observed changes in expression patterns of PR protein isoforms that occur during mammary gland development in the mouse. Overall, the goal of this project is to analyze the transcriptional regulation of the mouse progesterone receptor gene to determine the molecular basis for its differential regulation.

RESULTS

1. Regulation of PR Isoform Expression in Mouse and Human Mammary Epithelial Cells: Validation of Reporter Assays, Identification of Promoter Elements and Signaling pathways Responsible for Modulating PR Expression and Differentially Regulating PR Isoform Expression

a. Activating Protein-1

To help understand the role of the AP-1 proteins in regulating the mouse PR promoter, Jun and Fos isoform expression vectors were cotransfected with mouse PR promoter constructs. Additionally, we sought to determine if differential AP-1 isoform usage would lead to differing transcriptional activities for the mouse PRA and PRB promoters. Cotransfections were performed in the ER^+/PR^+ human mammary tumor cell line MCF-7 in which a PMA effect was initially observed. Different lengths of the mouse PR promoter driving expression of the firefly luciferase gene were used to separate the distal (PRB) and proximal (PRA) promoters. The long tandem promoter (LTP) combines the proximal promoter A (PPA) and long distal promoter B (long DPB) constructs and contains 2050 bp of additional 5' promoter sequence (Figure 3.1).

The sense PR promoters were all induced by c-Jun alone or c-Jun/c-Fos (Figure 3.2). The LTP was induced similarly by c-Jun alone (2.60) or c-Jun with any Fos family member (c-Jun/c-Fos 2.66 fold; c-Jun/Fra1 2.90 fold; c-Jun/Fra2 3.00 fold) (Figure 3.2). Although its basal level of transcriptional activity was very low, the short tandem promoter (STP) was still induced to a comparable magnitude as the LTP with c-Jun alone (2.83 fold), c-Jun/c-Fos (1.74 fold), and c-Jun/Fra1 (2.31 fold). Activation of STP with c-Jun/Fra2 (1.51 fold) was significantly lower than activation of LTP construct (3.00 fold) at the $p<0.05$ level. The short DPB was also comparable to the LTP when activated by c-Jun alone (2.89 fold), c-Jun/c-Fos

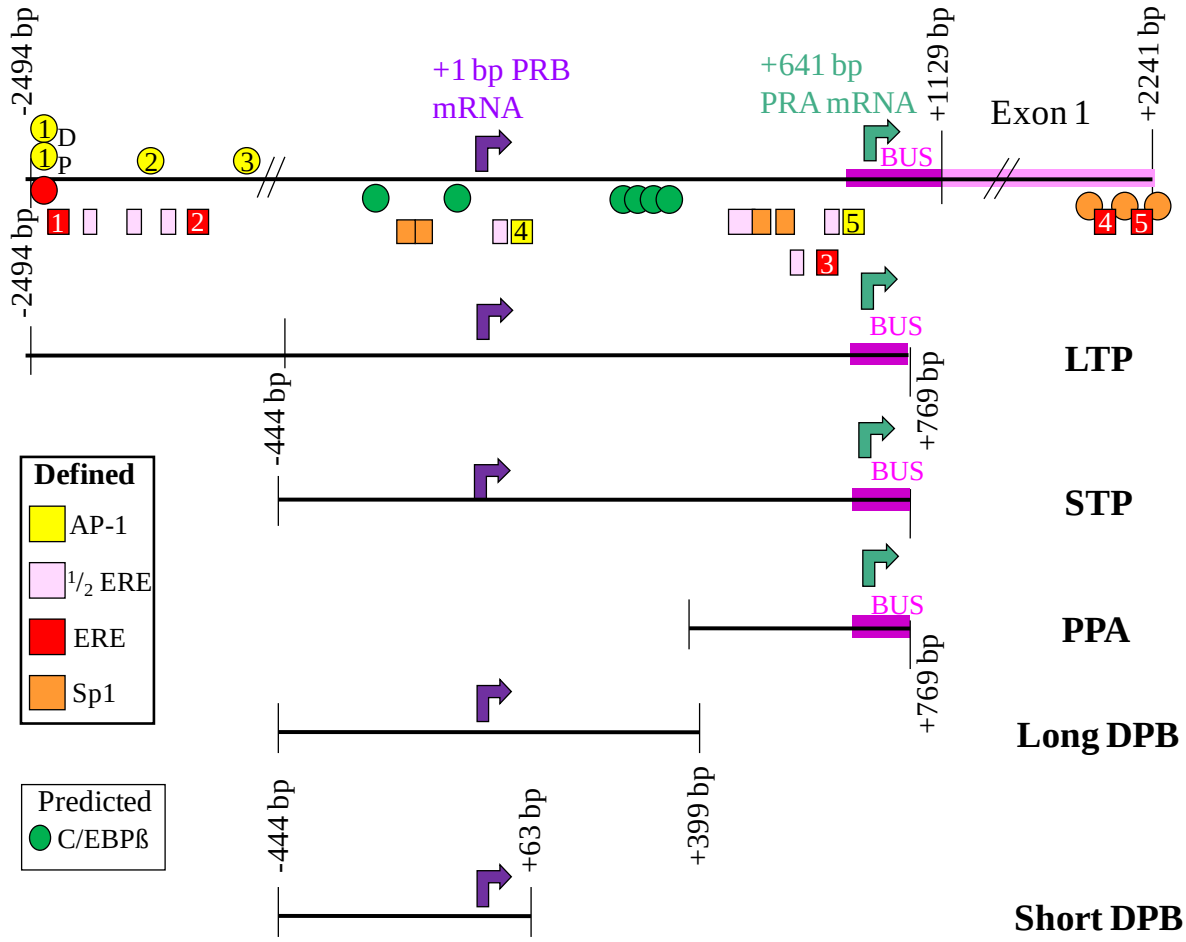

Figure 3.1: Mouse Pgr locus constructs: Long tandem PR promoter (LTP), short tandem PR promoter (STP), proximal promoter A (PPA), as well as long (843 bp) and short (507 bp) distal promoter B (DBP). Additionally, an estrogen response element (ERE) cassette of EREs 4 and 5 was added as an enhancer to the long tandem promoter construct (LTP-ERE) (not shown). All plasmids are promoter-reporter firefly luciferase constructs. Defined transcription factor binding sites are indicated as squares, while Genomatix MatInspector predicted sites are shown as circles (MatInspector 2005).

(2.85 fold), c-Jun/Fra1 (3.45 fold) and c-Jun/Fra2 (2.51 fold). The PPA was similar to the LTP and short DPB constructs with a 2.76 fold induction by c-Jun alone and 1.99 fold with c-Jun/c-Fos (Figure 3.2). Results with cotransfected c-Jun/Fra1 or c-Jun/Fra2 did not significantly differ from c-Jun/c-Fos or c-Jun alone (Figure 3.2), suggesting that the majority of the AP-1 effect was mediated by c-Jun rather than heterodimerization with a Fos partner or due to endogenous AP-1 proteins.

A region upstream of the distal PRB promoter appears to contain an AP1-dependent transcriptional enhancer based on its ability to stimulate promoter activity in response to PMA treatment or AP-1 cotransfection (Figures 3.1, 3.2). Truncation of the LTP at -444 bp removes 2050 bp of the 5'-end and gives rise to the STP (Figure 3.1). The basal transcriptional activity of the STP construct was lower than the activity of the LTP. The STP construct was induced 2.83 fold by c-Jun but only 1.74 fold by c-Jun/c-Fos (Figure 3.2). The LTP construct was similarly induced 2.60 fold by c-Jun and 2.66 fold by c-Jun/c-Fos. Increased reporter gene activity of the LTP construct compared to the truncated STP depended on activation of AP-1, either by treatment of transfected cells with PMA (see Figure 3.6) or cotransfection with c-Jun/c-Fos (Figure 3.2). Several copies of the AP-1 consensus sequence (TGAGTCA) are present in the -2494/-444 bp region of the PR promoter (Figure 3.1).

JunB alone or with any Fos member did not significantly induce or repress the STP, PPA, or short DPB constructs (Figure 3.3). The LTP appeared to be induced by JunB or JunB plus any Fos partner, but was only significantly induced by JunB/Fra1 (2.36 fold) and JunB/Fra2 (2.01 fold) (Figure 3.3). Unlike c-Jun, JunB was only apparently able to activate the LTP, presumably through synergism between the 2 defined and 4 putative AP-1 sites. JunD by itself weakly, but significantly, induced the LTP and the short DPB constructs (Figure 3.4). JunD plus

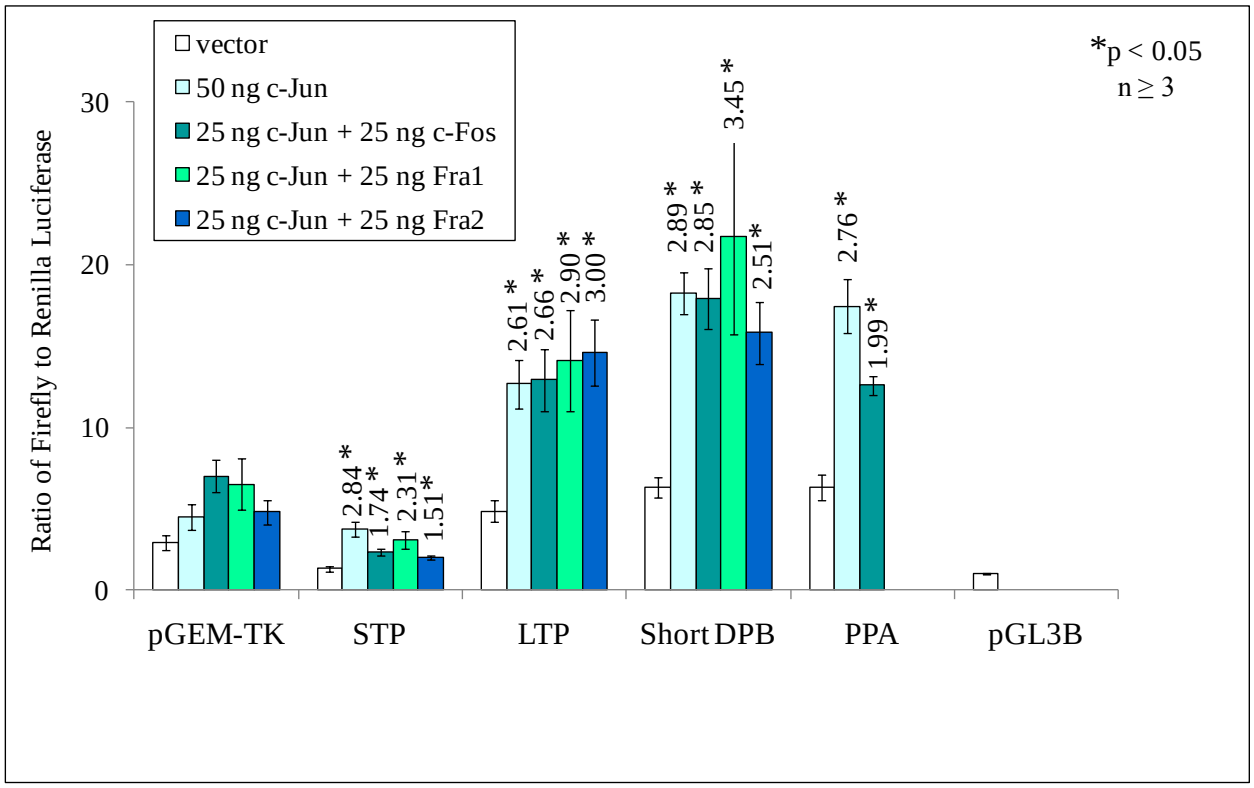

Figure 3.2: Cotransfection of mouse PR promoter constructs with c-Jun/Fos.
Cotransfections of mouse PR promoter constructs with 50 ng c-Jun or 25 ng of c-Jun plus 25 ng of a Fos partner (c-Fos, Fra1 or Fra2) in MCF-7 cells. Fold changes are given as mean induction of promoter activity when cotransfected with AP-1 over empty vector (pGL3B) ± SE. Promoter constructs used were: short tandem PR promoter (STP), long tandem PR promoter (LTP), short distal promoter B (short DPB), and proximal promoter A (PPA). pGEM-TK-luc is a control TK-luc vector . Datapoints represent triplicates in a minimum of 3 replicate experiments. Statistical analysis utilized Student's *t* test and statistical significance (*) is denoted when $p<0.05$.

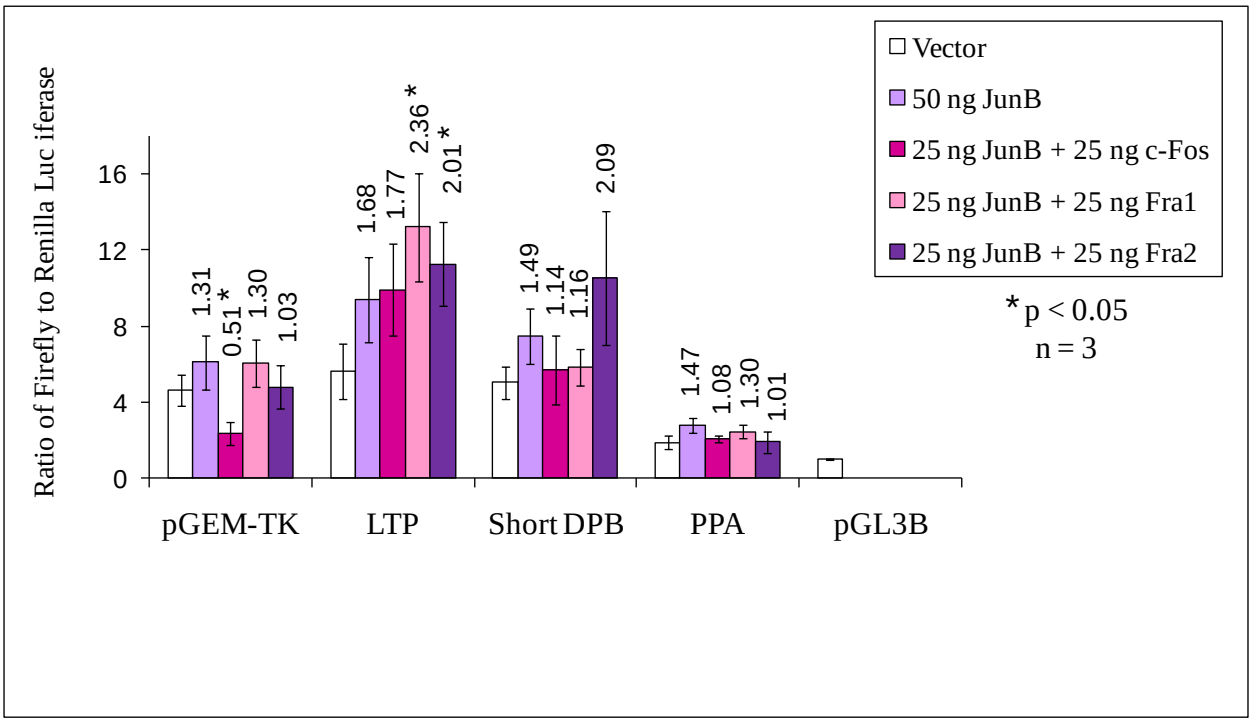

Figure 3.3: Cotransfection of mouse PR promoter constructs with JunB/Fos. Cotransfections of mouse PR promoter constructs with 50 ng JunB or 25 ng of JunB plus 25 ng of a Fos partner (c-Fos, Fra1 or Fra2) in MCF-7 cells. Fold changes are given as mean induction of promoter activity when cotransfected with AP-1 over empty vector (pGL3B) ± SE. Promoter constructs used were: long tandem PR promoter (LTP), short distal promoter B (short DPB), and proximal promoter A (PPA). pGEM-TK-luc is a control TK-luc vector. Datapoints represent triplicates in a minimum of 3 replicate experiments. Statistical analysis utilized Student's *t* test and statistical significance (*) is denoted when $p < 0.05$.

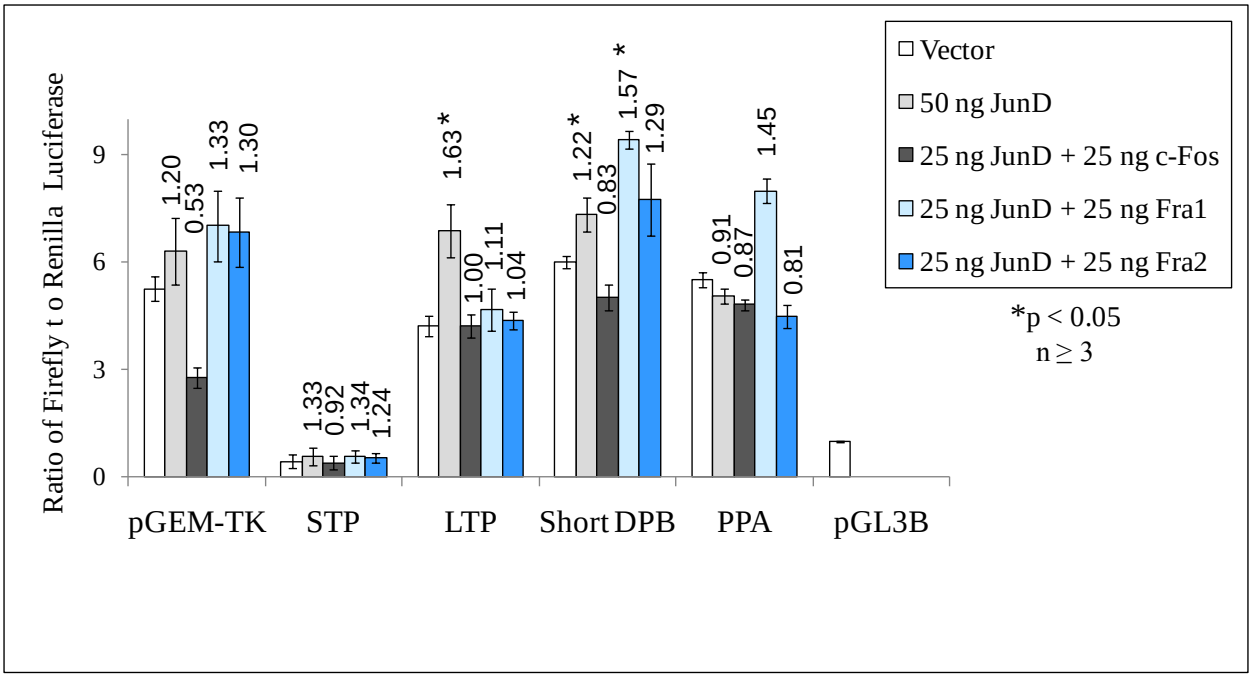

Figure 3.4: Cotransfection of mouse PR promoter constructs with JunD/Fos.
Cotransfections of mouse PR promoter constructs with 50 ng JunD or 25 ng of JunD plus 25 ng of a Fos partner (c-Fos, Fra1 or Fra2) in MCF-7 cells. Fold changes are given as mean induction of promoter activity when cotransfected with AP-1 over empty vector (pGL3B) ± SE. Promoter constructs used were: short tandem PR promoter (STP), long tandem PR promoter (LTP), short distal promoter B (short DPB), and proximal promoter A (PPA). pGEM-TK-luc is a control TK-luc vector. Datapoints represent triplicates in a minimum of 3 replicate experiments. Statistical analysis utilized Student's *t* test and statistical significance (*) is denoted when $p < 0.05$.

Fra1 also weakly activated the short DPB. JunD alone or with any Fos member failed to produce a statistically significant induction or repression of the STP or PPA constructs (Figure 3.4).

It is interesting to note that the basal strength of the LTP was about 3.7 fold greater than the STP, which differs only by the absence of the 5'-unique upstream region (Figure 3.2). This suggests that the 5'-unique region adds to the overall strength of the LTP. The STP is essentially comprised of the short distal and proximal promoter regions, but lacks the high basal activity seen in the short DPB construct (Figure 3.2). Taken together, the sense PR promoter constructs were all up-regulated by c-Jun but to varying degrees. In isolation the DPB and LTP showed the greatest transcriptional activity with c-Jun alone or c-Jun plus any Fos isoform. The same combinations of c-Jun and Fos subunits failed to activate transcription from the STP to the same absolute magnitude as with the short DPB construct. However, the relative fold inductions were comparable.

b. Hormone and Phorbol Ester Treatments

Constructs containing portions of the human and rat PR promoters are reported to be E_2-responsive (Petz LN 2004b); (Petz LN 2002); (Schultz JR 2003); (Kraus WL 1994), but it is unknown if the corresponding regions of the mouse Pgr gene show similar behavior. Additionally, in the rat, PRA expression has been shown *in vivo* to be entirely E_2-dependent (Kariagina A 2010). To address the question of whether the mouse PR promoters are E_2-reponsive, MCF-7 cells were transfected with the various PR promoter constructs and treated with E_2.

The activities of the mouse PR promoter constructs (LTP, STP, DPB and PPA) failed to show a significant response to E_2 (Figure 3.5), suggesting that the proximal and distal mouse PR promoter regions lack any functional EREs. Similar to their behavior in MCF-7 cells, none of these constructs showed a significant change in activity with E_2 treatment when tested in several mouse mammary tumor cell lines (MC7-L1, MC4-L2, and MC4-L3) that are reported to be steroid responsive (Lanari C 2001). Finally, attempts were unsuccessful to reproduce the more robust effects of E_2 that have been reported for the human PR promoter when analogous mouse PR luciferase constructs were cotransfected with ER in human osteosarcoma U2-OS cells (Petz LN 2002); (Petz LN 2004b); (Schultz JR 2003). In our hands, these experiments showed only repressive effects following E_2 treatment of transfected U2-OS cells (data not shown).

From these results we concluded that none of the AP-1/ERE or ERE/Sp1 sites that were described as being E_2-responsive in the case of the human or rat PGR genes appear to mediate a robust E_2 effect in the context of the mouse PR promoter. The explanation for this apparent difference remains elusive. It remains possible, however, that the AP-1 site which overlaps with the predicted start site of PRA transcription (i.e., the "+745 AP-1/ ERE" motif) may be involved in inhibiting PRA expression in certain contexts (Petz LN 2004a), a scenario that is at least consistent with the observed decrease in PRA expression in the mouse mammary gland during pregnancy (Aupperlee M 2005a).

To address the possibility that our PR reporter constructs may lack one or more essential regulatory elements present in the native mouse Pgr gene, we also constructed a derivative of the LTP (LTP-ERE) containing two additional EREs (ERE4 and ERE5) that were identified in the rat Pgr gene and reported to contribute greatly to its E_2-responsiveness (Kraus WL 1994). These

elements are situated downstream of the transcription start sites at the 3'-end of exon 1 (Figure 3.1). Comparison of the LTP construct with and without these additional EREs showed no significant difference in luciferase activity following E_2 treatment (Figure 3.6; data not shown).

The human PGR gene is reported to be Sp1-inducible and it has also been reported that ERα enhances Sp1 binding to each of two sets of Sp1 sites (-61 bp and +571 bp) within the distal and proximal promoters (Schultz JR 2003); (Petz LN 2000). Based on these human PR studies, we tested the effect of cotransfected Sp1 on our mouse PR promoter constructs with and without E_2 treatment. Again, treatment with E_2 alone or combined with cotransfected Sp1 failed to activate the mouse PR promoter constructs (Figure 3.6). This was especially surprising for the LTP construct containing the ERE(4,5) enhancer cassette, which contributes three additional putative Sp1 binding sites based on sequence analysis (MatInspector 2005). These experiments lead us to conclude that the core promoter region of the mouse Pgr gene, extending from –2494 to +769 bp with respect to the predicted PRB transcription start site, was not responsive to E_2, even in the presence of two additional hormone response elements that normally reside within the coding region of the gene near the end of exon 1. This differs from the situation described for both the human and rat PGR genes which appear to be more highly regulated by hormone, both *in vivo* and in transfection studies (Petz LN 2004b); (Petz LN 2002); (Schultz JR 2003); (Kraus WL 1994); (Kariagina A 2010).

Phorbol esters such as PMA mimic the function of the second messenger diacylglycerol, an activator of signaling kinases in the protein kinase C (PKC) pathway that activate c-Jun N-terminal kinase (JNK), and subsequently leads to AP-1 phosphorylation (Brose N 2002). To determine if PMA alone or cotransfected AP-1 could synergize with E_2 to activate transcription

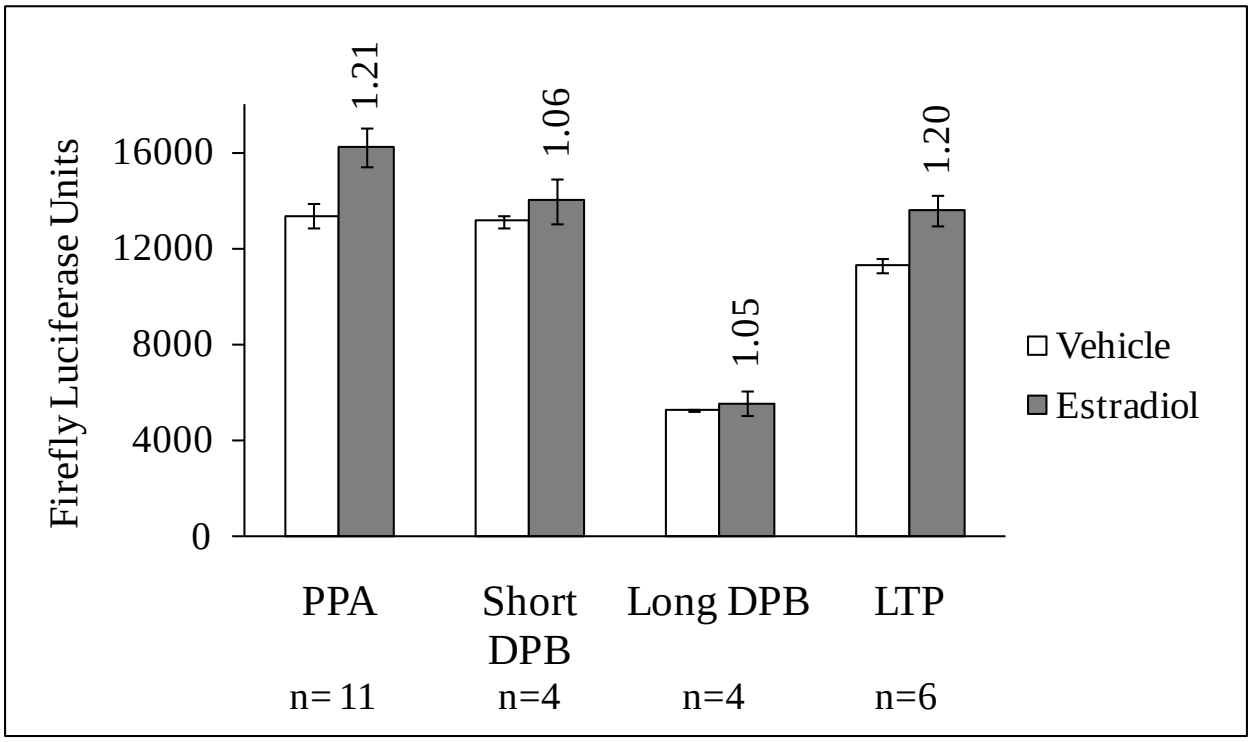

Figure 3.5: Transfection of mouse PR promoter constructs with and without estradiol. MCF-7 cell transfections of the proximal promoter A (PPA), short distal promoter B (short DBP), long distal promoter B (long DPB) and the long tandem PR promoter (LTP) constructs. Fold changes are given as mean induction after 24 hours of 10 nM estradiol (E_2) treatment compared to vehicle controls (± SE). Datapoints represent triplicates in a minimum of 3 replicate experiments in which firefly luciferase was normalized to 1 µg of protein. Statistical analysis utilized Student's *t* test. In all cases, however, changes relative to vehicle control were not significant.

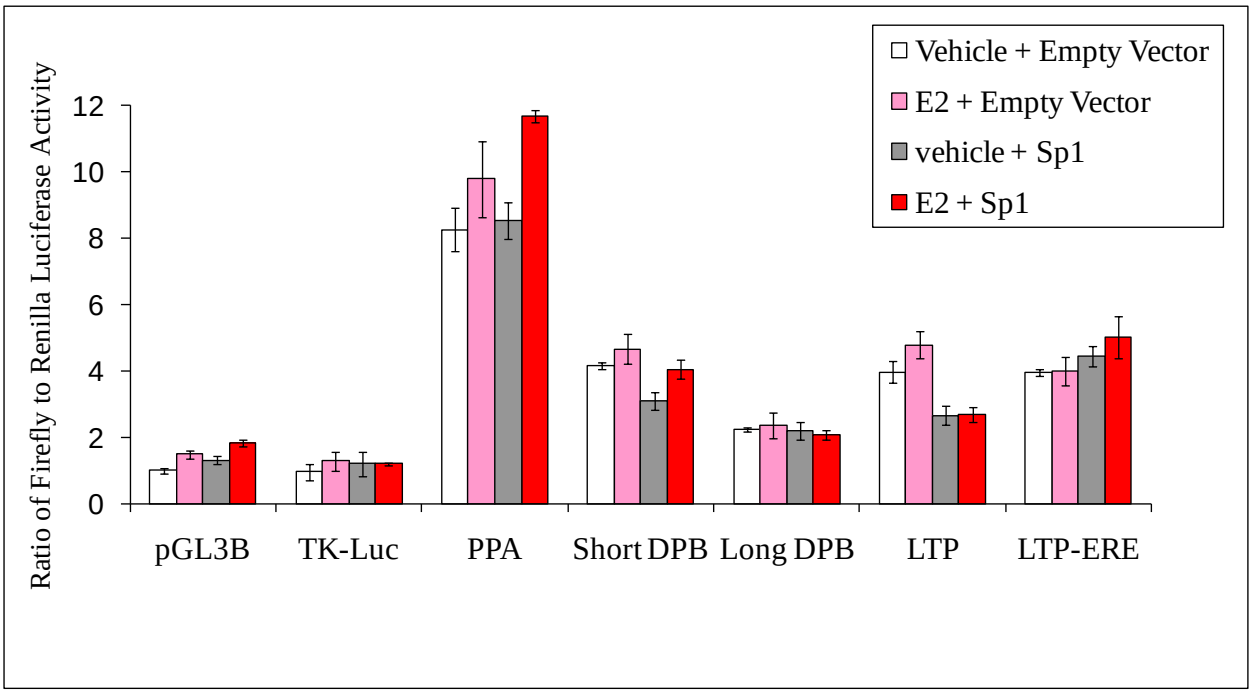

Figure 3.6: Transfection of mouse PR promoter constructs with and without estradiol and Sp1. MCF-7 cell transfections of thymidine kinase luciferase (TK-Luc) and PR promoter constructs: proximal promoter A (PPA), short distal promoter B (short DBP), long distal promoter B (long DPB), long tandem PR promoter (LTP) and tandem PR promoter with the ERE(4,5) enhancer cassette (LTP-ERE). Cells were cotransfected with 50 ng of empty vector or a Sp1 expression vector. Hormone treatment was with ethanol vehicle or 10 nM estradiol (E_2) for 24 hours. Datapoints represent triplicates in a representative experiment in which firefly luciferase was normalized to renilla luciferase and values are relative to pGL3B. Statistical analysis utilized Student's *t* test, however, changes relative to vehicle or vector control were not significant.

from the PR promoter constructs, MCF-7 cells were treated alone or in combination with E_2 and PMA. When combined with PMA, E_2 reduces, rather than augments the stimulatory activity of PMA on the LTP (Figure 3.7). Using PMA treatment alone, the LTP was highly induced (24.29 fold) by PMA in the context of endogenous AP-1 (Figure 3.7). Cotransfection of 25 or 50 ng each of c-Jun/c-Fos increased the basal activity of the LTP 5.94 and 7.38 fold, respectively, but the combined effect of c-Jun/c-Fos plus PMA treatment was no different than the transcriptional response to PMA alone (Figure 3.7). The effect that PMA and AP-1 had in our transfection studies on the activity of the LTP suggests that changes either in the level or composition of AP-1 or stimuli that activate AP-1 may give rise to increased amounts of PR *in vivo.* This could be accomplished by changes in the expression pattern of individual members of the AP-1 family (e.g., replacement of Fra1 by the more transcriptionally active c-Fos) or by changes in upstream signaling factors that influence AP-1 activity through JNK or other upstream kinases.

2. Analysis of PR Isoform Expression in Mouse Tissues and Mammary Cell Lines

a. Primer Extension Mapping of PR mRNA Start Sites

For a weakly expressed gene like mouse Pgr, cap analysis of gene expression (CAGE) analysis tends to predict multiple CAGE tags that are spread over CpG islands within the promoter region (Carninci P 2006). This is in contrast to TATA-containing promoters which show strong alignment of CAGE tags to a well defined single TSS (Carninci P 2006). Exonic promoter activity is usually highest in tissue-specific genes and does not correlate with the number of CAGE tags over the major promoter, but does correlate with a single dominant site of transcription initiation (Carninci P 2006). Of note, the FANTOM database lacks any CAGE tags

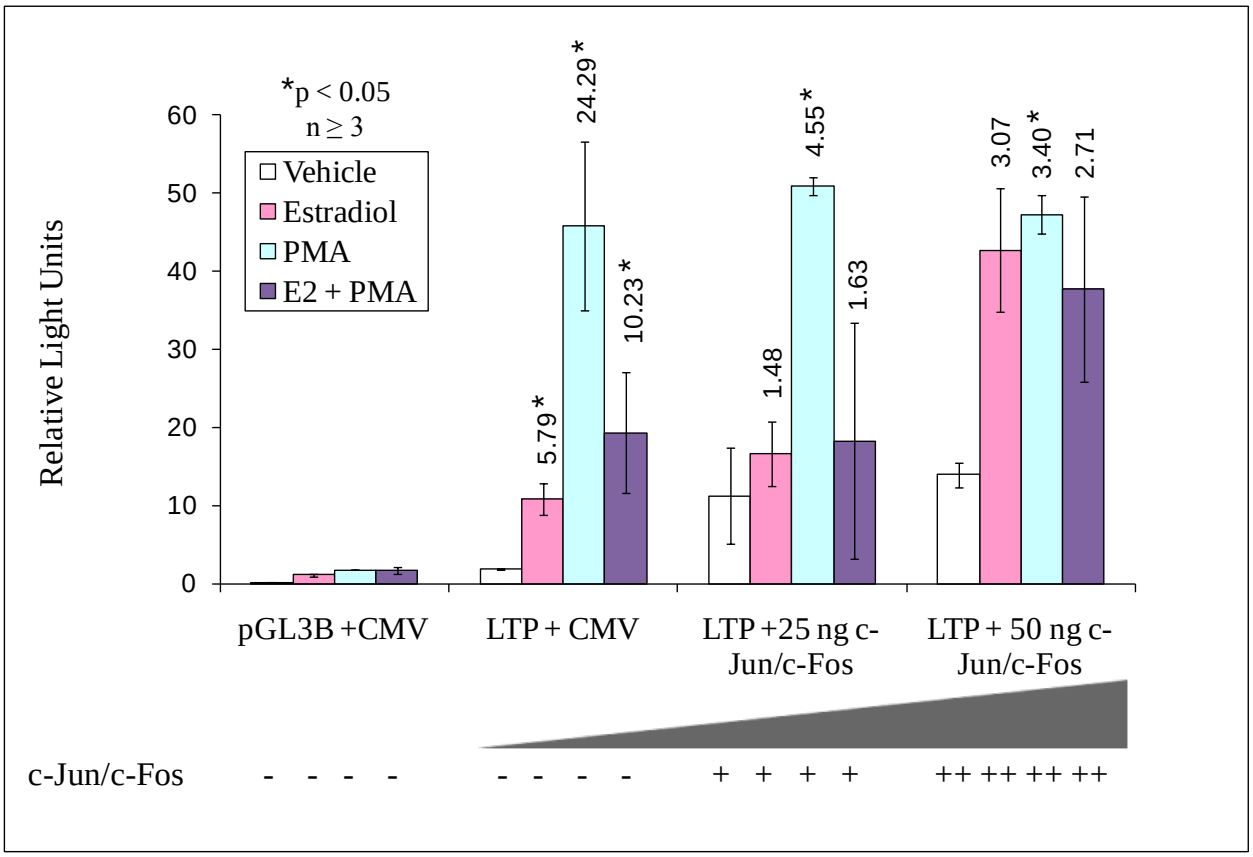

<u>Figure 3.7:</u> Cotransfection of mouse PR promoter constructs and c-Jun/c-Fos with and without estradiol, phorbol ester or estradiol and phorbol ester. Cotransfection of the long tandem PR promoter (LTP) and control vector pGL3Basic (pGL3B) with 25 or 50 ng of c-Jun and c-Fos expression vectors in MCF-7 cells. In order to maintain a constant amount of vector driven by cytomegalovirus (CMV), either pCMV empty vector, CMV-cJun, or CMV c-Fos were cotransfected. Fold changes are given as mean induction by 10 nM phorbol ester (PMA), 10 nM estradiol (E_2) or E_2 + PMA compared to vehicle controls (± SE). Datapoints represent triplicates in a representative experiment in which firefly luciferase was normalized to 1 µg of protein and light units are relative to pGL3B. Statistical analysis utilized Student's *t* test and significance (*) is denoted when $p < 0.05$.

in the distal promoter region of PRB, but contains a single CAGE tag at +630 bp, near the predicted proximal (PRA) TSS of +641 bp (Figure 3.8). The additional 4 CAGE tags for the mouse Pgr gene are dispersed throughout exon 1, mostly within the second CpG island (Figure 3.8), corresponding to a region that lies downstream of the PRA ATG and was therefore not analyzed by primer extension. CAGE tags located between the start site at the 5'-end of a gene and the 3'-UTR are common in CAGE analysis, mapping most often to exons (Carninci P 2006).

ESTs, cDNAs, and Riken clones for the mouse Pgr gene were generated largely by high throughput sequencing or targeted sequencing of tissues that may not express PRB (GenBank (NCBI) 2008). Therefore, the sequencing data is biased towards PRA since tissues such as mid-pregnant mammary gland, where PRB is high, were not included (GenBank (NCBI) 2008). The publicly available sequencing data for mouse Pgr is rather sparse compared to the more extensive studies that have been performed on rat and human PGR (GenBank (NCBI) 2008).

The 5'-ends of the human and rat PR transcripts were previously mapped by Kastner *et al.* and Kraus *et al.*, respectively, but they have yet to be delineated for the mouse Pgr gene (Kastner P 1990); (Kraus WL 1993). Additionally, the existence of one or two promoters needs to be confirmed for mouse PR, since this is central to the question of whether or not there is differential regulation of the PRA and PBR isoforms occurring at the transcriptional level. For these studies, primer extension (PE) analysis was used with lower strand primers for PRB (Distal 1, 2, 3) and PRA (Proximal 1, 2, 3) depicted in Figure 3.9.

Primer extension was used to map the 5'-end of mouse PR transcripts (i.e., presumptive $PR^{(B)}$ and $PR^{(A)}$ mRNAs) to help clarify if two classes of PR RNA exist in the mouse. Endogenous mRNA levels in several mouse cell lines were compared for total $PR^{(A+B)}$ and

$PR^{(B)}$ only message, as well as regulation of the gene in response to hormone or PMA treatment. Additionally, primer extension was carried out in tissue harvested from virgin adult mice that were either ovary-intact or ovariectomized (ovx). PR start sites were then analyzed in RNA extracted from mouse mammary gland, uterus and liver. Six different lower strand primers (Figure 3.9) were used to map the 5'-ends of PR mRNA and to determine the level of these transcripts in various mouse tissues and mouse mammary cell lines. Figure 3.10a shows the most abundant primer extension products from +215 to +224 bp and one faint band at approximately -9 bp in liver from ovary-intact mice using the Distal 2 (D2) primer. Although initially thought to be a PR-negative tissue, the mouse liver does indeed have PR mRNA present at detectable levels. Semi-quantitative PCR also confirmed the presence of a faint band for liver using primers in the common region of PRA and PRB (see Figures 3.12b, d), but it is not known if PR protein is expressed in the liver or what role PR-dependent signaling may play in liver function.

PE experiments using total RNA from virgin adult and mid-pregnant mouse mammary gland were also carried out to determine the abundance of mRNAs for both PR isoforms in two developmental states that show high levels of PRA and high PRB protein, respectively (Aupperlee M 2005a). Liver RNA from ovary-intact mice yielded primer extension products clustering from +215 to +224 bp (Figures 3.10a, 3.S2) with the D2 primer. Unfortunately, even 40 µg of input total RNA from the mammary gland failed to yield primer extension products (Figure 3.S2).

Uterine total RNA was annealed at two different temperatures (U_1 and U_2) with the Proximal 2 (P2) primer (Figure 3.10b). The transcription start sites (TSSs) that mapped upstream of the PRB ATG at +634 bp may give rise to PRB or PRA proteins, while start sites

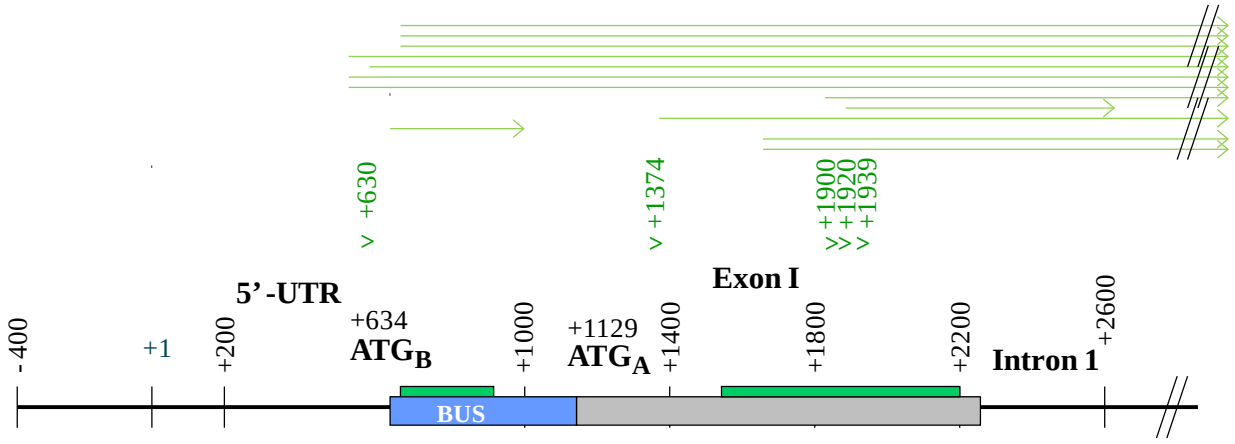

Figure 3.8: ***In Silico*** **data for the sense strand of the mouse Pgr locus.** Location of progesterone receptor RIKEN clones and cDNAs (arrows) compared to cap analysis of gene expression (CAGE) tags (carrots). The position of the two CpG islands (green boxes) are + 659 to +884 bp and +1572 to +2197 bp, both are located within exon 1. The region of the mouse Pgr gene shown includes the 5'-untranslated region (5'-UTR), PRB upstream sequence (BUS), exon 1 and intron 1.

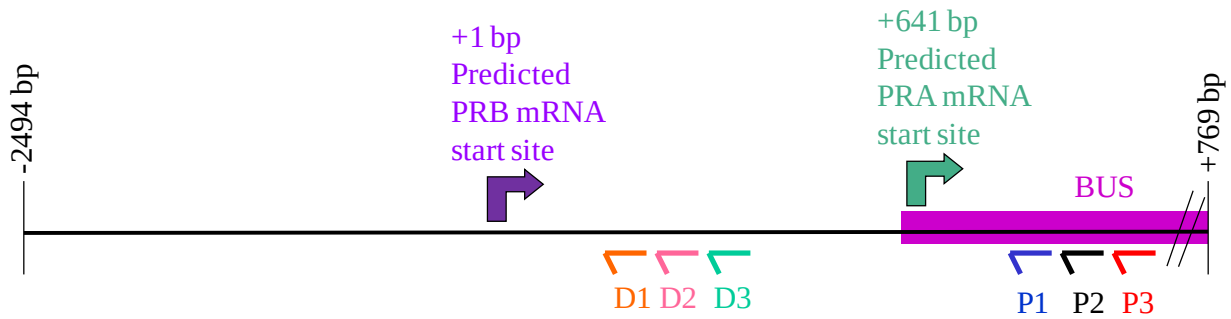

	Primer	Distance from predicted start site
PRB	Distal 1	131 bp
	Distal 2	234 bp
	Distal 3	378 bp
PRA	Proximal 1	110 bp
	Proximal 2	204 bp
	Proximal 3	313 bp

Figure 3.9: Location of the lower strand oligos used for primer extension analysis of the mouse Pgr gene. The primers are numbered left to right with the primers for PRB labeled distal 1, 2, 3 (D1, D2, D3) and for PRA labeled proximal 1, 2, 3 (P1, P2, P3). The principal start site predicted for PRB mRNA based on homology with the human PGR gene is denoted +1 bp, while the homologous predicted PRA start site is shown as +641 bp.

located downstream of +634 bp can only produce the PRA protein isoform. Using the Proximal 1 (P1) primer, combined with the data from the P2 primer described above, PRA transcriptional start sites in uterine RNA clustered primarily from +635 to +725 bp (data not shown). Since these transcriptional start sites lie downstream of the PRB ATG at +634 bp, by definition they correspond to $PR^{(A)}$ transcripts that can only produce PRA protein. In contrast to what has been reported by Kastner and colleagues for the human PGR gene (Kastner P 1990), transcription start sites mapped using a total of six primers derived from the homologous 5'-untranslated region (UTR) of the mouse Pgr gene are unexpectedly dispersed throughout the +114 bp to +221 bp distal region and the +635 bp to +725 bp (proximal) region with several isolated start sites located from +358 bp to +582 bp (Figures 3.10, 3.11; data not shown). These transcription start sites are further broken down by tissue source and whether or not ovarian hormones were present (Figure 3.11). Uterine RNA from ovary-intact mice showed very faint start sites for $PR^{(B)}$ transcripts ranging from +181 bp to +202 bp, with more prominent start sites for $PR^{(A)}$ message from +635 bp to +713 bp, as well as several difficult to classify TSSs at +499 bp and +582 bp that could represent either $PR^{(A)}$ or $PR^{(B)}$ transcripts (Figure 3.11).

Liver RNA from ovary-intact or ovariectomized mice both produced start sites at -9 bp and differed in many of the remaining start sites (Figure 3.11). Liver RNA from ovary-intact mice also displayed start sites at +190 and +196 bp for $PR^{(B)}$ transcripts and $PR^{(A)}$ transcripts that ranged from +678 to +718 bp (Figure 3.11). Liver RNA from ovariectomized mice had PR start sites at +188, +192, +200, +201 bp for $PR^{(B)}$ message (Figure 3.11). Start sites for ovariectomized liver RNA using the proximal primers were not determined and attempts to detect PR mRNA from mouse mammary gland tissue using the PE technique was unsuccessful

Figure 3.10: Representative primer extension reactions using total RNA extracted from the liver (L) using primer Distal 2 (D2) and uterine RNA (U) with the Proximal (P2) primer.

(a) Liver RNA from ovary-intact (Int) virgin adult BALB/c mice was analyzed in primer extension using 40 μg of RNA per reaction. GATC lanes represent the four sequencing reactions of mouse PR plasmid DNA initiated with the corresponding primers and run in parallel.
(b) Primer extension reactions used 40 μg of total RNA extracted from the uterus of virgin adult BALB/c mice, annealed at either 47 ˚C (U_1) or 44 ˚C (U_2), with the Proximal P2 primer. GATC lanes represent the four sequencing reactions of mouse PR plasmid DNA initiated with the corresponding primers and run in parallel.

Figure 3.10 (Cont'd.)

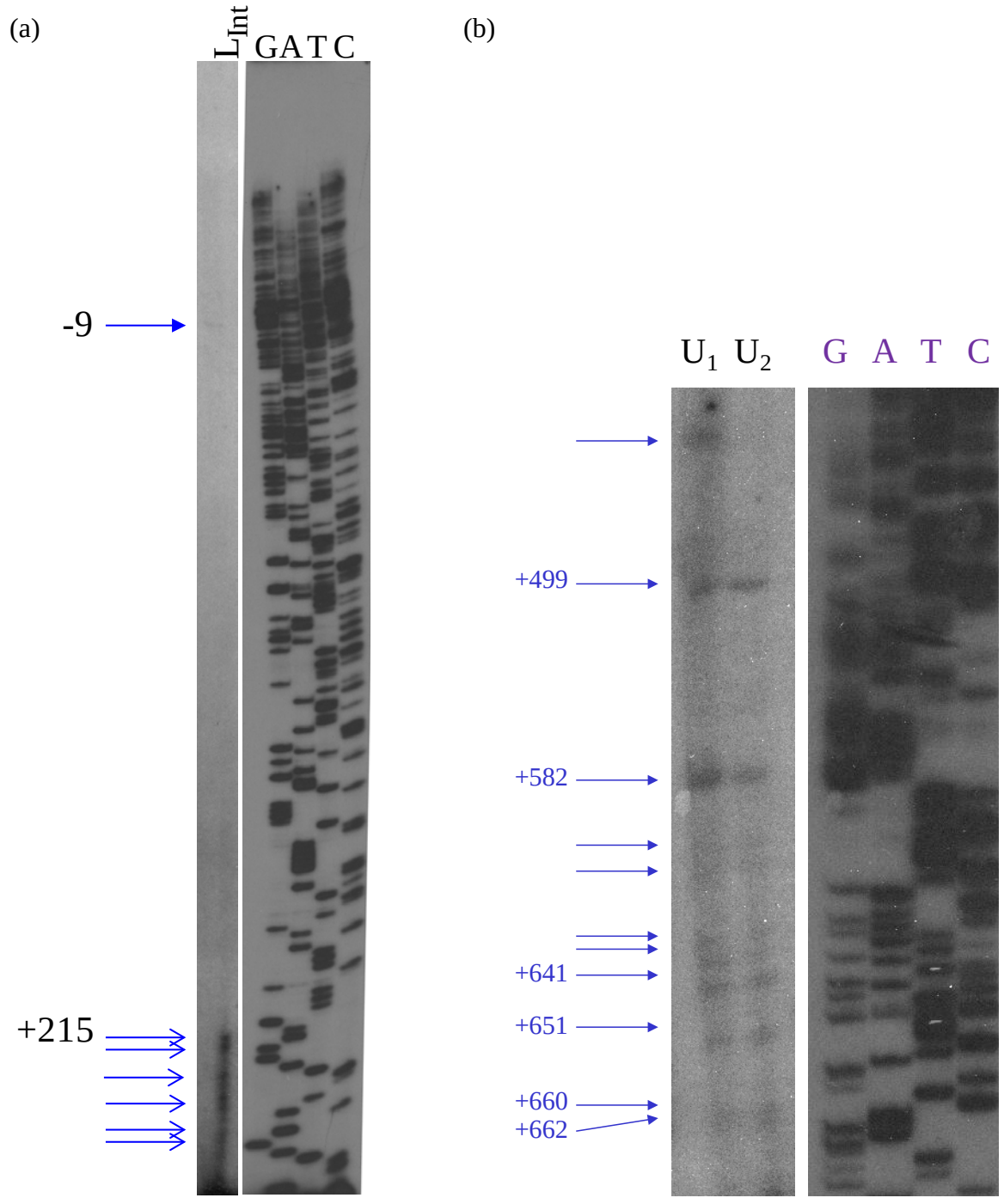

(Figure 3.S2). The overall pattern of transcription initiation was consistent with the fact that the 5'-flanking region of mouse PR is distinctly GC-rich and lacks a recognizable TATA box (GenBank (NCBI) 2008); (MatInspector 2005). Note the consistency in the 5'-end location mapping for mouse PR between the *in silico* data presented in Figure 3.8 and our primer extension results summarized in Figure 3.11. Based on this distribution of TSSs, it has been difficult to conclude whether a subset of mouse PR mRNA start sites exists that are truly isoform specific. Clearly, however, transcripts that initiate downstream of the PRB ATG can only support the production of PRA protein through initiation at the downstream PRA ATG.

b. Semi-Quantitative PCR of Total $PR^{(A+B)}$ and $PR^{(B)}$–Specific mRNA Transcripts

A mouse mammary cell line is desirable to enable later study of endogenous $PR^{(A)}$ and $PR^{(B)}$ mRNAs, to demonstrate PR isoform expression levels, and to examine transcriptional regulation of the endogenous mouse PR promoters. Currently, there are no well characterized mouse mammary cell lines that are ER^{+}/PR^{+} and behave similarly to normal mouse mammary tissue *in vivo*. We selected a few candidate steroid receptor positive mouse mammary cell lines to confirm if they express PR and to test their hormone responsiveness (MC7-L1, MC4-L2, MC4-L3, and UMD-208 cells). Hormone treatments were given for the final 24 hours prior to harvest, and included: E_2, R5020, or the combination of E_2+R5020.

Candidate cell lines were analyzed initially using semi-quantitative PCR that employed a lower strand primer in the 3'-UTR of the mouse Pgr gene to prepare a strand-specific PR cDNA. A lower strand PR primer was chosen over a conventional oligo(dT) primer to avoid assay interference from possible antisense transcripts (see Chapter 4) which are often known to be

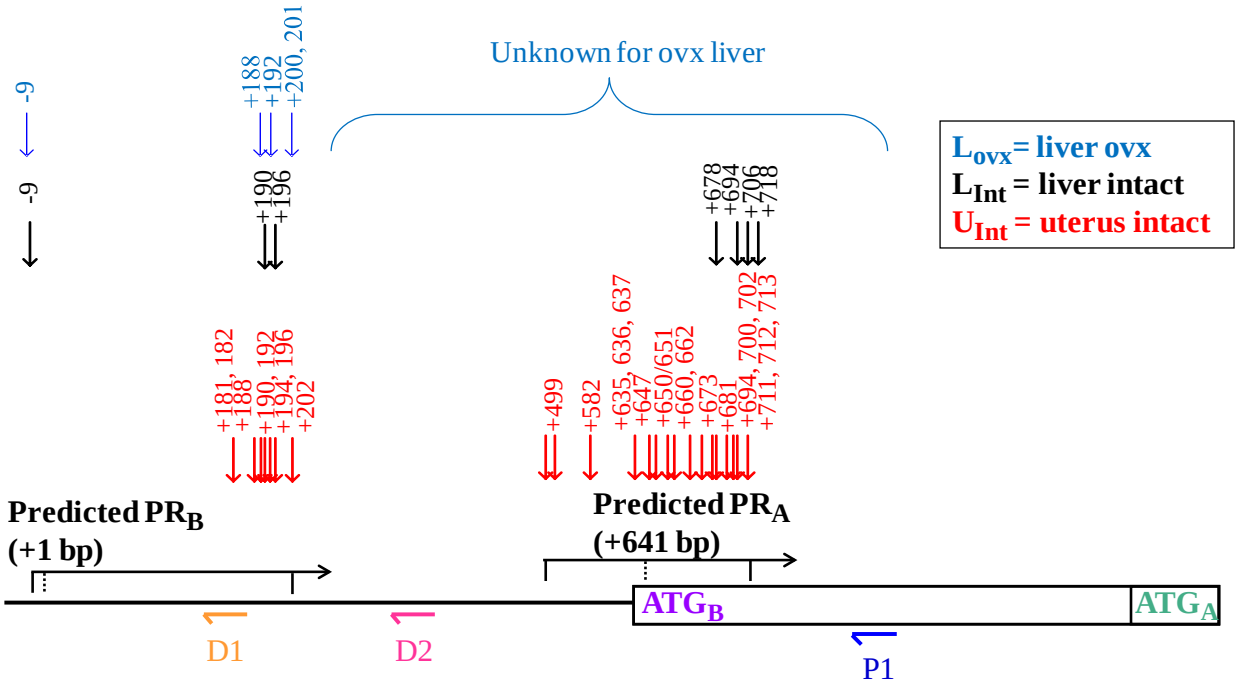

Figure 3.11: Transcription start sites mapped for the progesterone receptor gene using primer extension (vertical arrows; minimum of 2 experiments per primer). The location of lower strand primers for distal (D) promoter B and proximal (P) promoter A are shown as horizontal colored arrows (D1, D2, and P1). Also shown are the location of the predicted "+1 bp" and "+641 bp" start sites (dashed lines) based on sequence alignment with the human and rat progesterone receptor genes. Tissues used were: liver from ovaractomized mice (L_{ovx}), liver from ovary-intact mice (L_{Int}) and uterus from ovary-intact mice (U_{Int}).

polyadenylated. The primer set used for PCR amplification spans exon 4 to exon 5 within the ligand binding domain (LBD) and detects both $PR^{(A)}$ and $PR^{(B)}$ transcripts (Figure 3.12e). Because this PCR primer set straddles the relatively large fourth intron, interference from contaminating genomic DNA could be avoided. All four candidate cell lines were $PR^{(A+B)}$-positive (Figures 3.12a, b, d) by this criterion and were compared to mouse tissues to extrapolate message abundance and primer efficiency. In Figure 3.12a, the cycle number appeared to be saturating for detecting PR transcripts in all tissues and cell lines examined except for liver and NMuMG which had little if any PR message present that corresponded to the body of the mouse Pgr gene. When amplified at a lower cycle number, UMD-208 cells showed apparent down-regulation of PR message with R5020 treatment and an increase in PR message with combined E_2+R5020 treatment, but showed little change with E_2 treatment alone (Figure 3.12b). Vehicle control treated MC7-L1 cells were positive for PR message and the amount of mRNA was not altered by 24 hours of treatment with vehicle, E_2, R5020, or E_2+R (Figure 3.12c). Similarly, treatment of MC7-L1 cells with PMA for 2 or 18 hours also did not change the PR mRNA levels (Figure 3.12c). For the mouse tissues examined, 28 cycles of PCR amplification was saturating for both uterine samples as judged from similarly intense PR bands for ovariectomized and ovary-intact mouse uterine RNA (Figure 3.12d). However, PCR amplification using a lower cycle number would have made detection of PR mRNA in ovarectomized mammary gland difficult since it displays fairly low levels of total PR compared to uterus (Figure 3.12d). Of note, ovariectomy resulted in a decrease in total PR message in the mammary glands of BALB/c mice relative to ovary-intact controls (Figure 3.12d).

(a)

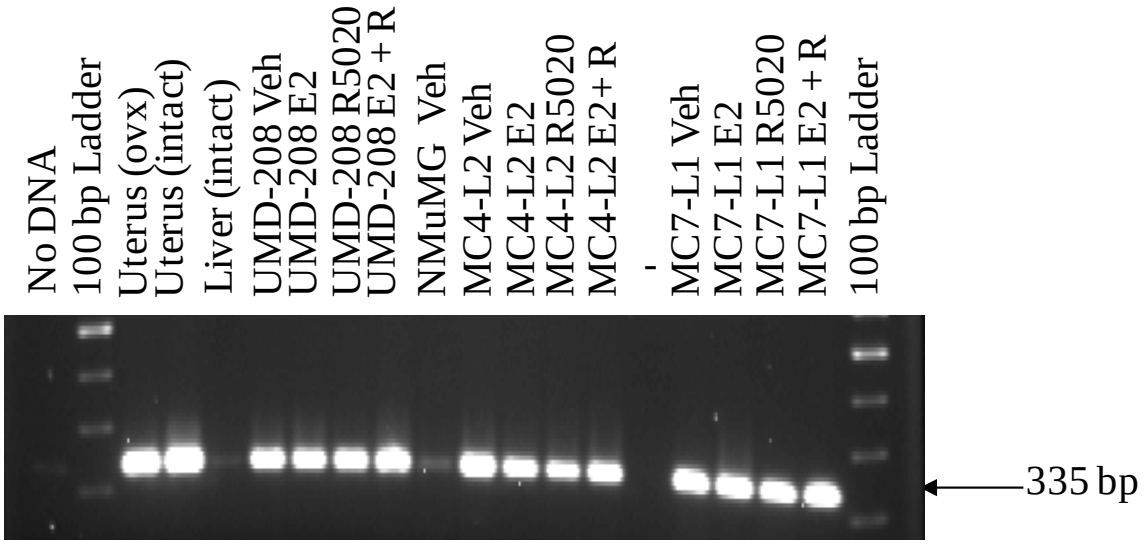

Figure 3.12: Semi-quantitative PCR of mouse mammary cell lines and tissues with an exon 4/5 primer set.

(a) Semi-quantitative PCR of mouse mammary cell lines and mouse tissues amplified for 36 cycles using a PCR primer set spanning exons 4 and 5 to detect total $PR^{(A+B)}$.

(b) Semi-quantitative PCR of UMD-208 cells and mouse tissue using 28 cycles of PCR amplification using a PCR primer set spanning exons 4 and 5 to detect total $PR^{(A+B)}$.

(c) Semi-quantitative PCR of MC7-L1 and NMuMG mouse mammary cells amplified for 36 cycles using an exon 4/5 primer set. MC7-L1 cells were treated for 24 hours with vehicle, E_2, R5020, or E_2+R. Alternatively, MC7-L1 cells were treated for 2 or 18 hours with phorbol myristate acetate (PMA). Sense strand PR cDNA was prepared using a lower strand primer located in the 3'-UTR of the Pgr gene. The positive control PCR reaction used the cloned PR cDNA plasmid as a template.

(d) Semi-quantitative PCR mouse tissues and NMuMG mouse mammary cells using 28 cycles of PCR amplification using a PCR primer set spanning exons 4 and 5 to detect total $PR^{(A+B)}$.

(e) A 3'-untranslated region (UTR) lower strand primer was used to prime cDNA synthesis in the mouse Pgr gene. For semi-quantitative PCR the PCR primer set spanned exons 4 and 5. The negative control PCR reaction was no template DNA. Additionally, a PRB-specific set of primers were used for PCR located in the PRB 5'-UTR.

Figure 3.12 (Cont'd.)

(b)

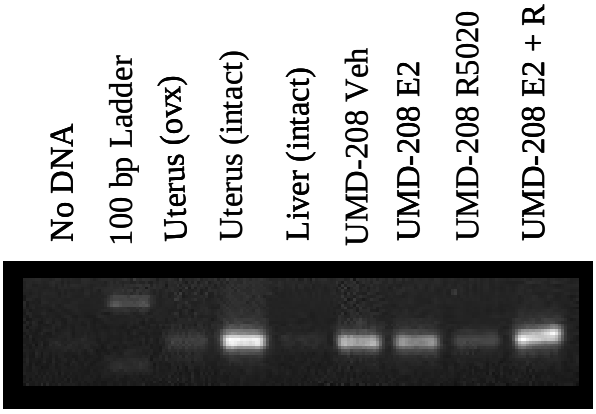

(c)

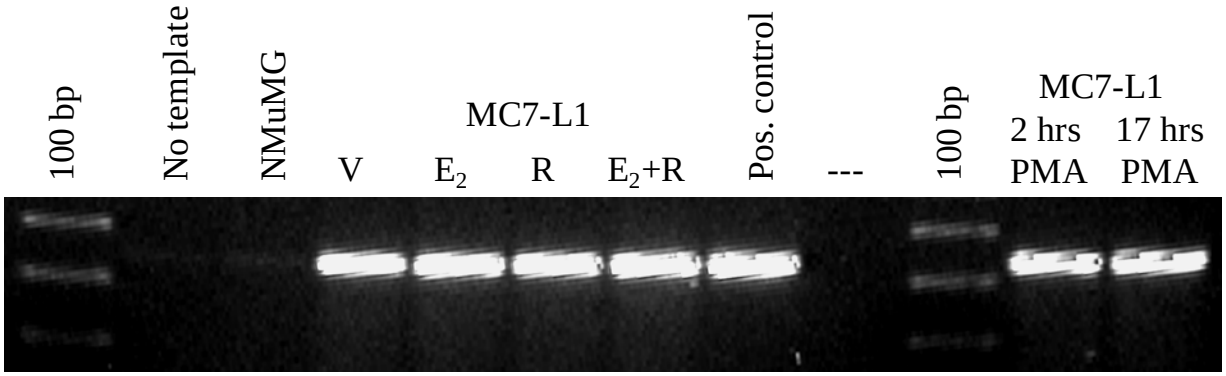

(d)

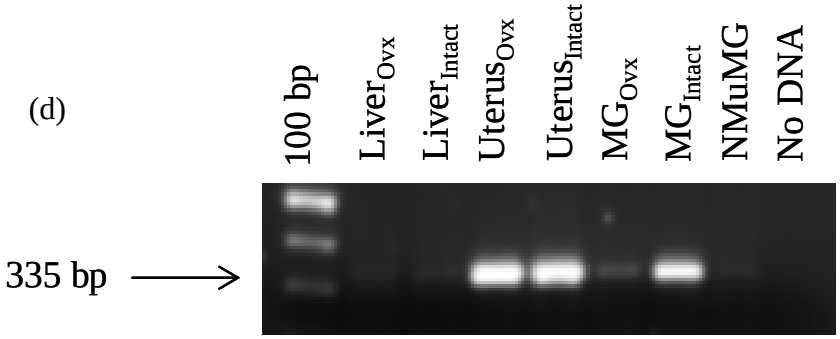

(e)

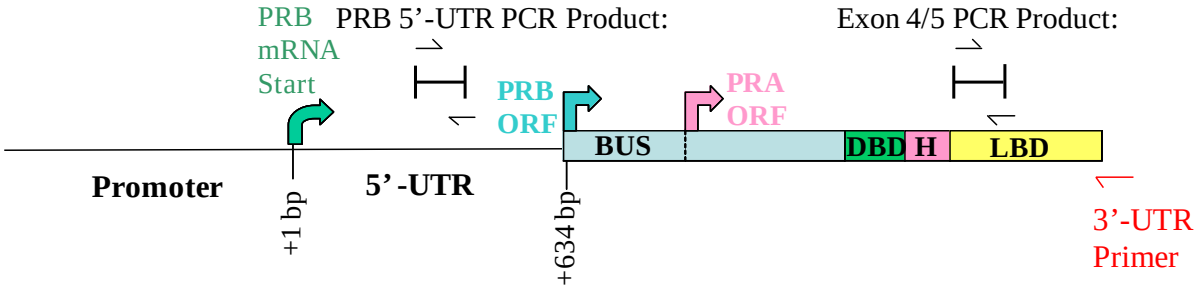

In an effort to detect $PR^{(B)}$-specific transcripts, semi-quantitative PCR was also performed using a PCR primer set located in the region homologous to the rat and human PRB 5'-UTR. This PCR primer set was located at +144 to +444 bp, relative to the predicted +1 bp PRB mRNA start site. Regardless of the hormone receptor-positive cell line or tissue used, PCR amplification was reproducibly negative for a PRB-specific transcript in the PRB 5'-UTR region (data not shown). This confirms the primer extension analysis in the PRB 5'-UTR region where there were no detectable transcription start sites located upstream of +181 bp, suggesting that the majority of PRB start sites are located downstream of +181 bp (Figures 3.8; 3.11).

Alternatively, a PCR primer set located within exon 1 in the vicinity of the PRB ATG (ATG_B) was used for PCR amplification (Figure 3.13a), priming from +634 to +1004 bp. In the uterus samples, the level of $PR^{(B)}$ transcript was higher in the ovary-intact mice than in ovariectomized mice as expected (Figure 3.13a). The ATG_B primer also detected low levels of $PR^{(B)}$ message in liver, which was also increased in the tissues from ovary-intact mice versus ovariectomized in general agreement with our results using primer extension analysis. The ATG_B primer set detected a faint PRB band in NMuMG cells (Figure 3.13a), which was lacking in experiments using the PRA+B exon 4/5 primer set described above (Figure 3.12). PR was not detected in either of the virgin adult mammary gland samples using the exon 1 ATG_B primer (Figure 3.13a), possibly because most of the transcripts at this stage represent PRA and initiate downstream of this region (Figure 3.11).

To further characterize the levels of PR mRNA in various tissues, a sense strand cDNA was primed within exon 4 and then amplified with PCR primers located in exon 1 and exon 2,

spanning the first intron (Exon 1/2 primers) (Figure 3.13d). For all treatments, MC7-L1 cells had low levels of $PR^{(A+B)}$ message, which was slightly increased following treatment with either E_2 or E_2+R5020 (Figure 3.13c). RNA from ovary-intact or ovariectomized mouse liver lacked detectable levels of PR message, but the livers of ovariectomized mice treated for 5 days with E_2+P displayed a very low level of $PR^{(A+B)}$ mRNA (Figure 3.13c). Uterine RNA from ovary-intact or ovariectomized mice had moderate to high $PR^{(A+B)}$ RNA levels, but message levels were noticeably higher in an independent sample set extracted from ovariectomized virgin adult mice treated for 5 days with vehicle, E_2, P or E_2+P (Figure 3.13c). After 5 days of vehicle or treatment with E_2+P, uterine $PR^{(A+B)}$ RNA levels were high, but were decreased upon E_2 or P treatment (Figure 3.13c). In the mammary gland samples from ovariectomized mice, $PR^{(A+B)}$ message was essentially absent. In comparison, $PR^{(A+B)}$ RNA was expressed at a low, but detectable level in mammary gland from ovary-intact mice (Figure 3.13c). An interesting, but consistent observation was that PR message was increasingly difficult to detect in RNA samples from nominally PR-negative tissues such as liver and cell lines such as NMuMG as the PCR priming site was moved progressively further from the 5'-end of the Pgr gene, suggesting that there may be abortive transcripts present in cells that express very low levels of PR protein.

c. Immunofluorescence Staining of PR Isoforms in Mouse Mammary Cell Lines

Experiments using PRB-specific PCR primers successfully detected $PR^{(B)}$ message in many of the mouse mammary cell lines as well as in mouse uterus (Figures 3.19a, c), therefore, confirming the presence of a bonafide separate $PR^{(B)}$ RNA transcript. Due to extensive overlap,

however, there isn't a reliable method to determine the separate contribution that $PR^{(A)}$ transcript makes to the PCR product amplified using a primer set common to both the $PR^{(A)}$ and $PR^{(B)}$ mRNA. An alternative method to assay for the number of PRA and PRB expressing cells is immunofluorescence analysis, which makes use of isoform-specific antibodies to detect the corresponding PR proteins. Immunofluorescence was therefore used to determine on a cell-by-cell basis if candidate mouse mammary cell lines express either PRA or PRB protein, as well as to estimate the effect of hormone treatment on expression of each PR isoform.

The first candidate cell line examined was UMD-208, a mouse mammary tumor cell line reported to be both ER^+/PR^+, to be growth inhibited by tamoxifen, and to show E_2-reglated PR expression in culture (Skildum A 2007). UMD-208 cells are luminal epithelial cells derived from a transgenic FBV/N mouse engineered to express a NRL-TGF-α transgene (rat neu related lipocalin-transforming growth factor-α) that spontaneously developed mammary tumors after receiving tamoxifen pellets at a young age (Rose-Hellekant TA 2003). The NRL promoter is mammary specific but not under the control of E_2 (Rose-Hellekant TA 2003). Mouse 208 from which the cell line was derived, showed increased steroid receptor expression in the tumor compared to non-tumor gland (Skildum A 2007). Proliferation of UMD-208 cells is stimulated by E_2, and sensitive to tamoxifen treatment (Skildum A 2007).

The second candidate cell line used was MC7-L1, which is a C7-H1 tumor-derived cell line model for steroid receptor-positive mouse mammary carcinomas (Lanari C 2001). MC7-L1 and its sister cell lines represent the first non-transgenic mouse mammary carcinoma cell lines that express both ER and PR. MC7-L1 cells are P-independent for growth *in vivo*, but P-dependent for growth *in vitro* (Lanari C 2001).

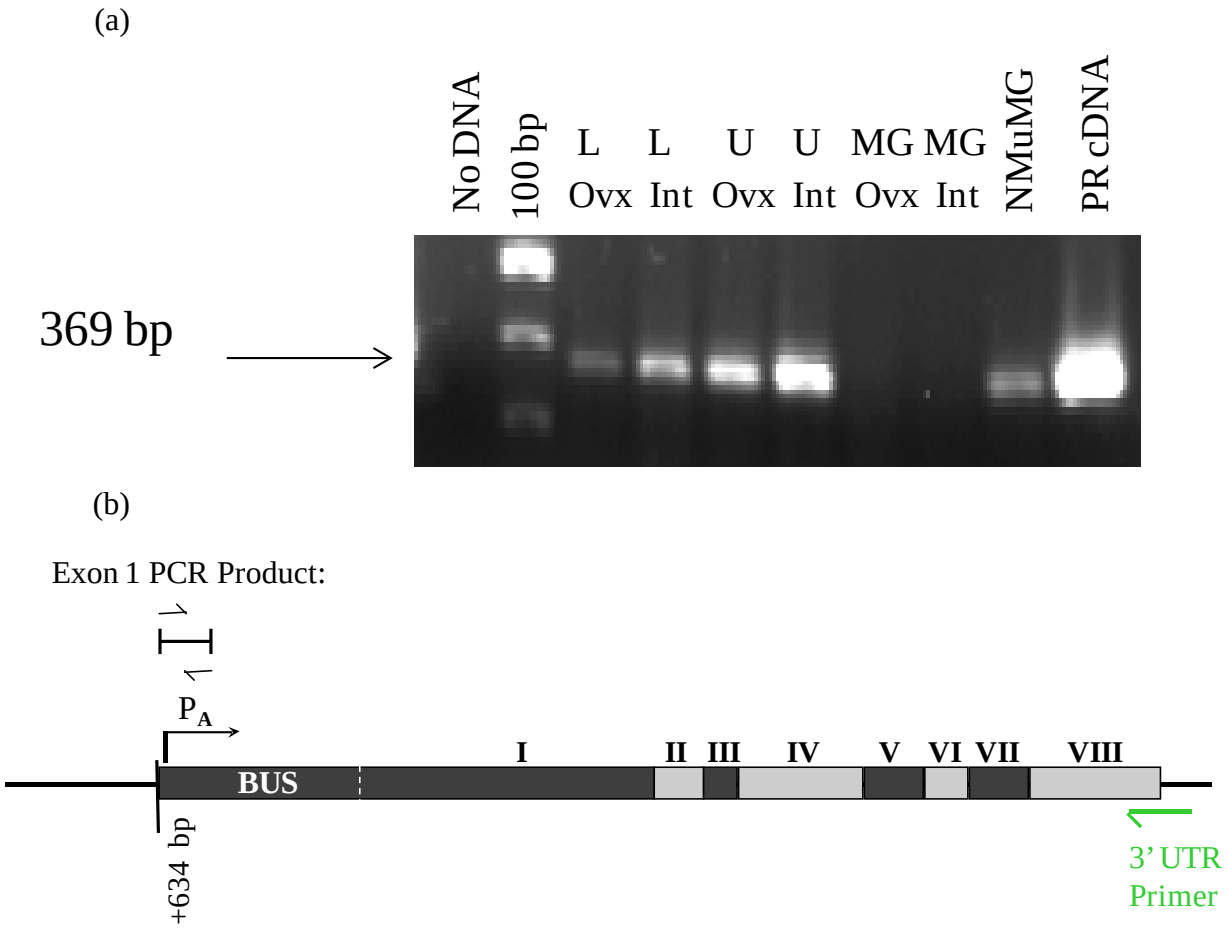

Figure 3.13: Semi-quantitative PCR of mouse mammary cell lines and tissues with exon 1 ATG_B or exon 1/2 primer sets.

(a) Semi-quantitative PCR of mouse tissues and NMuMG mammary cells amplified for 36 cycles using an exon 1 ATG_B primer set. Sense strand PR cDNA was prepared using a lower strand primer in the 3'-UTR/exon 8 common region of PR. The negative control was no template DNA while the positive control PCR reaction uses the cloned PR cDNA plasmid as a template.

(b) Location of the sense primers used to prepare the cDNA as well as the exon 1 ATG_B primer set used in the PCR reaction.

(c) Semi-quantitative PCR of mouse tissues, MC7-L1 and NMuMG mammary cells amplified for 36 cycles using an exon 1/2 primer set. Uterus and liver tissue were extracted from ovariectomized virgin adult BALB/c mice that were treated for 5 days with vehicle, E_2, P, or E_2+P. Sense strand PR cDNA was prepared using a lower strand primer in exon 4 within the common region of PR. The negative control was no template DNA while the positive control PCR reaction uses the cloned PR cDNA plasmid as a template.

(d) Location of the sense primers used to prepare the cDNA as well as the exon 1/2 primer set used in this PCR reaction.

Figure 3.13 (Cont'd.)

(c)

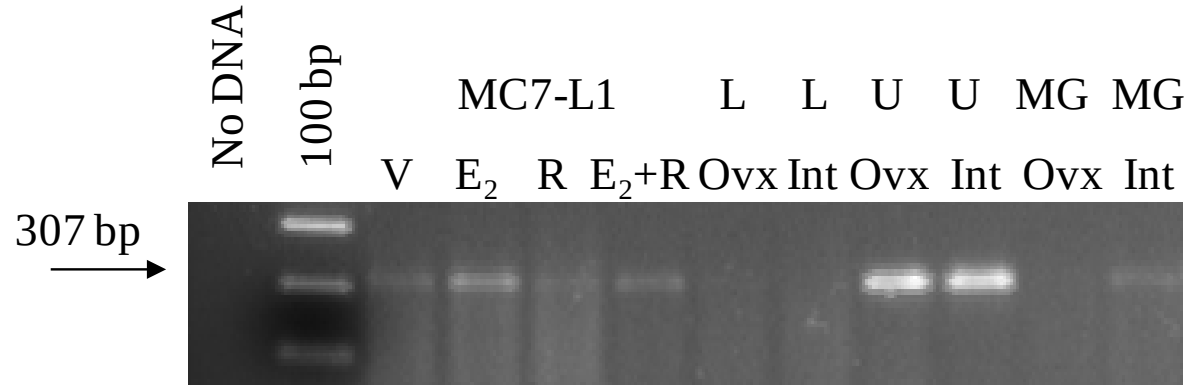

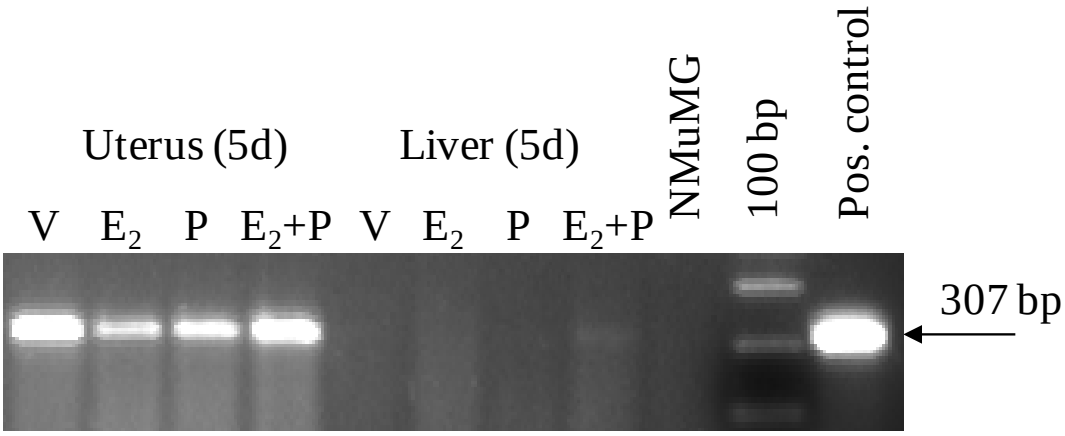

(d)

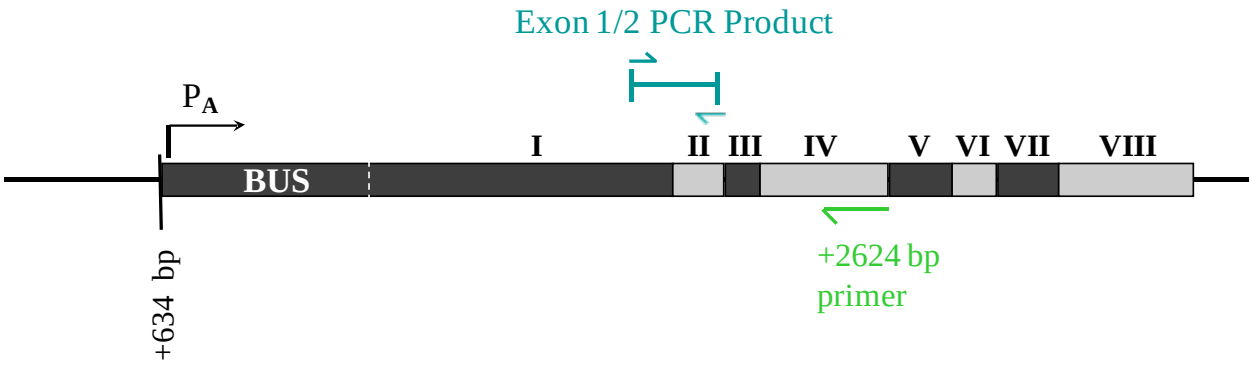

Using two candidate PR^+ mammary cell lines (UMD-208 and MC7-L1), the level of endogenous PRA and PRB protein was found to be low to undetectable by immunofluorescence (Figures 3.14, 3.15). UMD-208 cells treated with vehicle were very weakly positive for cytoplasmic PRA (data not shown), but negative for nuclear PRA. Hormone treatment did not increase the number of or intensity of PRA^+ cells (data not shown). Staining for PRB showed nuclear speckling in many of the UMD-208 cells cultured in the absence of hormone (Figure 3.14(ii)). Treatment with E_2, R5020, or E_2+R showed a trend towards more strongly staining of PRB with nuclear speckling, implying that hormone treatment may increase the amount of nuclear PRB protein or promote the intranuclear redistribution of PRB (Figure 3.14(iii-v)).

In comparison to UMD-208 cells, MC7-L1 cells treated with vehicle were weakly positive for nuclear PRA in a subset of cells (Figure 3.15(ii)), while E_2 treatment appeared to increase both the number of and intensity of PRA^+ cells (Figure 3.15(iii)). Treatment with R5020 was similar to vehicle control (Figure 3.15(iv)). The combination of E_2 + R5020 resulted in an intermediate staining pattern, resulting most likely from the induction of PRA due to E_2 and down regulation by R5020 (Figure 3.15(v)). Staining for PRB in control cells treated with vehicle showed nuclear speckling in many of the MC7-L1 cells (Figure 3.15(vi)). Treatment with E_2 showed a slight trend towards an increasing intensity of or number of nuclear speckles per cell (Figure 3.15(vii)). Treatment with R5020 or E_2 plus R5020 was similar to vehicle control (Figure 3.15(viii, ix)). In both UMD-208 and MC7-L1 cell lines, strong nuclear staining was detected only when PRA and PRB antibodies were used to stain cells transfected with the

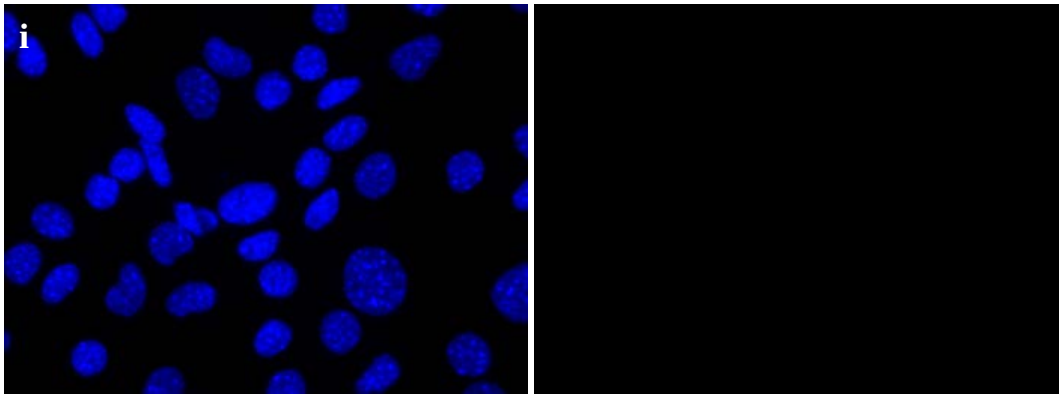

Figure 3.14: Immunofluorescence of UMD-208 cells using no primary antibody (i) or the B15 antibody to detect PRB (ii-v). Cells were treated with ethanol vehicle (ii), estradiol (iii), R5020 (iv) or estradiol + R5020 (v). Left panels are merged images of DAPI stained nuclei (blue) and PRB staining (green), right panels are PRB staining only (green). Hormone treatments were for 24 hours preceding cell fixation. Images are representative of 3 experiments.

Figure 3.14 (Cont'd.)

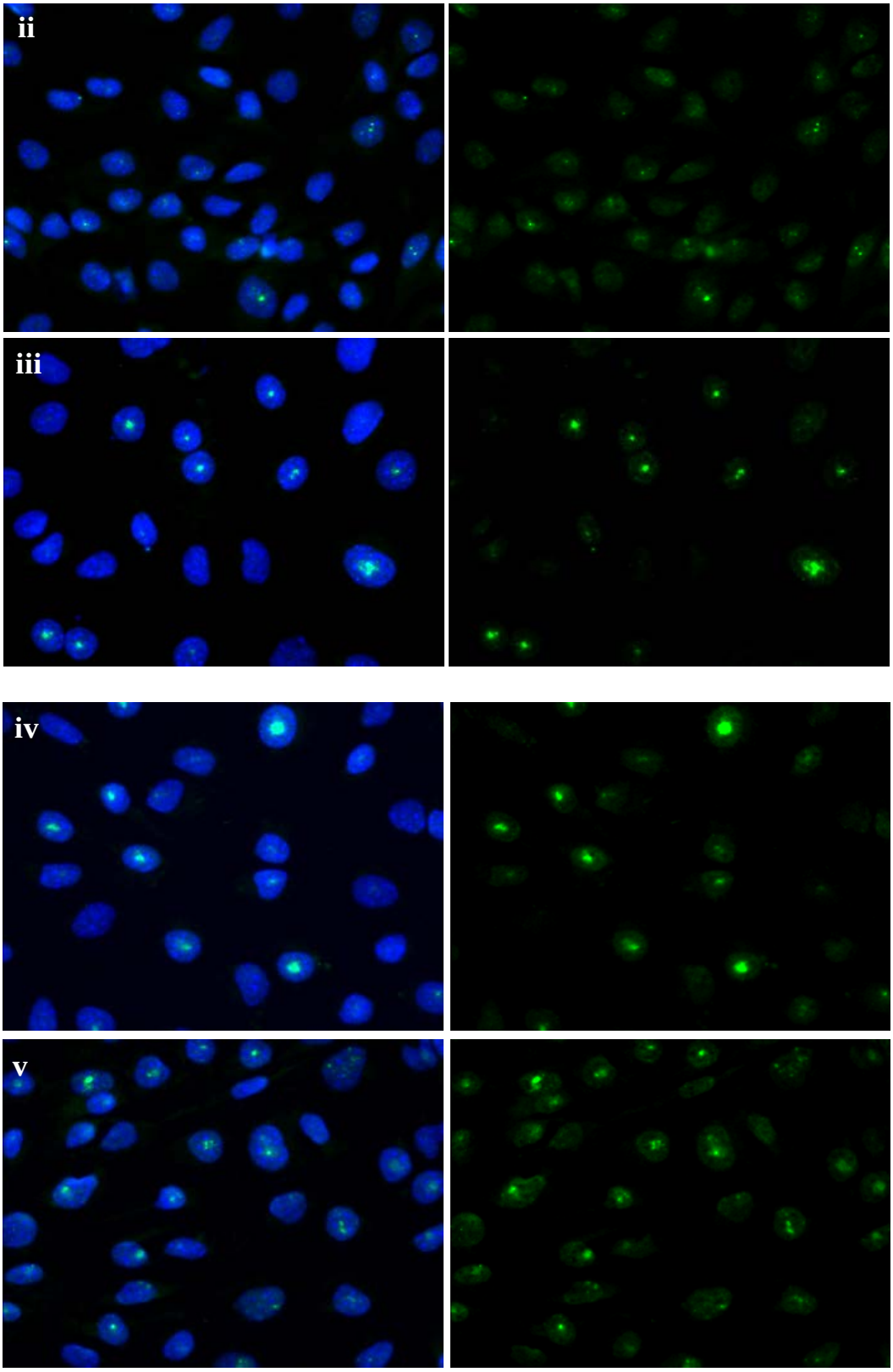

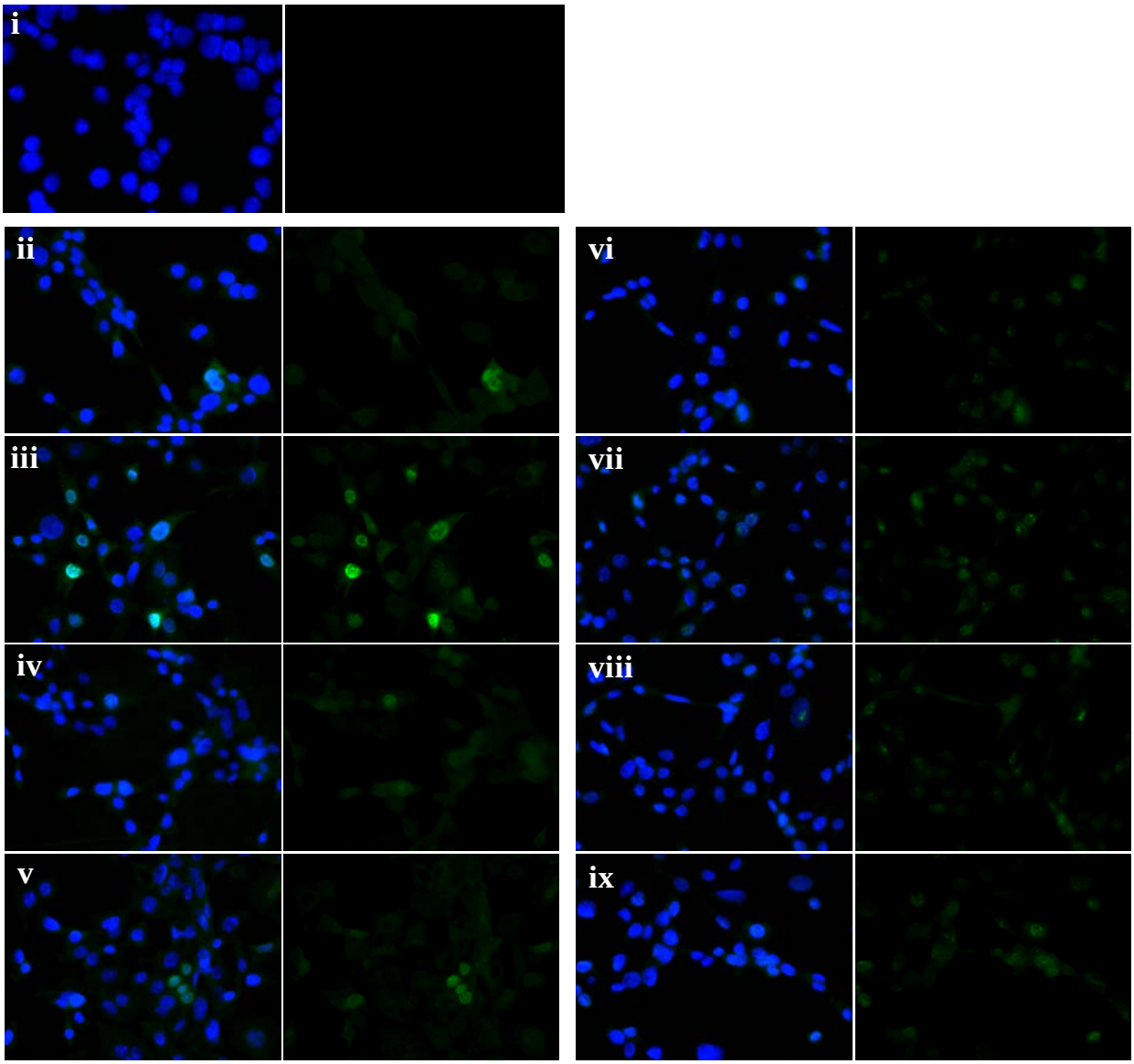

<u>Figure 3.15:</u> Immunofluorescence of MC7-L1 cells using no primary antibody, an antibody to detect PRA or an antibody to detect PRB. Immunofluorescence of MC7-L1 cells used no primary antibody (i), an antibody to detect PRA (hPRa7) (ii, iii, iv and v), or an antibody to detect PRB (B15) (vi, vii, viii and ix). MC7-L1 cells were treated with vehicle (ii and iv), estradiol ((E_2) iii and vii), R5020 ((R) iv and viii) or E_2+R (v and ix) for the 24 hours preceding fixation. Images are representative of 3 experiments.

corresponding receptor expression plasmid (pcDNA3.1(-).PRA or pcDNA3.1(+).PRB, respectively), confirming antibody specificity (Figure 3.S3; data not shown).

3. Developmental Study of the Mouse Mammary Gland: Colocalization of PR Isoforms with AP-1 Isoforms in Mammary Gland Tissue

Background

Expression of the mouse progesterone receptor (Pgr) gene is regulated not just by estrogen and progesterone (Shyamala G 1990); (Schott DR 1991); (Aupperlee MD 2007), but also by growth regulatory pathways that have the potential to signal through AP-1 and other transcription factors (Leonhardt SA 2003). Studies have shown that AP-1, especially the c-Jun/c-Fos heterodimer, plays an important role in up-regulating human PR via binding to an AP-1 site overlapping the PRB transcription start site (Petz LN 2002). Conversely, c-Jun/c-Fos binding to a similar AP-1 site overlapping the PRA mRNA start site is involved in down-regulating human PR (Petz LN 2004a). Changes in the expression pattern of individual AP-1 family members have not been systematically studied during mouse mammary gland development. The expression profile of AP-1 isoforms in the mouse mammary gland has only been studied during lactation and involution. In the AP-1 dimer, members of the Jun family show tissue specificity as well as differential expression during development in non-mammary tissues (Marti A 1994). Therefore, differential usage of AP-1 isoforms may lead to changes in the transcriptional activity of AP-1 responsive promoters, such as PR. Characterization of the relationship between AP-1 and PR may allow for a better understanding of the observed changes

in expression patterns of PR protein isoforms that occur during mammary gland development in the mouse.

Immunohistochemical analysis of lactating mouse mammary glands failed to detect c-Fos, c-Jun, phospho-c-Jun (Marti A 1999), or JunD (Jaggi R 1996). Electrophoretic mobility shift assay (EMSA) detected no binding on an AP-1 site in the lactating mammary gland (Marti A 1994). After 1 or 2 days of involution, AP-1 dimers consisted mostly of JunD/c-Fos, with some complexes also containing JunB, but not c-Jun (Marti A 1994). Immunohistochemical analysis of mammary glands at 2 days of involution detected nuclear c-Fos and JunD (Jaggi R 1996), while in another study at 3 days of involution, nuclear c-Fos, c-Jun and phospho-c-Jun were all detected (Marti A 1999). Since the number of luminal epithelial cells expressing PR is low (10-12 %) in mouse mammary gland during involution (Aupperlee M 2005a) at a time of low c-Jun expression, this is consistent with the notion that c-Jun may play a role in regulating PR expression.

AP-1 is known to regulate many physiological functions including proliferation, apoptosis, survival and differentiation (Shaulian E 2002). In the normal mammary gland, AP-1 controls the postnatal regulation of epithelial cell proliferation (Shen Q 2006). Whereas studies examining the role of AP-1 in tumorigenesis have found that in human mammary carcinomas, Fra-1 shows an inverse correlation with PRB (Bamberger AM 2000). Studies also confirmed earlier findings that most tumors have an altered PR ratio, expressing more PRA than PRB protein (Bamberger AM 2000). Another group tested neoplastic breast tissue and found that it was positive for nuclear Fra-1, regardless of whether it was benign or malignant tissue (Song Y 2006). Whereas adjacent normal tissue had much weaker nuclear staining in only a subset of the epithelial cells (Song Y 2006). In 90% of breast carcinomas studied, there was a shift from

exclusively nuclear Fra-1 staining to the simultaneous expression of Fra-1 in the nucleus and cytoplasm (Song Y 2006). Fra-1 expression is much more stable than c-Fos expression, possibly due to Fra-1 hyper-phosphorylation in exponentially growing cells (Song Y 2006). Fra-1 has been shown to be important for cell motility, invasion, and invasiveness in ER^+ MCF-7 cells and ER-negative MDA-MB231 cells (Belguise K 2005). Furthermore, since high Fra-1 expression is associated with a more malignant phenotype (Belguise K 2005), these studies establish Fra-1 as an important player in breast cancer progression.

Expression of the other AP-1 isoforms was determined for human mammary tumors, while c-Jun shows weak protein expression levels, JunB expression was moderate and Fra-2 levels were moderate to strong (Bamberger AM 1999). The protein levels of JunD varied greatly between specimens, with no clear pattern (Bamberger AM 1999). Since c-Jun is often the predominant Jun isoform in normal tissues, over-expression of c-Jun was tested in MCF-7 cells and leads to a tumorigenic, invasive, hormone resistant phenotype that is associated with an increase in Fra-1 expression and a loss of ER (Smith LM 1999).

In summary, since both AP-1 and PR play important roles in normal mammary gland development and tumorigenesis, their colocalization during mouse mammary gland development will be important in extrapolating their combined role in both the normal gland and in breast cancer. Human PR promoter studies demonstrated the importance of c-Jun/c-Fos in regulating PR (Petz LN 2002); (Petz LN 2004a) and tumorigenesis of the mammary gland (Bamberger AM 2000); (Song Y); (Belguise K 2005); (Bamberger AM 1999). Additionally, both Jun and Fos isoforms can play a role in normal mouse mammary gland development (Shen Q 2006). Thus, we hypothesized that AP-1, particularly a Jun isoform, would be important in the regulation of PR in the mouse mammary gland, specifically that the PRA and PRB promoters would respond

differently to the various hetero- and homodimers formed by the Jun and Fos isoforms. We examined the pattern of AP-1 isoform expression in mouse mammary gland during key stages of development and attempted to correlate this with expression of the PRA or PRB proteins. *In vivo* analysis was performed at three developmental stages of the BALB/c mouse mammary gland: pubertal, virgin adult, and age matched virgin adult mice treated for 14 days with E_2+P to provoke lobuloalveolar development. Dual-immunofluorescence was performed with rabbit antibodies specific for each Jun or Fos isoform (c-Jun, JunB, JunD, c-Fos, Fra1) or pan Jun together with the hPRa7 antibody which specifically detects only PRA (Aupperlee M 2005a); (Figure 3.S2). For PRB detection, a custom antibody (B15) raised against the first 15 amino acids of mouse PRB was used (Kariagina A 2007); (Figure 3.S2). PRB staining was performed only in 14 day E_2+P tissues, and since the available AP-1 antibodies were from rabbit, it was necessary to analyze serial sections due to lack of a PRB-specific antibody that was raised in a species other than rabbit.

Expression of Jun invariably correlates with that of PRA

Dual-immunofluorescence analysis of mouse mammary glands was carried out with a PRA antibody along with a pan Jun antibody. The pan Jun antibody detects an epitope in the Jun DNA binding domain, which is highly conserved between Jun family members and recognizes c-Jun, JunB, and JunD. In total, 49% of luminal epithelial cells were pan Jun^+ in the pubertal mammary gland, which decreased across development to 33% in the pregnancy-like gland ($p<0.05$) (Figure 3.16b). Of the pan Jun^+ luminal epithelial cells, a large proportion was also PRA^+ ranging from 69% of pan Jun^+ cells in pubertal glands to 42% in 14 day E_2+P treated

mice ($p<0.05$) (Figure 3.16a, b). There was a significant population of PRA-negative luminal epithelial cells that clearly expressed one or another Jun isoform based on pan Jun antibody staining, accounting for 31% of pan Jun^+ cells in pubertal mice, which increased across development to 58% in 14 day E_2+P treated mice ($p<0.05$). Virtually all of the PRA^+ cells (99-100%) were positive with the pan Jun antibody (Figures 3.16a, b). This supports the hypothesis that Jun is indeed important for efficient PRA expression. Of note, the proliferative cap cell layer displayed especially intense staining for pan Jun in terminal end buds (TEBs) of the pubertal mammary gland, which is PRA-negative (Figure 3.16a; data not shown).

c-Jun, JunB, and JunD Expression Vary During Mammary Gland Development

Since Jun correlated highly with PRA expression, we next sought to determine which Jun isoform(s) were expressed across developmental states in the mouse mammary gland. Based on the human PR promoter studies and the known transcriptional activity of the various Jun isoforms, it was hypothesized that c-Jun would constitute the predominant Jun isoform during development.

(a) c-Jun/PRA

c-Jun had the most widespread expression pattern of the Jun isoforms with only a minor difference in its expression between the various structures examined (small ducts, large ducts, TEBs, and lobules) (Figures 3.17a, b). In the pubertal and virgin adult mouse mammary gland, the percentage of c-Jun^+ alone or c-Jun^+/PRA^+ cells was essentially the same for luminal epithelial cells (Figure 3.17b). Compared to the pubertal and virgin adult mouse, the percentage of PRA^+ cells dramatically decreased in the pregnancy-like mammary gland (14 days E_2+P);

(a)

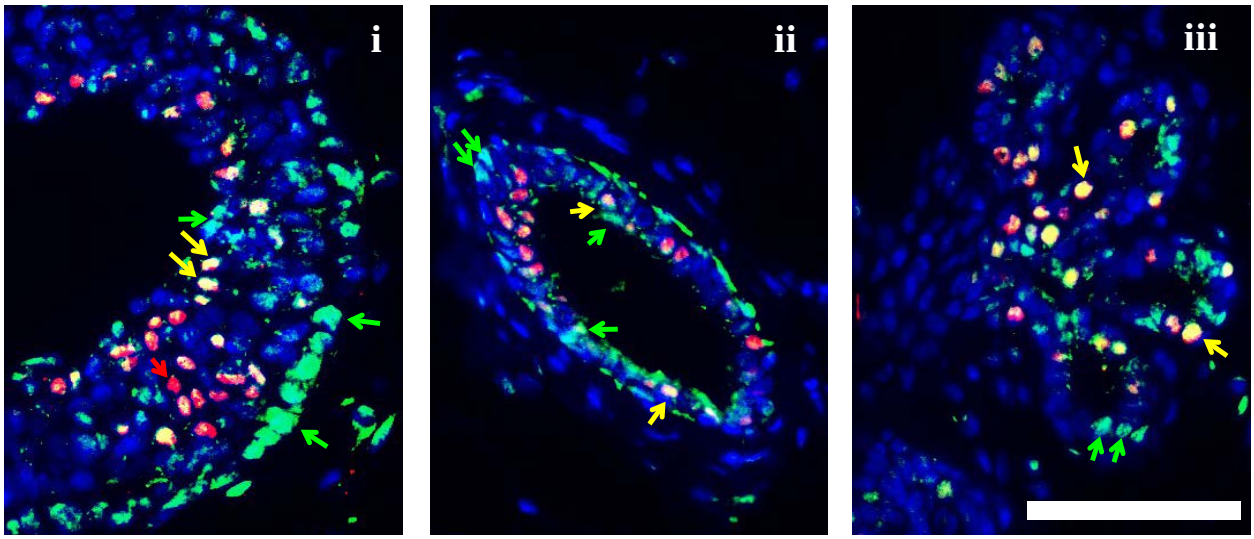

(b)

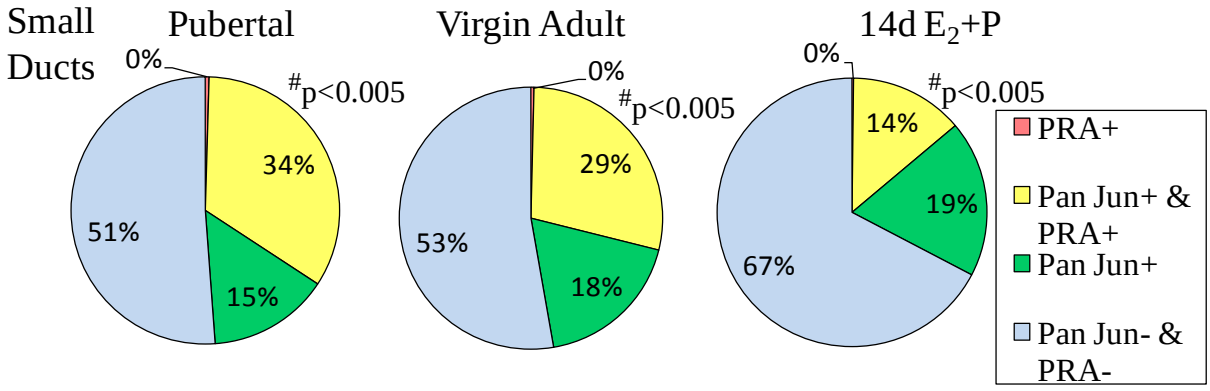

<u>Figure 3.16:</u> Developmental Profile of Pan Jun Expression and Colocalization with PRA. (a) Immunofluorescence staining was performed with mammary gland tissue from BALB/c mice and used an antibody to detect PRA (hPRa7) (red) or pan Jun (sc-44) (green). Nuclei were counterstained with DAPI (blue). Red arrows indicate PRA-positive cells, green arrows represent pan Jun-positive cells and yellow arrows show representative cells that are both PRA and pan Jun-positive (scale bar, 25 µm). (i) Terminal end bud in a pubertal mouse (6 weeks). Note the abundance of green pan Jun-positive cells in the PR-negative cap cell layer. (ii) Small duct in a virgin adult mouse (19 weeks). (iii) Lobule in an age-matched virgin adult mouse treated for 14 days with E_2+P.

(b) Quantitation values represent the mean ± SEM from three to four mice per group and a minimum of 500 cells/structure type/mouse analyzed. For statistical analysis a two-tailed Fischer's exact test was used for each structure type at each stage of development. Colocalization is statistically significant if $p<0.05$, with the level of significance indicated. The distribution of pan Jun and PRA in large ducts, terminal end buds, and lobules mirrored the pattern shown for small ducts (data not shown).

(Figure 3.17b), as has been previously reported in the mid-pregnant mouse mammary gland by Aupperlee, et *al*. (Aupperlee M 2005a). As a result, the percentage of c-Jun$^+$/PRA$^+$ luminal epithelial cells was also decreased in the pregnancy-like mammary gland, largely due to the decrease in PRA$^+$ cells (Figures 3.17a, b). For all three structures at all three developmental stages, there was a significantly higher percentage of c-Jun$^+$/PRA$^+$ cells than expected by chance (Fisher's exact test, $p<0.05$); (Figure 3.17c). Although c-Jun expression was not sufficient for PRA expression, it tended to colocalize in a relatively large proportion of cells such that its expression appears to correlate with other transcription factors that can up-regulate PRA, such as ERα (Kraus WL 1994); (Petz LN 2002); (Petz LN 2004a).

(b) JunD/PRA

The total number of JunD$^+$ cells (JunD$^+$ alone + JunD$^+$/PRA$^+$) was highest in the virgin adult and pubertal mouse and lower in the pregnancy-like mouse mammary gland ($p<0.05$); (Figure 3.18a). Reflecting this trend, the percentage of cells that expressed JunD in the absence of PRA was similar in the pubertal and virgin adult mouse, but decreased in hormone treated adult mammary gland (Figure 3.18a, b) (whereas the percentage of PRA-expressing cells also tended to decrease across these stages). The frequency of colocalization between JunD and PRA was also significantly greater than expected by chance for all three structures and all three developmental stages ($p<0.05$); (Figure 3.18b). This suggests that although JunD was not sufficient for PRA expression, JunD may contribute to the regulation of PRA, especially in the pubertal and virgin adult mammary gland where JunD showed the highest degree of colocalization with PRA.

(a)

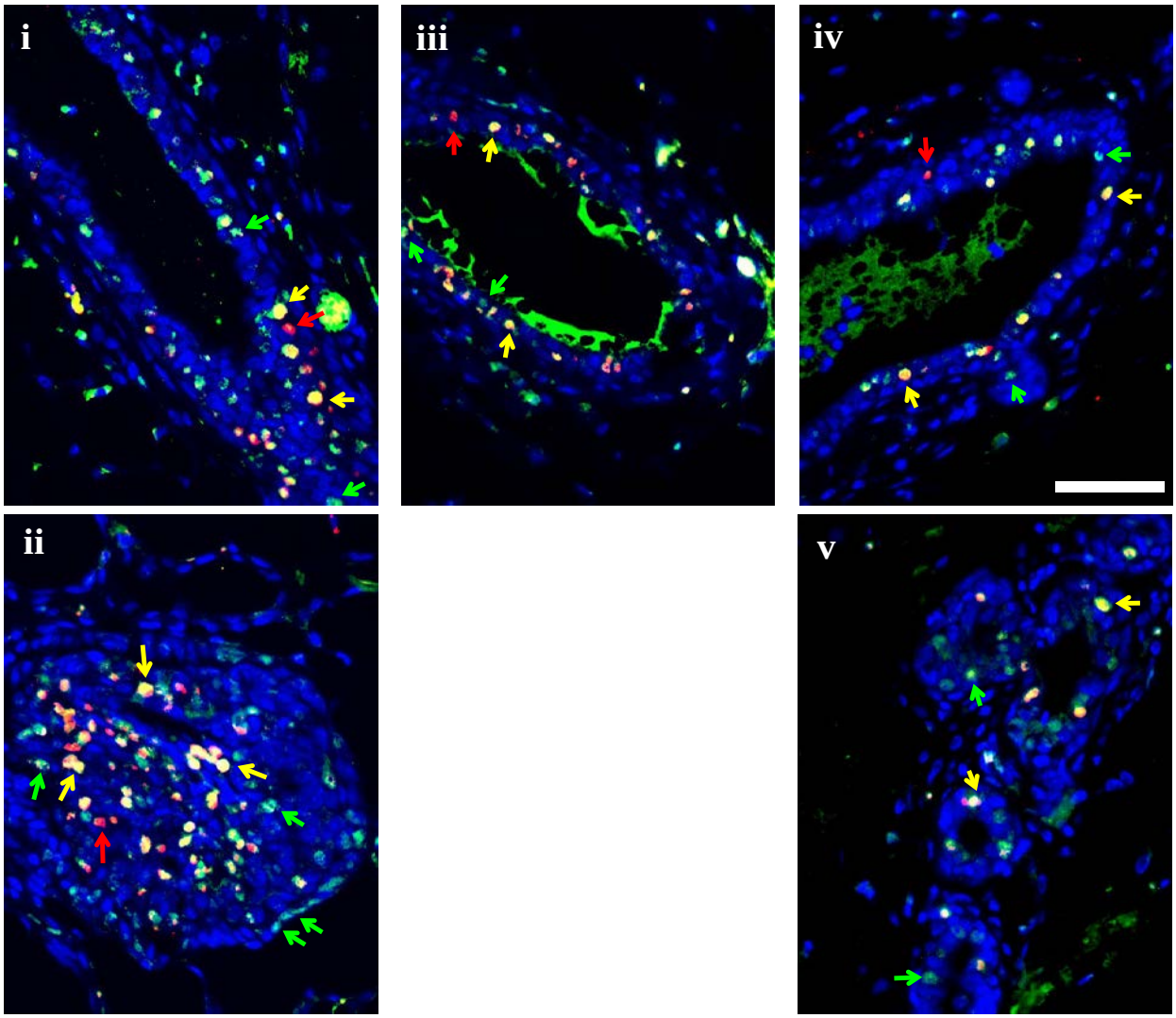

<u>Figure 3.17:</u> Developmental Profile of c-Jun Expression and Colocalization with PRA.
(a) Dual-immunofluorescence detection of mammary gland tissue from BALB/c (i, ii) pubertal (6 weeks), (iii) virgin adult (19 weeks) and (iv, v) age-matched virgin adult mice treated for 14 days with E_2+P. Immunofluorescence staining used an antibody to detect PRA (hPRa7) (red) or c-Jun (sc-1694) (green). Nuclei were counterstained with DAPI (blue). Arrows indicate representative cells: red arrow is a PRA^+ only cell, green arrow is a $c\text{-}Jun^+$ only cell and yellow arrow is a $c\text{-}Jun^+/PRA^+$ cell. Panel ii represents a terminal end bud, while panel v shows a mammary lobule (scale bar, 25 µm).
(b) Quantitation values represent the mean ± SEM from four to six mice per group and a minimum of 1000 cells/structure type/mouse analyzed.
(c) For statistical analysis a two-tailed Fischer's exact test was used for each structure type at each stage of development. Colocalization is statistically significant if $p<0.05$, with the level of significance indicated. The distribution of c-Jun and PRA in large ducts mirrored the pattern shown for small ducts (see part b; data not shown).

Figure 3.17 (Cont'd.)

(b)

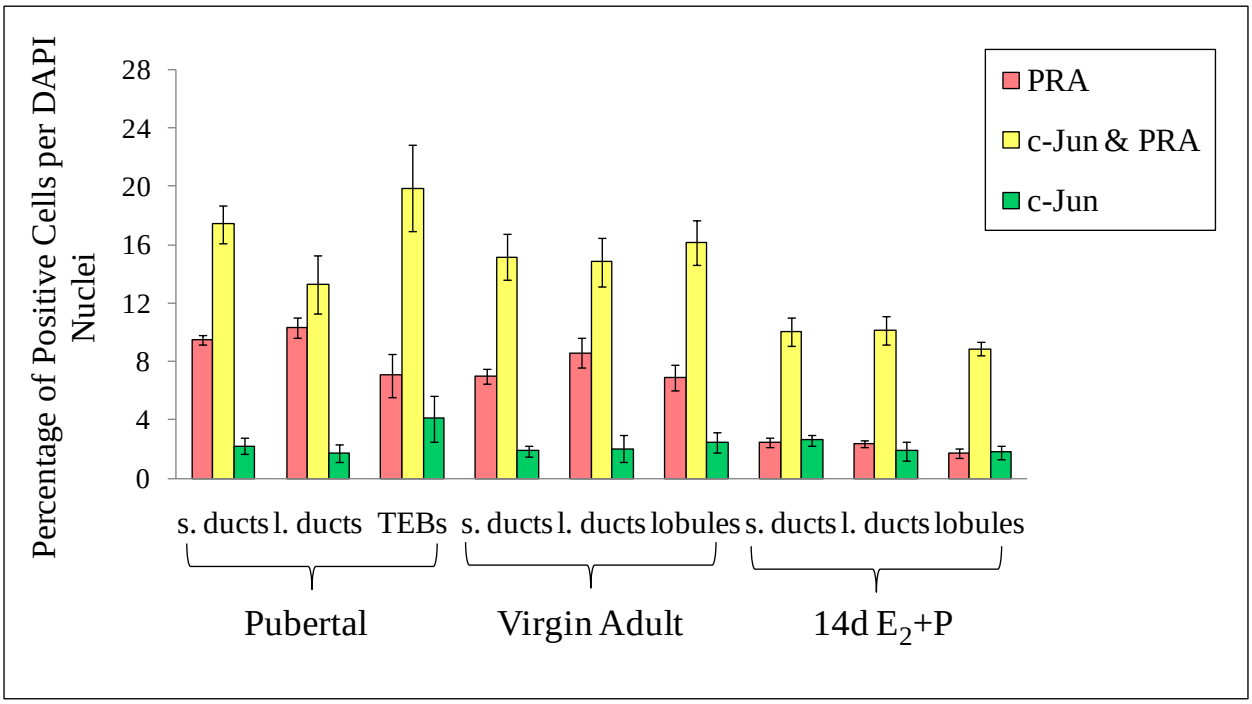

(c)

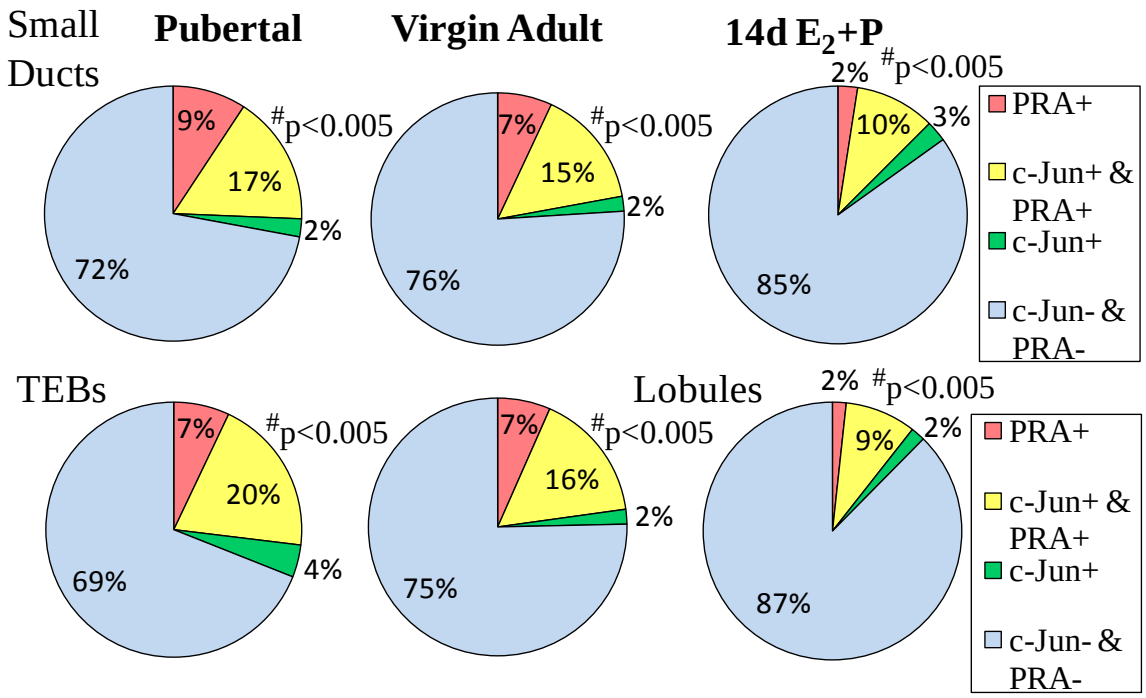

(c) JunB/PRA

The total percentage of $JunB^+$ positive cells ($JunB^+$ alone + $JunB^+/PRA^+$) significantly decreased across development in all structures examined ($p<0.05$); (Figure 3.19a). The percentage of cells that expressed JunB in the absence of PRA decreased during development with the lowest percentage seen in the pregnancy-like mouse mammary gland (Figure 3.19a, b). Although the percentage of $JunB^+$ cells that colocalized with PRA was the lowest compared to the other Jun isoforms, this frequency of colocalization remained significant in all structures at all developmental stages ($p<0.05$); (Figure 3.19b). JunB may therefore also contribute to PRA regulation but alone was not sufficient for its expression, similar to the pattern observed for c-Jun and JunD.

Using the pan Jun antibody that detects all of the Jun isoforms, we expected to see that the number of pan Jun^+ cells was either equal to the amount of c-Jun^+ cells (complete colocalization), equal to the sum of c-Jun^+, $JunB^+$ and $JunD^+$ cells (little to no colocalization) or somewhere in between. The percentage of pan Jun^+ cells was approximately equal to the sum of the c-Jun, JunB and JunD isoforms individually for all structures at all three developmental stages examined (Figure 3.16). Of particular interest was the proliferative cap cell layer of the TEB where there was a highly Jun^+ population of cells detected with the pan Jun antibody (Figure 3.16). Closer examination of the cap cell layer using Jun isoform specific antibodies showed that the pan Jun staining was predominantly composed of JunB (5.5% of cap cells) and c-Jun (3.9%) (Figure 3.17; data not shown). JunD was a minor component of the cap cell layer, accounting for only 0.4% of total cap cells (data not shown). The vast majority of pan Jun^+, $JunB^+$ or c-Jun^+ cap cells were located on the leading edge of the cap cell layer (Figures 3.16, 3.17; data not shown).

(a)

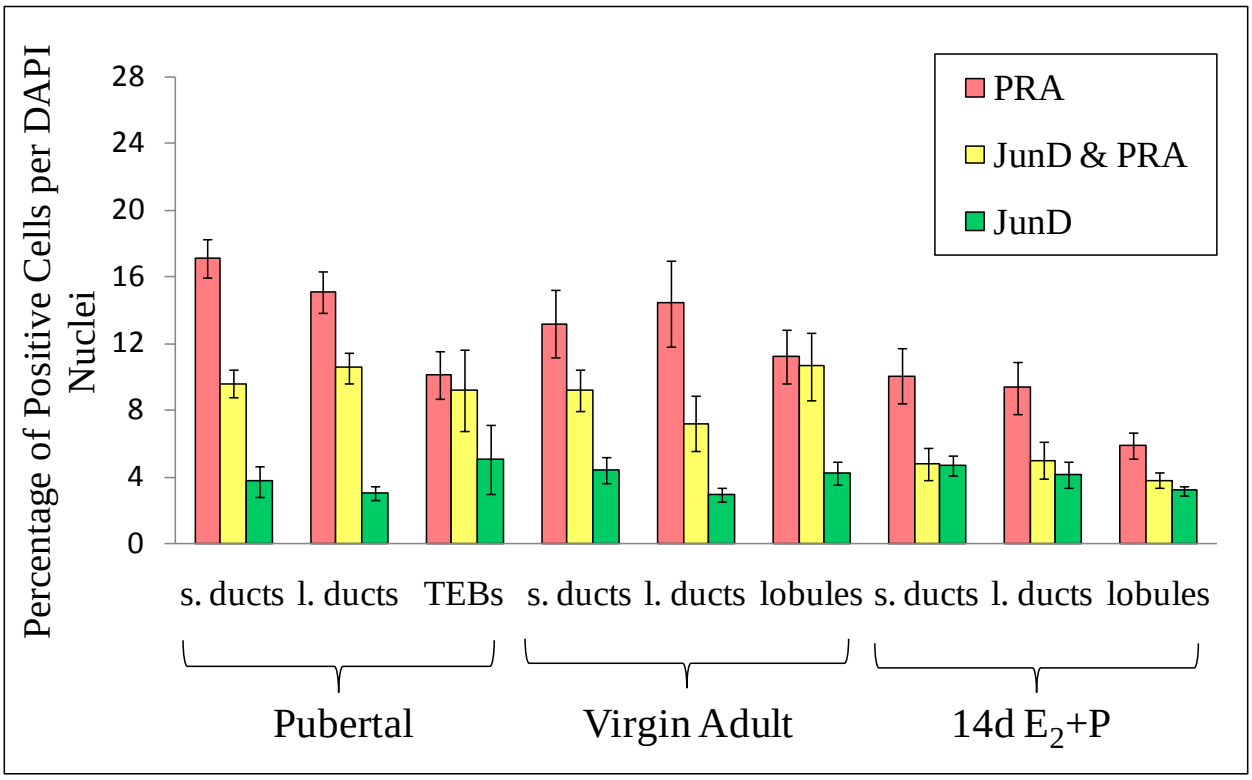

Figure 3.18: Developmental Profile of JunD Expression and Colocalization with PRA. Immunofluorescence of PRA utilized an anti-PRA antibody (hPRa7) on tissue sections from 6 week pubertal, 18 week virgin adult or in age-matched adult mice treated for 14 days with estradiol + progesterone (E_2+P) to achieve a pregnancy-like state. Colocalization with JunD used an anti-JunD antibody (sc-74). (a) Quantitation values represent the mean ± SEM from four to six mice per group and a minimum of 1000 cells/structure type/mouse analyzed.
(b) For statistical analysis a two-tailed Fischer's exact test was used for each structure type at the three developmental stages. Colocalization is statistically significant if $p<0.05$, with the level of significance indicated. The distribution of JunD and PRA in large ducts mirrored the pattern shown for small ducts (see part a; data not shown).

Figure 3.18 (Cont'd.)

(b)

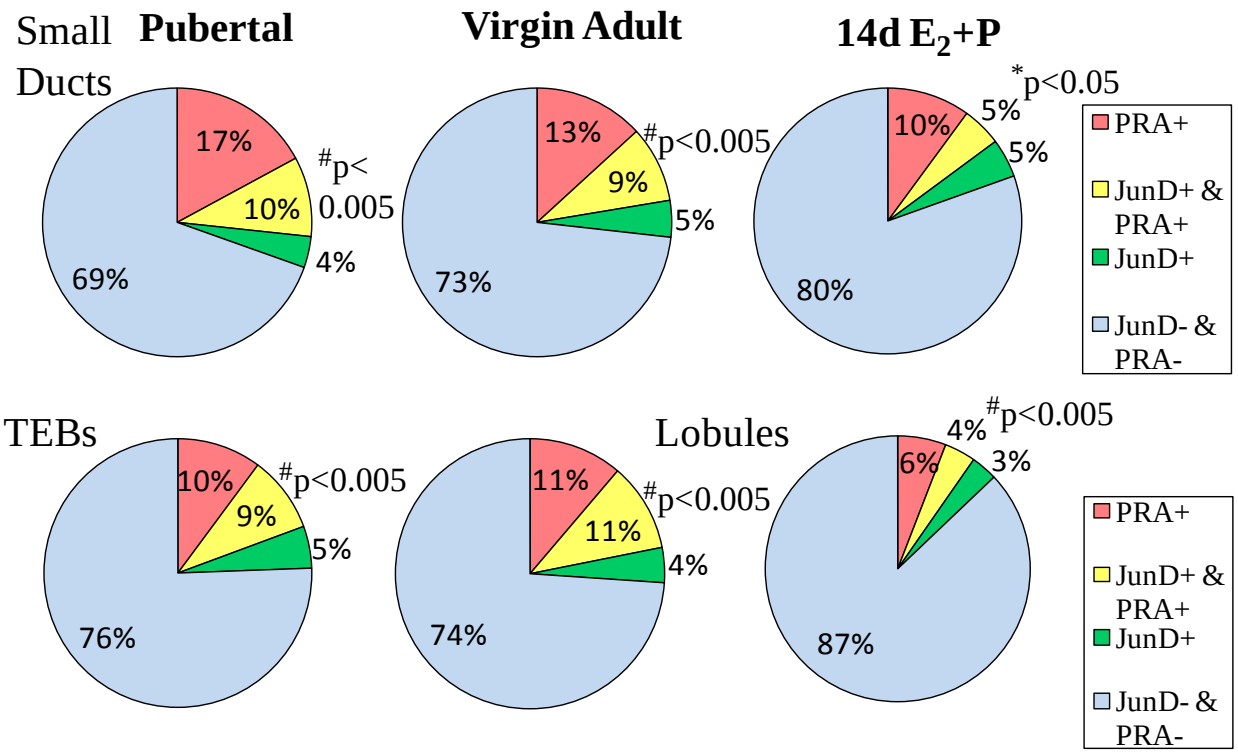

(a)

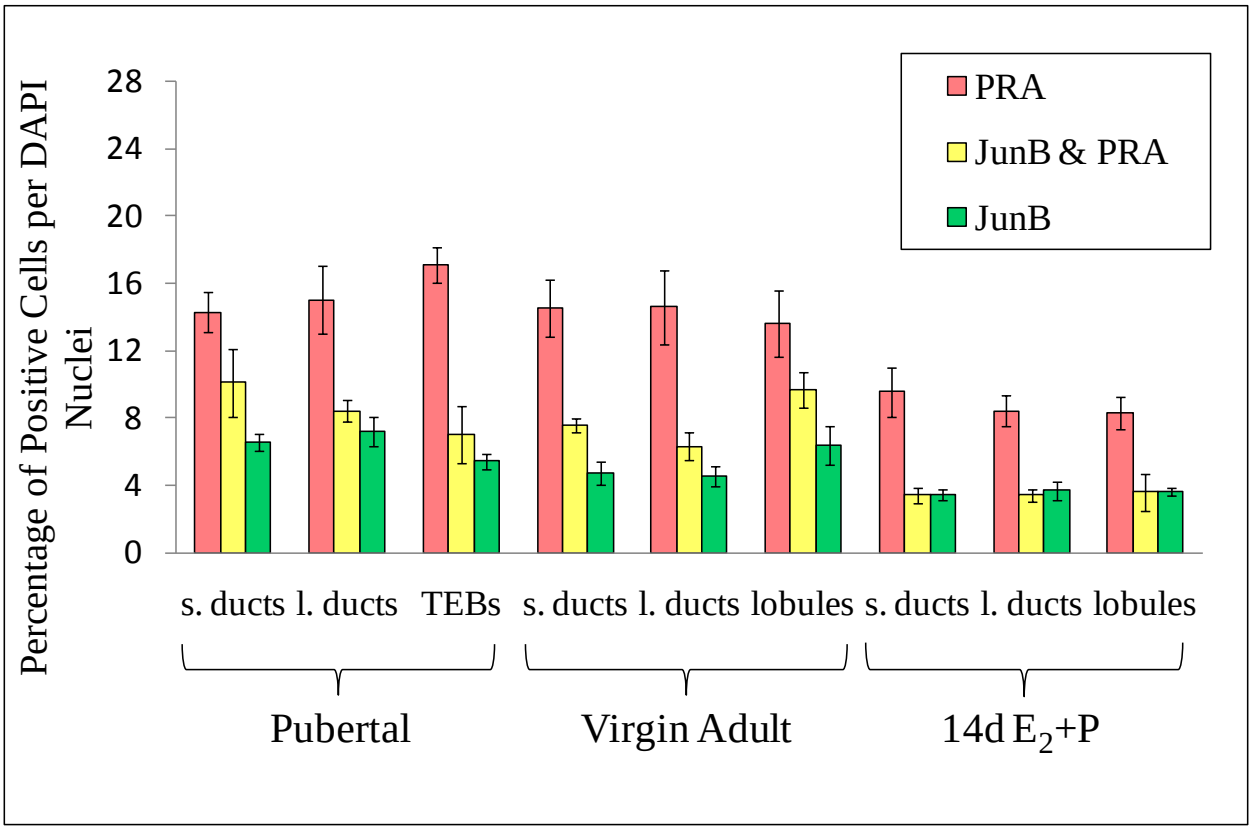

Figure 3.19: Developmental Profile of JunB Expression and Colocalization with PRA. Immunofluorescence of PRA utilized an anti-PRA antibody (hPRa7) on tissue sections from 6 week pubertal, 18 week virgin adult or in age-matched adult mice treated for 14 days with estradiol + progesterone (E_2+P) to achieve a pregnancy-like state. Colocalization with JunB used an anti-JunB antibody (sc-46). (a) Quantitation values represent the mean ± SEM from four to six mice per group and a minimum of 1000 cells/structure type/mouse analyzed.
(b) For statistical analysis a two-tailed Fischer's exact test was used for each structure type at the three developmental stages. Colocalization is statistically significant if $p<0.05$, with the level of significance indicated. The distribution of JunB and PRA in large ducts mirrored the pattern shown for small ducts (see part a; data not shown).

Figure 3.19 (Cont'd.)

(b)

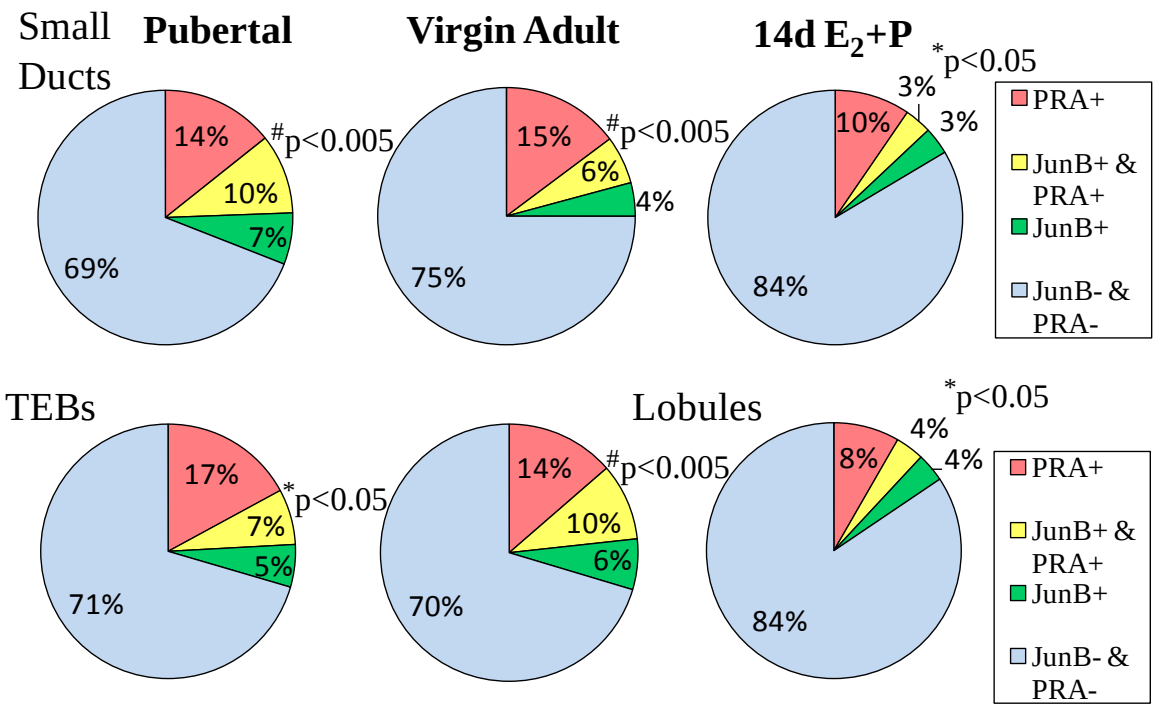

Fra1, not c-Fos, is the predominant Fos isoform

Since c-Jun expression was abundant and colocalized in the majority of cells with PRA, we hypothesized that c-Fos would also colocalize highly with PRA expression. Surprisingly, the percentage of total c-Fos (c-Fos$^+$ alone + c-Fos$^+$/PRA$^+$) positive luminal epithelial cells was extremely low in pubertal (1-2%), virgin adult (3-4%), and 14 day E_2+P treated mammary glands (5-8%) (Figures 3.20a, b). Cells that expressed c-Fos without PRA were rare in all three developmental stages, ranging from less than 1% to a maximum of 5% of total luminal epithelial cells (Figure 3.20b). Of all the AP-1 isoforms examined, c-Fos appeared to be the least abundant component of AP-1 dimers, especially in the pubertal and virgin adult mammary gland. The colocalization of PRA and c-Fos was random for all stages and structures examined (Figure 3.20b; data not shown).

Because the number of c-Fos$^+$ cells was so low, we examined other Fos family members such as Fra1. In the mouse mammary gland, the number of cells which expressed Fra1 was significantly higher at all stages and in all structures compared to cells that expressed c-Fos ($p<0.05$); (Figures 3.21a, b). The percentage of total Fra1 (Fra1$^+$ only + Fra1$^+$/PRA$^+$) positive cells was highest in the pubertal gland due to the large proportion of Fra1$^+$/PRA$^+$ cells (Figures 3.21a, b). The percentage of doubly positive Fra1/PRA-expressing cells was statistically different from each other at each developmental stage for each structure type ($p<0.05$) (Figure 3.21b). This trend towards decreased Fra1 expression overall during mammary development was also statistically significant for all developmental stages and in all structures ($p<0.05$) (Figure 3.21b). Of note, the percentage of cells that expressed Fra1 without PRA was highest in the pregnancy-like mammary gland (Figure 3.21b), suggesting an inverse correlation following hormone treatment.

(a)

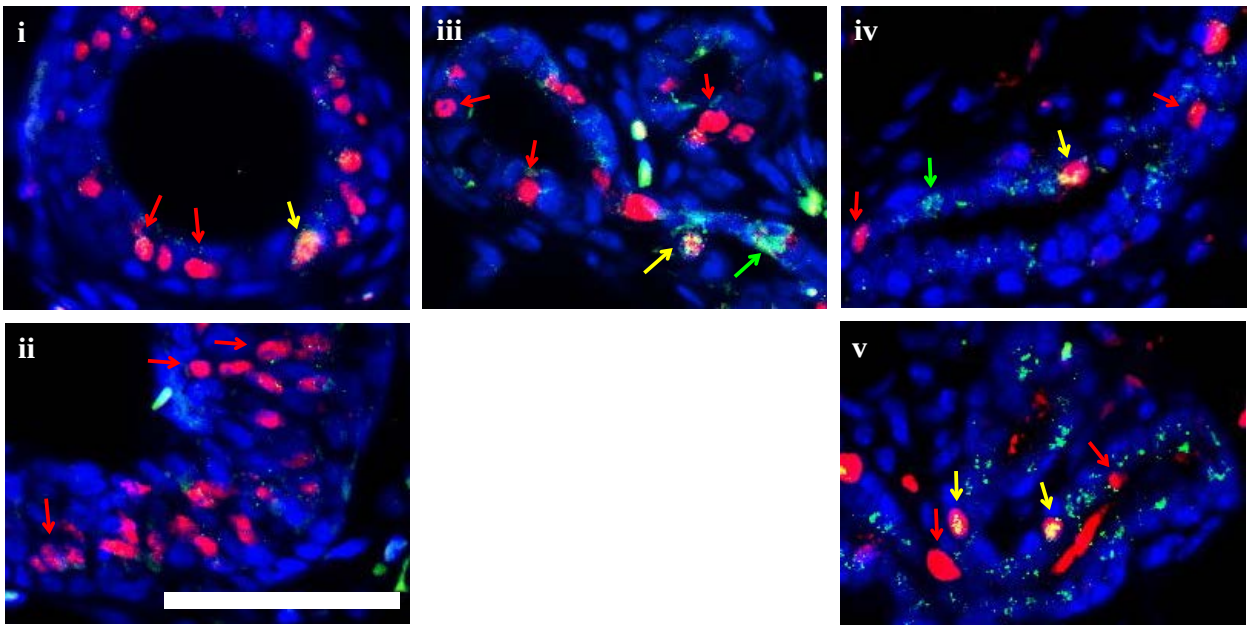

<u>Figure 3.20:</u> Developmental Profile of c-Fos Expression and Colocalization with PRA. Immunofluorescence of PRA utilized an anti-PRA antibody (hPRa7) on tissue sections from 6 week pubertal, 18 week virgin adult or in age-matched adult mice treated for 14 days with estradiol + progesterone (E_2+P) to achieve a pregnancy-like state. Colocalization with c-Fos used an anti-c-Fos antibody (sc-52). Red arrows indicate PRA^+ cells, green arrows show c-Fos^+ cells and yellow arrows show representative cells that are PRA^+/c-Fos^+ (scale bars, 25 µm). (a) Quantitation values represent the mean ± SEM from four to six mice per group and a minimum of 1000 cells/structure type/mouse analyzed. (b) For statistical analysis a two-tailed Fischer's exact test was used for each structure type at the three developmental stages. Colocalization is statistically significant if $p<0.05$, with the level of significance indicated.

Figure 3.20 (Cont'd.)

(b)

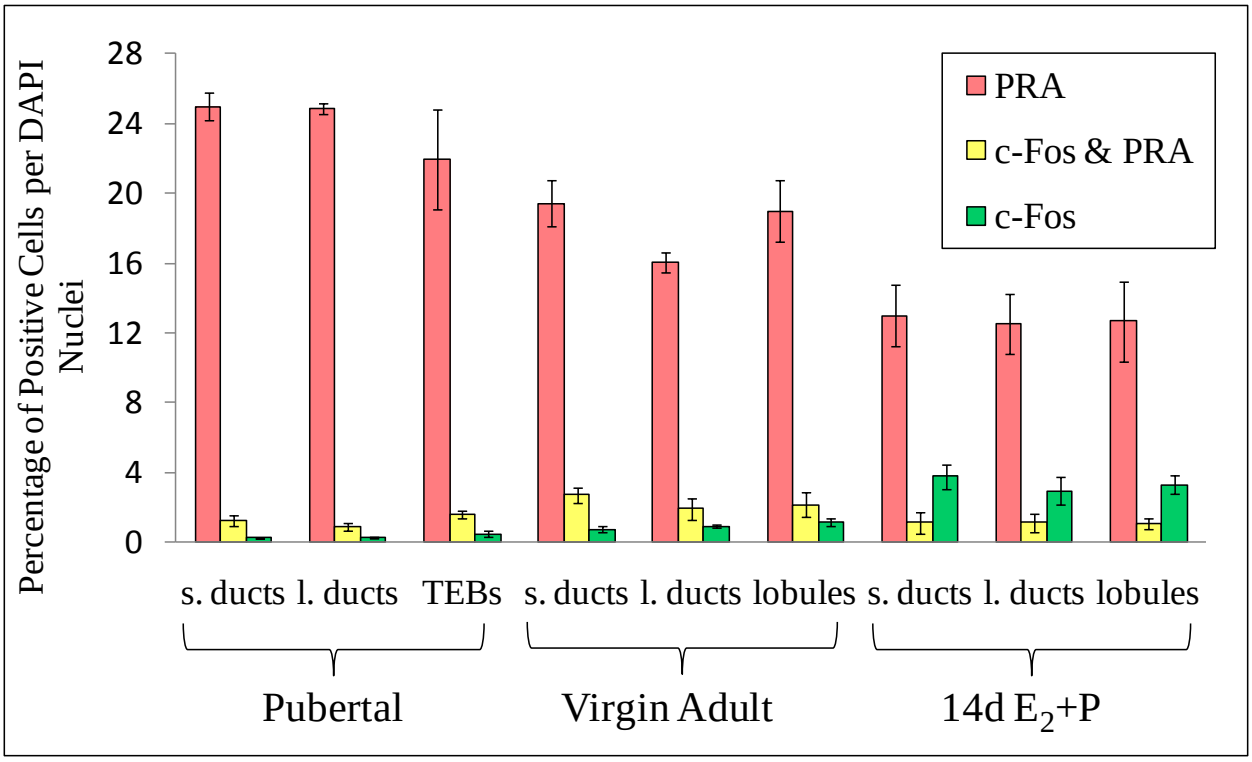

(a)

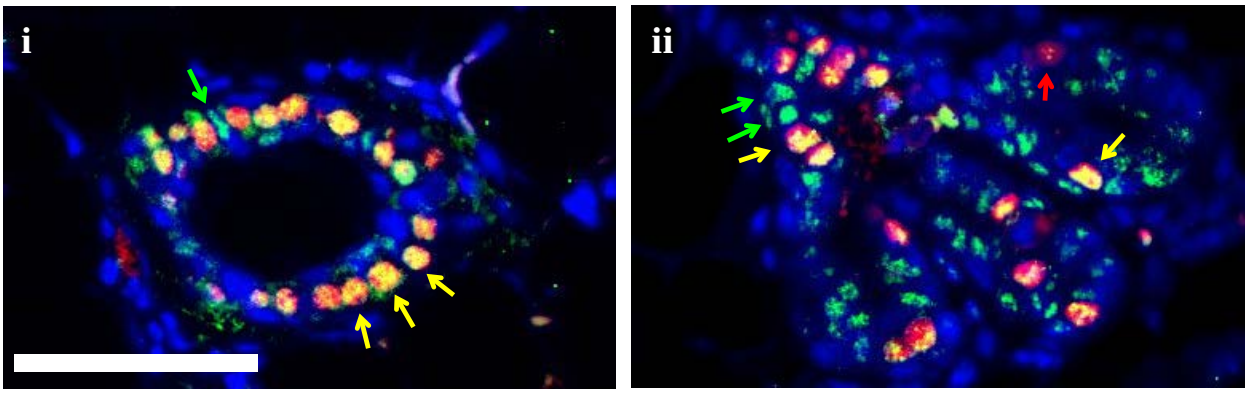

<u>Figure 3.21:</u> Developmental Profile of Fra1 Expression and Colocalization with PRA.
Dual-immunofluorescence detection of Fra1 and PRA in mammary gland tissue from BALB/c (i) pubertal (6 weeks) and (ii) 19 week old virgin adult mice treated for 14 days with E_2+P. Immunofluorescence staining used an antibody to detect PRA (hPRa7) (red) or Fra1 (sc-183) (green). Nuclei were counterstained with DAPI (blue).
(a) For the pubertal mouse, panel i represents a small duct, while for the 14 day E_2+P treated mouse, panel ii shows a mammary lobule. Red arrows indicate PRA^+ cells, green arrows show $Fra1^+$ cells and yellow arrows show representative cells that are $PRA^+/Fra1^+$ (scale bar, 25 µm).
(b) Quantitation also included 19 week old virgin adult mice and values represent the mean ± SEM from four to six mice per group. A minimum of 1000 cells/structure type/mouse were analyzed.

Figure 3.21 (Cont'd.)

(b)

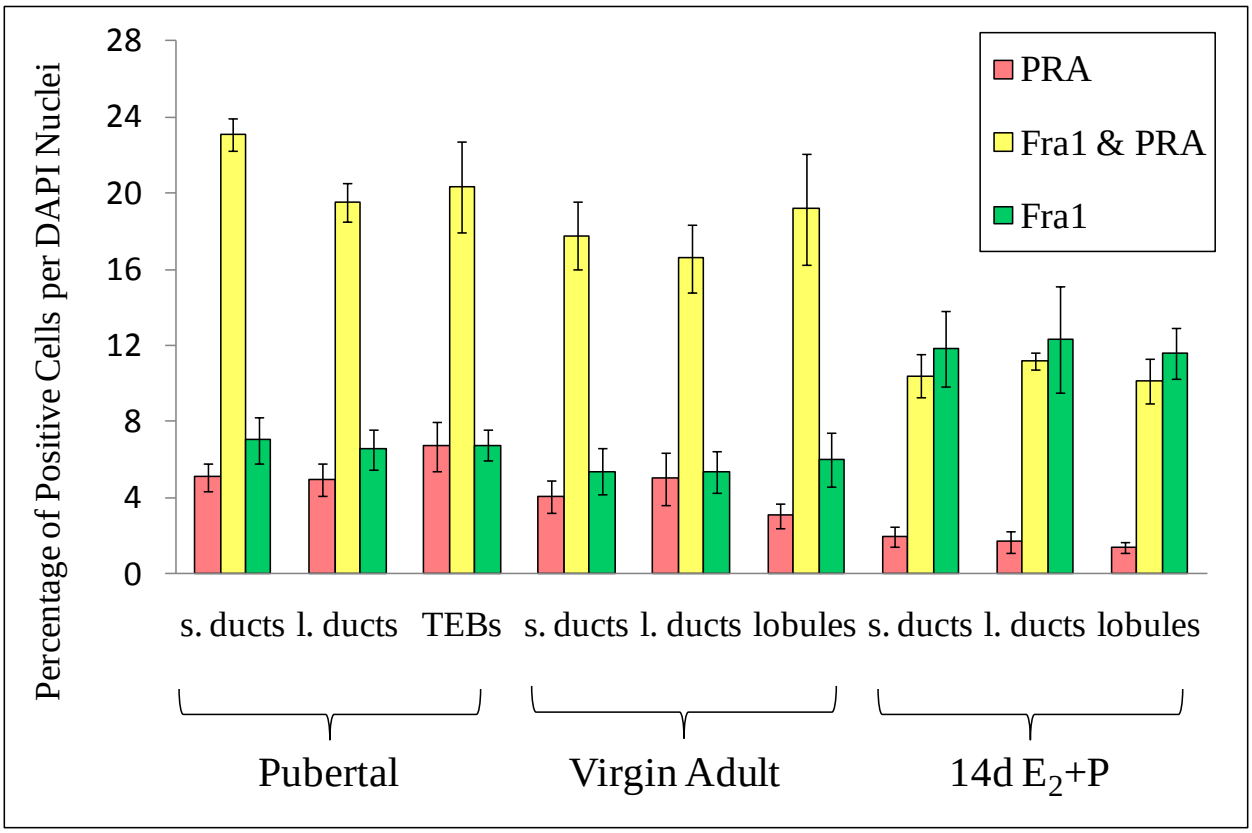

c-Jun and Fra1 Help Maintain PRA Expression in a Subset of PRB-Positive Cells After 14 Days of Treatment with E_2+P

Because both PRA and PRB isoforms are present in the mid-pregnant mouse (Aupperlee M 2005a), we investigated the abundance of PRB and PRA protein in the 14 day E_2+P treated mouse mammary gland and the relationship between AP-1 and PRB expression. A custom antibody (B15) raised against the first 15 amino acids of mouse PRB was generated (Kariagina A 2007) and compared against the hPRa7 antibody, which is reported to be specific for the PRA isoform (Aupperlee M 2005a).

Staining in the pregnancy-like mammary gland showed a relatively low percentage of PRA expressing luminal epithelial cells (10-12%) in which PRA almost invariably colocalized with PRB (Figure 3.22). As previously reported (Aupperlee M 2005a), the vast majority of PR^+ cells, representing 34-36% of luminal epithelial cells, expressed PRB in the absence of detectable PRA (Figure 3.22). The percentage of PRA^+/PRB^+ cells was greater than expected by chance alone in all structures examined ($p<0.05$); (Figure 3.22). Since almost all of the PRA^+ cells were also PRB^+, this suggests that in the pregnancy-like gland, PRB itself may contribute to the regulation of PRA expression along with other transcription factors. Neither PR isoform was absolutely required for expression of the other since PRA^+ and PRB^+ only cells were clearly observed at certain stages of development (Figures 3.17, 3.22).

Since cotransfection of a Jun isoform with and without a Fos isoform generally did not differ and there was a substantial population of $PRB^{+/}$PRA-negative cells, this suggests that one would expect a disconnect between the cells expressing PRB and AP-1. Although the PRA^+ cells were always PRB^+ in the pregnancy-like gland (Figure 7), there were not enough c-Jun^+/PRA^+, $Fra1^+/PRA^+$, or other $AP\text{-}1^+/PRA^+$ cells to account for the large number of PRB-expressing cells. Therefore, if there is a PR-specific role for AP-1 in the pregnancy-like

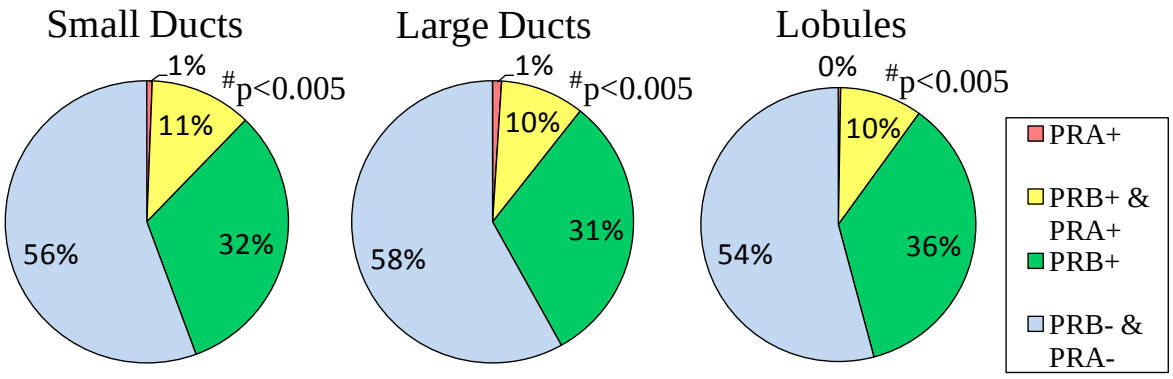

Figure 3.22: Profile of PRB Expression and Colocalization with PRA. Immunofluorescence of PRA utilized an anti-PRA antibody (hPRa7) on 18 week virgin adult mice treated for 14 days with estradiol + progesterone (E_2+P) to achieve a pregnancy-like state. Colocalization with PRB used a custom generated anti-PRB antipeptide antibody (B15).
Quantitation values represent the mean ± SEM from four mice per group and a minimum of 1000 cells/structure type/mouse analyzed. For statistical analysis, a two-tailed Fischer's exact test was used for each structure type in the 14 day E_2+P treated mouse. Colocalization was highly statistically significant ($p<0.005$), for all three structures examined.

mammary gland, it's in the maintenance of PRA expression, not in up-regulating PRB. Rather, in order to up-regulate PRB, AP-1 (specifically c-Jun and Fra1) may interact with other transcription factors that are highly expressed during mid-pregnancy such as signal transducer and activator of transcription 5a (Stat5a) (Santos SJ 2007) and CCAAT/Enhancer-Binding Protein β (C/EBPβ) (Grimm SL 2003).

4. Hormonal Effects on AP-1 Expression in the Mouse Mammary Gland and its Relation to Cell Proliferation: Colocalization of AP-1 with PRA and BrdU in Hormone Treated Mice

Background

The PR promoter from at least two species is reported to contain multiple hormone response elements (Petz LN 2002) (Kraus WL 1994) along with two functional AP-1 binding sites (Petz LN 2002); (Petz LN 2004a). Differential expression of AP-1 isoforms may lead to changes in transcriptional activity of AP-1 responsive promoters, such as PR. Additionally, the promoter regions of some AP-1 isoforms are themselves known to be responsive to hormone treatment, the best known of which is E_2 regulation of the c-fos promoter (Bjornstrom L 2005). The c-fos promoter is up-regulated via transcriptional interactions between ERα and Sp1 in the GC-rich region of the c-fos promoter (Bjornstrom L 2005), as well as by non-genomic mechanisms involving the mitogen-activated protein kinase (MAPK) and phosphoinositide (PI3)-kinase (PI3K) signaling pathways, which specifically target the Ets transcription factor family member Elk-1 and serum response factor (SRF) (Bjornstrom L 2005); (Janknecht R 1995). It has also been reported that c-Fos mRNA is transiently up-regulated in response to

acute P treatment (Musgrove EA 1991), but P regulation of the c-Fos protein has not been examined.

The effect that E_2 has on the c-Jun promoter *in vivo* in the context of the mouse mammary gland is unknown. Additionally, the role P plays in regulation of the c-Jun promoter has not been examined. The rat c-Jun promoter contains an estrogen response element (ERE) that is E_2-inducible in transient transfection assays in yeast and mammalian cells (H301 E_2-induced hamster kidney tumor cells) (Hyder SM 1995). Although the c-Jun ERE is imperfect compared to a consensus ERE, it is still capable of binding estrogen receptor (ER) in gel shift experiments (Hyder SM 1995). At a sequence level, the ERE half-sites within the rat and mouse c-Jun promoters are identical, as are their proximally flanking basepairs (Hyder SM 1995). In proliferating fibroblasts, the level of c-Jun protein is relatively constant during the cell cycle (Piechaczyk M 2008), therefore c-Jun levels are not expected to be drastically different between cycling cells in S phase versus any other stage of the cell cycle. However, since cell cycle progression in fibroblasts is E_2-independent, it is not known how the level of c-Jun proteins may differ during mammary gland development in luminal epithelial cells.

JunD protein on the other hand is reported to be down-regulated by E_2 in a JNK-dependent manner (Hernandez JM 2008). E_2 down-regulates the activity of JNK leading to decreased levels of phosphorylated JunD, which in turn decreases the expression of JunD mRNA (Hernandez JM 2008). Phospho-JunD also plays a role in the cell cycle by repressing transcription of cell proliferation target genes (i.e. p19) (Figure 3.29) and activating target genes involved in cell differentiation (Hernandez JM 2008). JunD differs from the other AP-1 isoforms in that, when tested in fibroblasts, it is the only isoform that is non-responsive to serum stimulation (Mechta-Grigoriou F 2001).

In ER^+ MCF-7 cells, microarray analysis identified JunB as one of the transcription factors down-regulated by E_2 (Frasor J 2003). The level of JunB mRNA was significantly decreased after 4 hours of E_2 treatment and remained down-regulated throughout the time course up through 48 hours of E_2 treatment (Frasor J 2003). Other studies have established that JunB opposes the pro-proliferative functions of c-Jun and c-Fos (Jochum W 2001), therefore E_2-dependent down-regulation of JunB is possibly a pre-requisite for S phase entry and cell cycle progression. Like other AP-1 isoforms, it is unknown if the JunB promoter is P-responsive or not. It is also unknown if the Fra1 promoter is under the control of either E_2 or P.

When normal cells are maintained in culture, the percentage of cells expressing Jun and Fos is generally low to moderate and each isoform has a distinct expression profile during cell cycle progression (Jochum W 2001). c-Jun positively regulates cell proliferation (specifically the transition from G_1 to S phase) by up-regulating cyclin D1 and repressing p53 (Schreiber M 1999); (Figure 3.29). c-Fos and FosB redundantly induce S phase entry and activate cyclin D1 expression (Jochum W 2001). Conversely, both JunB and JunD repress cell proliferation, antagonizing the effect of c-Jun (Jochum W 2001); (Figure 3.29). The expression of AP-1 isoforms varies greatly from normal mammary gland tissue to mammary carcinomas where overexpression of one or more AP-1 isoform is common (Bamberger AM 1999); (Bamberger AM 2000). Therefore, AP-1 expression levels in normal mouse mammary tissue are expected to represent an asynchronous cell population including cells that are both capable and incapable of proliferating, depending on their AP-1 expression profile.

Both the PR promoter and certain AP-1 promoters are known to be hormonally-responsive, but the PR promoter could also be differentially regulated by altering AP-1 dimer composition or AP-1 activity. In order to determine the effect of hormones on various AP-1

isoforms (c-Jun, JunB, JunD, c-Fos, Fra1) and the correlation with PRA expression, ovariectomized adult mice were treated with E_2, P, or E_2+P for 3 days. To investigate the relationship between AP-1 isoforms and proliferation, sections were double-labeled with antibodies against 5'-bromo-2'-deoxyuridine (BrdU) and c-Jun or c-Fos. Not only does c-Jun constitute the one of the major Jun isoforms expressed during mouse mammary gland development (Figure 3.17), but c-Jun is also required for cycle progression (Jochum W 2001). c-Fos, which also stimulates S phase entry (Jochum W 2001), constituted a much smaller proportion of luminal epithelial cells in the mouse mammary gland during development (Figure 3.20). However, this surprisingly small proportion of c-Fos$^+$ cells during development may under estimate the contribution of c-Fos to the AP-1 heterodimer, due to the rapid turnover of activated c-Fos protein (Gomard T 2008).

Expression of c-Fos in the Mouse Mammary Gland Requires Ovarian Steroids

Three days of E_2 or E_2+P treatment dramatically induced c-Fos expression from 0% in ovariectomized control mice to 25-31% of the total luminal epithelial cell population (Figures 3.23a, b); indicating that E_2 was sufficient to induce c-Fos expression in a subset of luminal epithelial cells. P treatment also induced the expression of c-Fos, but to a lesser extent than E_2 ($p<0.05$), accounting for 20% of luminal epithelial cells (Figures 3.23a, b). Treatment with E_2 increased the percentage of luminal epithelial cells co-expressing c-Fos and PRA (up to 28%, $p<0.05$), while P and E_2+P were slightly less efficient (up to 16-17%, $p<0.05$) (Figure 3.23b). After E_2 treatment, the vast majority of cells that expressed c-Fos (90%) co-expressed PRA (Figure 3.23b). Similarly after P treatment, 80% of c-Fos$^+$ cells also expressed PRA (Figure 3.23b). After E_2+P treatment 68% of the c-Fos expressing cells co-expressed PRA

protein accompanied by a small, but significant, increase in the percentage of cells expressing c-Fos without PRA compared to E_2 or P alone ($p<0.05$) (Figure 3.23b). PRA expression was not dependent on the presence of c-Fos since nearly 50% of luminal epithelial cells expressed PRA in ovariectomized control (Figures 3.23a, b). Although PRA expression was not dependent on the presence of c-Fos, the degree of colocalization between c-Fos and PRA was significant for E_2, P, or E_2+P treatment in both small and large ducts ($p<0.05$, Fischer's exact test) (Figure 3.23b).

c-Jun is Not Dependent on Hormones for Basal Expression

The number of total c-Jun-positive cells (c-Jun$^+$ alone + c-Jun$^+$/PRA$^+$) was slightly higher after E_2, P, or E_2+P treatments compared to ovariectomized control mice ($p<0.05$). There was a high degree of colocalization between c-Jun and PRA in ovariectomized control mice and those treated with E_2, P, or E_2+P and varied from 26-36% of the total luminal epithelial cell population (Figures 3.24a, b). Of the c-Jun$^+$ cells in control or E_2 treated mice, there was a 84-90% likelihood that the cell also co-expressed PRA (Figure 3.24b). In the E_2+P treated mice, c-Jun$^+$ cells colocalized with PRA in 79% of cells, while c-Jun$^+$ cells showed slightly lower colocalization with PRA in P treated mice (67%) (Figure 3.24b). Colocalization was highly significant between c-Jun and PRA in control and hormone treated mice ($p<0.05$) (Figure 3.24b). The expression of c-Jun was not hormone dependent since control ovariectomized mice expressed c-Jun protein in 31% of cells (Figures 3.24a, b). Hormone treatments did not influence the percentage of cells expressing PRA alone or both c-Jun and PRA. However, the percentage of cells expressing c-Jun alone was significantly higher after P or E_2+P treatment compared to control or E_2 treated mice ($p<0.05$) (Figure 3.24b). Nevertheless, there was a

(a)

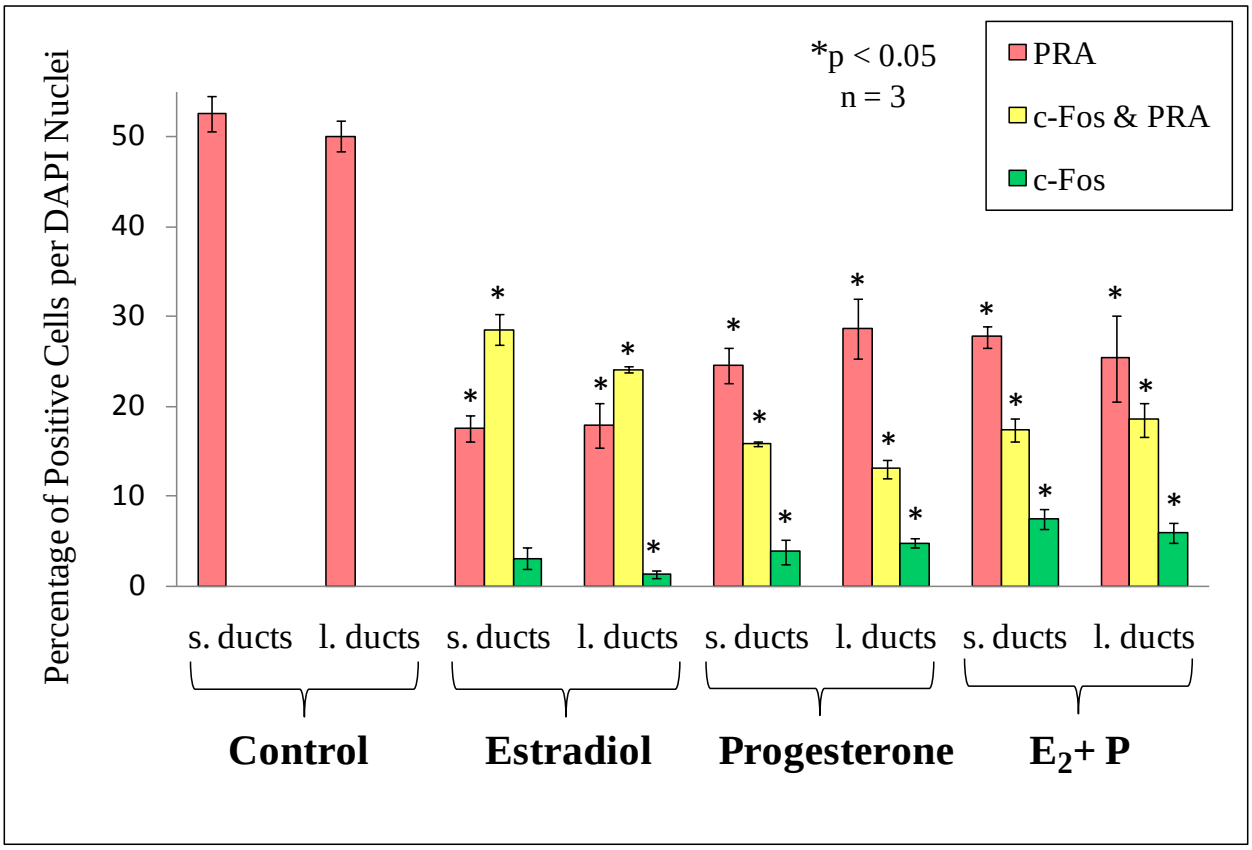

Figure 3.23: Hormonal regulation of c-Fos expression and colocalization with PRA. Immunofluorescence of PRA utilized an anti-PRA antibody (hPRa7) on tissue sections from 18-22 week virgin adult mice treated for 3 days with control, estradiol (E_2), progesterone (P) or E_2+P. Colocalization with c-Fos used an anti-c-Fos antibody (sc-52). Quantitation values represent the mean ± SEM from three to four mice per group and a minimum of 500 cells/structure type/mouse analyzed. (a) Statistical analysis utilized Student's *t* test and significance is denoted: *p<0.05. (b) For statistical analysis a two-tailed Fischer's exact test was used for each structure type for each treatment. Colocalization is statistically significant if p<0.05, with the level of significance indicated. The distribution of c-Fos and PRA in large ducts mirrored the pattern shown for small ducts (data not shown).

Figure 3.23 (Cont'd.)

(b)

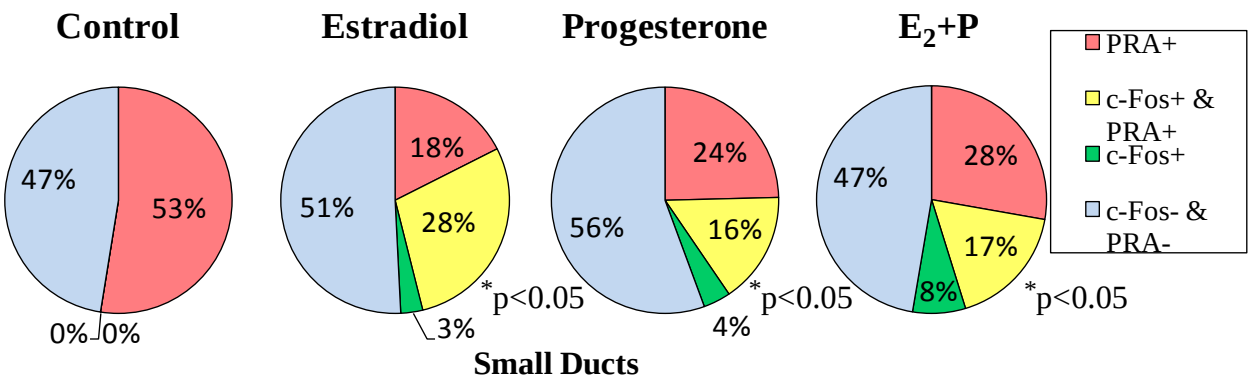

(a)

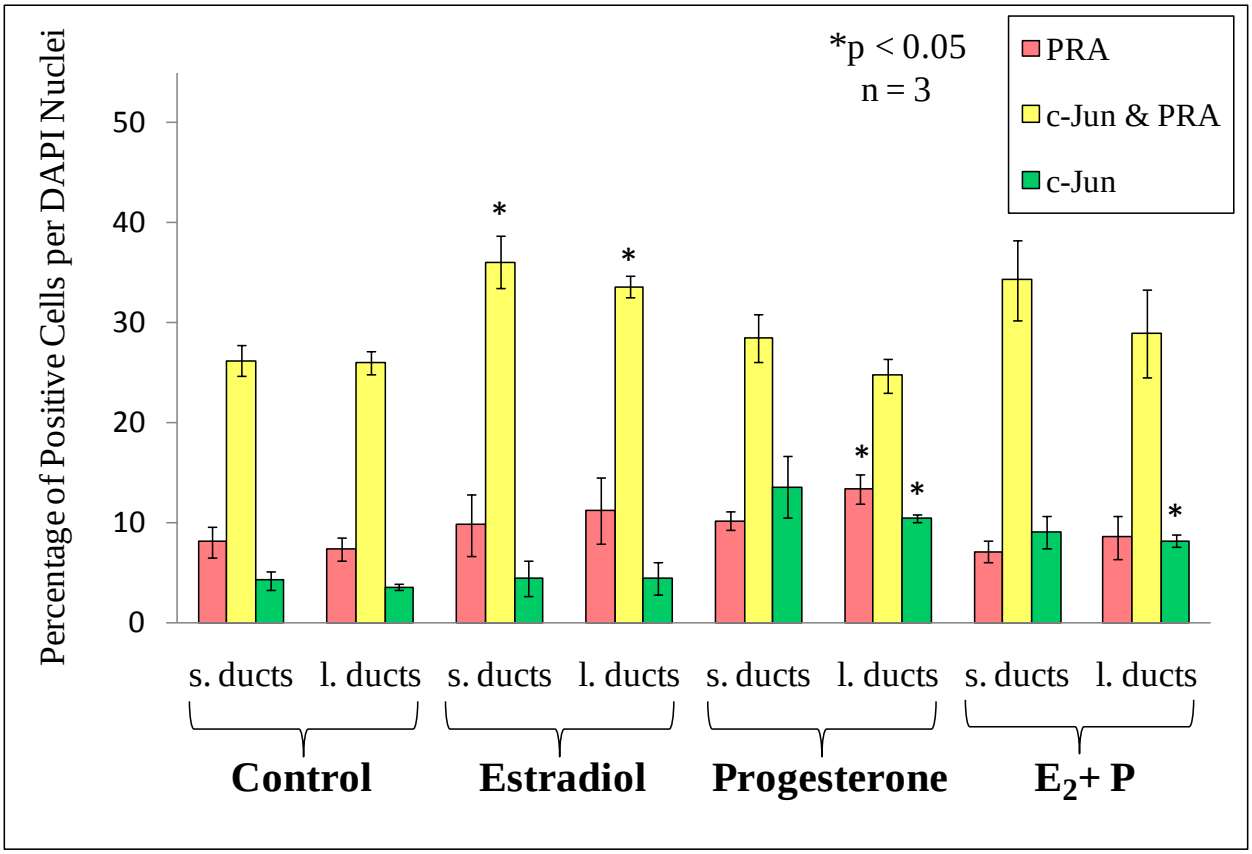

Figure 3.24: Hormonal regulation of c-Jun expression and colocalization with PRA. Immunofluorescence of PRA utilized an anti-PRA antibody (hPRa7) on tissue sections from 18-22 week virgin adult mice treated for 3 days with control, estradiol (E_2), progesterone (P) or E_2+P. Colocalization with c-Jun used an anti-c-Jun antibody (sc-1694). Quantitation values represent the mean ± SEM from three to four mice per group and a minimum of 500 cells/structure type/mouse analyzed. (a) Statistical analysis utilized Student's *t* test and significance is denoted: *p<0.05. (b) For statistical analysis a two-tailed Fischer's exact test was used for each structure type for each treatment. Colocalization is statistically significant if p<0.05, with the level of significance indicated. The distribution of c-Jun and PRA in large ducts mirrored the pattern shown for small ducts (data not shown).

Figure 3.24 (Cont'd.)

(b)

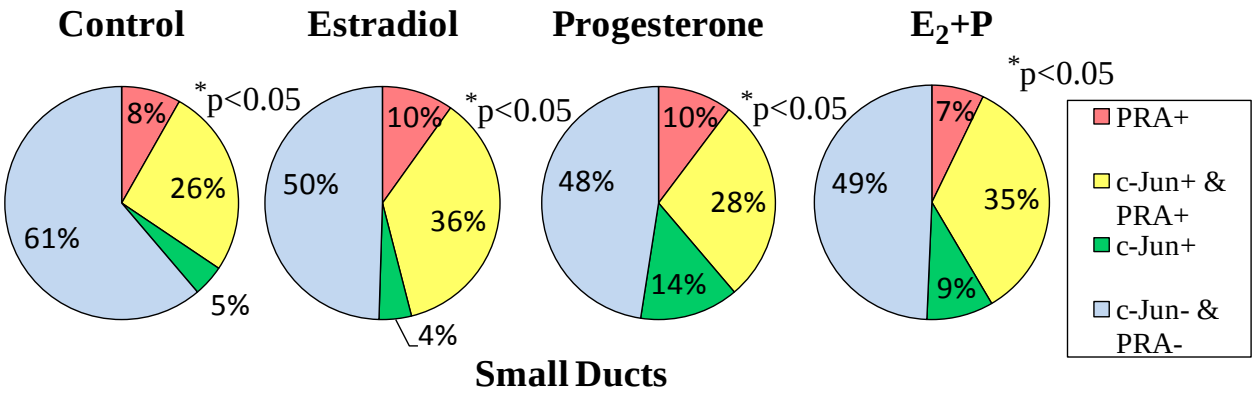

significant population of cells that expressed PRA but did not express c-Jun (7-10%), or conversely that expressed c-Jun without PRA (4-14%) (Figure 3.24b). Overall, c-Jun and PRA expression correlated highly in the adult mouse mammary gland, but c-Jun was neither necessary nor sufficient for PRA expression in the adult mouse.

JunB, JunD and Fra1 are Not Regulated Strongly by Hormones in the Mouse Mammary Gland

The number of cells expressing total JunB ($JunB^+$ alone + $PRA^+/JunB^+$) was significantly higher after E_2 treatment in small and large ducts ($p<0.05$), but not altered by P or E_2+P (Figure 3.S5). JunB was expressed in 38% of luminal epithelial cells in ovariectomized control mice (Figure 3.S5). Of the $JunB^+$ cells in control mice, 66% co-expressed PRA protein (Figure 3.S5), whereas, of the PRA^+ cells in control mice, 58% also expressed JunB protein (Figure 3.S5). There was a small, but significant increase in the population of $PRA^+/JunB^+$ cells after E_2 treatment, particularly in small ducts ($p<0.05$) (Figure 3.S5). This increase in double-positive cells was accompanied by a slight decrease in the number of cells expressing PRA only ($p<0.05$). Treatment with P or E_2+P did not significantly alter the proportion of PRA^+, $JunB^+$ or $PRA^+/JunB^+$ expressing cells. The colocalization of PRA with JunB was highly significant and greater than expected by chance ($p<0.05$) (Figure 3.S5). However, JunB was also neither necessary nor sufficient for PRA expression in luminal epithelial cells in the adult mouse.

The total number of cells expressing JunD ($JunD^+$ alone + $PRA^+/JunD^+$) was not significantly altered by hormone treatment and ranged from 60-63% of luminal epithelial cells. Furthermore, JunD expression was not hormone-dependent since in ovariectomized control mice, 63% of total luminal epithelial cells expressed JunD (Figure 3.S6). In control mice, 67% of the $JunD^+$ cells also co-expressed PRA (Figure 3.S6). Of the PRA^+ luminal epithelial cells, 89% co-

expressed JunD protein (Figure 3.S6). Even though the majority of PRA^+ cells co-expressed JunD, there was still a small subpopulation of cells expressing only PRA (Figure 3.S6). The degree of colocalization between JunD and PRA was highly significant for all treatments and control for both small and large ducts ($p<0.05$) (Figure 3.S6). However, like the other AP-1 subunits, JunD was neither necessary nor sufficient for PRA expression in the adult mouse mammary gland, although their correlation was greater than random.

The percentage of luminal epithelial cells that were both $PRA^+/Fra1^+$ was highest in the control mice and decreased slightly with any of the hormone treatments, especially P alone ($p<0.05$) (Figures 3.25a, b). The total number of cells expressing Fra1 ($Fra1^+$ alone + $PRA^+/Fra1^+$) was not significantly altered by treatment with either hormone and ranged from 41-50% of luminal epithelial cells (Figure 3.25b). Colocalization between PRA and Fra1 was significantly greater than expected by chance for both small and large ducts in control and hormone treated mice ($p<0.05$) (Figure 3.25b). When E_2 was combined with P, there was a significant increase in the proportion of cells that expressed PRA alone or Fra1 alone ($p<0.05$) (Figures 3.25a, b). Although there was a significant population of $Fra1^+$ cells that failed to express PRA (and vice versa), Fra1 was therefore neither necessary nor sufficient for PRA expression in adult mice with or without hormone treatments, but expression of Fra1 increased the likelihood that PRA would also be expressed.

Proliferation Correlates Best with c-Jun-Positive or c-Fos-Positive Cells

Double-immunofluorescence for BrdU on mouse mammary gland sections showed that only P and E_2+P treated cells were proliferative following 3 days of hormone treatment. In total, 21% and 30% of luminal epithelial cells were $BrdU^+$ when mice were treated with P and E_2+P,

(a)

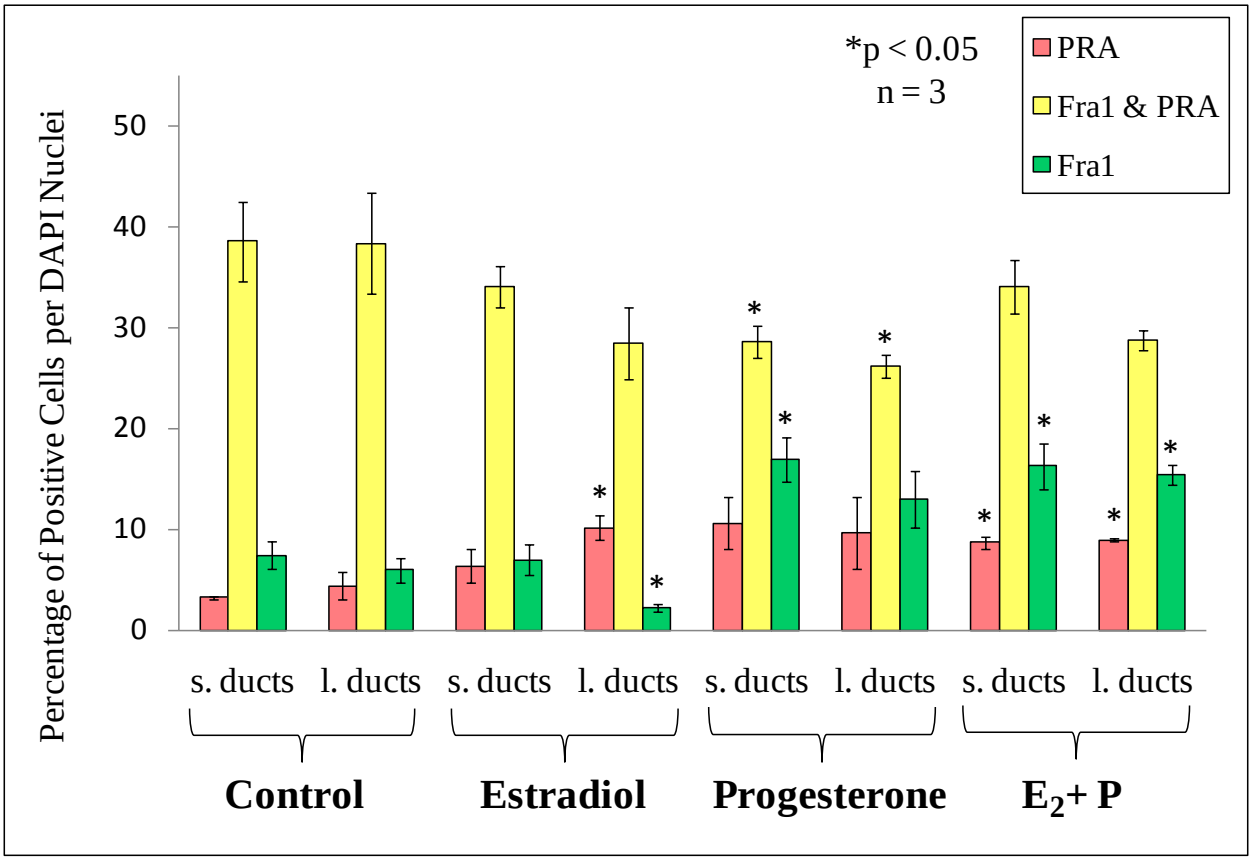

Figure 3.25: Hormonal regulation of Fra1 expression and colocalization with PRA. Immunofluorescence of PRA utilized an anti-PRA antibody (hPRa7) on tissue sections from 18-22 week virgin adult mice treated for 3 days with control, estradiol (E_2), progesterone (P) or E_2+P. Colocalization with Fra1 used an anti-Fra1 antibody (sc-183). Quantitation values represent the mean ± SEM from three to four mice per group and a minimum of 500 cells/structure type/mouse analyzed. (a) Statistical analysis utilized Student's *t* test and significance is denoted: *p<0.05. (b) For statistical analysis a two-tailed Fischer's exact test was used for each structure type for each treatment. Colocalization is statistically significant if p<0.05, with the level of significance indicated. The distribution of Fra1 and PRA in large ducts mirrored the pattern shown for small ducts (data not shown).

Figure 3.25 (Cont'd.)

(b)

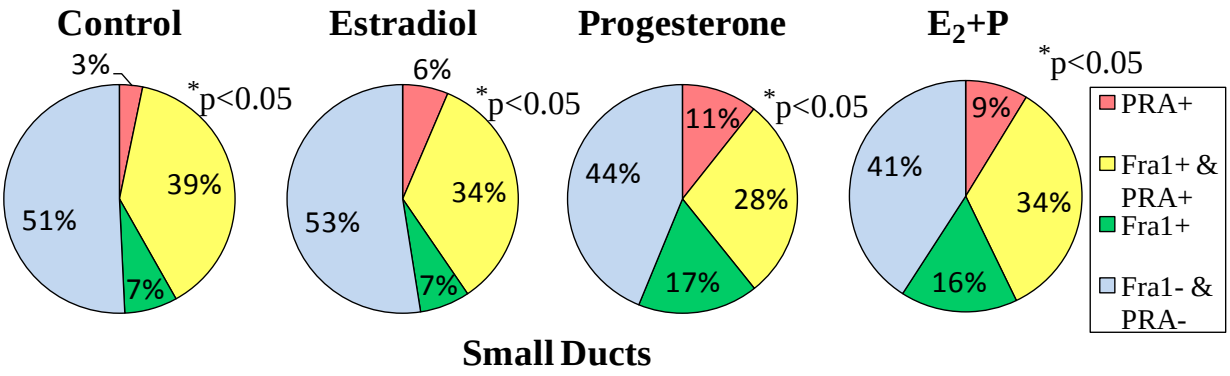

respectively (Figure 3.26a). A subset of the luminal epithelial cells proliferated in treatments that contained P (Figures 3.26a, b; data not shown). The percentage of cells positive for total c-Jun was significantly increased by all hormone treatments, as compared to control mice ($p<0.05$). Under these conditions, 31% of the total number of luminal epithelial cells were c-Jun$^+$ in the P treatment group and 38% after E_2+P treatment (Figure 3.26a). About 62-63% of the BrdU$^+$ cells were also c-Jun$^+$ for the P or E_2+P treatment groups (Figure 3.26a). The percentage of c-Jun$^+$ cells that are also BrdU$^+$ did not significantly differ between P and E_2+P treatments, ranging from 42-50% (Figures 3.26a, b). Colocalization between BrdU and c-Jun was significantly greater than random for all structures examined in mice treated with P or E_2+P (small ducts, $p<0.05$) (Figure 3.26a). A proliferating (BrdU$^+$) luminal epithelial cell in the P or E_2+P treated mammary gland is at least 2.5 times more likely to express c-Jun than a non-proliferating cell (BrdU-negative).

Ovariectomized control mouse mammary gland did not express c-Fos and were non-proliferative (BrdU-negative) (Figures 3.27a, b). The total number of c-Fos$^+$ cells that were also positive for BrdU was similar following treatment with P or E_2+P, ranging from 58-60% (Figure 3.27a). Both P and E_2+P treatments showed significant colocalization between c-Fos and BrdU in small ducts ($p<0.05$) (Figures 3.27a, b). c-Fos appears to be neither necessary nor sufficient for proliferation in luminal epithelial cells since a small population of cells expressed c-Fos without incorporated BrdU, and vice versa. However, rapid turnover of c-Fos following phosphorylation may occur for cells entering S phase, causing an underestimation of the c-Fos$^+$ population (Jariel-Encontre I 1997); (Gomard T 2008). Regardless, c-Fos was much more likely to be expressed in a luminal epithelial cell that was BrdU$^+$ than a BrdU-negative cell, about 5 fold more likely in P or E_2+P treated mouse mammary gland. Taken together, a proliferative

luminal epithelial cell was much more likely to express c-Jun and/or c-Fos than a non-proliferative cell.

(a)

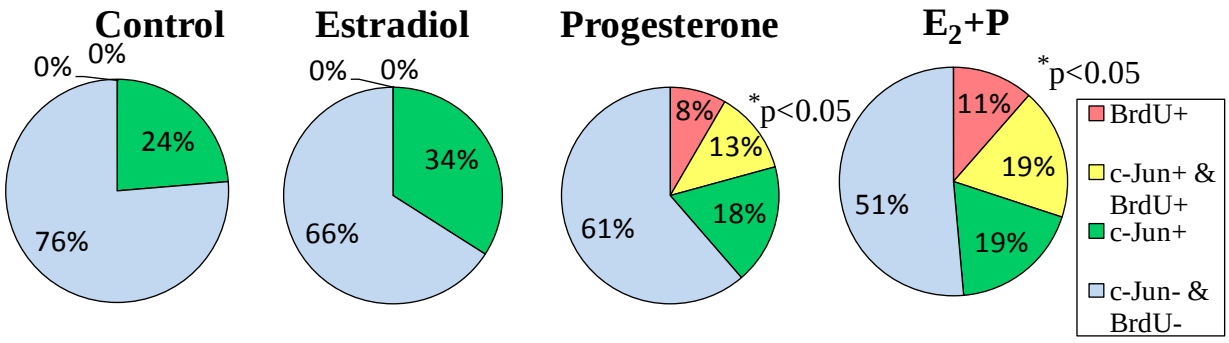

(b)

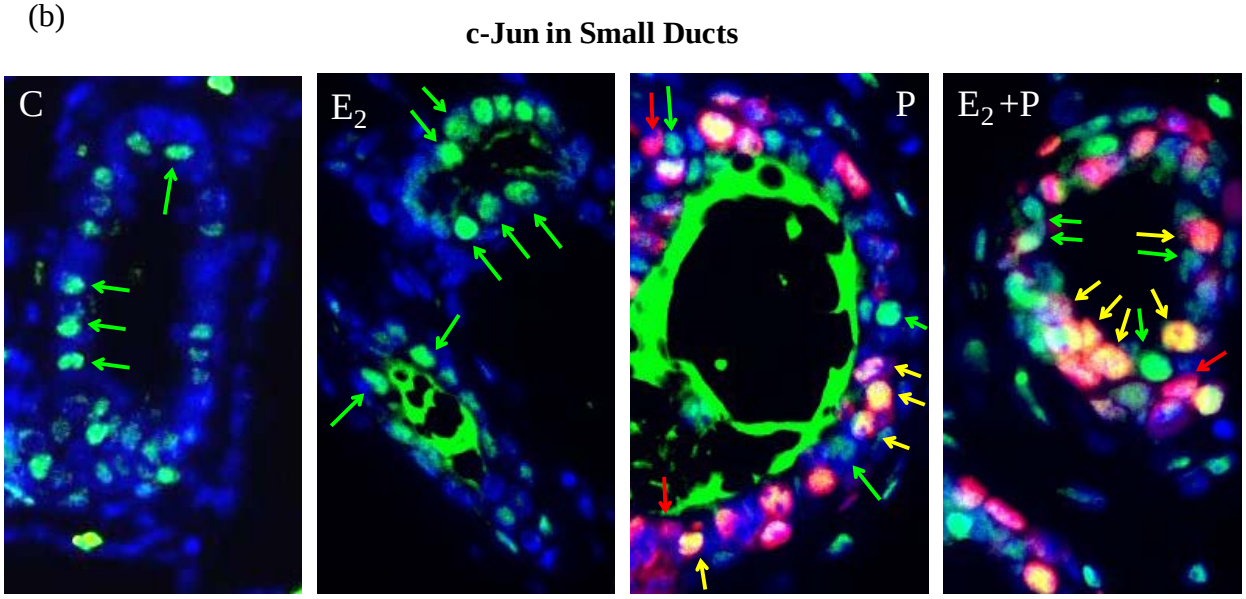

<u>Figure 3.26:</u> Hormonal regulation of c-Jun expression and its relation to cell proliferation. Immunofluorescence of c-Jun utilized an anti-c-Jun antibody (sc-1694) on ovariectomized virgin adult mice treated for 3 days with estradiol (E_2), progesterone (P), or the combination E_2+P. Colocalization with the proliferation marker BrdU (5-bromo-2'-deoxyuridine) used an anti-BrdU antibody (RPN202). Quantitation values represent the mean ± SEM from three to four mice per group and a minimum of 500 cells/structure type/mouse analyzed. (a) For statistical analysis a two-tailed Fischer's exact test was used for each structure type for each treatment. Colocalization is statistically significant if $p<0.05$, with the level of significance indicated. The distribution of c-Jun and BrdU in large ducts mirrored the pattern shown for small ducts (data not shown). (b) Red arrows indicate $BrdU^+$ cells, green arrows show $c\text{-}Jun^+$ cells and yellow arrows show representative cells that are $BrdU^+/c\text{-}Jun^+$ (scale bar, 25 µm).

(a)

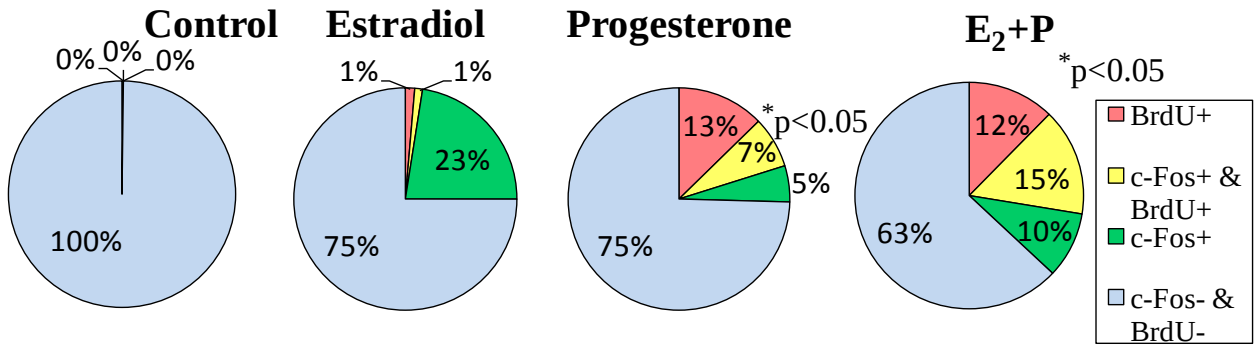

(b)

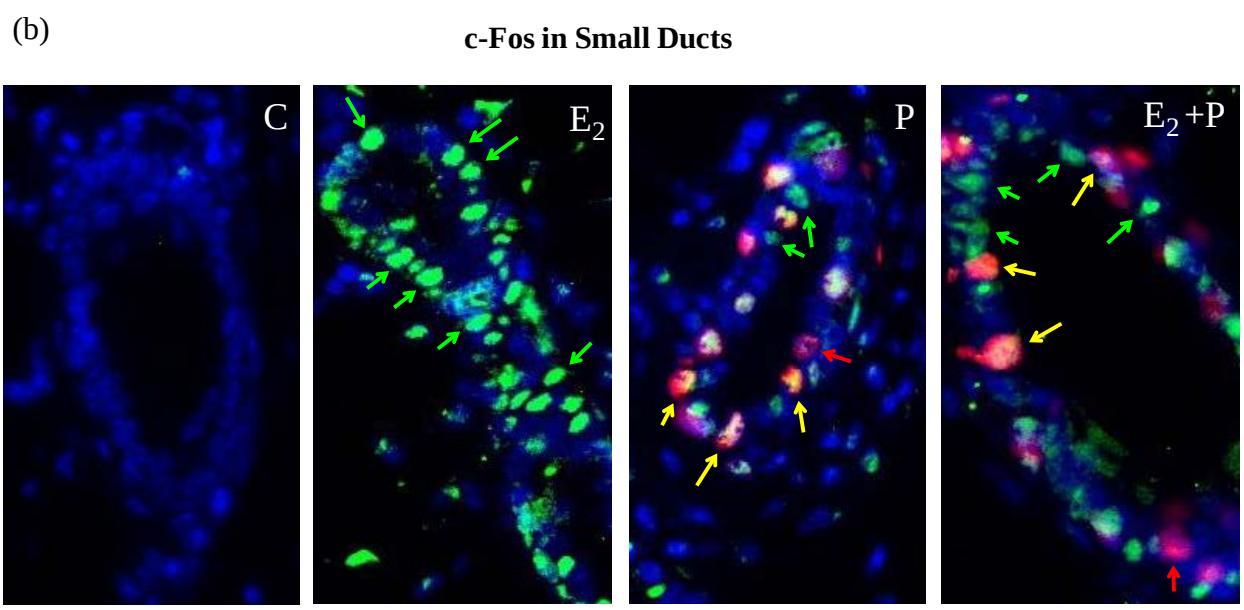

Figure 3.27: Hormonal regulation of c-Fos expression and its relation to cell proliferation. Immunofluorescence of c-Fos utilized an anti-c-Fos antibody (sc-52) on ovariectomized virgin adult mice treated for 3 days with estradiol (E_2), progesterone (P), or the combination E_2+P. Colocalization with the proliferation marker BrdU (5-bromo-2'-deoxyuridine) used an anti-BrdU antibody (RPN202). Quantitation values represent the mean ± SEM from three to four mice per group and a minimum of 500 cells/structure type/mouse analyzed. (a) For statistical analysis a two-tailed Fischer's exact test was used for each structure type for each treatment. Colocalization is statistically significant if $p<0.05$, with the level of significance indicated. The distribution of c-Fos and BrdU in large ducts mirrored the pattern shown for small ducts (data not shown). (b) Red arrows indicate $BrdU^+$ cells, green arrows show $c\text{-}Fos^+$ cells and yellow arrows show representative cells that are $BrdU^+/c\text{-}Fos^+$ (scale bar, 25 µm).

DISCUSSION

1. Regulation of PR Isoform Expression in Mouse and Human Mammary Epithelial Cells: Validation of Reporter Assays, Identification of Promoter Elements and Signaling Pathways Responsible for Modulating PR Expression and Differentially Regulating PR Isoform Expression

a. Activating Protein-1

Pathways leading to activation of AP-1 were targeted using cotransfected AP-1 expression vectors or phorbol ester treatment of the cells. PMA can act through different PKC isozymes to yield diverse effects on cell fate by activating or inhibiting cell proliferation or apoptosis (Kazanietz MG 2005). PKC is thought to play a role in breast cancer and tumor progression since its activity is often increased in malignant breast tissue as well as in the most aggressive breast carcinoma cell lines (Platet N 1998). In breast cancer cell lines, the effect of PMA is dependent on the length of exposure (Sengupta K 2006) as well as the concentration (Roos W 1986). Short exposure to PMA (less than 20 hours) stimulates cell proliferation in many ER^+ breast cancer cell lines (Sengupta K 2006), whereas long exposure to PMA (more than 20 hours) causes growth arrest of many ER^+ and ER-negative breast cancer cell lines (Sengupta K 2006).

In the normal mouse mammary cell line NMuMG, up to 90 minutes of PMA treatment increased cell proliferation by activating the mitogen-activated protein kinase/extracellular signal-regulated kinases (MAPK/ERK kinase) ERK 1 and ERK2, as well as enhancing expression of cyclin D1 (Grossoni VC 2007). Activation of MAPKs by growth factors or PMA can lead to phosphorylation of the PR on Serine 294 which allows unliganded PR to accumulate in the nucleus (Faivre E 2005). Both PRA and PRB can activate transcription of target genes in the absence of ligand, however PRA is a much stronger unliganded transactivator and can

activate more target genes than PRB (Jacobsen BM 2005). PR activation upon PMA treatment may be due to MAPK phosphorylation of the PR, by phosphorylation of MAPK targets such as Jun-kinase and AP-1, or some combination of phosphorylation events. Activated Jun/Fos proteins could theoretically activate or inhibit transcriptional activity of one or both PR isoforms leading to changes in the mRNA levels of PR. In addition, feedback loops controlling PR mRNA levels at the transcriptional level are also possible in this complex MAPK signaling cascade.

In transient transfection assays, basal activity of the various PR promoter constructs varied dramatically. Relative to the short tandem promter (STP), the long tandem promoter (LTP) was 3.6 fold more active ($p<0.05$), while the short distal promoter B (DPB) and proximal promoter A (PPA) each have 4.7 fold more activity ($p<0.05$) (Figure 3.2). However, the basal activity of the LTP, DPB and PPA constructs did not differ significantly from one another (Figure 3.2).

Transient transfection of PR promoter-reporter constructs driving luciferase demonstrated the importance of c-Jun in up-regulating PRA, PRB, PRA+B (LTP) or the 5' truncated PRA+B promoter (STP) (Figure 3.2). Cotransfection of c-Fos with a Jun isoform did not enhance transcriptional activation of any of the PR promoters, while cotransfections with Fra1 or Fra2 had promoter-specific effects depending on the heterodimer (Jun) partner. This suggests that either the majority of the AP-1 effect was mediated by c-Jun rather than heterodimerization with a Fos partner or the effect of cotransfecting a Fos isoform was minimal due to high endogenous levels of c-Fos (Milde-Langosch K 2004). Thus, c-Jun was either the only Jun isoform able to reproducibly induce transcription or, alternatively, that c-Jun on its own was the strongest Jun activator of the PR promoters. In a study on human PR, the +90 AP-1 site located in the distal

promoter region showed activation by direct c-Jun/c-Fos DNA binding (Petz LN 2002). The effect of c-Jun appears to be similar at the DPB AP-1 site in mouse PR since the short DPB showed the greatest increase in transcriptional activity when cotransfected with c-Jun or c-Jun/c-Fos (Figure 3.2). Cotransfection with a Fos isoform (c-Fos, Fra1, Fra2) was not significantly different than activation by c-Jun alone on the LTP, STP or short DPB promoters (Figure 3.2). This suggests that Jun homodimers, rather than a Jun/Fos heterodimer may be the predominant AP-1 isoform binding to AP-1 sites in this promoter region or alternatively, that there are sufficient levels of endogenous Fos proteins in MCF-7 cells to readily form heterodimers (Milde-Langosch K 2004).

Unlike the results with c-Jun, the DPB AP-1 site within mouse PR was not significantly activated by JunB (Figure 3.3). Promoter analysis failed to detect any additional putative AP-1 binding sites within the mouse DPB constructs, other than the +18 bp AP-1 site (analogous to the +90 bp site in human PR). Similarly, the PPA AP-1 site within mouse PR was not significantly activated by JunB (Figure 3.3) and promoter analysis did not uncover any putative AP-1 binding sites in addition to the +635 bp AP-1 site in mouse (analogous to the human +745 bp site). JunB is known to have a low potential for forming JunB/JunB homodimers, but more easily forms heterodimers with Fos family members which have greater inherent transcriptional activity and increased DNA binding affinity (Deng T 1993); (Passegue E 2002). The transcriptional activity of a JunB/Fos heterodimer is also increased greatly when there are multiple AP-1 binding sites nearby to allow synergism of a higher order complex (Passegue E 2002). On an isolated AP-1 site, JunB can antagonize c-Jun induced transcriptional activation (Passegue E 2002). This antagonism could occur through JunB titrating out active c-Jun dimers by heterodimerizing with c-Jun, forming a suboptimal AP-1 complex that binds DNA with reduced affinity and only

weakly activates transcription (Deng T 1993). Second, with all the c-Jun protein bound in inactive complexes, JunB can form homodimers which have low DNA binding affinity and low to no transcriptional activity on a single AP-1 binding site (Deng T 1993); (Passegue E 2002). Therefore, the ratio of c-Jun to JunB is important in determining the overall level of expression for an AP-1 target gene (Mechta-Grigoriou F 2001). On a promoter with multiple AP-1 sites, such as the LTP, which contains 2 defined and 4 putative AP-1 sites, JunB/c-Jun, JunB/JunB, and JunB/Fos dimers may still activate transcription through synergism (Figure 3.3). But on a promoter with just a single AP-1 site (like the short DPB or PPA), JunB appears to be unable to cooperate with other JunB-containing dimers and therefore failed to activate transcription to the same extent as c-Jun.

JunB and c-Jun do share some features in common, they are both highly induced by serum stimulation and both are considered early response genes (Hirai SI 1989). JunD however, is the most atypical member of the Jun family showing a divergent tissue expression pattern, a lack of induction upon serum treatment, and constitutive expression in quiescent cells (Hernandez JM 2008). The regulatory interactions between c-Jun and JunD have not been well characterized, but the interactions of JunD with c-Fos have been examined in transient transfection studies in NIH 3T3 cells (Hirai SI 1989). Using a TRE-TK-CAT (TPA response element Tymidine Kinase-Chloramphenicol Acetyltransferase) reporter, these experiments showed that in the absence of c-Fos, c-Jun is a better transcriptional activator than JunD (Hirai SI 1989). But when c-Fos is cotransfected, then JunD/c-Fos activates transcription to a greater extent than c-Jun/c-Fos (Hirai SI 1989). Although c-Fos is capable of potentiating transcriptional activation of both c-Jun and JunD, c-Fos/JunD is clearly a stronger transactivator in this system. This may be a cell type or promoter-specific effect since in our hands,

cotransfections of c-Fos, Fra1 or Fra2 with JunD did not enhance transactivation of the LTP, STP, short DPB or PPA constructs (Figure 3.4). The exception was the short DPB, which was weakly, but significantly activated by JunD/Fra1 (Figure 3.4).

Based on the transient transfection assays, the most likely AP-1 isoforms binding to the 6 AP-1 sites are as follows: AP-1(1_D), AP-1(1_P), AP-1(2), and AP-1(3) sites (-2288, -2269, -1306, -708 bp, respectively) (Figure 3.1) which are unique to the LTR, most likely bind JunB/Fra1, JunB/Fra2, or c-Jun/any Fos family member. The AP-1(4) site, located upstream of the PRB mRNA start site (+19 bp) in the DPB, STP, and LTP constructs, most likely binds JunD/Fra1 or c-Jun/any Fos family member. The AP-1(5) site, overlapping the PRB ATG (+635 bp), is most likely occupied by c-Jun/any Fos family member. However, an electrophoretic mobility shift assay (EMSA) would need to be performed in order to confirm these predicted binding preferences.

b. Hormone and Phorbol Ester Treatments

i. The Promoter Proximal Region of the Mouse Pgr Gene is Not Regulated by E_2

In the rat Pgr gene, five consensus EREs were mapped along with dispersed half-EREs (Kraus WL 1994). Sequence alignment with the mouse Pgr gene showed a high degree of conservation. The percentage indentify for ERE(1) through ERE(5) was: 90, 80, 100, 90 and 100%, respectively. Based on sequence similarity to the rat and human sequence as well as transfection experiments showing that both the human and rat PR promoters are strongly E_2-responsive (Petz LN 2004b); (Petz LN 2002); (Schultz JR 2003); (Kraus WL 1994) we hypothesized that the mouse PR promoter should behave similarly. However, regardless of the human or mouse cell line used, the mouse Pgr gene was not significantly activated by E_2 in

transfected cells (Figure 3.5). This was especially surprising considering the published rat and human PR data. However, in mouse studies, the number of luminal epithelial cells expressing PRA protein is not altered by ovariectomy or by treatment with E_2 following ovariectomy (Aupperlee MD 2007). Rather, the PRA staining intensity is decreased by ovariectomy and is increased by treatment with E_2, albeit not to the same extent as ovary-intact controls (Aupperlee MD 2007). This suggests that in the mouse, E_2 is only able to exert a weak effect on PRA regulation and is not essential for PRA expression. This action of E_2 on expression of the Pgr gene may therefore be either direct (via distant EREs) or indirect.

Most of the human PR studies were carried out in human U2-OS cells, but repeating these cotransfections with mouse PR promoter constructs and ERα in U2-OS cells actually showed repression rather than induction by E_2 (data not shown). We also considered the possibility that our constructs were missing one or more nearby ERE elements that could lead to E_2-responsiveness. There is an ERE(4/5) enhancer cassette located at the 3'-end of exon 1 that is reported to be strongly E_2-responsive in the rat (Kraus WL 1994) but was absent from the LTP construct. We added an ERE(4/5) cassette onto the LTP construct, but this did not alter the E_2-inducibility of the LTP (Figure 3.6; data not shown). However, addition of the ERE(4/5) cassette did increase the basal level of transcription from the LTP in U2-OS cells (data not shown). We concluded that the E_2-responsive human AP-1/ERE and ERE/Sp1 sites are not able to activate the mouse PRA or PRB promoters in tissue culture to the extent described for human PR.

In vivo, the number of PRA protein positive cells and intensity of PRA staining are down-regulated in adult ovariectomized mice treated with P for 5 or 10 days as well as 10 days with

E_2+P (Aupperlee MD 2007). Conversely, 10 days of treatment with E_2+P up-regulated PRB expression from below the level of detection to 25% of luminal epithelial cells (Aupperlee MD 2007). Therefore, we tested whether the mouse PR promoter constructs were P-responsive. However, like the results with E_2, transcriptional activity of the various mouse PR promoter constructs was not altered by 24 hours of P treatment (data not shown). Although the dose of P was standard (10 nM), the length of the treatment may not have been long enough. For example, the action of P down-regulation of PRA and up-regulation of PRB requires 5-10 days before there was a quantitative difference in the number of PR^+ cells and difference in the intensity of PR staining (Aupperlee MD 2007), suggesting that the action of P in the mouse mammary gland is not a direct effect.

The human PGR gene contains two sets of Sp1 sites located at -61 bp and +571 bp which are both regulated by ERα (Schultz JR 2003); (Petz LN 2000). The -61 bp site is near a putative CCAAT box but lacks a consensus ERE binding sequence. Although ERα does not directly bind to this region, it enhances Sp1 binding to the Sp1 sites especially the proximal -61 bp Sp1 site when treated with E_2 (Schultz JR 2003). The +571 Sp1 sites are adjacent to a half ERE binding site. Sp1 is associated with the +571 bp site in the presence and absence of E_2, but ERα only binds in the presence of E_2 (Petz LN 2000). ERα enhances Sp1 binding additively to the proximal and distal Sp1 sites (Petz LN 2000). Based on these human PR studies, we hypothesized that Sp1 would increase transcriptional activity from both the proximal and distal promoters along with the LTP. Sequence comparison of the human and mouse promoters showed that the pair of Sp1 sites located at -61 bp and +571 bp in human PR are 89%, 89%, 100% and 50% conserved in the mouse, respectively. The construct most likely to respond to

cotransfected Sp1 was the LTP-ERE construct (containing the ERE(4,5) enhancer cassette), because it has the distal and proximal Sp1 sites plus an additional 3 putative Sp1 binding sites flanking ERE(4) and ERE(5) (MatInspector 2005); (Figure 3.1). However, the addition of cotransfected Sp1 with or without E_2 did not differ from empty vector control (Figure 3.6). These experiments lead us to conclude that the core promoter region of the mouse Pgr gene, extending from –2494 to +769 bp with respect to the predicted PRB transcription start site, is not E_2-responsive, even in the presence of two additional hormone response elements.

One possible explanation for the disconnect between *in vivo* and tissue culture E_2 regulation of the mouse PR is that there are one or more critical EREs lacking from our promoter constructs. Although our mouse promoter constructs contained a comparable amount of upstream promoter sequence to the rat studies, the 5 well defined EREs in rat (Kraus WL 1994) were not responsive in the context of the mouse PR promoter. A recent report on human PR, demonstrated E_2-dependent long-range control of PR at the transcriptional level (Boney-Montoya J 2010). Specifically, there are eight regions of the human PGR gene that contribute to E_2-responsiveness ranging from 311 kb upstream to 4 kb downstream of the PRB start site (Boney-Montoya J 2010). All eight of the upstream regions contain one or more EREs, but these ERE containing enhancer regions differ in their ability to physically bind ERα and the level of E_2-dependent transactivation that they support (Boney-Montoya J 2010). The +4 kb enhancer was particularly interesting due to its relatively close proximity to the human PRA and PRA promoters. A BLAST search for the homologous 600 bp region in mouse mapped this putative enhancer to 350 kb downstream of the mouse Pgr gene, far outside of the promoter proximal region examined in our transfection studies above (BLAST 2010).

In another human genome-wide screen of ER binding sites, three functional ER enhancer regions were mapped to the PGR locus at approximately -205 , -168 and +100 kb relative to the PRB transcription start site (+1 bp) (Carroll JS 2006). Two of these upstream enhancer regions (-205 and -168 kb) coincide with ER enhancer regions mapped by Boney-Montoya, *et al.* and both were shown by both groups to bind ERα by ChIP and activate transcription in a E_2-dependent manner in transient transfection assays (Boney-Montoya J); (Carroll JS 2006). Therefore, there is strong evidence to support the notion that the human PGR gene is under long-range E_2-dependent regulation, but it is unknown if the mouse Pgr gene is regulated similarly.

ii. Phorbol Ester Activates the Long Tandem Promoter

Although PMA treatment increased the transcriptional activity of the LTP, PMA+E_2 did not lead to synergism, rather it reduced the transactivation potential of the LTP (Figure 3.7). Antagonism between AP-1 and ER has been previously reported in MCF-7 cells that were transfected with an ERE-TK-CAT reporter and treated with E_2 plus PMA, showing approximately 70% reduction in ERE activity (Tzukerman M 1991). Such a reduction indicates that the AP-1 elements unique to the 5'-region of LTP may differ from many hormone-responsive AP-1 sites which typically synergize with ERα in response to PMA (Tzukerman M 1991). It appears that the AP1-dependent induction of the LTP reporter in MCF-7 cells was limited primarily by activation of AP-1, rather than the amount of AP-1 protein since the addition of c-Jun and c-Fos had relatively modest effects in the absence of PMA treatment. Alternatively, if the majority of the PMA activity was thru another transcription factor such as

nuclear factor-κ light-chain-enhancer of activated B cells (NF-κB) or activating protein-2 (AP-2), cotransfecting additional c-Jun/c-Fos wouldn't augment PR transcriptional activity.

It has been shown in MCF-7 cells that human PR mRNA and protein are up-regulated by increased PKA activation after treatment of cells with 8-bromo-cAMP (cyclic adenosine 3',5'-monophosophate) (Cho H 1994). Similarly, rat PR is up-regulated by treatment with 8-bromo-cAMP and other PKA activators, such as forskolin, in rat granulosa cells (Park-Sarge OK 1995). Since PKC pathway activation due to PMA treatment led to increased transcriptional activity of the mouse LTP, we also investigated whether protein kinase A (PKA) activation induced the PR promoter constructs. Treatment with forskolin, forskolin+R5020 or forskolin+PMA did not differ from vehicle for any of the mouse PR promoter constructs tested in MCF-7 cells (data not shown). Mechta *et al.* examined PMA stimulation of the various AP-1 isoforms before and after cAMP treatment (Mechta F 1989). By increasing PKA signaling (via increased cAMP levels) they show strong up-regulation of JunB and c-Fos expression, along with weaker up-regulation of JunD upon PMA activation (Mechta F 1989). Although c-Jun is normally a highly PMA-inducible gene, when treated with cAMP, there was complete inhibition of PMA-inducible c-Jun expression (Mechta F 1989). Therefore, our forskolin experiments described above most likely led to an increase in JunB, c-Fos and JunD inducibility, but a complete loss of c-Jun inducibility by PMA. Since c-Jun is the only AP-1 isoform able to efficiently activate the mouse PR promoters, this explains the lack of an increase in transactivation of any of the PR promoters. These forskolin experiments represent another difference in the regulation of the human and rat PGR genes compared to the mouse Pgr gene.

2. Analysis of PR Isoform Expression in Mouse Tissues and Mammary Cell Lines

a. Primer Extension Mapping of PR mRNA Start Sites

One limitation in mapping the transcription start sites for the mouse Pgr gene was the inability of traditional methods for RNA analysis (Northern blots and PCR) to accurately differentiate between transcription initiating at the proximal (PRA) and distal (PRB) promoters, combined with relatively low levels of PR mRNA in the tissue of interest (mammary gland). Previous attempts to quantify this using RNAse protection assays (data not shown) were relatively unconvincing even for our positive control samples (uterine RNA) and failed to detect $PR^{(A)}$ or $PR^{(B)}$ transcripts in mouse mammary gland RNA in the regions predicted from the human and rat PGR genes. Later experiments using primer extension to identify start sites for PR transcription within uterine RNA suggested that the proximal promoter may in fact lie downstream of the region previously analyzed by RNAse protection. Using this technique, start sites were dispersed over a 440 bp region beginning approximately 150 bp upstream of the PRB ATG initiation codon, with the majority of sites actually occurring downstream of ATG_B. Similarly, we were unable to observe $PR^{(B)}$ transcripts corresponding to the predicted +1 bp start site based on homology to the human PGR gene, but instead saw evidence of transcription initiation being dispersed over a broad region from +114 to +372 bp, which was downstream of the predicted PRB start site. This represents an additional difference comparing mouse PR with the human and rat systems and increases the likelihood that a mechanism unique to the mouse Pgr gene exists to shift transcription from the proximal to the distal promoter, accounting for the loss of PRA protein expression and the appearance of PRB that accompanies lobuloalveolar development during pregnancy.

Using primer extension, the PRB start sites were localized to +181 to +202 bp for liver and uterine mouse RNA (Figure 3.11). In liver RNA samples from both ovary-intact and ovariectomized mice there was an additional start site mapped to -9 bp (Figures 3.10, 3.11). A recent study on nuclear receptors in mouse tissues failed to detect PR or PRB protein in the liver using immunoblotting (Takegoshi S 2009). This suggests that although the PR RNA exists, there isn't any functional protein produced or it is expressed at such a low level that it was not detected in this nuclear receptor study. In the uterus, sites of strong PRB initiation were mapped to the +181 to +202 bp region which was far downstream of the predicted PRB mRNA start site of +1 bp. Although the start site predictions were based on homology to both rat and human PR sequence, we concluded that in hormone dependent tissues, the transcription start sites for mouse PR mRNA were actually located 180 bp further downstream.

The predicted PRA start site is at +641 bp, but in uterine RNA, the mapped start sites were dispersed from +635 to +713 bp (Figures 3.10b, 3.11; data not shown). Any $PR^{(A)}$ mRNAs that initiate at +635 bp would have a 494 bp 5'-UTR before the PRA ATG at +1129 bp, which is considered unfavorable. Most vertebrate mRNAs examined have a 5'-UTR sequence of only 20 to 100 nt, while those with long, GC-rich 5'-UTR sequences are translated inefficiently (Lapidot M 2006). Since the $PR^{(A)}$ transcripts initiating at +635 bp have a long predicted 5'-UTR sequence (494 bp) and span the first CpG island (+659 to +884 bp) these are predicted to have poor translation efficiency. In addition, the PRA ATG is located in an unfavorable Kozak sequence context with 5 deviations from the consensus [GCC$^{A}/_{G}$CC**AUG**G] (Kozak M 1991a). The PR ATG_A translational start sequence is: <u>C</u>C<u>GCU</u>C**AUG**<u>A</u>, with divergences from the consensus underlined and the initiation codon indicated in bold.

Start sites located upstream of +634 bp appear to represent a potentially heterogeneous mRNA population of both $PR^{(B)}$ and $PR^{(A)}$ transcripts. The $PR^{(B)}$/$PR^{(A)}$ transcript start sites clustered around +114 to +125 bp, +181 to + 221 bp, +358 to +372 bp, +499 and +582 bp (Figures 3.11; data not shown). All of these start sites are capable of producing $PR^{(B)}$ or $PR^{(A)}$ transcripts, even the +582 bp TSS which would only have a 53 nt leader sequence. A minimum of a 12 nt 5'-UTR is required for ribosome initiation, while at least 20 nt of 5'-UTR sequence is needed for fidelity of initiation (Lapidot M 2006). One regulatory mechanism that these PR transcripts may be subject to is "promoter switching" (Kozak M 1991b), where the first AUG (AUG_B) is in a strong context and under the control of promoter B, so AUG_A is silent in the full length $PR^{(B)}$ mRNA. A second mRNA is under the control of promoter A and has a 5'-end between the two AUGs. This shorter $PR^{(A)}$ mRNA initiates at the internal start codon (AUG_A), which is in a weaker context. In both cases, the ribosomes initiate only at the first AUG codon (Kozak M 1991b). The PRB Kozak sequence [G<u>U</u>CG<u>U</u>C**AUG**<u>A</u>] differs from consensus at the 3 underlined positions, but retains the critical purine in position -3, relative to the +1 assignment of adenine in AUG (Kozak M 1991b). A transcript initiating at the furthest upstream TSS of +114 bp would have a PRB leader sequence of 520 nt, which is comparable in length to the PRA leader sequence. This 520 nt PRB leader sequence also has about 48% GC content, which is lower than the PRA leader GC content of about 61%. Overall, the PRB AUG is not only preceded by a less-structured, lower GC content leader sequence, but also found in the context of a stronger Kozak sequence, suggesting stronger translation initiation for the B isoform of PR.

The presence of multiple weaker transcription start sites in primer extension experiments of mouse PR is supported by multiple lines of evidence. First, it is established that vertebrate

promoters can change to a shorter leader sequence that is translated more efficiently (Kozak M 1991b). This is often due to either a developmental or environmental cue, such as serum stimulation (Kozak M 1991b). Since the PRA and PRB isoforms show different spatial and temporal regulation during development (Aupperlee M 2005a), it is probable that the mouse PR mRNAs show 5'-end heterogeneity. Second, mouse PR mRNA transcripts are known to range in size from 8.7 kb to less than 4.2 kb (Schott DR 1991). The most abundant transcripts in mouse uterus or vagina are the 8.7 and 6.9 kb sizes, which are ovarian hormone dependent (Schott DR 1991). In the intact virgin adult mammary gland, the most abundant transcripts are 6.9 and 8.7 kb, with relative abundances of 6.9 > 8.7 > 3.5 > 2.7 > 4.2 kb (Shyamala G 1990). Third, alignment of ESTs and RIKEN cDNAs mapped a heterogeneous 5'-end localized mostly around +640 bp or +1800/+1900 bp (Figure 3.8). Fourth, the mouse PR promoter is a TATA-less promoter, belonging to the CpG-rich class of promoters which is known for broadly dispersed transcription start sites (Carninci P 2006); (GenBank (NCBI) 2008).

b. Semi-Quantitative PCR of Total $PR^{(A+B)}$ and $PR^{(B)}$–Specific mRNA Transcripts

In order to study transcriptional regulation of the PR, a mouse mammary cell line that expresses the receptors for both E_2 and P would be ideal. Several candidate cell lines were tested for PR expression levels as well as hormone responsiveness using semi-quantitative PCR. The UMD-208, MC4-L2 and MC7-L1 cell lines along with mouse uterus were all $PR^{(A+B)}$-positive, as reported (Figure 3.12a). Mouse liver and mouse NMuMG cells both had low to no PR RNA detectable, as expected for the NMuMG cells and predicted for the liver RNA (Figure 3.12a). Again using the common region exon 4/5 primer set, UMD-208 cells showed similar hormonal regulation to endogenous mouse PR *in vivo*. $PR^{(A+B)}$ message was down-regulated by

R5020 alone, while E_2 + R5020 increased the level of PR RNA, but E_2 alone did not increase the level of PR as seen *in vivo* (Figure 3.12b) (Aupperlee M 2005b). Using the exon 4/5 primer set, PCR amplification of MC7-L1 cell RNA resulted in robust PR message expression in vehicle control, all hormone, and PMA treatments (Figure 3.12c). However, there was no significant difference between the various treatments and vehicle control. In the endogenous virgin adult mouse, there was no PR detected in the liver, low levels in ovariectomized mammary gland, moderate levels in mammary gland from ovary-intact mice and the highest levels were seen in uterus samples from ovariectomized or ovary-intact mice (Figure 3.12d).

A second primer set was used that is located in exon 1 overlapping ATG_B (Figure 3.13b). This primer set preferentially detects PRB transcript, but can also detect PRA transcripts that contain a long 5'-UTR and extend upstream to include + 634 bp. Again, the level of PR message was highest in the uterus, with uterus from an ovary-intact mouse expressing more PR than uterine RNA from an ovariectomized mouse (Figure 3.13a). When assaying for PR transcripts in the liver, primers within exon 1, such as the ATG_B set, detected PR message in both ovary-intact and ovariectomized mouse RNA (Figure 3.13a). However, PR message was not detected in liver RNA preparations using a primer set that included exons 2 to 5 (Figure 3.13b, c; data not shown). This may reflect a difference in primer efficiency, transcript abundance or transcript integrity/length. Nacent transcripts for PR message were detectable in liver samples since the 5'-end of PR was mapped using primer extension (Figures 3.10a, 3.11).

With the ATG_B primer set, there were no $PR^{(B)}$/ $PR^{(long\ A)}$ transcripts detected in the mammary gland of ovary-intact or ovariectomized mice (Figure 3.13a). It has been established by immunofluorescence staining that PRB protein is not detected in the virgin adult mouse

mammary gland and that PRA protein is the only isoform detected (Aupperlee M 2005a). Transcripts leading to the expression of both PRB and PRA proteins may be present, but only those transcripts initiating at the PRA start sites should produce functional protein in the virgin adult mammary gland. Since $PR^{(A+B)}$ mRNA was detected with this same virgin adult mammary gland cDNA preparation using a common region exon 4/5 primer set (Figure 3.12d), this implies that $PR^{(A)}$ transcripts spanning this region are either not being expressed or not being detected. Primer extension mapping of start sites in the +634 bp region revealed that the majority of start sites which could lead to PRA protein initiate from +635 to +725 bp, significantly further downstream from the region initially predicted. However, if a $PR^{(A)}$ transcript initiated downstream of the ATG_B primer, anywhere downstream of +656 bp, then it would give a negative PCR result using this primer pair since the forward PCR primer sequence is not present.

The third primer set used was the exon 1/2 set, which detects both $PR^{(A)}$ and $PR^{(B)}$ message. The overall primer efficiency did not appear to be as high compared to the exon 4/5 or ATG_B primer sets, as was evident in the lower levels of $PR^{(A+B)}$ in the uterus samples from ovary-intact and ovariectomized mice (Figure 3.13c). This primer set was able to detect a low amount of $PR^{(A+B)}$ message in ovary-intact mouse mammary gland, but the transcript level in mammary gland from ovariectomized mice was below the level of detection in this system (Figure 3.13c). Since the exon 1/2 primer set detects both $PR^{(A)}$ and $PR^{(B)}$ message, it was able to amplify a small amount of PR transcript, presumably mostly $PR^{(A)}$ RNA since this is the only protein isoform detected in virgin adult mouse mammary gland (Aupperlee M 2005a). This

confirms the PCR results with the ATG_B primer set which failed to detect PR transcripts at +634 bp in virgin adult mouse mammary gland (Figure 3.13a).

c. Immunofluorescence Staining of PR Isoforms in Mouse Mammary Cell Lines

One downfall of semi-quantitative PCR based analysis is the inability to determine the actual amount of PRA mRNA present or the percent of mouse mammary cells that are positive for PRA protein. At best, a subtractive method could be used to estimate the amount of PRA based on the amount of total PR ($PR^{(A+B)}$) minus the amount of $PR^{(B)}$. This assumes equal priming efficiency, which is an unknown variable. A definitive way to determine whether or not the candidate mouse mammary cell lines are PRA and PRB protein-positive is using immunofluorescence for each PR isoform. Surprisingly, even though PR RNA was abundant enough to detect by PCR, PR protein was barely detectable by immunofluorescence. UMD-208 cells were only weakly positive for cytoplasmic PRA, but nuclear PRA was undetectable even upon E_2 treatment (Figure 3.14). PRB protein was detected as nuclear speckling, which increased in both the number of speckles per cell and the number of positive cells after E_2 treatment (Figure 3.14). MC7-L1 cells were at best weakly PRA^+ positive, even after E_2 treatment, while hormone treatments did not appreciably alter the level of PRB or the number of PRB^+ cells (Figure 3.15). However, since the relative abundance of both PRA and PRB protein in UMD-208 and MC7-L1 cells was so low, the quantitative number of positive cells was not calculated.

The main goal of characterizing several mouse mammary cells lines was to identify those that are PR^+, presumably ER^+, and show hormonal regulation comparable to mouse tissues *in*

vivo. The best two candidate mouse mammary cell lines, UMD-208 and MC7-L1 cells, were weakly PR^+, reported to be ER^+ but show differing hormonal regulation. Neither cell line perfectly mirrors the up-regulation by E_2 and down-regulation by P seen in mouse mammary gland tissue. To study both PRA and PRB isoforms, the MC7-L1 cell line is the best option currently available, while UMD-208 cells represent a good model to study mid-pregnancy when the predominant isoform is PRB.

3. Developmental Study of the Mouse Mammary Gland: Colocalization of PR Isoforms with AP-1 Isoforms in Mammary Gland Tissue

Developmental Profile of Jun Isoform Expression and Colocalization

(a) Pan Jun

Immunofluorescence staining with a pan Jun antibody that recognizes c-Jun, JunB and JunD showed that essentially all PRA^+ cells were Jun^+ (Figure 3.16). Combined with the transient transfection data, this suggests that the presence of a Jun isoform is important for efficient PRA expression. The percentage of pan Jun^+ cells was equal to the sum of the individual Jun isoforms, which implies that the Jun isoforms rarely colocalize and rather usually represent individual populations of cells. This decreases the chance for Jun heterodimers, but still allows the cell to manipulate the ratio of Jun to Fos, ATF, or Maf dimer partner.

Since there were virtually no PRA^+/pan Jun-negative cells, Jun alone may be necessary for efficient PRA expression, but was not sufficient for PRA expression. Many studies implicate ERα as a transcription factor that is necessary for PRA expression, especially since ERα colocalizes in essentially all PRA^+ luminal epithelial cells (Aupperlee MD 2007). However, if

the interaction of ERα is direct, it must be through a distant ERE not found in the distal or proximal PR promoter regions examined in the above transfection studies (see Chapter 3, Section 1b). Rather, the transfection data suggest that ERα indirectly leads to PRA up-regulation, perhaps through ERα tethering to another transcription factor already bound to the PRA promoter (i.e. AP-1) or distant EREs, such as those described for human PR (Boney-Montoya J 2010); (Carroll JS 2006). In addition, our studies have shown a direct effect of hormone upon c-Jun and c-Fos levels therefore indirectly modulating PR transcription. In $PRA^+/AP1^+$ cells, it is unlikely that only one AP-1 isoform is present at any one time or in any single mammary gland structure. Therefore, various combinations of Jun and Fos homo- and heterodimers must be considered. The pan Jun staining suggests that although the majority of cells expressed a single Jun isoform (for the most part Jun isoforms did not colocalize), this does not appear to be a structure specific phenomenon. Combined with the transfections studies (see Ch. 3, section 1), the *in vivo* colocalization data was most consistent with the notion that that Jun is necessary for PRA expression. Although it doesn't rule out the possibility that both PRA and Jun family genes are regulated by an as yet unidentified third factor.

(b) c-Jun

c-Jun expression was widespread and did not significantly vary between the developmental stages or structures (Figures 3.17a, b). Although the colocalization between c-Jun and PRA was highly significant, there was still a population of $c\text{-}Jun^+$ or PRA^+ only expressing cells meaning that c-Jun was neither necessary nor sufficient for PRA expression. It is noteworthy that the half-lives of c-Jun (and c-Fos) protein are very short (about 1 hour) (Gomard T 2008), compared to PR protein, which has a half-life of 6 hours (Ramamoorthy S

2010). Therefore, in the PRA^+ population of cells, there may be a subset of cells in which c-Jun and c-Fos were expressed and were subsequently degraded.

In transfected MCF-7 cells, c-Jun was the only Jun isoform able to significantly activate the PPA, DPB, STP, and LTP constructs (Figure 3.2). c-Jun is usually found to be the strongest activator of promoters either as a c-Jun homodimer or more robustly as a c-Jun/c-Fos heterodimer (Shaulain E 2001). The overall strength of c-Jun in our *in vitro* transient transfection experiments is consistent with other promoter studies, but the PR promoters appear to differ from other well characterized promoters (i.e. collagenase) in that the addition of c-Fos is not required to achieve maximal promoter activation (Deng T 1993). This was also reflected in the extremely low number of cells which expressed c-Fos at all developmental stages and in all structures examined. Expression of PRA or PRB protein appears to be independent of c-Fos expression since the presence of PR failed to correlate with c-Fos expression in the mouse mammary gland.

(c) JunD

In PRA^+cells, there was a slight increase in the ratio of JunD to c-Jun from the pubertal to the virgin adult mammary gland (1.3 fold for ducts). This ratio decreased slightly from the virgin adult to the pregnancy-like mammary gland, mirroring the total percentage of $JunD^+$ cells which tended to decrease with hormone treatment (Figure 3.18). The decreased ratio was most evident in lobules, where there was a 1.8 fold decrease in the ratio of JunD to c-Jun for PRA co-expressing cells. Of the PRA^+ cells, 37-42% colocalized with JunD in the pubertal mouse, 39-50% in virgin adult and 33-40% in the 14 day E_2+P mouse (Figure 3.18). Although JunD was

clearly not necessary for PRA expression, JunD does have the potential to homodimerize with itself or heterodimerize with c-Jun and regulate PRA at all stages of development. Similar to JunB, the total level of JunD decreased in the pregnancy-like gland, where 50-57% of $JunD^+$ cells were also PRA^+ (Figure 3.18). The role of JunD in AP-1 homo- or heterodimers is not well understood, but can serve as either an activator or repressor depending on the stimulus and its heterodimer partner (Hernandez JM 2008). Since c-Fos accounted for such a small proportion of positive cells, it is an unlikely dimer partner with JunD (Figure 3.18). However, c-Jun, JunB, and Fra1 all remain possible heterodimer partners with JunD along with JunD itself especially in $AP\text{-}1^+$ cells that showed colocalization with PRA (Figures 3.17, 3.19, 3.21).

(d) JunB

Changing the composition of the AP-1 dimer can dramatically alter its transcriptional activity and DNA binding activity. In PRA^+ cells, the ratio of JunB to c-Jun decreased during development by a factor of 1.8 fold (small ducts), 1.65 fold (large ducts) and 1.5 fold (lobules) (Figures 3.17, 3.19; data not shown). This is potentially significant since the role of JunB in a c-Jun/JunB heterodimer is to reduce the DNA binding activity as well as the transcriptional activity of c-Jun (Deng T 1993). However, based on the pan Jun staining, the population of $cJun^+/JunB^+$ cells was relatively small.

The percentage of PRA^+ cells that colocalized with JunB in ducts during development varied from 38-42% in the pubertal mouse to 25-28% in the virgin adult, similar to the 14 day E_2+P treated mouse (23-33%) (Figure 3.19). PRA^+ cells in lobules also showed a statistically significant decrease in colocalization with JunB from 42% in the virgin adult compared to 33% in the 14 day E_2+P mammary gland (Figure 3.19). From the standpoint of JunB expression in

the pregnancy-like mammary gland, 50% of $JunB^+$ cells also expressed PRA, not unlike pubertal and virgin adult mice where 56-60% of $JunB^+$ cells co-expressed PRA. It is possible that in PRA^+ cells, JunB is one of multiple transcription factors contributing to the down-regulation of PRB in the pubertal and virgin adult mammary gland. Alternatively, PRB expression may not need to be suppressed or the inducer for PRB is absent in the pubertal and virgin adult mouse mammary gland.

(e) c-Fos

Although the Jun proteins can homo- and heterodimerize amongst themselves, generally higher transcriptional activity is seen upon dimerization with a Fos binding partner due to greater stability and increased binding activity (Deng T 1993). Of the Fos isoforms, c-Fos is known to regulate the human PR promoter (Petz LN 2002); (Petz LN 2004a) and combined with c-Jun usually forms the strongest trans-activating AP-1 dimer when tested on an AP-1 responsive promoter such as collagenase (data not shown); (Deng T 1993). However, for the Fos isoforms, c-Fos was expressed in such a small percentage of cells in the pubertal and virgin adult mouse that it was unlikely to have a significant role in PRA regulation in the mouse mammary gland (Figures 3.20a, b). Only 4-6% of luminal epithelial cells were positive for c-Fos in the pregnancy-like gland, significantly less than what was observed for any of the Jun isoforms ($p<0.05$). The possibility for Jun/c-Fos interactions was severely limited when only 1-2% of the c-Fos expressing cells also expressed PRA (Figure 3.20b).

(f) Fra1

Although previous studies have established Fra-1 as an important player in breast cancer progression (Belguise K 2005), the role, if any that Fra1 plays in the normal mammary gland is not well understood. Unlike c-Fos, Fra1 was expressed in a much greater percentage of luminal epithelial cells. Since Fra1 colocalized with PRA in 9-23% of these cells, it was much more likely to heterodimerize with the Jun proteins compared to c-Fos. Specifically, 68-82% of PRA^+ cells colocalized with Fra1 in the pubertal mouse, 70-76% in virgin adult and 82-91% in the 14 day E_2+P treated group (Figure 3.21b). This high degree of colocalization suggests that either Fra1 is contributing to the regulation of PRA or that both genes are co-regulated by another factor or factors. Although originally described as an inhibitor of transcription, recent reports have shown that Fra1 is capable of inducing transcriptional activation (Young MR 2006). However, the exact mechanism of this activation is still under investigation since Fra1 lacks a transactivation domain (Young MR 2006). The phosphorylation state of Fra1 along with the identity of its binding partner play a major role in determining whether these AP-1 dimers activate or inhibit transcription (Young MR 2006). This means that, similar to JunD, Fra1 has the capacity to activate or inhibit PR transcription.

(g) PRB

The mouse PR proximal promoter, capable of supporting expression of only the shorter PRA isoform, is active predominantly in the pubertal mammary gland, when the basic architecture of the ductal tree is established by a combination of steroid- and growth factor-driven ductal elongation and side-branching (Aupperlee M 2005a). PRB expression may depend upon *de novo* activation of a second set of transcripts arising within a distal promoter further

upstream. Since PRB is restricted to luminal cells of lobules and ducts in mid- to late-pregnancy, its appearance seems to require a developmental program that is initiated by the combined effects of E_2 and P in the hormonal environment of pregnancy (Aupperlee M 2005a). Dual-immunofluorescence of PRB and PRA in the pubertal and virgin adult mouse mammary gland failed to detect PRB at either stage and rather only detected PRA (Aupperlee M 2005a); (Kariagina A 2007).

In the pregnancy-like mouse mammary gland, none of the AP-1 isoforms were expressed in a greater percentage of cells compared to earlier stages of development. In fact, the total percentage of AP-1 positive cells (Jun^+ only + Jun^+/PRA^+) was similar to that in pubertal animals for c-Jun and decreased for JunB and JunD (Figure 3.17b, 3.18, 3.19). This contrasts with the dramatic rise in PRB expression during pregnancy, which increased from below the level of detection in pubertal and virgin adult mice (Aupperlee M 2005a), to 43-46% of luminal epithelial cells in the pregnancy-like mouse (Figure 3.22). Since PRA expression was observed in only a subset of PRB^+ cells, PRA was clearly not sufficient for PRB expression. However PRA/PRB colocalization was non-random and PRA-only expressing cells were rare, suggesting that PRB may contribute to regulation of PRA but not the converse. We hypothesize that in a subset of PRB^+ cells, the presence of c-Jun and Fra1 helps to maintain PRA expression since all four of these proteins colocalized in 9-11% of cells in the 14 day E_2+P treated mammary gland (Figures 3.17, 3.21, 3.22). Furthermore, PRA only, c-Jun only, and Fra1 only expressing cells were very rare in the pregnancy-like gland, but colocalized with PRA to a similar extent (i.e. approximately 10%). This phenomenon does not appear to hold for pubertal or virgin adult mice where cells expressing only PRA were more common, ranging from 5-10%, and where colocalization with PRA was less common compared to the 14 day E_2+ P-treated gland. AP-1

may still have the potential to affect PRA expression in a sub-population of $PRA^+/AP1^+$ cells. For each AP-1 isoform in the pregnancy-like gland there was a subset of PRB^+/AP-1-negative cells, in which AP-1 cannot have a direct effect on PRB expression.

Of note, the percentage of $AP\text{-}1^+$ cells does not account for the greater than 40% PRB-expressing cells observed in the 14 day E_2+P treated mammary gland. Therefore, AP-1 is neither necessary nor sufficient to up-regulate PRB expression by itself. *In vivo*, E_2 can up-regulate PRB expression, but it is believed to be an indirect effect since the majority of PRB^+ cells are ERα-negative (Aupperlee M 2005b). Interestingly, when PRB expression levels are increased, this correlates with a decrease in the level of ERα expression (Aupperlee MD 2007), suggesting that high ERα levels are incompatible with high PRB expression levels. However, in order to up-regulate PRB, AP-1 may interact with other transcription factors that are highly expressed during mid-pregnancy such as Stat5a (Santos SJ 2007) and C/EBPβ (Grimm SL 2003).

Luminal epithelial cells in the mouse mammary gland are not a homogeneous population of cells, but rather consist of many different cell subtypes capable of differing interactions and signaling pathways. Cells that are positive for JunB or JunB/Fra1 have the capacity to inhibit downstream AP-1 target genes, while JunD or JunD/Fra1 are able to either activate or inhibit downstream target genes (Figure 3.28). Cells that are positive for c-Jun or c-Jun/Fra1 can transactivate downstream AP-1 target genes. Regardless of their AP-1 expression status, PR^+ cells are capable of acting in PR signaling pathways that are either genomic or nongenomic. However, the double positive cells $PR^+/AP\text{-}1^+$ (predominantly composed of c-Jun/Fra1) define a sub-population of luminal epithelial cells capable of showing AP-1/PR crosstalk. Based on the

(a)

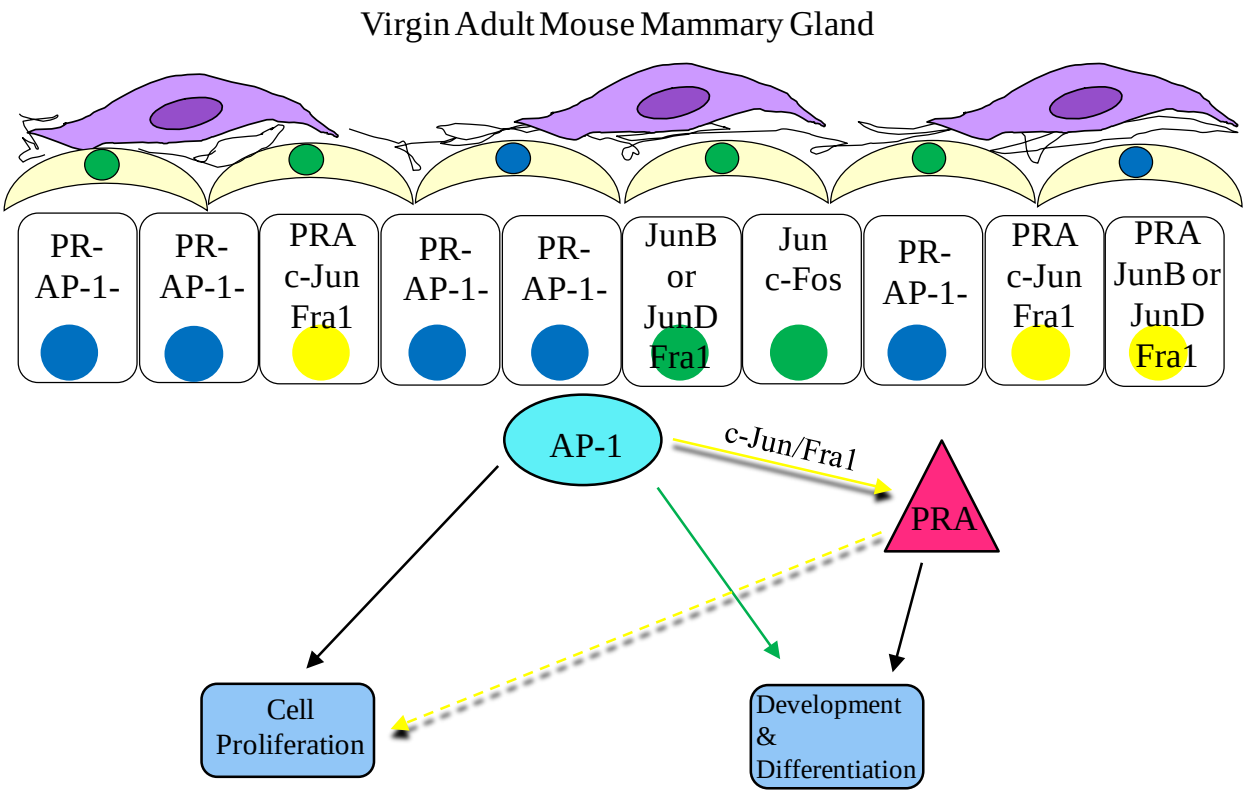

<u>Figure 3.28:</u> Representative cells types found in the mouse mammary gland of a virgin adult mouse (a) and a mid-pregnant mouse (b). Luminal epithelial cells are indicated as white rectangles, myoepithelial cells are tan and fibroblasts are purple spindle-shaped. For the luminal epithelial cells: AP-1^+ cells have a green nucleus, PR^+ a red nucleus, PR^+/AP-1^+ cells have a yellow nucleus and AP-1-negative /PR-negative cells have a blue nucleus. In the virgin adult (a), AP-1 can act alone to alter cell proliferation (c-Jun/c-Fos), differentiation (Jun/Fra1), and development (Jun/Fra1) in addition to its effects on PRA (c-Jun/Fra1). In the mid-pregnant mouse (b), AP-1 can act alone to alter cell proliferation (c-Jun/c-Fos), differentiation (Jun/Fra1), and development (Jun/Fra1) in addition to its effects on PRA (c-Jun/Fra1). AP-1 can also cooperate with other transcription factors that may regulate PRB. PRB exerts its effect on cell proliferation through a paracrine mechanism, while PRA^+ cells rarely proliferate.

Figure 3.28 (Cont'd.)

(b)

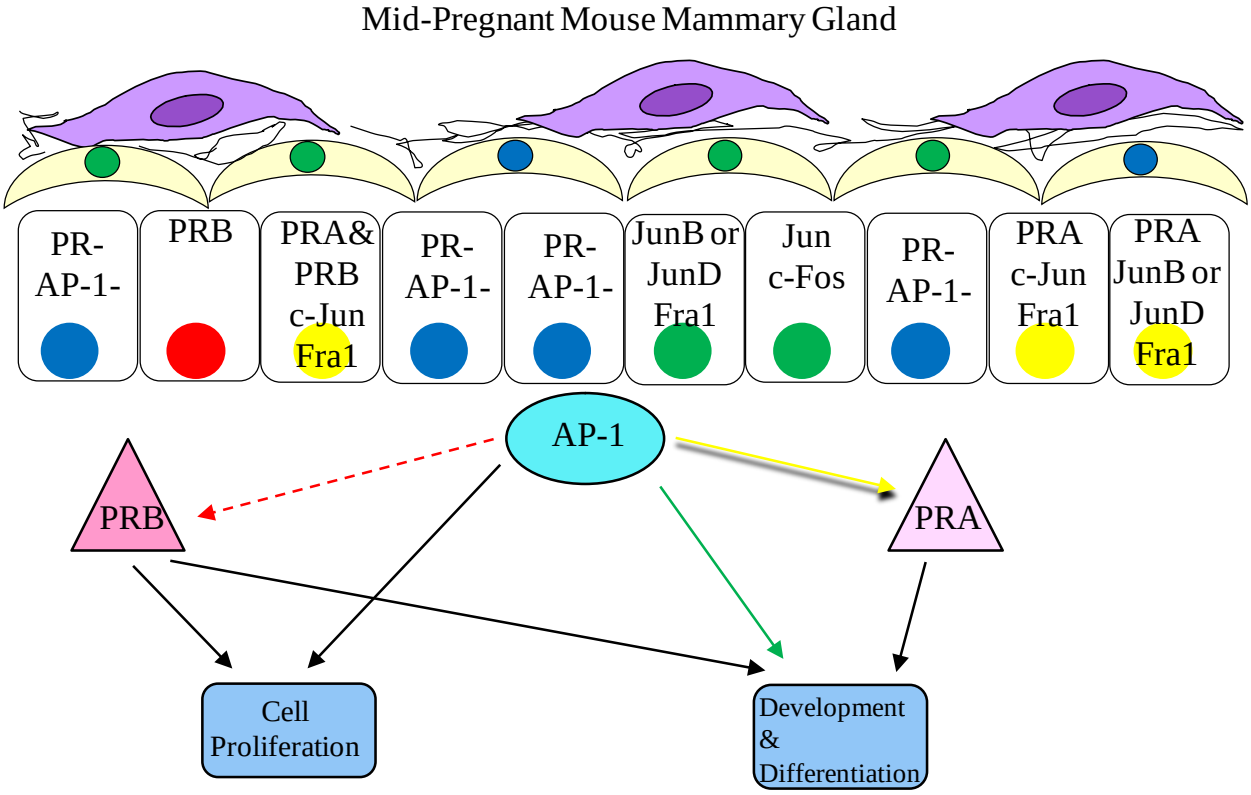

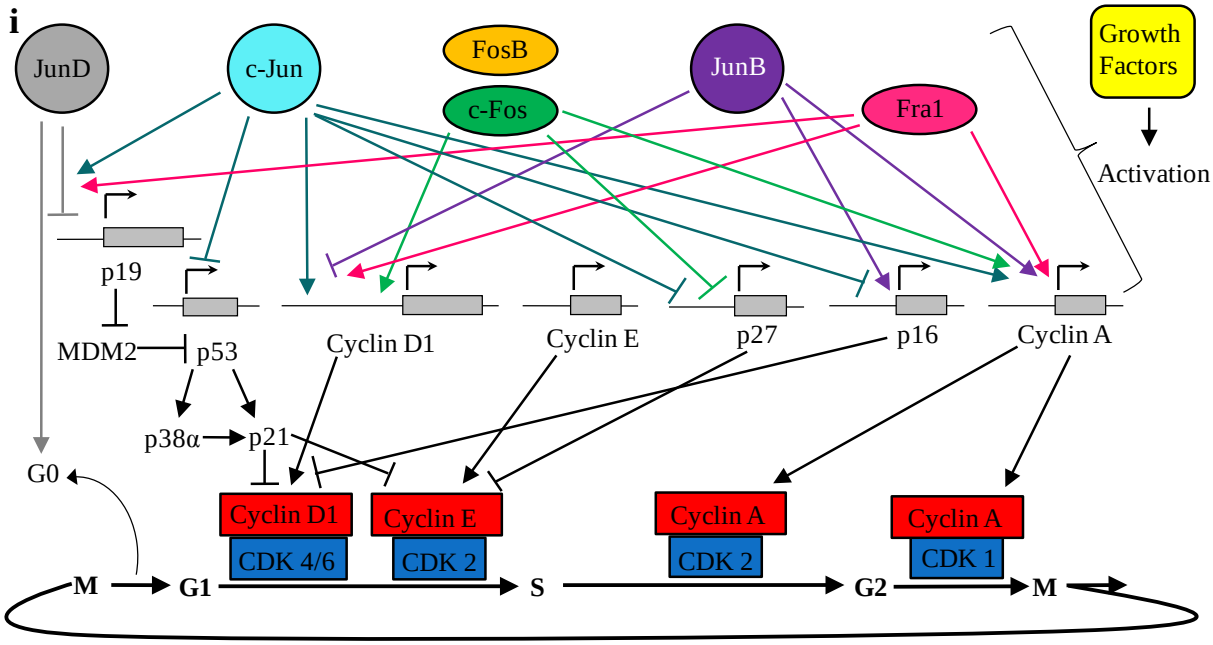

Figure 3.29: The role of AP-1 in cell cycle progression.

(i) c-Jun induces cyclin D1 and cyclin A, stimulating the transition from G_1 to S phase (Schreiber M 1999); (Verde P 2007). c-Jun represses p53 leading to reduced p21 levels (Schreiber M 1999). Similarly, c-Fos and FosB stimulate entry into S phase and induce cyclin D1 (Jochum W 2001). c-Jun is also able to down-regulate p16, opposing the action of JunB, which up-regulates p16 (Passegue E 2002); (Verde P 2007). JunB also antagonizes the action of c-Jun by repressing cyclin D1 and inhibiting the G_1 to S phase transition (Passegue E 2002). JunD controls the Ras/p53 pathway by down-regulating p19, thereby inhibiting S phase entry and increasing the pool of resting cells (Weitzman JB 2000). At the cyclin A promoter, c-Jun, JunB, Fra1 all up-regulate transcription (Verde P 2007). Fra1 also up-regulates cyclin D1 and p19, similar to the effects of c-Jun (Verde P 2007). Transcription at the p27 promoter is inhibited by c-Jun and c-Fos (Khattar E 2010). At the cyclin E promoter, c-Fos and JunB both up-regulate transcription, while cyclin E protein is inhibited by p21 and p27 (Hess J 2004); (Khattar E 2010).

(ii) Summary of immunofluorescence quantitation of the relative amounts of total c-Jun, c-Fos, Fra1 and BrdU-positive cells after ovariectomy and 3 days of treatment with estradiol (E_2), progesterone (P), or the combination E_2+P in the virgin adult mouse.

(iii) Quantitation of immunofluorescence for the proliferation marker BrdU (5-bromo-2'-deoxyuridine) using an anti-BrdU antibody (RPN202). Ovariectomized virgin adult mice were treated for 3 days with estradiol (E_2), progesterone (P), or the combination E_2+P. The values represent the mean ± SEM from three to four mice per group and a minimum of 500 cells/ structure type/mouse analyzed. Statistical analysis utilized Student's *t* test and significance is denoted: $^*p<0.05$.

Figure 3.29 (Cont'd.)

ii

3 Days:	Ovx	E_2	P	E_2+P
c-Jun	+	++	++	++
c-Fos	-	++	+	++
Fra1	++	++	++	++
BrdU	-	-	+	++

iii

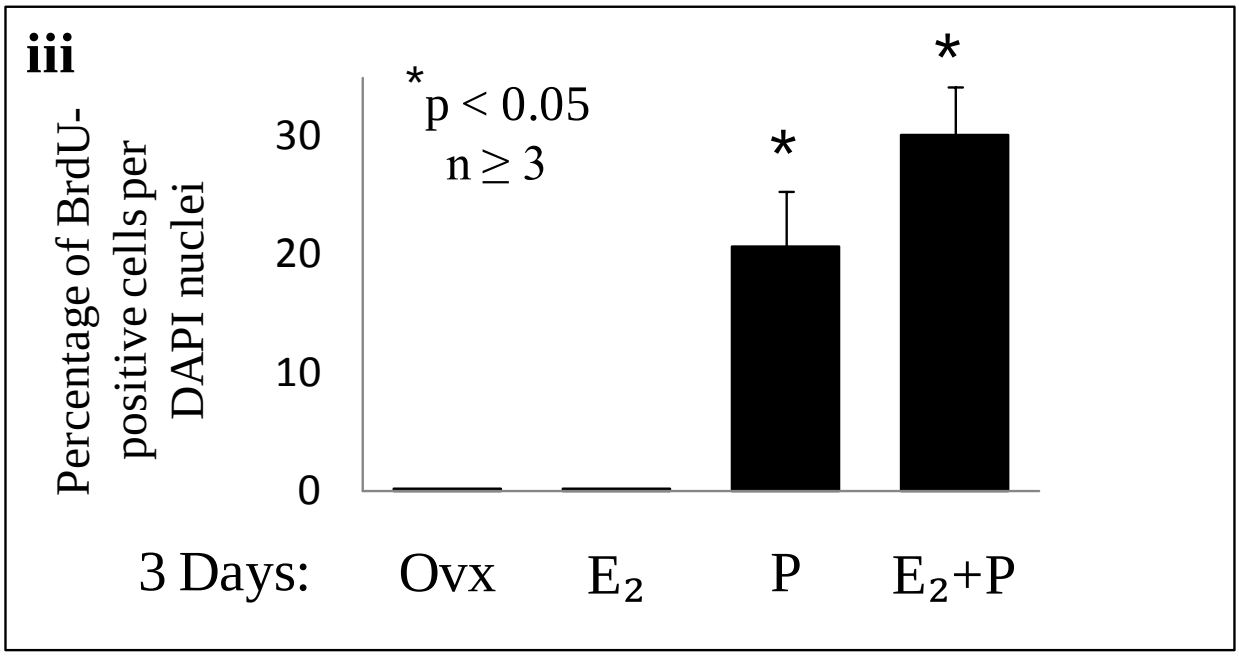

established role of AP-1 in promoting cell cycle progression (Jochum W 2001), it is possible that the co-expression of PR and AP-1 defines a subpopulation of cells with altered proliferative potential.

4. Hormonal Effects on AP-1 Expression in the Mouse Mammary Gland and its Relation to Cell Proliferation: Colocalization of AP-1 with PRA and BrdU in Hormone Treated Mice

c-Fos has been shown to be an important regulator of AP1-dependent breast cancer cell growth (Lu C 2005); (Milde-Langosch K 2004). Other studies have focused on fibroblasts derived from AP-1 knockout mice. The fibroblasts which were derived from a *c-fos*$^{-/-}$ or a *fosB*$^{-/-}$ mouse were able to proliferate normally, however the double knockout *c-fos*$^{-/-}$ *fosB*$^{-/-}$ fibroblasts had a significantly reduced ability to proliferate (Shaulian E 2002). These studies support the role of c-Fos as an important player in proliferation in breast cancer cells and fibroblasts, but the role of c-Fos in luminal epithelial cells of the normal mouse mammary gland has not been extensively studied.

The direct role of the other Fos isoforms, Fra1 and Fra2, in cell cycle regulation is less well understood. In MCF-7 cells, Fra1 over-expression leads to an increase in cell proliferation as well as an increase in the proportion of cells in S phase (Belguise K 2005). Whereas Fra2 over-expression in MCF-7 cells does not change the level of proteins that promote cell cycle progression (i.e. cyclin D1, cyclin E), nor is cell proliferation altered (Milde-Langosch K 2008). Studies examining the dimer composition in fibroblasts found that in late G_1, Jun/Fos heterodimers are mostly composed of Jun with Fra1 and Fra2 (Kovary K 1992). As for a

specific role in cell cycle regulation, Fra1 and Fra2 are implicated in cell cycle progression, specifically during the G_0 to G_1 transition as well as during exponential growth in fibroblasts (Kovary K 1992), but this may differ in other cell types.

Hormonal Regulation of AP-1 and its Colocalization with PRA

(a) c-Fos/PRA

c-Fos was not expressed in ovariectomized control mice, but of all of the AP-1 isoforms examined, c-Fos was the most E_2-inducible, showing a dramatic increase in the percentage of c-Fos expressing cells after E_2 treatment (Figures 3.23a, b). Both E_2 and E_2+P treatment can lead to rapid activation of MAPK signaling via non-genomic actions of ER (Bjornstrom L 2005). Activated ERK1 and ERK2 phosphorylate ternary complex factor (TCF) protein, which is already bound to the serum response element (SRE) together with serum response factor (SRF) at the c-Fos promoter (Karin M 1995). TCF phosphorylation in turn leads to rapid activation of c-Fos transcription (Karin M 1995). The surprising result came from P treatment where 20% of luminal epithelial cells expressed c-Fos compared to 0% in ovariectomized control (Figure 3.23b). The c-Fos promoter does not contain any canonical progesterone response elements (PREs), but P alone was reported to increase transcriptional activity from the c-Fos promoter in human breast cancer cells (T47-D and ZR-75 cell lines) (Carvajal A 2005). Furthermore, treatment of ZR-75 cells with P followed by exposure to epidermal growth factor (EGF) leads to both an increase in c-Fos promoter activity and nuclear localization of c-Fos protein (Carvajal A 2005). The EGF effect is thought to be mediated through epidermal growth factor receptor (EGFR) interaction with Stat proteins bound at the *sis* inducible element (SIE) in the promoter proximal region of the c-Fos gene (Janknecht R 1995). The P-inducibility of the

c-Fos promoter may be due to the ability of P to up-regulate the Stat proteins, specifically Stat5a (Santos SJ 2007) or Stat5b (Carvajal A 2005).

Based on these results, it is clear that c-Fos can be induced by both E_2 and P, however, this ligand-dependent regulation can only occur in PR^+/ER^+ cells. It has been previously shown in the ovariectomized virgin adult mouse that essentially every PRA^+ cell co-expresses ERα in all treatment groups (control, E_2, P and E_2+P) following 3, 5 or 10 days of hormone treatment (Aupperlee MD 2007). The strong correlation observed between c-Fos and PRA expression may therefore be due to the underlying correlation between PRA and ERα and the fact that both P and E_2 are capable of independently inducing c-Fos. In addition, once c-Fos protein expression is induced by steroid hormone treatment, it can dimerize with c-Jun and act in a positive regulatory loop to further promote PR expression in $ER\alpha^+$ cells.

(b) c-Jun/PRA

Since ovariectomized mice still expressed c-Jun protein in 24-30% of cells, this means that c-Jun was not dependent on ovarian hormones for its expression (Figures 3.24a, b, 3.26b). The rat c-Jun promoter is reported to contain an ERE capable of binding ER in hamster and yeast cell lines (Hyder SM 1995), but this ERE's functionality has not been examined in the mouse. However, what is interesting is that compared to control, E_2, P or E_2+P treatment all increased the expression of c-Jun to a small but significant extent ($p<0.05$) (Figures 3.24a, b). This suggests that although the basal number of c-Jun expressing cells was already high in the adult mouse mammary gland, the mouse c-Jun promoter may still be weakly E_2-reponsive. P may be exerting its effect through non-genomic interaction with Src, which could in turn activate JNK (Lange C 2008). JNK is the main activator of c-Jun and once pre-existing c-Jun (and ATF2)

proteins are phosphorylated, a positive auto-regulatory loop is activated leading to a rapid increase in c-Jun protein (Mechta-Grigoriou F 2001). Alternatively, P acting through PR may act genomically by tethering to the Sp1 sites located in the c-Jun promoter to aid in transactivation.

(c) JunB/PRA

Overall, JunB expression was not strongly altered by hormone treatment in the adult mouse mammary gland. E_2 treatment lead to a slight, but significant decrease in cells that expressed PRA alone and a corresponding increase in cells that co-expressed PRA and JunB ($p<0.05$) (Figure 3.S5). The number of total $JunB^+$ cells was slightly decreased after P treatment (Figure 3.S5). Treatment with E_2+P did not significantly alter the percentage of positive cells for PRA, JunB, or PRA/JunB (Figure 3.S5). The JunB promoter contains two serum response elements, the first of which (SRE1) can be induced by growth factors and recruits ternary complex factors (TCF) (Mechta-Grigoriou F 2001). The other site, SRE2, is both distantly located from SRE1 and non-responsive to growth factors (Mechta-Grigoriou F 2001). The JunB promoter is not reported to be hormone-responsive. However, P may exert indirect effects upon the JunB promoter by tethering to Sp1 protein bound at the GC-rich region of the JunB promoter (Mechta-Grigoriou F 2001). Alternatively, when PRB is expressed, P may act through the c-Src pathway to activate JNKs (Lange C 2008), which could in turn phosphorylate JunB. The JNK phosphorylation sites present in c-Jun are absent from JunB, but JunB does contain other motifs that can be phosphorylated (Mechta-Grigoriou F 2001). JunB is activated by PKA signaling, but PKA inhibits c-Jun (Mechta-Grigoriou F 2001); (Mechta F 1989), therefore, activation of PKA signaling can up-regulate JunB, but would down-regulate c-Jun expression.

(d) JunD/PRA

The number of cell expressing JunD alone or combined with PRA did not significantly change following hormone treatment (Figure 3.S6). The JunD promoter is reported to be the least serum responsive of the AP-1 isoforms and its major regulator is constitutively bound octamer-binding transcription factor 1 (Oct1) (Mechta-Grigoriou F 2001). Phospho-JunD is reported to repress transcription of genes involved in cell proliferation (Hernandez JM 2008), however, the role of JunD varies depending upon its AP-1 dimer binding partner, post-transcriptional, and post-translational regulation (Hernandez JM 2008). In the context of the adult mouse mammary gland, 3 days of E_2 treatment failed to induce proliferation (Figures 3.26, 3.27) and did not alter the number of $JunD^+$ cells (Figure 3.S6). If phospho-JunD down-regulates genes involved in proliferation in the mammary gland this change is not apparent in the JunD staining. Alternatively, JunD may not be involved prominently in cell cycle regulation in the mouse mammary gland.

(e) Fra1/PRA

In human breast samples, one group found that all of the neoplastic breast tissue tested was positive for nuclear Fra-1, regardless of whether it was benign or malignant tissue (Song Y 2006). Whereas adjacent normal tissue had much weaker nuclear staining in only a subset of the epithelial cells (Song Y 2006). In 90% of breast carcinomas studied, there was a shift from exclusively nuclear Fra-1 staining to the simultaneous expression of Fra-1 in the nucleus and cytoplasm (Song Y 2006). Fra-1 expression is much more stable than c-Fos expression, due to the presence of a single destabilizer element in Fra1 protein compared to two destabilizers in c-Fos (Gomard T 2008). Fra-1 has been shown to be important for cell motility, invasion, and

invasiveness in ER^+ MCF-7 cells and ER-negative MDA-MB231 cells (Belguise K 2005). Furthermore, since high Fra-1 expression is associated with a more malignant phenotype (Belguise K 2005), this establishes Fra-1 as an important player in breast cancer progression.

Colocalization between Fra1 and PRA was significantly greater than random after all hormone treatments, however, unlike the other AP-1 isoforms, this association was the greatest in control mice (Figure 3b). Therefore, there was an anti-correlation between Fra1 expression and hormone treatment. Since ERα colocalizes in essentially all PRA^+ cells (Aupperlee MD 2007), these results showed an increase in the ERα- negative/PRA-negative/$Fra1^+$ population of cells and corresponding decrease in $ER\alpha^+/PRA^+/Fra1^+$ cells. In human mammary tumor cell lines, the expression level of Fra1 varies dramatically depending on the hormone receptor status (Belguise K 2005). In the ER^+ cell lines, such as MCF-7, Fra1 expression levels are low, while in the ER-negative cell lines, such as MDA-MB231, Fra1 is highly over-expressed (Belguise K 2005). The non-proliferative $PRA^+/ER\alpha^+$ cells are capable of paracrine signaling with adjacent PR-negative cells (Aupperlee MD 2007); (Aupperlee M 2005a), therefore after 3 days of P or E_2+P treatment there was a larger proportion of $Fra1^+$/PRA-negative /ERα-negative cells that may be capable of proliferating. It has been previously shown that E_2 down-regulates ERα after 3 days of treatment (Aupperlee MD 2007), but it is interesting that rather than E_2, it was treatments containing P that were capable of increasing the number of PRA-negative/ERα-negative/$Fra1^+$ cells. These *in vivo* results were similar to breast tumor cell lines where Fra1 and PR/ER expression are inversely correlated (Belguise K 2005).

Treatment with E_2+P may lead to Increased Transactivation Potential of AP-1

Although the Jun proteins can homo- and heterodimerize amongst themselves, generally higher transcriptional activity is seen upon dimerization with a Fos binding partner due to greater stability and increased binding activity (Deng T 1993). Of the Fos isoforms, c-Fos is known to regulate the human PR promoter (Petz LN 2002); (Petz LN) and combined with c-Jun usually forms the strongest trans-activating AP-1 dimer when tested on an AP-1 responsive promoter such as collagenase (data not shown); (Deng T 1993) (Suzuki T 1991). Therefore, the change from no c-Fos and low c-Jun expression levels in the control ovariectomized mouse to moderate levels of both c-Fos and c-Jun after 3 days of E_2+P treatment may have a drastic effect on the transactivation potential of AP-1 (Figure 3.30). Additionally, the transcriptional activity of AP-1 parallels the proliferative state of the mammary gland. In control ovariectomized mice, there was no proliferation and AP-1 transactivation potential was relatively low, whereas after 3 days of treatment with E_2+P luminal epithelial cells in the mammary gland were highly proliferative and AP-1 transactivation potential was high (Figure 3.30).

Hormonal Regulation of AP-1 Expression and its Relation to Cell Proliferation

Although c-Fos was largely an E_2-inducible gene product, its colocalization with the proliferation marker BrdU was non-random and significant after P or E_2+P treatment in ovariectomized mouse mammary gland (Figures 3.27a, b). c-Fos was not expressed in control mice, but expression was highly induced after E_2 treatment, where there was essentially no proliferation in luminal epithelial cells (Figure 3.27a). Likewise, c-Jun showed significant colocalization with BrdU after P or E_2+P treatment in ovariectomized mouse mammary gland (Figures 3.26a, b). Even though c-Jun was expressed in mice treated with control and E_2, there

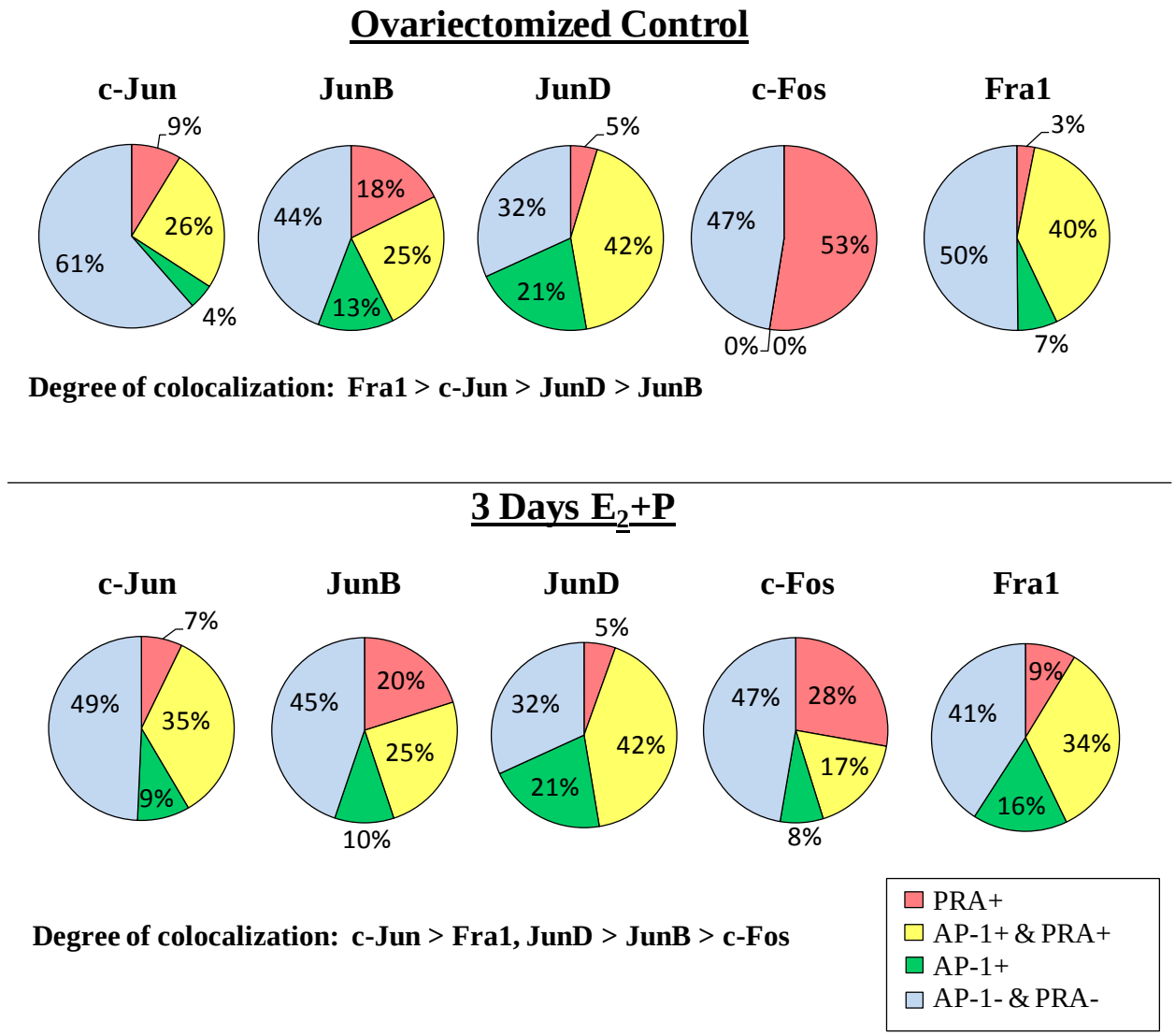

Figure 3.30: Hormonal regulation of AP-1 expression and colocalization with PRA. Immunofluorescence of PRA utilized an anti-PRA antibody (hPRa7) on tissue sections from 18-22 week virgin adult mice treated for 3 days with control or estradiol + progesterone (E_2+P). Colocalization with AP-1 used an anti-c-Jun antibody (sc-1694), an anti-JunB antibody (sc-46), an anti-JunD antibody (sc-74), an anti-c-Fos antibody (sc-52), or an anti-Fra1 antibody (sc-183). Quantitation values represent the mean ± SEM from three to four mice per group and a minimum of 500 cells/structure type/mouse analyzed. For statistical analysis a two-tailed Fischer's exact test was used for each structure type for each treatment. Colocalization was statistically significant ($p < 0.05$) for PRA and all AP-1 isoforms examined. The degree of colocalization was ranked based on Fischer's exact test value for significance. The distribution of AP-1 and PRA in large ducts mirrored the pattern shown for small ducts (data not shown).

was almost no proliferation in luminal epithelial cells (Figure 3.26a), as has also been shown previously by Aupperlee, *et al.* (Aupperlee MD 2007). Liganded PRA and ERα can participate in crosstalk with c-Jun, and once c-Jun expression is induced, c-Jun (specifically c-Jun/c-Fos) can also act on PR in $PRA^+/ER\alpha^+$ cells in a feed-forward amplification mechanism. These observations are consistent with the established role of c-Jun and c-Fos in regulation of the cell cycle (Figure 3.29); (Jochum W 2001).

Luminal epithelial cells in control ovariectomized mice or those treated with E_2 appeared to be proliferatively deficient due to a lack of P. In human breast cancer cell lines, there is an initial acceleration of cells from G_1 to S phase after P treatment, but once the cell cycle has been completed, these cells arrest in G_1 (Pestell RG 1999). The P-mediated increase in cell cycle progression also leads to an induction of cyclin D1 (Pestell RG 1999). Cyclin D1 is up-regulated by E_2, but E_2+P leads to a synergistic enhancement of the E_2-mediated induction (Pestell RG 1999). Therefore, proliferation, as assayed by BrdU staining (Figure 3.29(iii)), is often greatest in luminal epithelial cells from mice treated with E_2+P (or P) due to the combined effects of both E_2 and P on cell cycle target genes such as cyclin D1 (Figure 3.29).

Based on results from our developmental study in the mouse mammary gland (Figure 3.16), PRA^+ cells were found to nearly always colocalize with c-Jun and also with Fra1 protein expression. c-Jun in particular is known to be an important inducer of cell proliferation along with c-Fos due to their up-regulation of the cyclin D1 gene (Figure 3.29); (Jochum W 2001). c-Jun is also reported to be necessary for proliferation based on its ability to down-regulate p53 (Figure 3.29); (Jochum W 2001). However, based on these immunofluorescence studies, there was still a significant portion of $BrdU^+$ cells that were c-Jun-negative and c-Fos-negative (Figures 3.26b, 3.27b). Therefore either c-Jun/c-Fos are not required for progression

into S phase, they may be turned over more rapidly (after phosphorylation) (Jariel-Encontre I 1997) than incorporated BrdU, or other Jun isoforms can drive cell cycle progression (Figure 3.29).

Overall, expression of c-Fos and c-Jun are regulated by steroid hormones. As expected, c-Fos was not expressed in control ovariectomized mice but was highly up-regulated following E_2 treatment. Surprisingly, c-Fos was also modestly up-regulated by P or E_2+P. c-Jun was expressed in a moderate number of cells in control mice and was slightly, but significantly, up-regulated by E_2, P, or E_2+P treatment. Colocalization of AP-1 with proliferating cells (i.e. those that incorporate BrdU) showed that in control mice, there was abundant c-Jun but no c-Fos expression, along with a complete lack of proliferation in luminal epithelial cells. Although there was sufficient c-Jun and c-Fos in E_2 treated mice, BrdU staining indicates that the mammary epithelium remains proliferatively quiescent under these conditions. The reason why short term (3 day) treatment with P or E_2+P, but not with E_2 alone, was able to stimulate proliferation remains unclear, however, there are several possibilities. First, AP-1 proteins must be phosphorylated in order to exert their transcriptional actions on target genes involved in cell cycle progression (Shaulian E 2002). Second, it has been proposed that non-proliferative ER^+/PR^+ cells are growth arrested by high levels of inhibitors like p21 and p27 (Figure 3.29) (Lange C 2008). It appears likely that P is therefore more efficient than E_2 in promoting the expression of key cell cycle regulatory proteins as well as in priming the signaling pathways (i.e. MAPK) that are necessary for AP-1 activation. Since AP-1 acts as an extracellular signal responsive transcription factor complex located at the end of a vast array of signaling cascades, it may indeed be the link between growth factor signaling and cell cycle control.

Future Directions

Two main candidates for cooperation with AP-1 in PRB^+ cells are the Stat proteins, especially Stat5a, along with C/EBPβ, both of which have been shown to be highly expressed during mid- to late-pregnancy in the mouse mammary gland (Santos SJ 2007); (Grimm SL 2003). It would be interesting to determine which AP-1 isoform colocalizes with Stat5a and C/EBPβ in the mouse mammary gland during mid- to late-pregnancy. We hypothesize that c-Jun and Fra1 are the most likely to colocalize with Stat5a and C/EBPβ due to their high expression levels in the pregnancy-like mammary gland. Furthermore, if Stat5a, C/EBPβ, and AP-1 are all cooperating in the regulation of PRB expression, one could determine which binding sites in the PRB promoter are actually occupied by each of these transcription factors. Similarly, the AP-1 binding sites in the PRA promoter could be definitively mapped.

Based on the growth factors and hormones present during pregnancy, particularly the high levels of E_2 and P, c-Fos may show transient high expression in the pregnant mouse mammary gland. In an ovary-intact virgin adult mouse, treatment for 14 days with E_2+P only led to low levels of c-Fos expression, but after ovariectomy, a shorter 3 day treatment with E_2, P, or E_2+P led to a dramatic increase in the number of cells expressing c-Fos compared to control mice. This suggests that c-Fos is capable of being expressed in a robust, but transient manner, the kinetics of which are unknown. An appropriate follow-up experiment would be to determine the timing and relative expression level of c-Fos in the pregnant state (late-pregnancy) along with in the ovariectomized mouse at 5, 10 and 14 days of hormone treatment. One would predict that in the ovariectomized mouse, c-Fos expression is still relatively high after 5 days of hormone treatment but decreases by 14 days of treatment.

One possible direction for future work would be to determine the effect of post-transcriptional regulation on the PR transcripts, including processing, export, localization, turnover and translation of the PR message. Another would be to determine the effect of translational/post-translational regulation on the PR proteins, including translation initiation and protein modifications such as phosphorylation. The ultimate goal of examining regulation at levels following transcription would be to tease apart the precise nature of the differential regulation of the PRB and PRA promoters in the mouse mammary gland.

From a physiological standpoint, the most interesting follow-up experiment would involve determining if there is a mammary gland phenotype in the various AP-1 knock-out mice during development (puberty, virgin adult, early-, mid- and late-pregnancy, along with lactation and involution). Since many of the AP-1 knock-out mice were embryonic lethal (c-Jun, JunB and Fra1), this leaves only the c-Fos, FosB and JunD knock-out mice as a possibility to study in adulthood (Jochum W 2001). Because c-Jun and Fra1 showed the highest degree of correlation with PRA, these would be the most probable isoforms to show a mammary defect. To get around the embryonic lethality issue, one could use a either a conditional mammary gland specific knock-out or alternatively a knock-in strategy. For the knock-in mice, floxed AP-1 mice (c-Jun or Fra1) could be crossed with mouse mammary tumor virus-Cre recombinase (MMTV-Cre) mice.

Summary and Conclusions

The mouse progesterone receptor gene is composed of two promoters, which give rise to PRA and PRB proteins in a spatially and temporally distinct pattern. The proximal promoter, which is the predominant isoform in the pubertal and virgin adult mammary gland, gives rise to

PRA protein. The distal promoter, which is the predominant isoform during mid- to late-pregnancy, gives rise to a second set of transcripts that initiate upstream of the proximal promoter and encode the PRB isoform but may also encode the PRA isoform. The PRA and PRB protein isoforms only colocalized in a small subset of cells during mid- to late-pregnancy, further suggesting that the promoters are under differing control. In luminal epithelial cells, PRA colocalized highly with c-Jun and Fra1, as well as JunB and JunD to a lesser extent, across developmental states. This differs from PRB, which only colocalized with AP-1 isoforms in the small percentage of cells that co-expressed PRA. Transient transfection experiments demonstrated the ability of c-Jun in up-regulating the PRA, PRB and PRA+PRB promoter luciferase constructs. JunB alone was not able to transactivate any of the PR promoter constructs, but JunD had a weak activating effect upon the long tandem promoter. Taken together with the immunofluorescence data, this supports a role for AP-1 in up-regulating the PRA promoter during development, especially c-Jun and Fra1.

Interestingly, in the ovariectomized virgin adult mouse, the prevalence of Jun isoforms is reversed from an ovary-intact age-matched mouse. In an ovary-intact mouse, the prevalence of Jun isoforms was c-Jun, JunB, JunD, whereas in the ovariectomized mouse JunD was the predominant isoform followed by JunB and c-Jun. Fra1 was expressed in a large number of cells across development in an ovary-intact mouse as well as in an ovariectomized adult mouse. The greatest difference in Fos isoforms was seen in the expression of c-Fos, which was expressed in a very small percentage of cells across development in an ovary-intact mouse, but completely absent in an ovariectomized adult mouse. In the ovariectomized adult mouse, treatment with E_2 or E_2+P induced c-Fos expression in a subpopulation of luminal epithelial cells. Hormone treatments in the ovariectomized adult mouse did not have an effect on JunB or JunD expression

or colocalization with PRA. However, the number of luminal epithelial cells expressing c-Jun was significantly increased by treatment with E_2, P or E_2+P. Transient transfection of the PR promoter constructs followed by hormone treatment did not alter promoter activity suggesting that the main effect of E_2 on the PR promoters is indirect or due to distant EREs. Rather, changes in the levels of c-Fos and c-Jun, mediated by E_2 and P, had a more dramatic effect on PRA promoter activity. Although the PRB promoter was induced by various AP-1 isoforms in transfection assays, immunofluorescence staining showed that AP-1 alone cannot account for the large proportion of AP-1-negative/PRB^+ cells in the mid-pregnant mammary gland. This implies that other transcription factors (Stat5a, C/EBPβ) known to be highly expressed during pregnancy may be needed for PRB expression. Therefore, expression of the mouse PR gene is regulated not just by E_2 and P, but also by growth regulatory pathways that signal through AP-1 and other transcription factors. The results reported herein show that the subunit composition of AP-1 and its expression pattern correlated more closely with expression of PRA compared to PRB. Specifically, the c-Jun subunit correlated highly with PRA expression, and PRA^+ cells invariably express one Jun isoform or another.

APPENDIX

CHAPTER 3

APPENDIX

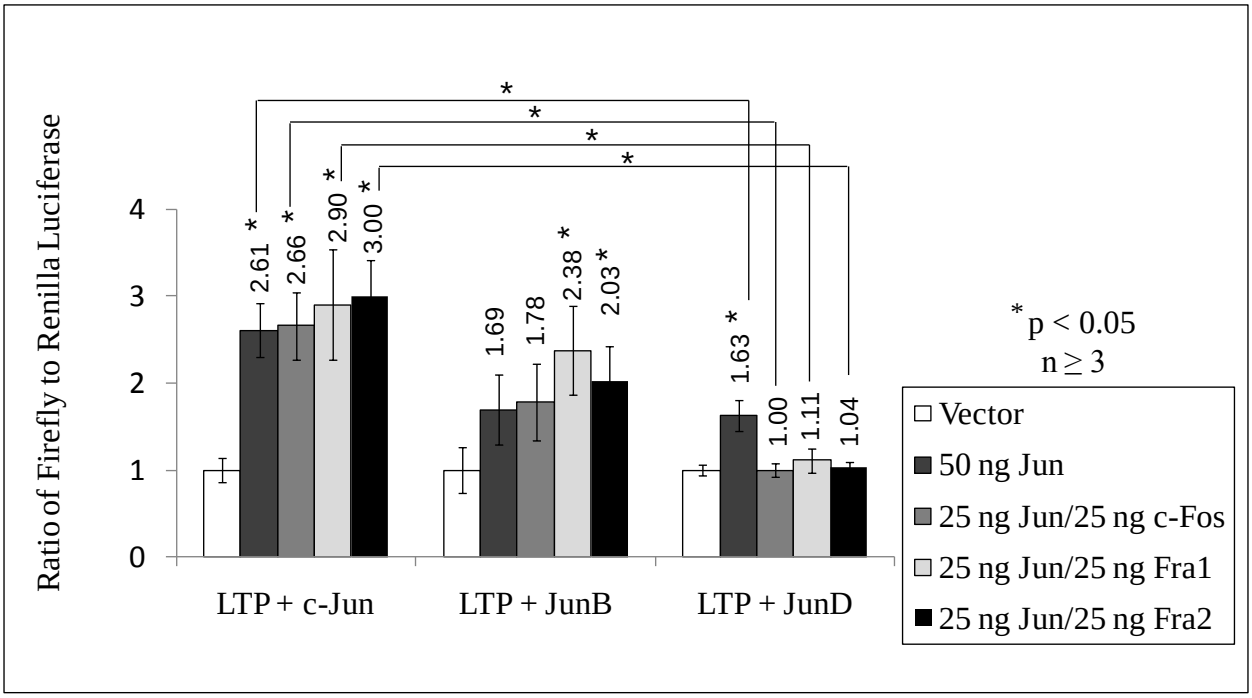

Figure 3.S1a: Cotransfection of mouse long tandem promoter construct with Jun/Fos. The mouse long tandem PR promoter (LTP) construct was transfected with 50 ng Jun (c-Jun, JunB or JunD) or 25 ng Jun plus 25 ng of a Fos partner (c-Fos, Fra1 or Fra2) in MCF-7 cells. Mean of the normalized ratio of firefly to renilla luciferase activity for promoter reporter constructs cotransfected with empty vector or AP-1 ± SE. Normalization was based on induced promoter activity relative to basal expression. Fold change values represent the ratio of induction relative to vector control. Differences between the Jun isoforms are indicated with brackets. Datapoints are derived from a minimum of 3 replicate experiments containing triplicate determinations. Statistical analysis utilized Student's *t* test and statistical significance (*) is denoted when $p<0.05$.

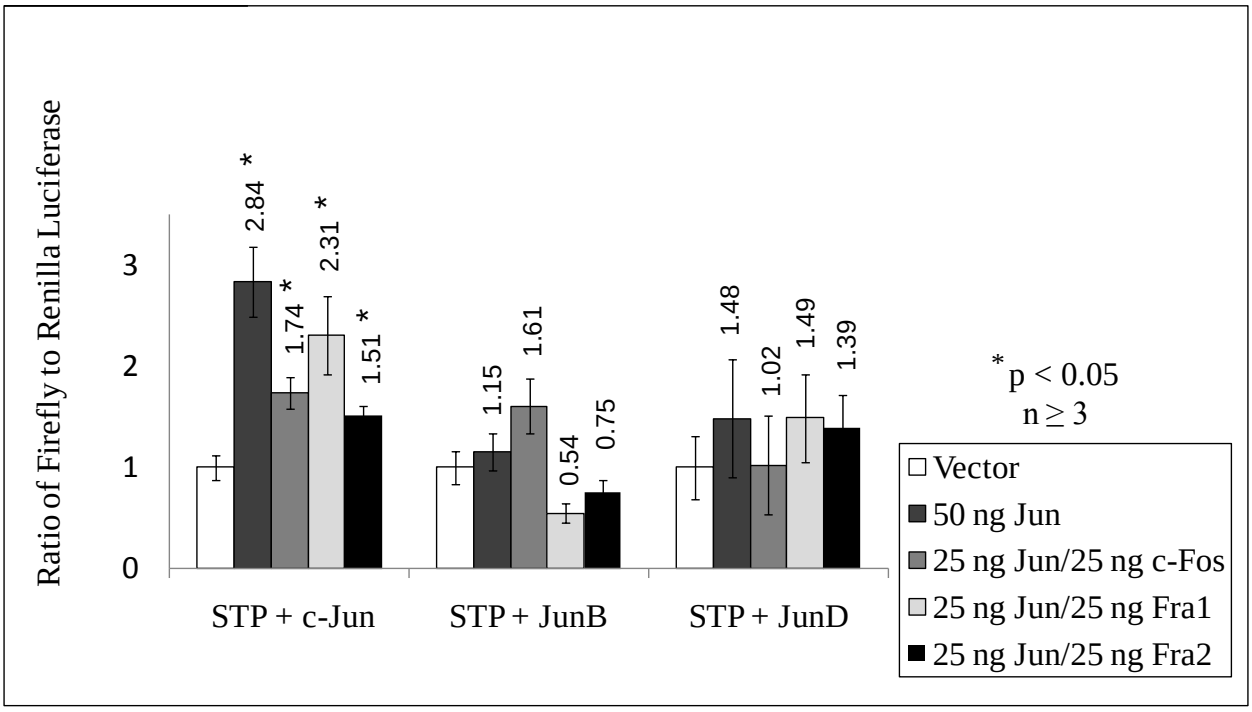

Figure 3.S1b: Cotransfection of mouse short tandem promoter construct with Jun/Fos. The mouse short tandem PR promoter (STP) construct was transfected with 50 ng Jun (c-Jun, JunB or JunD) or 25 ng Jun plus 25 ng of a Fos partner (c-Fos, Fra1 or Fra2) in MCF-7 cells. Mean of the normalized ratio of firefly to renilla luciferase activity for promoter reporter constructs cotransfected with empty vector or AP-1 ± SE. Normalization was based on induced promoter activity relative to basal expression. Fold change values represent the ratio of induction relative to vector control. Datapoints are derived from a minimum of 3 replicate experiments containing triplicate determinations. Statistical analysis utilized Student's *t* test and statistical significance (*) is denoted when $p<0.05$.

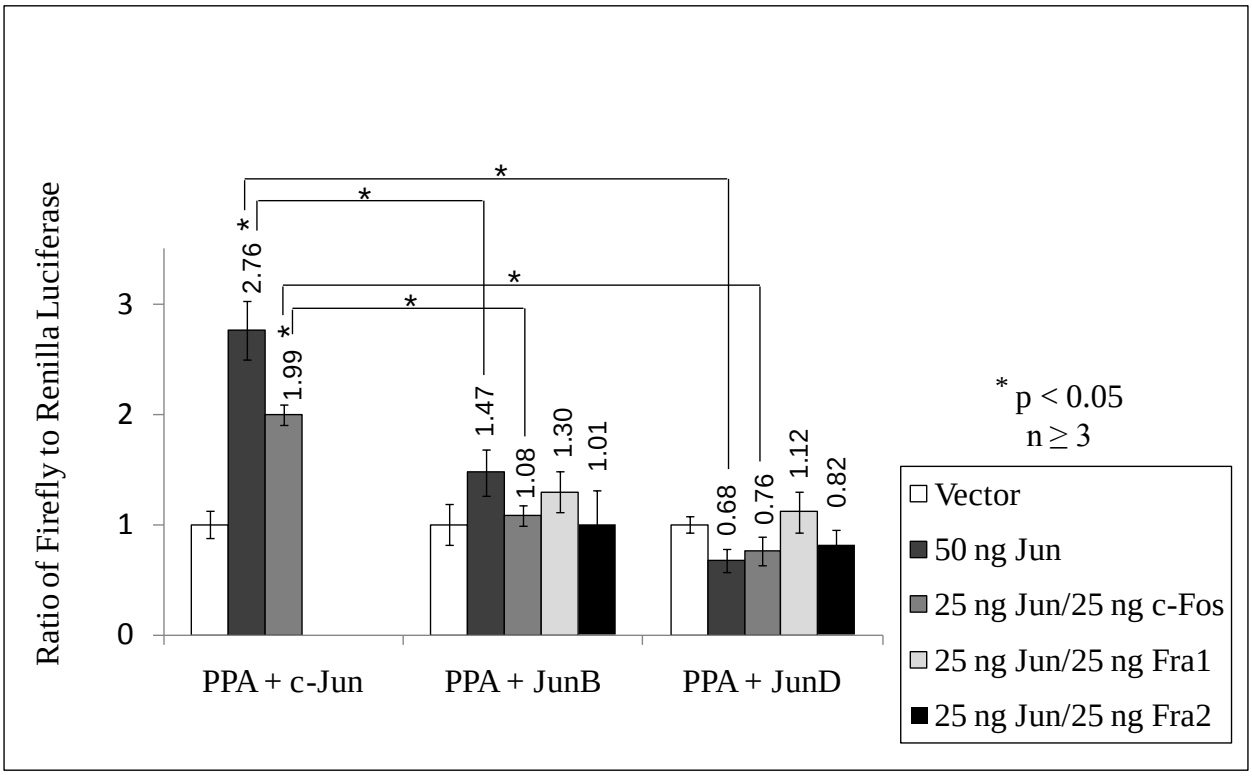

Figure 3.S1c: Cotransfection of mouse proximal promoter A construct with Jun/Fos. The mouse proximal promoter PRA (PPA) construct was transfected with 50 ng Jun (c-Jun, JunB or JunD) or 25 ng Jun plus 25 ng of a Fos partner (c-Fos, Fra1 or Fra2) in MCF-7 cells. Mean of the normalized ratio of firefly to renilla luciferase activity for promoter reporter constructs cotransfected with empty vector or AP-1 ± SE. Normalization was based on induced promoter activity relative to basal expression. Fold change values represent the ratio of induction relative to vector control. Differences between the Jun isoforms are indicated with brackets. Datapoints are derived from a minimum of 3 replicate experiments containing triplicate determinations. Statistical analysis utilized Student's *t* test and statistical significance (*) is denoted when $p<0.05$.

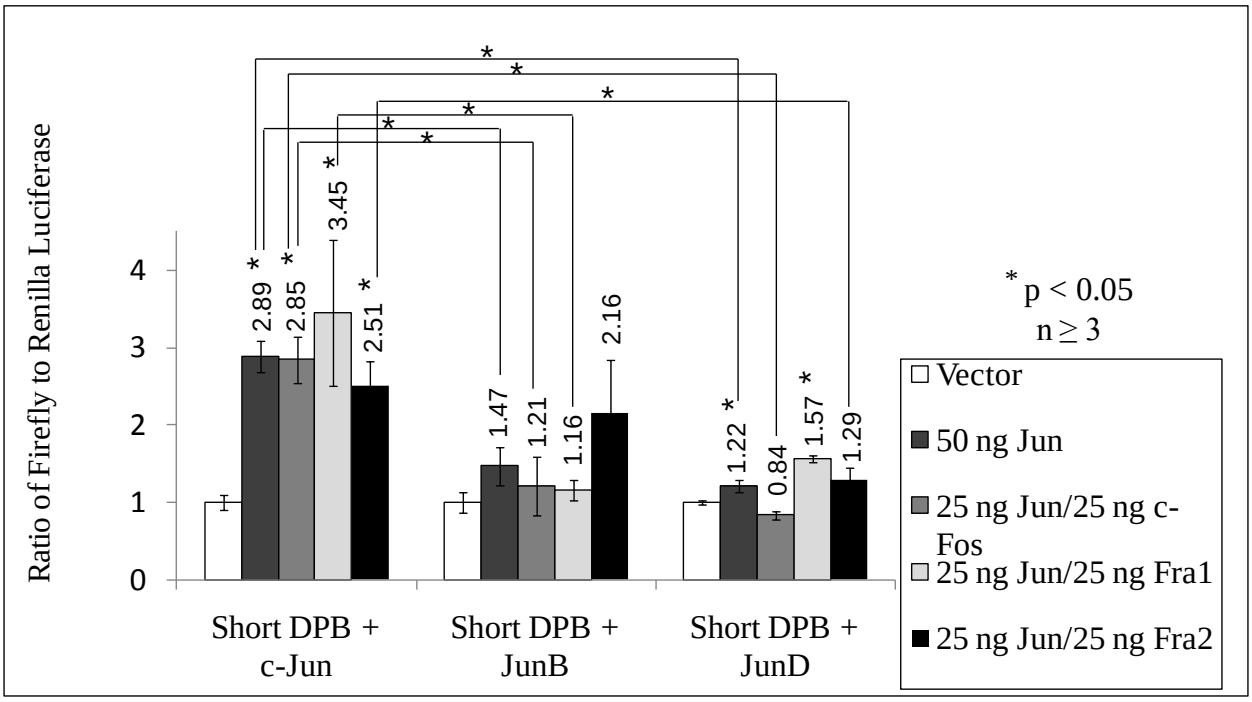

Figure 3.S1d: Cotransfection of mouse short distal promoter B construct with Jun/Fos. The mouse short distal promoter B (Short DPB) construct was transfected with 50 ng Jun (c-Jun, JunB or JunD) or 25 ng Jun plus 25 ng of a Fos partner (c-Fos, Fra1 or Fra2) in MCF-7 cells. Mean of the normalized ratio of firefly to renilla luciferase activity for promoter reporter constructs cotransfected with empty vector or AP-1 ± SE. Normalization was based on induced promoter activity relative to basal expression. Fold change values represent the ratio of induction relative to vector control. Differences between the Jun isoforms are indicated with brackets. Datapoints are derived from a minimum of 3 replicate experiments containing triplicate determinations. Statistical analysis utilized Student's *t* test and statistical significance (*) is denoted when $p<0.05$.

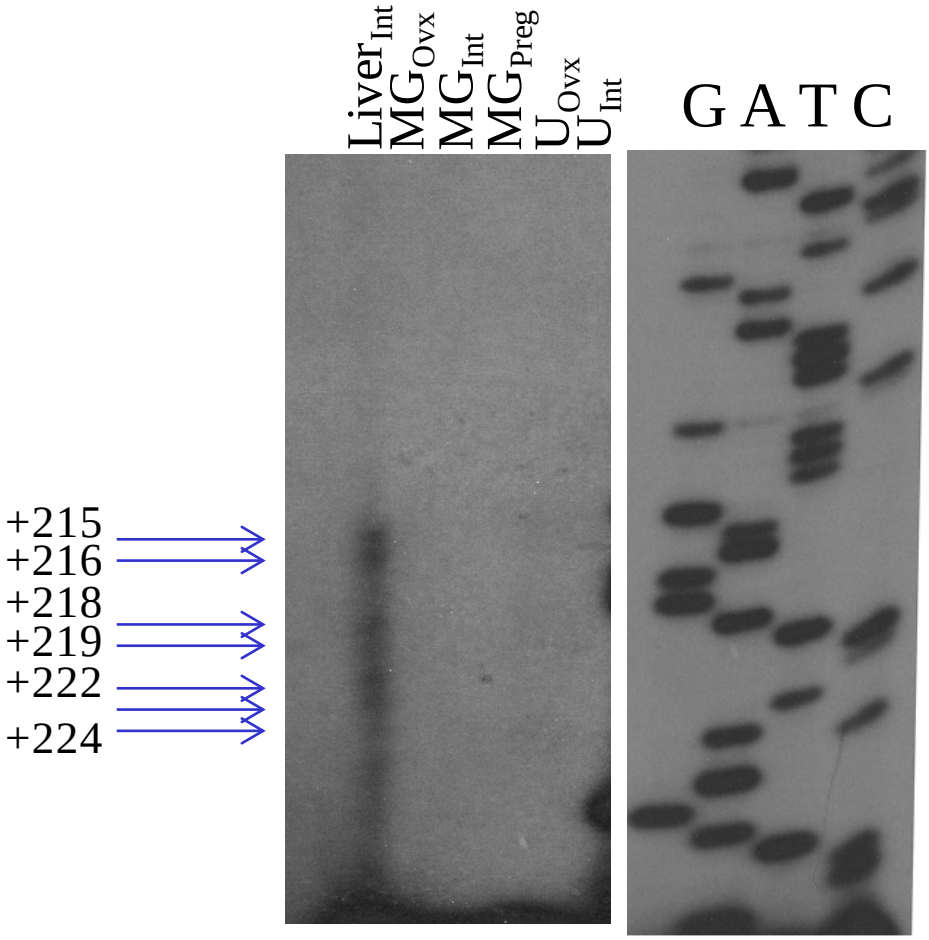

Figure 3.S2: Representative primer extension reactions using total RNA extracted from the liver (L), uterus (U) and mammary gland (MG) using primer Distal 2 (D2).
Virgin adult BALB/c mice were either ovary-intact (Int) or ovariectomized (Ovx) and 40 μg of RNA was used per reaction. Total RNA from a 10 day pregnant mouse (MG_{preg}) was also used for comparison. GATC lanes represent the four sequencing reactions of mouse PR plasmid DNA initiated with the corresponding primers and run in parallel.
Bands for liver RNA clustered from +215 to +224 bp, but there was a virtual absence of bands from mammary gland or uterine RNA using the D2 primer to detect the presence of PRB mRNA.

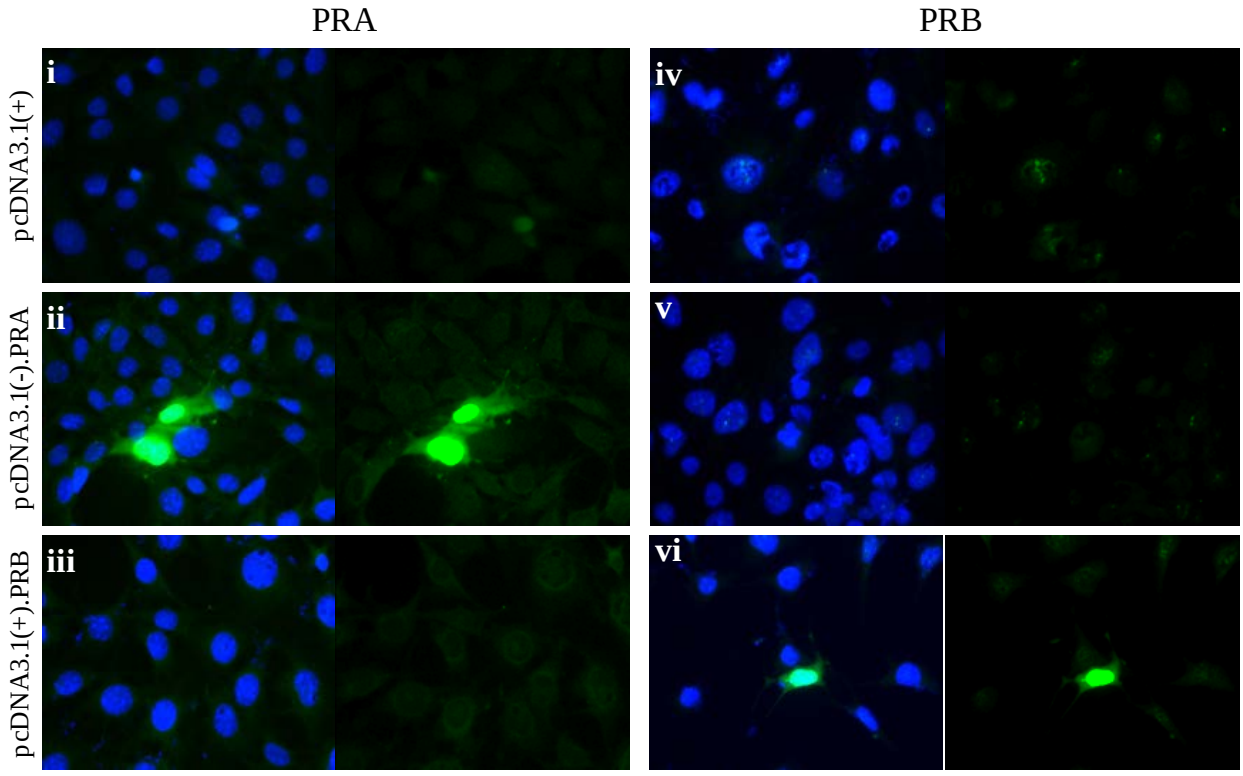

Figure 3.S3: Immunofluorescence of UMD-208 cells using an antibody to detect PRA (hPRa7) (i, ii and iii) or PRB (B15) (iv, v and vi). UMD-208 cells were transiently transfected with empty vector pcDNA3.1(+) (i and iv), a PRA expression vector (pcDNA3.1(-).PRA) (ii and v) or a PRB expression vector (pcDNA3.1(+).PRB) (iii and vi). Transfection with pcDNA3.1(+) was the same as untransfected (i and iv). (ii) PRA expression vector transfected cells stained with PRA antibody show specific intense nuclear staining which is absent in PRB transfected cells (iii). (vi) PRB transfected cells stained with PRB show specific intense nuclear staining which is absent in PRA transfected cells (v). UMD-208 cells were cultured in 5% fetal calf serum and were transfected 24 hours prior to cell fixation.

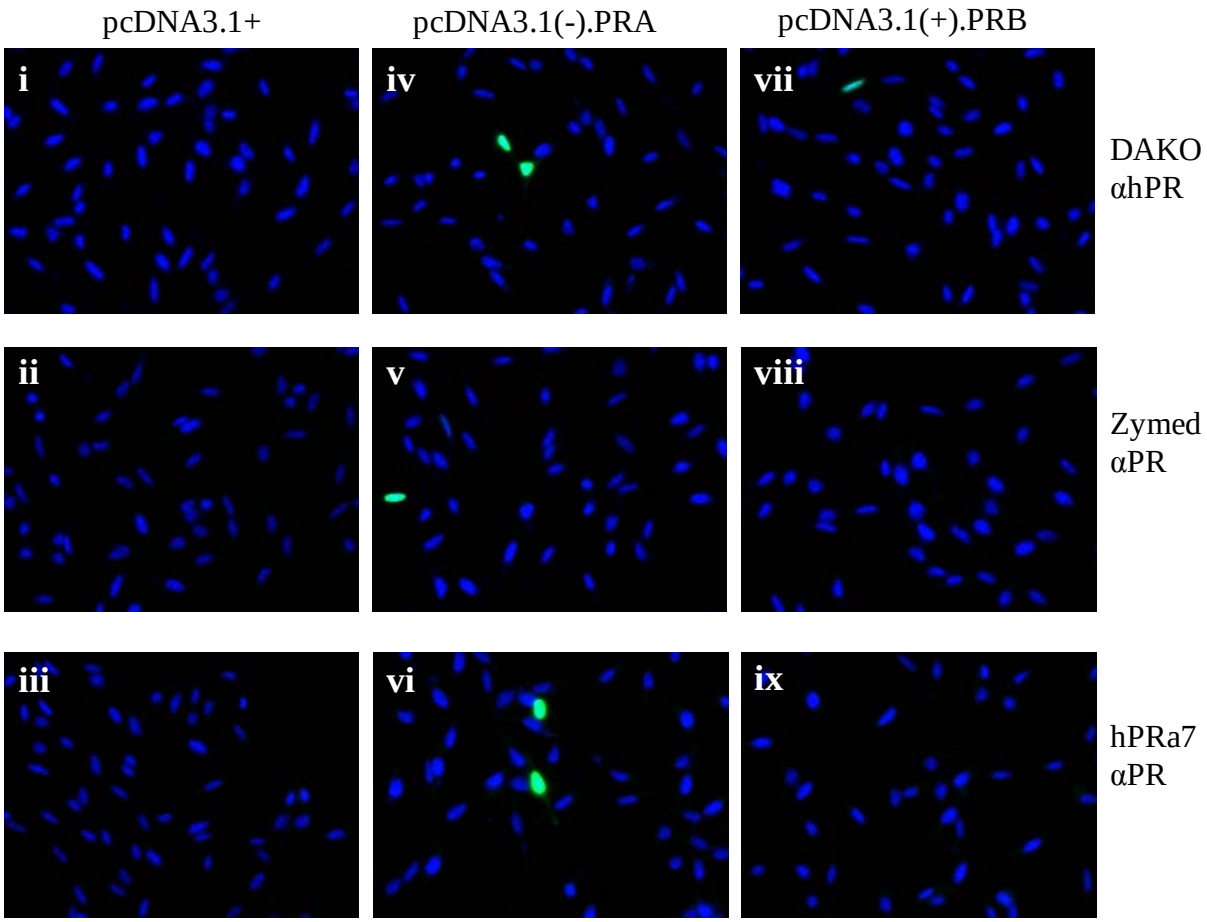

Figure 3.S4: Immunofluorescence of mouse L cells using a panel of antibodies to detect PRA. Merged images show DAPI counterstained nuclei (blue) and PRA staining (green). (i, iv and vii) staining with the DAKO anti-human PR antibody was detected in cells transfected with a PRA expression construct (pcDNA3.1(1).PRA) (iv) and weakly in a small number of cells transfected with a PRB expression construct (pcDNA3.1(+).PRB). (ii, v and viii) staining with the Zymed anti-PR antibody was only detected in cells transfected with a PRA expression vector (pcDNA3.1(-).PRA). (iii, vi and viii) staining with Neomarkers hPRa7 anti-human PR antibody was only detected in cells transfected with a PRA expression construct (pcDNA3.1(-).PRA).

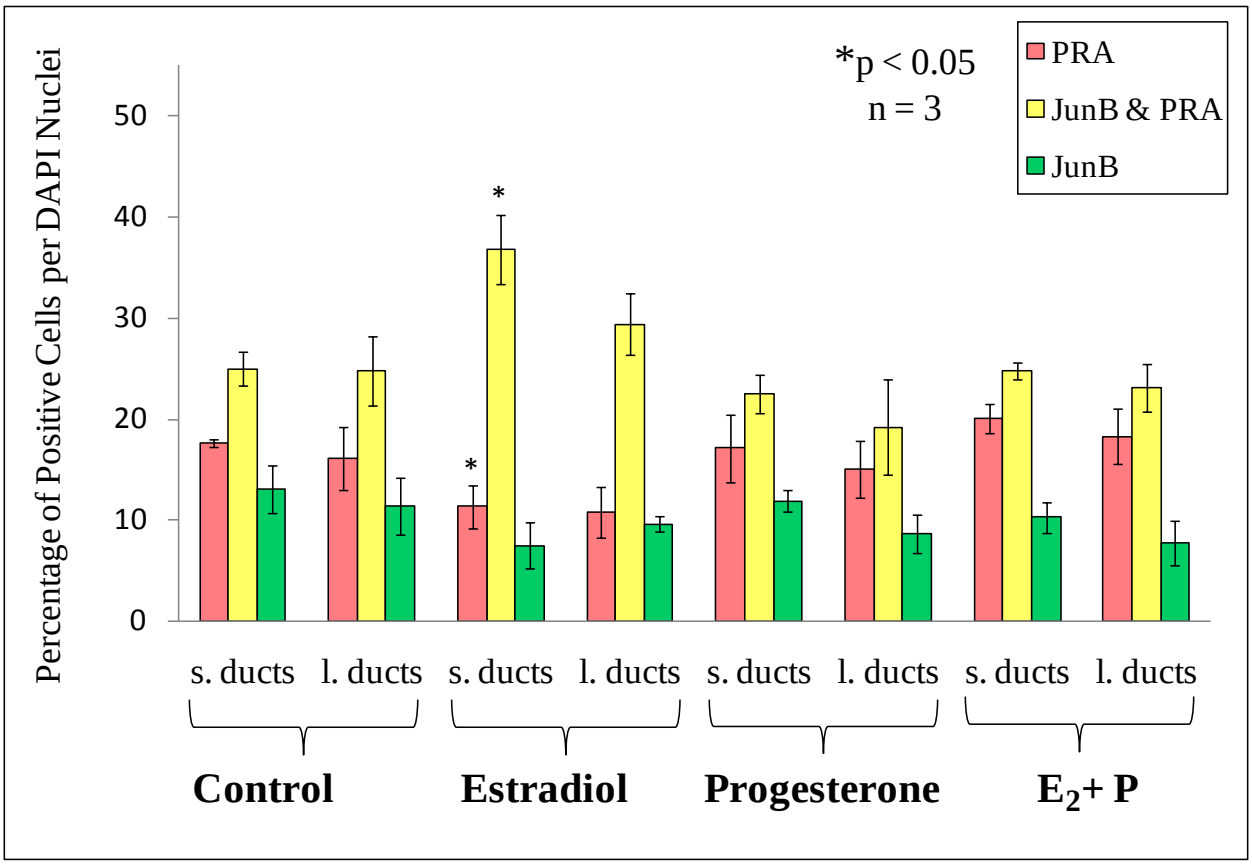

Figure 3.S5: Hormonal regulation of JunB expression and colocalization with PRA. Immunofluorescence of PRA utilized an anti-PRA antibody (hPRa7) on tissue sections from 18-22 week virgin adult mice treated for 3 days with control, estradiol (E_2), progesterone (P) or E_2+P. Colocalization with JunB used an anti-JunB antibody (sc-46). Quantitation values represent the mean ± SEM from three to four mice per group and a minimum of 500 cells/structure type/mouse analyzed. Statistical analysis utilized Student's *t* test and significance is denoted: *p<0.05.

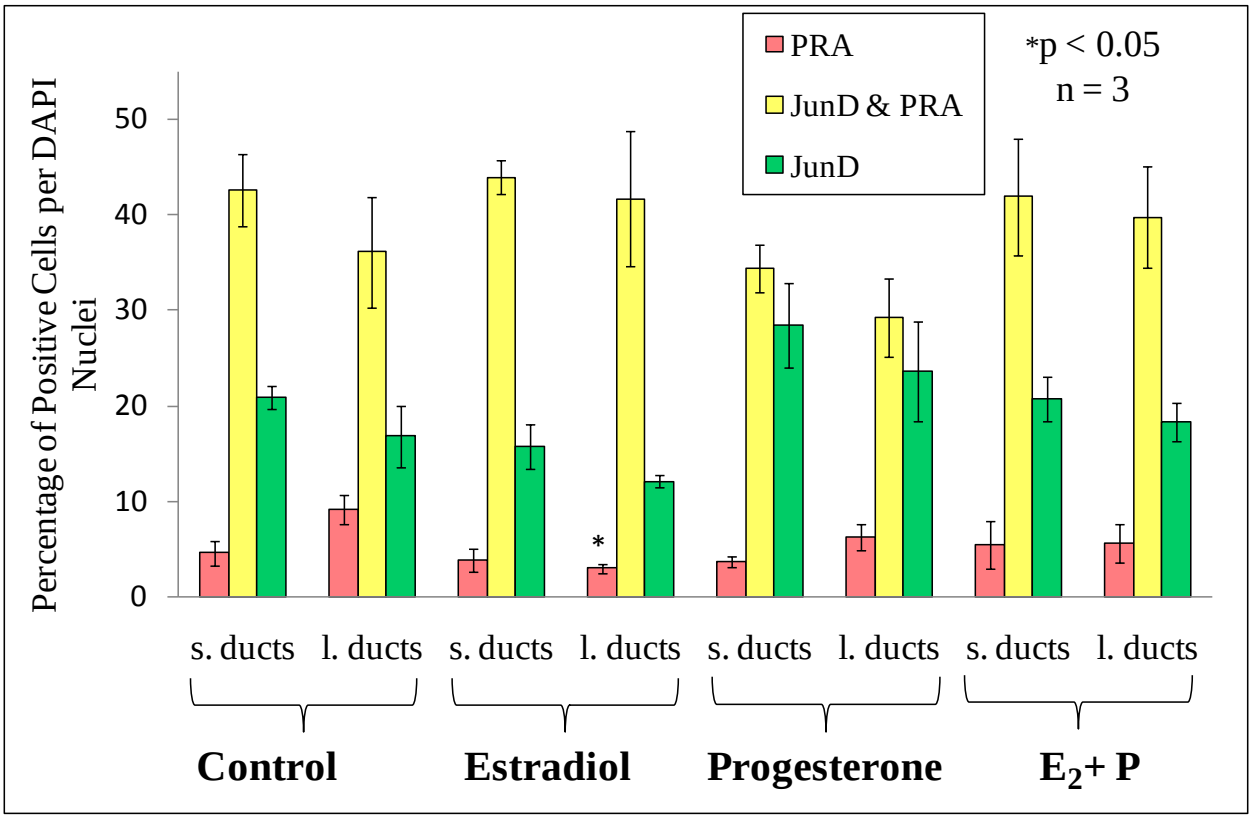

Figure 3.S6: Hormonal regulation of JunD expression and colocalization with PRA. Immunofluorescence of PRA utilized an anti-PRA antibody (hPRa7) on tissue sections from 18-22 week virgin adult mice treated for 3 days with control, estradiol (E_2), progesterone (P) or E_2+P. Colocalization with JunD used an anti-JunD antibody (sc-74). Quantitation values represent the mean ± SEM from three to four mice per group and a minimum of 500 cells/structure type/mouse analyzed. Statistical analysis utilized Student's *t* test and significance is denoted: *p<0.05.

REFERENCES

REFERENCES

Aupperlee M, Smith KT, Kariagina A, Haslam SZ. "Progesterone Receptor Isoforms A and B: Temporal and Spatial Differences in Expression during Murine Mammary Gland Development." Endocrinology 146.8 (2005a): 3577-3588.

Aupperlee M, Kariagina A, Osuch J, Haslam SZ. "Progestins and Breast Cancer." Breast Disease 24 (2005b): 37-57.

Aupperlee MD, Haslam SZ. "Differential Hormonal Regulation and Function of Progesterone Receptor Isoforms in Normal Adult Mouse Mammary Gland." Endocrinology 148.5 (2007): 2290-2300.

Bamberger AM, Methner C, Lisboa BW, Stadtler C, Schulte HM, Loning T, Milde-Langosch K. "Expression Pattern of the AP-1 Family in Breast Cancer: Association of fosB Expression with a Well-Differentiated Receptor-Positive Tumor Phenotype." International Journal of Cancer 84 (1999): 533-538.

Bamberger AM, Milde-Langosch K, Schulte HM. "Progesterone Receptor Isoforms, PRB and PRA, in Breast Cancer: Correlations with Clinicopathologic Tumor Parameters and Expression of AP-1 factors." Hormone Research 54 (2000): 32-37.

Belguise K, Kersual N, Galtier F, Chalbos D. "FRA-1 Expression Level Regulates Proliferation and Invasiveness of Breast Cancer Cells." Oncogene 24 (2005): 1434-1444.

Bjornstrom L, Sjoberg M. "Mechanisms of Estrogen Receptor Signaling: Convergence of Genomic and Nongenomic Actions on Target Genes." Molecular Endocrinology 19 (2005): 833-842.

BLAST 2010. (BLAST) Basic Local Alignment Search Tool. <www.ncbi.nlm.nih.gov/blast/>.

Boney-Montoya J, Ziegler YS, Curtis CD, Montoya JA, Nardulli AM,. "Long-Range Transcriptional Control of Progesterone Receptor Gene Expression." Molecular Endocrinology 24.2 (2010): 346-358.

Brose N, Rosenmund C. "Move Over Protein Kinase C, You've Got Company: Alternative Cellular Effectors of Diacylglycerol and Phorbol Esters." Journal of Cell Science 115 (2002): 4399-4411.

Carninci P, Sandelin A, Lenhard B, Katayama S, Shimokawa K, Ponjavic J, Semple CA, Taylor MS, Engström PG, Frith MC, Forrest AR, Alkema WB, Tan SL, Plessy C, Kodzius R, Ravasi T, Kasukawa T, Fukuda S, Kanamori-Katayama M, Kitazume Y, Kawaji H, Kai C,. "Genome-wide analysis of mammalian promoter architecture and evolution." Nature Genetics 38.6 (2006): 626-635.

Carroll JS, Meyer CA, Song J, Li W, Geistlinger TR, Eeckhoute J, Brodsky AS, Kransickas Keeton E, Fertuck KC, Hall GF, Wang Q, Beriranov S, Sementchenko V, Fox EA, Silver PA, Gingeras TR, Liu XS, Brown M. "Genome-wide Analysis of Estrogen Receptor Binding Sites." Nature Genetics 38.11 (2006): 1289-1297.

Carvajal A, Espinoza N, Kato S, Pinto M, Sadarangani A, Monso C, Aranda E, Villalon M, Richer JK, Horwitz KB, Brosens JJ, Owen GI. "Progesterone Pre-treatment Potentiates EGF Pathway Signaling in the Breast Cancer Cell Line ZR-75." Breast Cancer Research and Treatment 94 (2005): 171-183.

Cho H, Aronica SM, Katzenellenbogen BS. "Regulation of Progesterone Receptor Gene Expression in MCF-7 Breast Cancer Cells: A Comparison of the Effects of Cyclic Adenosine 3',5'-Monophosphate, Estradiol, Insulin-Like Growth Factor-I, and Serum Factors." Endocrinology 134.2 (1994): 658-664.

Deng T, Karin M. "JunB Differs From c-Jun in its DNA-Binding and Dimerization Domains, and Represses c-Jun by Formation of Inactive Heterodimers." Genes & Development 7 (1993): 479-490.

Faivre E, Skildum A, Pierson-Mullany L, Lange CA. "Interactions of Progesterone Receptor Mediated Rapid Signaling and Nuclear Actions in Breast Cancer Cell Models: Role of Mitogen-Activated Protein Kinases and Cell Cycle Regulators." Steriods 70 (2005): 418-426.

Frasor J, Danes JM, Komm B, Chang KCN, Lyttle CR, Katzenellenbogen BS. "Profiling of Estrogen Up- and Down-Regulated Gene Expression in Human Breast Cancer Cells: Insights into Gene Networks and Pathways Underlying Estrogenic Control of Proliferation and Cell Phenotype." Endocrinology 144.10 (2003): 4562-4574.

GenBank (NCBI) 2008. GenBank. <http://www.ncbi.nlm.nih.gov/Genbank/>.

Gomard T, Jariel-Encontre I, Basbous J, Bossis G, Mocquet-Torcy G, Piechaczyk M. "Fos Family Protein Degradation by the Proteasome." Biochmical Society Transactions 36.5 (2008): 858-863.

Grimm SL, Rosen JM. "The Role of C/EBPBeta in Mammary Gland Development and Breast Cancer." Journal of Mammary Gland Biology and Neoplasia 8.2 (2003): 191-204.

Grossoni VC, Falbo KB, Kazanietz MG, Bal de Kier Joffe ED, Urtreger AJ. "Protein Kinase C Delta Enhances Proliferation and Survival of Murine Mammary Cells." Molecular Carcinogenesis 46.5 (2007): 381-390.

Hernandez JM, Floyd DH, Weilbaecher KN, Green PL, Boris-Lawrie K. "Multiple Facets of JunD Gene Expression are Atypical Among AP-1 Family Members." Oncogene 27 (2008): 4757-4767.

Hess J, Angel P, Schorpp-Kistner M. "AP-1 Subunits: Quarrel and Harmony Among Siblings." Journal of Cell Science 117 (2004): 5965-5973.

Hirai SI, Ryseck RP, Mechta F, Bravo R, Yaniv M. "Characterization of junD: A New Member of the jun Proto-oncogene Family." The EMBO Journal 8.5 (1989): 1433-1439.

Hovey RC, Trott JF, Vonderhaar BK. "Establishing a Framework for the Functional Mammary Gland: From Endocrinology to Morphology." Journal of Mammary Gland Biology and Neoplasia 7.1 (2002): 17-38.

Hyder SM, Nawaz Z, Chippetta C, Yokoyama K, Stancel GM. "The Protooncogene c-jun Contains an Unusual Estrogen-inducible Enhancer within the Coding Sequence." The Journal of Biological Chemistry 270.15 (1995): 8506-8513.

Jacobsen BM, Schittone SA, Richer JK, Horwitz KB. "Progesterone-Independent Effects of Human Progesterone Receptors (PRs) in Estrogen Receptor-Positive Breast Cancer: PR Isoform-Specific Gene Regulation and Tumor Biology." Molecular Endocrinology 19.3 (2005): 574-587.

Jaggi R, Marti A, Guo K, Feng Z, Friis RR. "Symposium: Control of Mammary Cell Growth. Regulation of a Physiological Apoptosis: Mouse Mammary Involution." Journal of Dairy Science 79.6 (1996): 1074-1084.

Janknecht R, Cahill MA, Nordheim A. "Signal Integration at the c-fos Promoter." Carcinogenesis 16.3 (1995): 443-450.

Jariel-Encontre I, Salvat C, Steff AM, Pariat M, Acquaviva C. "Complex Mechanisms for c-fos and c-jun Degradation." Molecular Biology Reports 24 (1997): 51-56.

Jochum W, Passegue E, Wagner EF. "AP-1 in Mouse Development and Tumorigenesis." Oncogene 20 (2001): 2401-2412.

Kariagina A, Aupperlee MD, Haslam SZ. "Progesterone Receptor Isoforms and Proliferation in the Rat Mammary Gland during Development." Endocrinology 148.6 (2007): 2723–2736.

Kariagina A, Xie J, Leipprandt JR, Haslam SZ. "Amphiregulin Mediates Estrogen, Progesterone, and EGFR Signaling in the Normal Rat Mammary Gland and in Hormone-Dependent Rat Mammary Cancers." (n.d.).

Karin M, Hunter T. "Transcriptional Control by Protein Phosphorylation: Signal Transmission From the Cell Surface to the Nucleus." Current Biology 5.7 (1995): 747-757.

Kastner P, Krust A, Turcotte B, Stropp U, Tora L, Gronemeyer H, Chambon P. "Two Distinct Estrogen-Regulated Promoters Generate Transcripts Encoding the Two Functionally Different Human Progesterone Receptor Forms A and B." The EMBO Journal 9.5 (1990): 1603-1614.

Kazanietz MG. "Targeting Protein Kinase C and "Non-Kinase" Phorbol Ester Receptors: Emeeging Concepts and Therapeutic Implications." Biochemica et Biophysicia Acta 1754 (2005): 296-304.

Khattar E, Kumar V. "Mitogenic Regulation of p27Kip1 Gene is Mediated by AP-1 Transcription Factor." The Journal of Biological Chemistry 285.7 (2010): 4554-4561.

Kovary K, Bravo R. "Existence of Different Fos/Jun Complexes During the G0-to-G1 Transition and During Exponential Growth in Mouse Fibroblasts: Differential Role of Fos Proteins." Molecular and Cellular Biology 12.11 (1992): 5015-5023.

Kozak M. "Structural Features in Eukaryotic mRNAs That Modulate the Initiation of Translation." The Journal of Biological Chemistry (1991a): 19867-19870.

Kozak M. "An Analysis of Vertebrate mRNA Sequences: Intimations of Translational Control." Journal of Cell Biology 115.4 (1991b): 887-903.

Kraus WL, Montano MM, Katzenellenbogen BS. "Cloning of the Rat Progesterone Receptor Gene 5' Region and Identification of Two Functionally Distinct Promoters." Molecular Endocrinology 7 (1993): 1603-1616.

Kraus WL, Montano MM, Katzenellenbogen BS. " Identification of Multiple, Widely Spaced Estrogen-Responsive Regions in the Rat Progesterone Receptor Gene." Molecular Endocrinology 8 (1994): 952-969.

Lanari C, Luthy I, Lamb CA, Fabris V, Pagano E, Helguero LA, Sanjuan N, Merani S, Molinolo AA. "Five Novel Hormone-responsive Cell Lines Derived from Murine Mammary Ductal Carcinomas: In Vivo and in Vitro Effects if Estrogens and Progestins." Cancer Research 61 (2001): 293-302.

Lange C. "Challenges to Defining a Role for Progesterone Receptor in Breast Cancer." Steroids 73 (2008): 914-921.

Lapidot M, Pilpel Y. "Genome-wide Natural Antisense Transcription: Coupling its Regulation to its Different Regulatory Mechanisms." EMBO Reports 7.12 (2006): 1216-1222.

Leonhardt SA, Boonyaratanakornkit V, Edwards DP. "Progesterone Receptor Transcription and Non-Transcription Signaling Mechanisms." Steroids 68 (2003): 761-770.

Lu C, Shen Q, DuPre E, Kim H, Hilsenbeck S, Brown PH. "cFos is Critical for MCF-7 Breast Cancer Cell Growth." Oncogene 24 (2005): 6516-6524.

Marti A, Jehn B, Costello E, Keon N, Ke N, Martin F, Jaggi R. "Protein Kinase A and AP-1 (c-Jun/FosD) are Induced During Apoptosis of Mouse Mammary Epithelial Cells." Oncogene 9 (1994): 1213-1223.

Marti A, Lazar H, Ritter P, Jaggi R. "Transcription Factor Activities and Gene Expression During Mouse Mammary Gland Involution." Journal of Mammary Gland Biology and Neoplasia 4.2 (1999): 145-152.

MatInspector 2005. Genomatix MatInspector. 2005. <http://www.genomatix.de/cgi-bin/sessions/login.pl?s=5fea7747b00c3b1638b142a04b37e562>.

Mechta F, Piette J, Hirai SI, Yaniv M. "Stimulation of Protein Kinase C or Protein Kinase A Mediated Signal Trasduction Pathways Shows Three Modes of Response Among Serum Inducibile Genes." New Biologist 3 (1989): 297-304.

Mechta-Grigoriou F, Gerald D, Yaniv M. "The Mammalian Jun Proteins: Redundancy and Specificity." Oncogene 20 (2001): 2378-2389.

Milde-Langosch K, Roder H, Andritzky B, Aslan B, Hemminger G, Brinkmann A, Bamberger CM, Loning T, Bamberger AM. "The Role of the AP-1 Trancription Factors c-Fos, FosB, Fra-1 and Fra-2 in the Invasion Process of Mammary Carcinomas." Breast Cancer Research and Treatment 86 (2004): 139-152.

Milde-Langosch K, Janke S, Wagner I, Schroder C, Streichert T, Bamberger AM, Janicke F, Loning T. "Role of Fra-2 in Breast Cancer: Influence on Tumor Cell Invasion and Motility." Breast Cancer Research and Treatment 107 (2008): 337-347.

Musgrove EA, Lee CSL, Sutherland RL. "Progestins Both Stimulate and Inhibit Breast Cancer Cell Cycle." Molecualr and Cellular Biology 11.10 (1991): 5032-5043.

Park-Sarge OK, Sarge KD. "Cis-Regulatory Elements Conferring Cyclic 3',5'-Adenosine Monophosphate Responsiveness of the Progesterone Receptor Gene in Transfected Rat Granulosa Cells." Endocrinology 136.12 (1995): 5430-5437.

Passegue E, Jochum W, Behrens A, Ricci R, Wagner EF. "JunB Can Substitute for Jun in Mouse Development and Cell Proliferation." Nature Genetics 30.2 (2002): 158-166.

Pestell RG, Albanese C, Reutens AT, Segall JE, Lee RJ, Arnold A. "The Cyclins and Cyclin-Dependent Kinase Inhibitors in Hormonal Regulation of Proliferation and Differentiation." Endocrine Reviews 20.4 (1999): 501-534.

Petz LN, Nardulli AM. "Sp1 Binding Sites and an Estrogen Response Element Half-Site are Involved in Regulation of the Human Progesterone Receptor A Promoter." Molecular Endocrinology 14.7 (2000): 972-985.

Petz LN, Ziegler YS, Loven MA, Nardulli AM. " Estrogen Receptor α and Activating Protein-1 Mediate Estrogen Responsiveness of the Progesterone Receptor Gene in MCF-7 Breast Cancer Cells." Endocrinology 143.12 (2002): 4583-4591.

Petz LN, Ziegler YS, Schultz JR, Nardulli AM. "Fos and Jun Inhibit Estrogen-Induced Transcription of the Human Progesterone Receptor Gene Through an Activator Protein-1 Site." Molecular Endocrinology 18.3 (2004a): 521-532.

Petz LN, Ziegler YS, Schultz JR, Kim H, Kemper JK, Nardulli AM. "Differential Regulation of the Human Progesterone Receptor Gene Through an Estrogen Response Element Half Site and Sp1 Sites." The Journal of Steroid Biochemistry and Molecular Biology 88 (2004b): 113-122.

Piechaczyk M, Farras R. "Regulation and Function of JunB in Cell Proliferation." Biochemical Society Transactions 36.5 (2008): 864-867.

Platet N, Prevostel C, Derocq D, Joubert D, Rochefort H, Garcia M. "Breast Cancer Cell Invasiveness: Correlation with Protein Kinase C Activity and Differential Regulation by Phorbol Ester in Estrogen Receptor-Positive and -Negative Cells." International Journal of Cancer 75.5 (1998): 750-756.

Ramamoorthy S, Dhananjayan SC, Demayo FJ, Nawaz Z. "Isoform-Specific Degradation of PR-B by E6-AP Is Critical for Normal Mammary Gland Development." Molecular Endocrinology 24.11 (2010): 2099-2113.

Roos W, Fabbro D, Kung W, Costa SD, Eppenberger U. "Correlation Between Hormone Dependency and the Regulation of Epidermal Growth Factor Receptor by Tumor Promoters in Human Mammary Carcinoma Cells." Proceedings of the National Academy of Sciences, USA 83 (1986): 991-995.

Rose-Hellekant TA, Arendt LM, Schroeder MD, Gilchrist K, Sandgren EP, Schuler LA. "Prolactin Induces ERa-positive and ERa-negative Mammary Cancer in Transgenic Mice." Oncogene 22 (2003): 4664-4674.

Santos SJ, Haslam SZ, Conrad SE. "Estrogen and Progesterone are Critical Regulators of Stat5a Expression in the Mouse Mammary Gland." Endocrinology 149.1 (2007): 329-338.

Schott DR, Shyamala G, Schnneider W, Parry G. "Molecular Cloning, Sequence Analyses, and Expression of Complementary DNA Encoding Murine Progesterone Receptor." Biochemistry 30 (1991): 7014-7011.

Schreiber M, Kolbus A, Piu F, Szabowski A, Mohle-Steinlein U, Tian J, Karin M, Angel P, Wagner EF. "Control of Cell Cycle Progression by c-Jun is p53 Dependent." Genes & Development 13 (1999): 607-619.

Schultz JR, Petz LN, Nardulli AM. "Estrogen Receptor α and Sp1 Regulate Progesterone Receptor Gene Expression." Molecular and Cellular Endocrinology 201 (2003): 165-175.

Sengupta K, Banerjee S, Dhar K, Saxena NK, Mehta S, Campbell DR, Banerjee SK. "WISP-2/CCN5 is Involved as a Novel Signaling Intermediate in Phorbol Ester-Protein Kinase Calpha-Mediated Breast Tumor Cell Proliferation." Biochemistry 45 (2006): 10698-10709.

Shaulain E, Karin M. "AP-1 in Cell Proliferation and Survival." Oncogene 20 (2001): 2390-2400.

Shaulian E, Karin M. "AP-1 as a Regulator of Cell Life and Death." Nature Cell Biology 4 (2002): E131-E136.

Shen Q, Zhang Y, Uray IP, Hill JL, Kim HT, Lu C, Young MR, Gunther EJ, Hilsenbeck SG, Chodosh LA, Colburn NH, Brown PH. "The AP-1 Transcription Factor Regulates Postnatal Mammary Gland Development." 295 (2006): 589-603.

Shyamala G, Schneider W, Schott D. "Developmental Regulation of Murine Mammary Progesterone Receptor Gene Expression." Endocrinology 126.6 (1990): 2882-2889.

Skildum A 2007. personal communication 2007.

Smith LM, Wise SC, Hendricks DT, Sabichi AL, Bos T, Reddy P, Brown PH, Birrer MJ. "c-Jun Overexpression in MCF-7 Breast Cancer Cells Produces a Tumorigenic, Invasive and Hormone Resistant Phenotype." Oncogene 18.44 (1999): 6063-6070.

Song Y, Song S, Zhang D, Zhang Y, Chen L, Qian L, Shi M, Zhao H, Jiang Z, Guo N. "An Association of a Similtaneous Nuclear and Cytoplasmic Localization of Fra-1 with Breast Malignancy." BMC Cancer 6 (2006): 298-304.

Suzuki T, Okuno H, Yoshida T, Endo T, Nishina H, Iba H. "Difference in Transcription Regulatory Function Between c-Fos and Fra-2." Nucleic Acids Research 19.20 (1991): 5537-5542.

Takegoshi S, Jiang S, Ohashi R, Savchenko AS, Iwanari H, Tanaka T, Hasegawa G, Hamakubo T, Kodama T, Naito M. "Protein expression of nuclear receptors in human and murine tissues." Pathology International 59.2 (2009): 61-72.

Tzukerman M, Zhang X, Pfahl M. "Inhibition of Estrogen Receptor Activity by the Tumor Promoter 12-0-Tetradeconylphorbol-13-Acetate: A Molecular Analysis." Molecular Endocrinology 5 (1991): 1983-1992.

Verde P, Casalino L, Talotta F, Yaniv M, Weitzman JB. "Deciphering AP-1 Functions in Tumorigenesis: Fra-ternizing on Target Promoters." Cell Cycle 6.21 (2007): 2632-2639.

Weitzman JB, Fiette L, Matsuo K, Yaniv M. "JunD Protects Cells From p53-Dependent Senescence and Apoptosis." Molecular Cell 6 (2000): 1109-1119.

Young MR, Colburn NH. "Fra-1 a Target For Cancer Prevention or Intervention." Gene 379 (2006): 1-11.

CHAPTER 4

ANTISENSE TRANSCRIPTION AT THE MOUSE PROGESTERONE RECEPTOR (Pgr) LOCUS

ABSTRACT

The mouse progesterone receptor (Pgr) gene forms a *cis*-sense/antisense pair with a naturally occurring, non-coding antisense transcript ($PR^{antisense}$). The $PR^{antisense}$ transcript overlaps the majority of PR sense exon 1, with transcription initiating at the 3'-end of exon 1. Herein, we confirm the presence of this novel transcript in both mouse cell lines and tissues. Additionally, the antisense PR promoter was characterized and mapped to a position in the antisense strand located near the end of exon 1. The antisense PR promoter is induced by treatment with R5020, a synthetic progestin, and repressed by phorbol myristate acetate treatment. The antisense PR promoter also shows transactivation by AP-1, specifically JunD, JunB, or c-Jun either alone or complexed with c-Fos, Fra1, or Fra2. *In situ* hybridization was used to localize PR^{sense} and $PR^{antisense}$ transcripts to the majority of cells in a mouse mammary tumor cell line (MC7-L1). *In vivo*, the $PR^{antisense}$ transcript was localized to the same cells that expressed PR^{sense} message and PRA protein during mouse mammary gland development. When the $PR^{antisense}$ transcript was transiently over-expressed in *trans*, it was not able to alter PR^{sense} transcript levels in PR-positive (MC7-L1) cells. Although under certain conditions, the $PR^{antisense}$ transcript may interfere with PR protein expression, this may not be the case *in vivo* because co-expression of the sense and antisense mRNAs appears to be compatible. Since the $PR^{antisense}$ transcript was co-expressed at the cellular level and appears to be co-regulated with the PR^{sense} transcripts, it cannot be ruled out as a player in regulation of the Pgr locus. The role of the $PR^{antisense}$ transcript may also differ between the healthy breast and in breast cancer,

where an imbalance between PR^{sense} and $PR^{antisense}$ transcripts could have an effect on tumorigenesis.

INTRODUCTION

A mouse mammary cell line that expresses receptors for both estrogen and progesterone would be an invaluable resource to study hormonal regulation of progesterone receptor (PR) expression in normal mouse mammary tissue. Towards this aim, PCR was used to determine the PR and estrogen receptor (ER) status of a variety of candidate murine cell lines. However, semi-quantitative PCR experiments yielded conflicting results compared to reports in the literature on whether cells were ER-, PRB-, or PRA-positive. To help resolve these discrepancies, we performed a comprehensive *in silico* analysis of the mouse progesterone receptor (Pgr) locus using the GenBank and Fantom databases. Interestingly, there is evidence of a polyadenylated transcript in the antisense orientation that overlaps the PRA and PRB promoter region as well as the majority of exon 1. This observation raises an important consideration in designing primers for PCR that are used to evaluate PR expression, but also helps to explain some of the contradictory PCR results from previous studies. Specifically, primers that map to the first 2 kb of the mouse PR cDNA, especially those that purport to measure transcription which initiates uniquely in the PRB-specific region of the transcription unit *cannot* be used to measure the amount of protein-coding PR mRNA *unless* these measurements are based on a strand-specific cDNA prepared using an antisense PR oligonucleotide. This is a particular concern for studies using quantitative real time PCR, where the prevailing practice involves use of oligo (dT) or

random primers to copy total RNA into single-stranded cDNA prior to PCR amplification. When prepared in this manner, the first two-thirds of the protein coding region of the mouse PR message are represented in both the coding and con-coding strands within the cDNA library, since the antisense, as well as the sense transcript is polyadenylated. Of note, there are no published reports using PCR to measure PR message levels that take the confounding effects of antisense transcription into consideration. At the present time, there is no evidence of a protein-coding gene or a significant open reading frame present in the antisense strand and overlapping the 5'-end of the mouse Pgr gene. However this raises the possibility that the non-coding antisense transcript may play a role in regulation of PR mRNA levels or PR protein expression.

Additional *in silico* analysis predicted that a similar situation exists in the case of the human PGR gene and that both the mouse and human PGR genes represent the sense partner in a *cis*-sense/antisense pair. Evidence of a human $PR^{antisense}$ transcript was also reported in MCF-7 and T47-D human mammary cell lines, in which the $PR^{antisense}$ mRNA acts in a regulatory mechanism as a scaffold molecule between genomic DNA in the PGR locus and synthetic anti-gene peptides (Schwartz JC 2008). There is no known naturally occurring equivalent to the anti-gene peptides used by Schwartz and colleagues, however, this suggests that a pathway may exist in which the $PR^{antisense}$ mRNA plays a critical role in regulating gene expression from the human PGR locus. The authors proposed a blockade mechanism in which a RNA-RNA-protein complex interacts with PRB promoter DNA to prevent transcription initiation at the major start sites (Schwartz JC 2008). Additionally, there are multiple other transcriptional and translational mechanisms that the antisense PR transcript could utilize in regulating the human or mouse PGR locus. These include, but are not limited to: *trans* regulation of the PR promoters, regulation of mRNA stability, and regulation of mRNA translateability.

Since the antisense PR gene and its promoter overlap the sense Pgr gene, they share many known regulatory sequences for transcription factor binding sites. The mouse Pgr gene is regulated by estrogens, progestins, and growth regulatory pathways (Shyamala G 1990); (Schott DR 1991); (Aupperlee MD 2007) that signal through AP-1 and other transcription factors (Leonhardt SA 2003). Shared regulatory elements in a *cis*-sense/antisense pair usually results in either co-regulation or anti-regulation of the transcripts. It is unknown which type of regulation the Pgr gene and its antisense partner exhibit in mouse or human cell lines and tissues. This is the first report of a naturally occurring $PR^{antisense}$ transcript in mouse cell lines and tissues, but what role the $PR^{antisense}$ message plays *in vivo* has not yet been examined for any species. This role may differ between humans and mice and may also be different comparing the normal versus cancer state in the mammary gland. For this reason, we have undertaken the characterization of the antisense transcription unit within the mouse Pgr gene locus, and begun to analyze potential patterns of regulation.

RESULTS

1. Confirmation of an Antisense Promoter and Transcript at the Pgr Locus

a. *In Silico* Evidence: Cap Analysis of Gene Expression (CAGE) Tags, Expressed Sequence Tag (EST) Clones, and Riken cDNAs

PRA and PRB proteins have been shown in mouse mammary epithelial cells to be both spatially and temporally regulated (Aupperlee M 2005a). At the RNA levels PR transcripts appear to be even more heterogeneous (Schott DR 1991), with transcription occurring from multiple start sites for both PRB and PRA (Kastner P 1990). Regulation of the distal and proximal promoters which drive the already complex mouse Pgr gene may be even more complicated than previously thought due to the presence of a previously undefined antisense promoter that gives rise to $PR^{antisense}$ transcripts initiating at the 3'-end of exon 1.

A total of 17 antisense CAGE tags have been mapped to the mouse Pgr locus with clusters in the second half of exon 1 and flanking the predicted PRB mRNA start site (Kawaji H 2006); (Katayama S 2005). The most concentrated cluster of CAGE tags is in the +1800 to +2000 bp region of exon 1 with additional tags flanking this region (Figure 4.1a). The antisense PR ESTs from GenBank and the RIKEN database cluster into two sets of transcripts located in the second half of exon 1 and overlapping the predicted PRB mRNA start site (Figure 4.1a). The RIKEN Group used the FANTOM2 and FANTOM3 dataset to map CAGE tags and cDNA transcripts across the mouse genome (Kawaji H 2006); (Kiyosawa H 2003); (Katayama S 2005); (Carninci P 2005). Ten RIKEN clones map in the antisense orientation to the Pgr locus. These antisense PR RIKEN clones also cluster into two sets of transcripts, one located in the second half of exon 1 and the other overlapping the predicted PRB mRNA start site (Figure 4.1a). It is

worth noting that the presumptive RNA start sites within the antisense strand are associated with one of the two CpG islands located at the beginning of the Pgr gene (Figure 4.1a).

Analysis across the mouse genome showed that about half of the *cis*-sense/antisense pairs comprise a transcription unit (TU) pair of coding-noncoding transcripts (Kiyosawa H 2003); (Katayama S 2005); (Carninci P 2005), including the mouse Pgr locus. There are two antisense transcripts from GenBank assigned to the *cis*-sense/antisense mouse PR pair along with three sense PR ESTs and the PR reference sequence cDNA (M68915) (Schott DR 1991); (FANTOM3 S/AS 2005); (Su AI 2004) (Figure 4.1a).

The two GenBank antisense PR mRNAs in the sense/antisense pair span exon 1 all the way past the predicted PRB mRNA start site, connecting these two clusters of antisense ESTs (Figure 4.1a). One of these is a RIKEN clone (AK083181; C630024B11) extending from +1986 to -314 bp, while the other is an IMAGE clone (BC059021) from +1765 to -948 bp. The UniGene entry for mouse Pgr describes the BC059021 clone as being polyadenylated. Additionally, two of the antisense ESTs contain polyadenylation signals and a poly(A) tail as well as share the same 3'-end as AK083181. Predictions were made for finding polyadenylation signals in mouse genomic sequence using Polyadq software. Polyadq predicts the same polyadenylation signal at -928 bp in the BC059021 clone as well as a second putative polyadenylation signal at approximately -2500 bp, also in the antisense strand (Tabaska JE 1999).

Using Genomatix MatInspector, a computer algorithm for predicting transcription factor binding sites, the predicted promoter and 5'- untranslated region (UTR) of the antisense transcript were analyzed (MatInspector 2005). The first region analyzed was exon 1 of the Pgr gene from downstream of the PRA open reading frame (ORF) to the 3'-end of exon 1. There

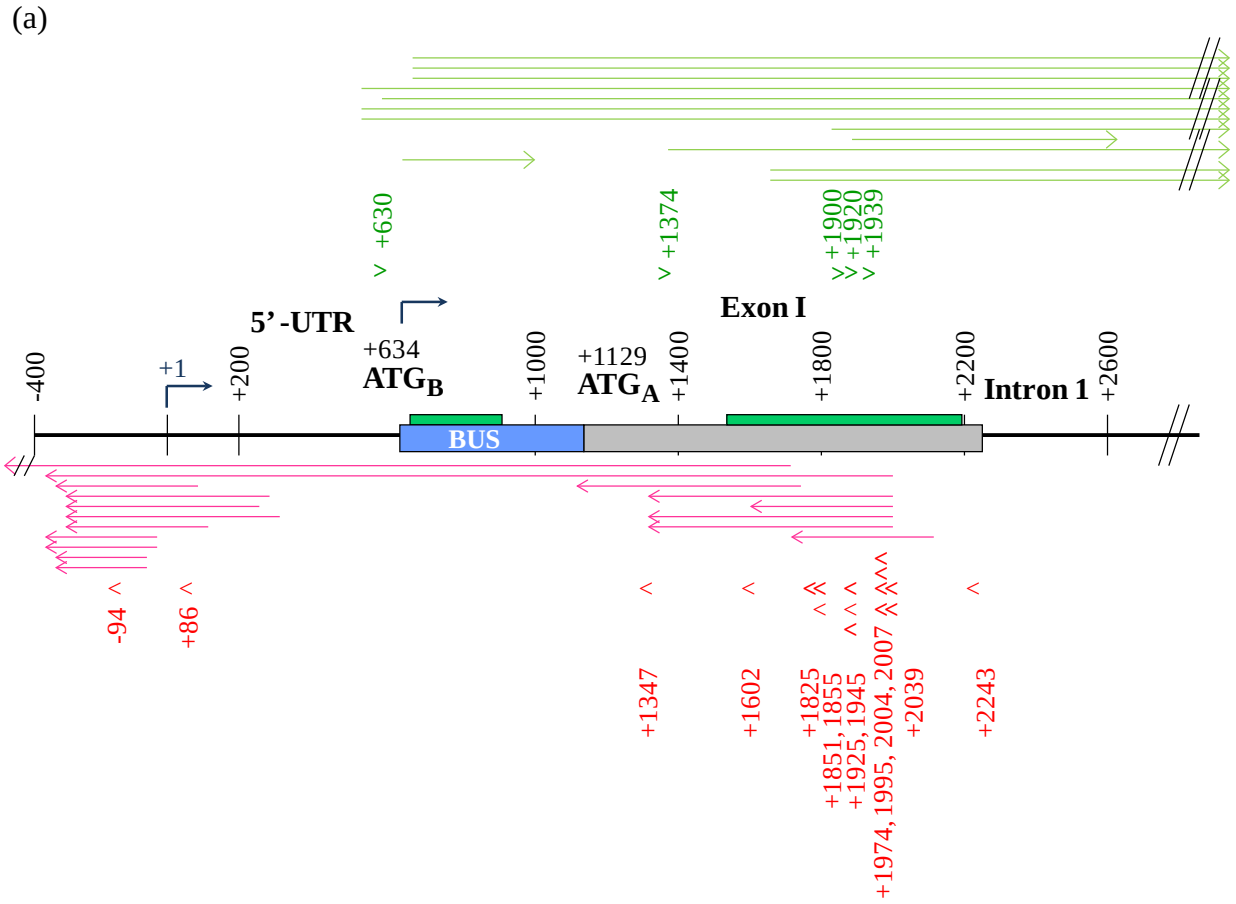

Figure 4.1: (a) Cap analysis of gene expression (CAGE) tags at the mouse progesterone receptor (Pgr) locus. CAGE tags of the sense strand are shown as green carrots and the antisense strand as red carrots. Expressed sequence tags (ESTs) and RIKEN cDNA clones are indicated as arrows in green (sense strand) and pink (antisense strand). The B-upstream sequence (BUS), exon 1 and intron 1 of progesterone receptor are indicated along with the two CpG islands (green boxes). **(b) Mouse progesterone receptor *cis*-sense/antisense pair.** The sense transcription unit (top) contains the promoter for PRB (P_B) and PRA (P_A) which give rise to transcripts spanning the eight exon Pgr locus. The PRB and PRA transcripts encode the full length PRB and amino-terminally truncated PRA proteins, respectively. The antisense transcription unit (bottom) contains the promoter for $PR^{antisense}$ RNA ($P_{antisense}$) and is shown in red overlapping all of exon 1, including the distal and proximal sense PR promoters.

Figure 4.1 (Cont'd.)

(b)

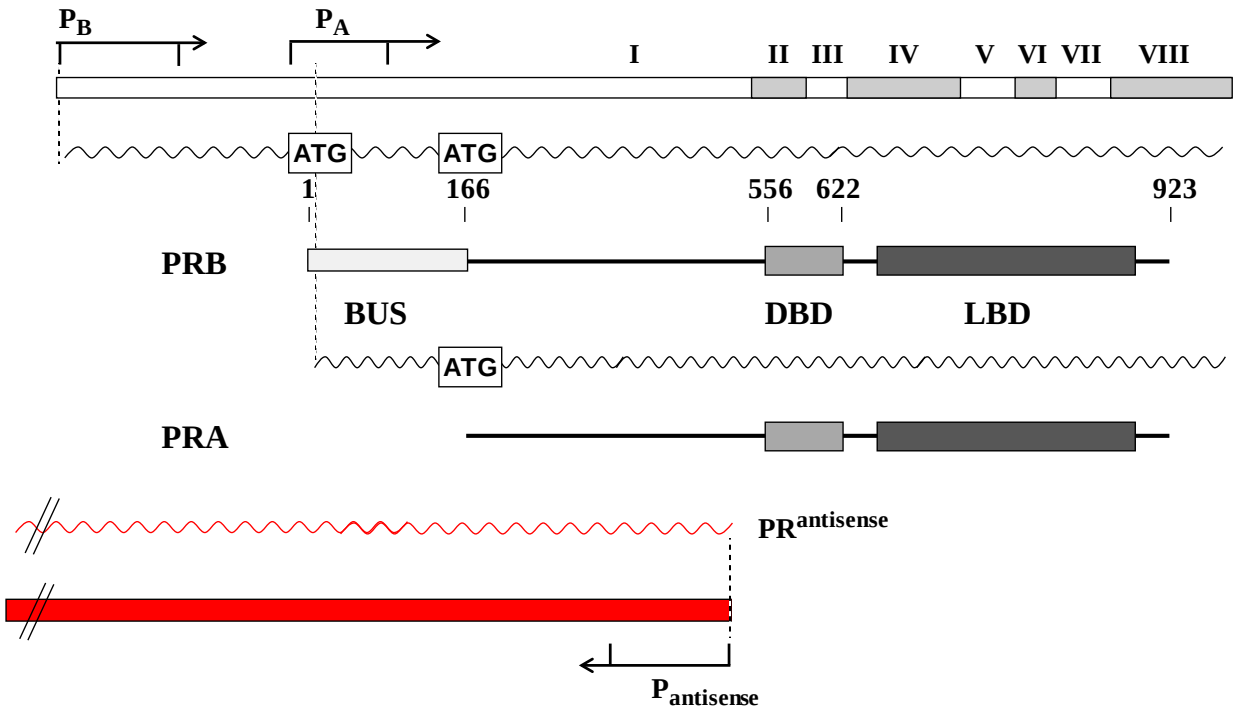

were binding sites predicted in the lower strand for a variety of core transcription factors: 4 Specificity protein (Sp1) sites, 1 CRE (cyclic adenosine monophosphate (cAMP) response element), and 2 CCAAT boxes. Also of note were estrogen response element 4 (ERE(4)) and ERE(5) previously described by Kraus, *et al.* in the human PGR gene (Kraus WL 1994), which are clustered near 3 putative Sp1 sites in what may be a minimal promoter (see Figure 3.1). The TATA boxes predicted in intron 1 are greater than 25 bp away from the 5'-end of the antisense RNA cluster at +1900/+2000 bp and therefore do not appear to be spaced correctly in order to be functional. Additionally, none of the predicted TATA boxes have the classical TATA containing promoter arrangement of a GC box at -40 bp and/or a CCAAT box at -110 bp. Therefore, it seems more likely that the antisense PR promoter is actually a TATA-less promoter and is controlled, at least in part, by the minimal promoter region of Sp1 sites and EREs that are located near the cluster of antisense CAGE tags at +1986 bp. Consistent with this is the presence of a nearby CpG Island (Figure 4.1a).

The $PR^{antisense}$ ESTs, RIKEN clones, and cDNAs were analyzed for open reading frames to determine if there could be a protein produced from any of these transcripts. The two Genbank mRNAs spanning exon 1 past the predicted PRB mRNA start site had the longest ORF of all the sequences analyzed, measuring 312 nt (104 aa). Although this hypothetical protein product was predicted to be approximately 10 kDa in size, it lacked any recognizable motifs in the SwissProt or National Center for Biotechnology Information (NCBI) Conserved Domains databases. Overall, the *in silico* protein analysis along with the lack of a reported protein product make it very unlikely the $PR^{antisense}$ transcript actually codes for a protein, leading us to classify this transcript as a non-coding RNA (nc-RNA). It is well established that the progesterone receptor is spliced into a mature-mRNA (GenBank (NCBI) 2008), however, there

is no evidence that the corresponding antisense message is spliced using a computer algorithm to predict exons and introns. The antisense transcript is collinear with genomic DNA, consistent with the $PR^{antisense}$ message being a single exon transcript lacking introns (Figure 4.1b).

b. *In Vitro* Evidence: Primer Extension and Strand-Specific Semi-Quantitative PCR

In silico data mapped a concentrated cluster of CAGE tags in the +1800 to +2000 bp region of PR exon 1 near with the 5'-end of many ESTs and RIKEN cDNA clones. Combined with *in silico* promoter analysis, this provided a solid framework supporting the hypothesis that there is a functional promoter located at the end of Pgr exon 1 that drives transcription in the antisense direction. Initially, it was necessary to experimentally determine where these antisense transcripts initiate and whether they are found in hormonally regulated tissues or not. Primer extension was utilized to map the antisense transcription initiation sites using upper strand primers located upstream of the cluster of CAGE tags in exon 1 designated forward primer 1, 2, and 3 (F1, F2, F3) (Figure 4.2a).

Given the relatively large amount of RNA required for these experiments, analysis was limited to the uterus of control animals and the livers from ovary-intact versus ovariectomized mice. Experiments with limited amounts of RNA from mouse mammary gland or ovariectomized uterus yielded unsatisfactory results (data not shown). Primer Forward 1 (F1) from +1565 to +1583 bp was initially tested to characterize PR antisense start sites in the region of approximately +1600 to +1850 bp (Figure 4.2b). Not only do these start sites in the antisense PR strand exist, but the $PR^{antisense}$ message seems to have a well defined 5'-end as can be seen in Figure 4.2 by the intense primer extension products and tight clusters of bands. The pattern of antisense PR start sites differs depending on both tissue and hormonal status. Using Forward

primer 1 (F1) for RNA from liver, start sites tended to cluster from +1613 to +1630 bp, where RNA from uterus displayed two prominent doublets of start sites at +1615/+1616 bp and +1686/+1687 bp (Figure 4.2b).

Forward strand primers closer to the predicted antisense start site were used in primer extension experiments to map additional start sites in the +1770 to +2000 bp region using mouse liver from ovariectomized and ovary-intact mice. Primer forward 2 (F2) from +1771 to +1790 bp, yielded a few faint putative start sites at the bottom of the gel very close to the primer, but nothing near the expected start sites (data not shown). Using primer F3 from +1861 to +1881 bp, start sites clustering around +1892 to +1989 bp were mapped near the majority of the antisense CAGE tags in RNA from the liver of ovariectomized versus ovary-intact mouse (Figure 4.2c). The furthest upstream antisense start site mapped near ERE(4) in the 3'-end of exon 1, at +2016 bp. A qualitative summary of these results is provided in Figure 4.3.

A second type of *in vitro* evidence for PR antisense transcription was obtained using semi-quantitative PCR. Due to the greater sensitivity of this method compared to RNase protection (data not shown), samples could be included from tissues available in smaller amounts such as mouse mammary gland and ovariectomized uterus. $PR^{antisense}$ cDNA was prepared using an upper strand primer at -146 bp in the mouse PRB promoter region (RMK 76, Table 2.2a). The primer set used for PCR is located at the beginning of the PRB reading frame (RMK 64/65, Table 2.2b) from +634 to +1004 bp and can detect antisense transcripts near the PRB ATG (Figure 4.4f). Since the furthest downstream polyadenylation signal in the antisense transcription unit is at -928 bp, the cDNA was primed further upstream at -146 bp (Figure 4.4f). The ATG_B primer set detected moderate to high expression levels of $PR^{antisense}$ transcripts in all of the tissues examined from both ovariectomized and ovary-intact mice as well as in NMuMG

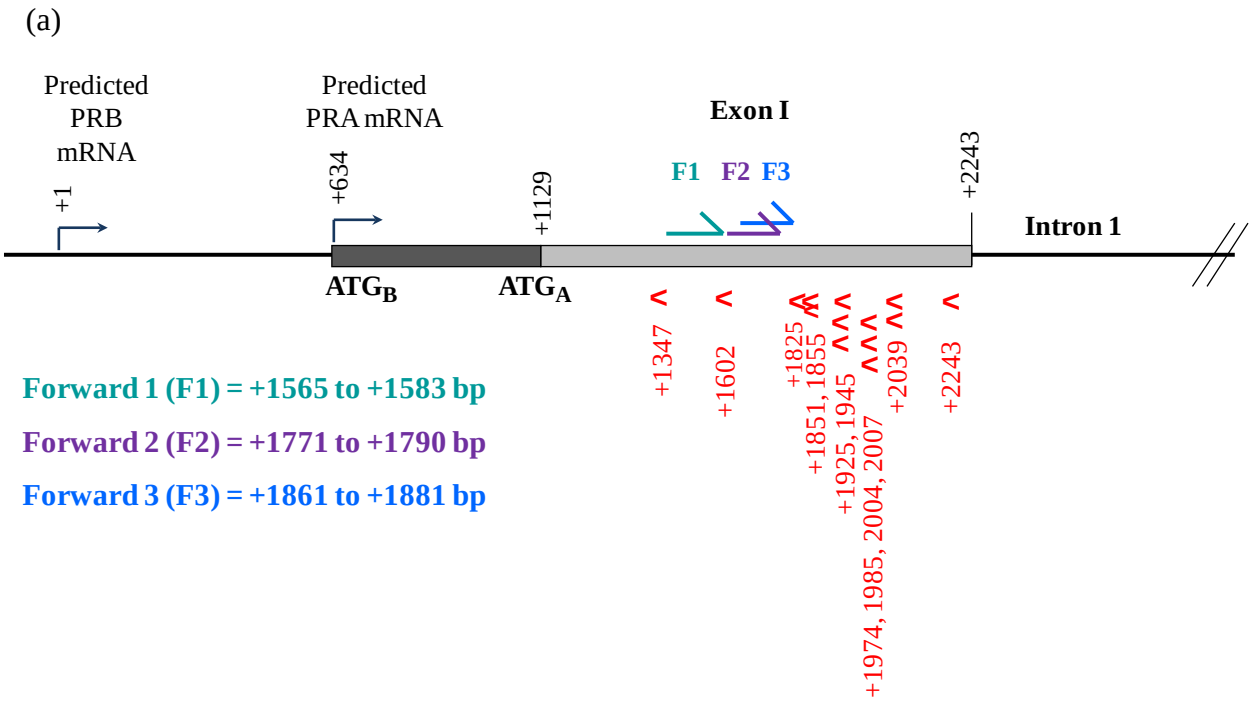

<u>Figure 4.2:</u> (a) Alignment of antisense cap analysis of gene expression (CAGE) tags and primer extension primers in the mouse Pgr gene. The antisense CAGE tags in the mouse Pgr gene are indicated in red and the location is given for the three forward primers (F1, F2, F3) designed to detect and map the 5'-ends of antisense PR message. Coordinates are relative to the predicted PRB mRNA start site (+1 bp) based on homology to human and rat sequences. The PRA mRNA start site is predicted at +641 bp. The PRB ATG (ATG_B) is located at +634 bp and the PRA ATG (ATG_A) is located at +1129 bp.
(b) Representative primer extension reactions using total RNA extracted from the uterus (U) or liver (L) of virgin adult BALB/c mice using primer (b) Forward 1 (F1) or (c) Forward 3 (F3). Mice were either ovary-intact (Int) or ovariectomized (Ovx) and 40 µg of RNA was used per reaction. Total yeast RNA (tRNA) was used as a negative control for each primer, 40 µg per reaction. GATC lanes represent the four sequencing reactions of mouse PR plasmid DNA initiated with the corresponding primers and run in parallel. (b) Notice the different pattern of antisense PR start sites found in the ovary versus liver of intact mice. (c) Comparison of the antisense start site pattern in the liver of ovariectomized versus ovary-intact mice.

Figure 4.2 (Cont'd.)

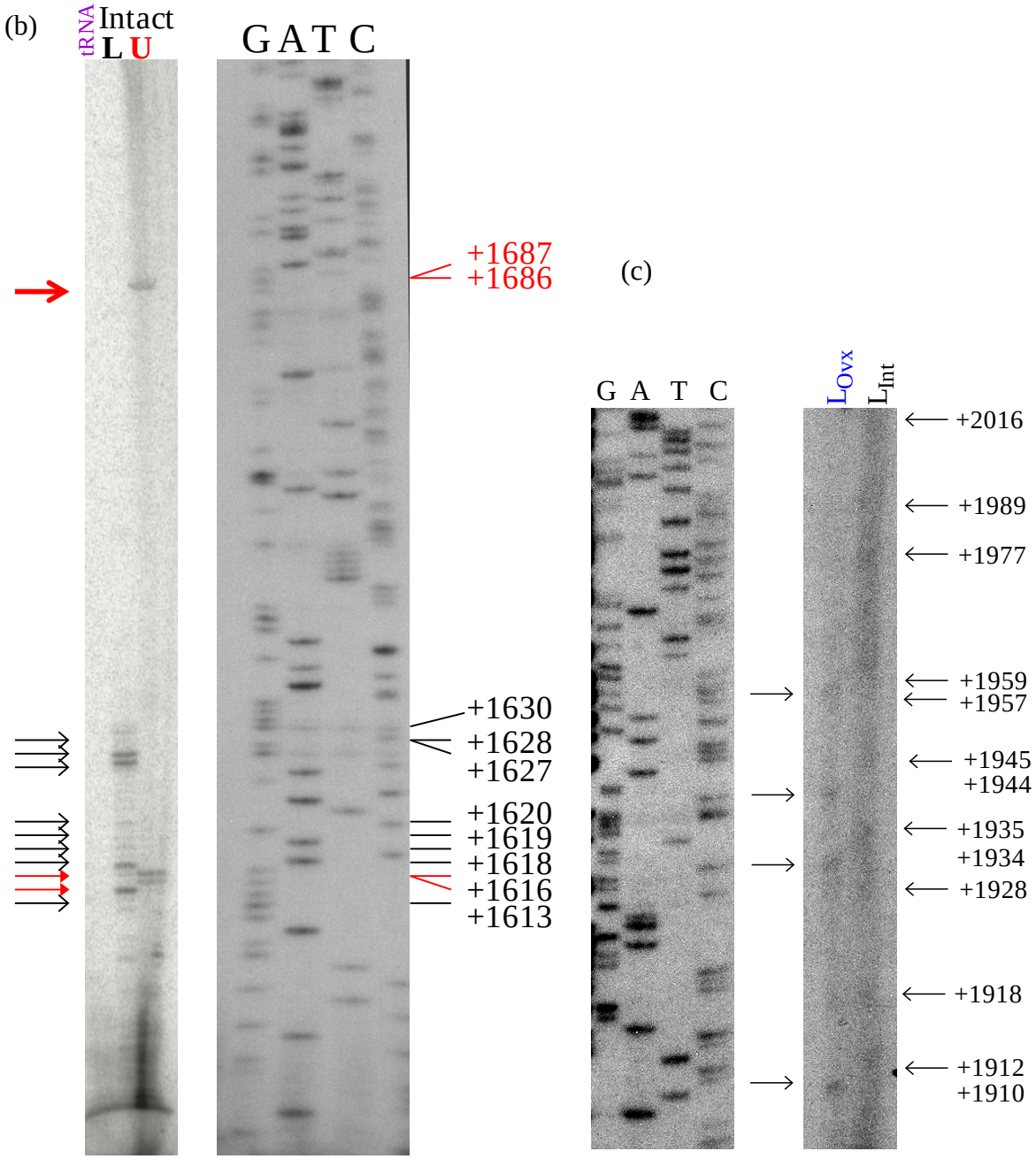

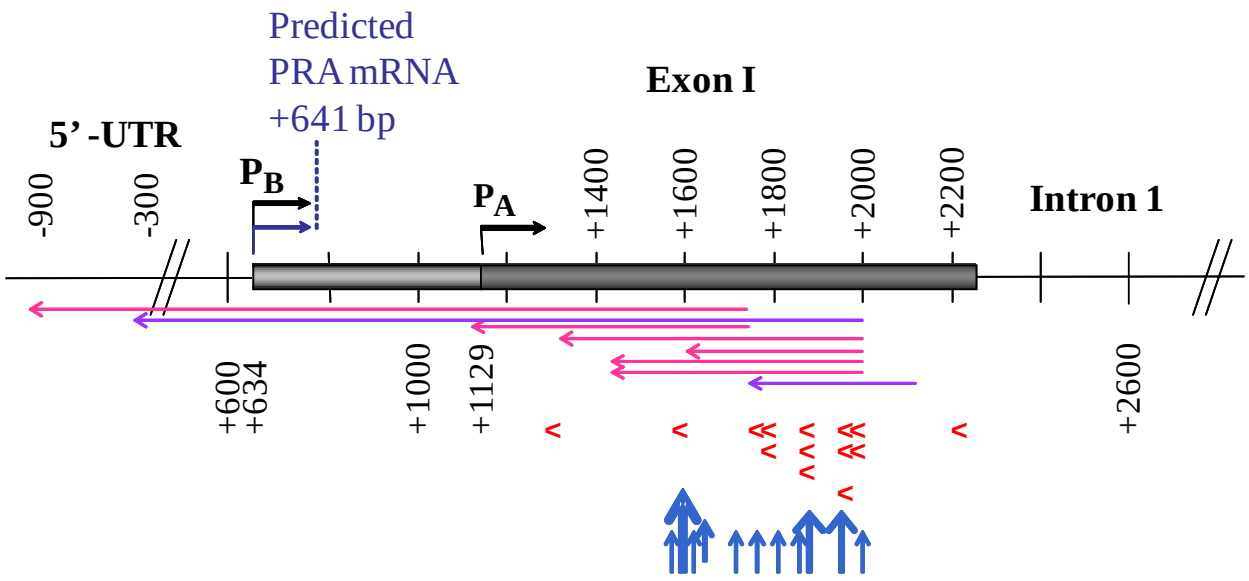

Figure 4.3: Summary of antisense *in silico* and *in vitro* data using primer extension. Antisense expressed sequence tags (ESTs) (pink arrows), RIKEN cDNA clones (purple arrows), and cap analysis of gene expression (CAGE) tags (red carrots) aligned with PR antisense primer extension start sites (vertical blue arrows) in the mouse Pgr gene. Size and thickness of the vertical arrows denotes the density of transcription start sites mapped. Horizontal arrows indicate the predicted mRNA start sites for PRB (+1 bp) and PRA (+641 bp).

cells (Figure 4.4a). In both liver and mammary gland sample sets, the level of $PR^{antisense}$ transcript increased from the ovariectomized to the ovary-intact samples (Figure 4.4a). In the uterus, the level of $PR^{antisense}$ transcript was consistently higher in the ovariectomized tissue compared to the uterus from ovary-intact mice (Figure 4.4a).

For comparison, the exon 1 ATG_B primer set was also tested on a sense strand PR cDNA primed in the 3'-UTR of the Pgr sequence (Figure 4.4f). Sense PR transcript measured by PCR was most abundant in the uterus from an ovary-intact mouse, as expected (Figure 4.4b). PR transcript levels showed estrogen dependent up-regulation in both liver and uterus samples from low levels seen in ovariectomized mice to higher levels in ovary-intact mice (Figure 4.4b). Sense PR mRNA was not detected in either of the virgin adult mammary gland samples using the exon 1 ATG_B primer set (Figure 4.4b). Using a mouse mammary carcinoma cell line (UMD-208), there was down regulation of $PR^{antisense}$ message with E_2 treatment or the combination of E_2+R5020, a synthetic progestin (Figure 4.4c). Treatment with R5020 alone had no effect on $PR^{antisense}$ message levels (Figure 4.4c). This is consistent with primer extension experiments, which showed E_2-dependent down regulation of $PR^{antisense}$ message in mouse liver (Figure 4.2c). Unlike the UMD-208 cells, semi-quantitative PCR with MC7-L1 mouse mammary carcinoma cells showed no detectable $PR^{antisense}$ mRNA prior to hormone treatment (Figure 4.4e). $PR^{antisense}$ message was increased slightly by treatment for 24 hours with E_2 or 17 hours with phorbol myristate acetate (PMA) (Figure 4.4e). Both R5020 alone and R5020 plus E_2

(a)

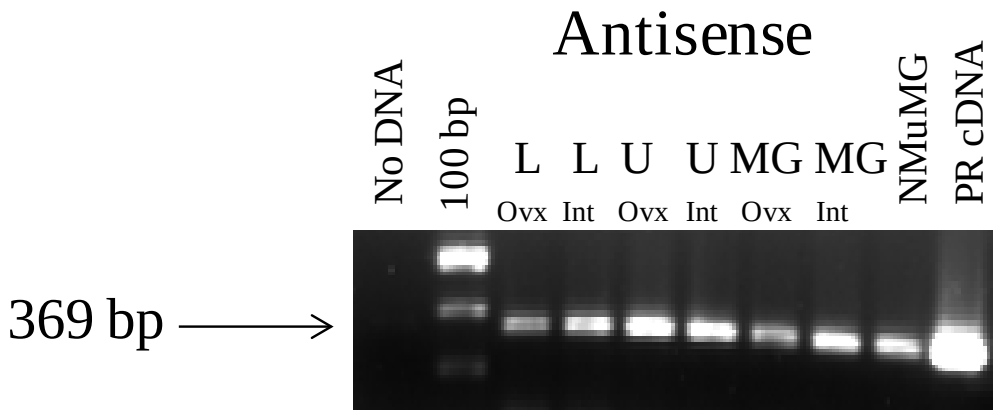

(b)

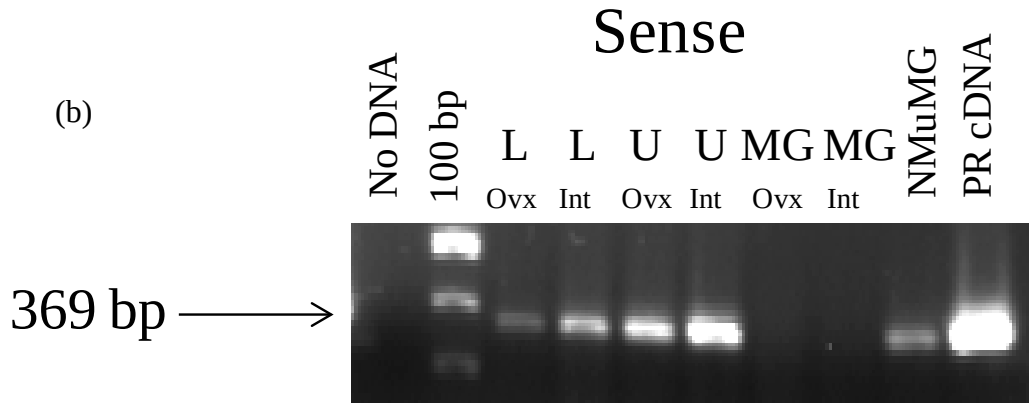

Figure 4.4: Semi-quantitative PCR of mouse tissues and cell lines to detect sense and antisense PR. Semi-quantitative PCR of mouse tissues along with UMD-208 and NMuMG mammary cells using an exon 1 ATG_B primer set. PCR products were amplified for 36 cycles (a, b, d) or 32 cycles (c). The positive control PCR reaction uses the cloned PR cDNA plasmid as a template. The negative control was no template DNA. (a, c, d) Antisense strand PR cDNA was prepared using an upper strand primer in the promoter region at -146 bp. (b) Sense strand PR cDNA was prepared using a lower strand primer in the 3'-UTR/exon 8 common region of PR. (c, d) Treatments were: vehicle (V), estradiol (E_2), R5020 (R), and estradiol plus R5020 (E_2+R) for 24 hours; 2 hours of phorbol ester (PMA) and 17 hours of PMA. (e) Location of the sense and antisense primers used to prepare the cDNAs as well as the exon 1 ATG_B primer set used in the PCR reaction.

Figure 4.4 (Cont'd.)

(c)

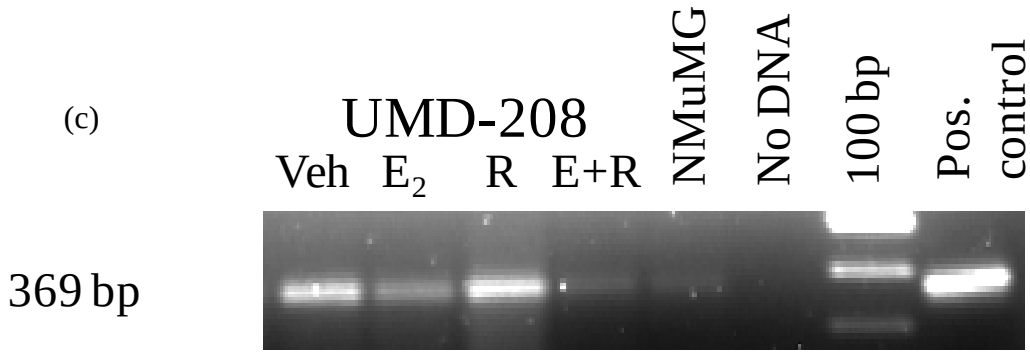

(d)

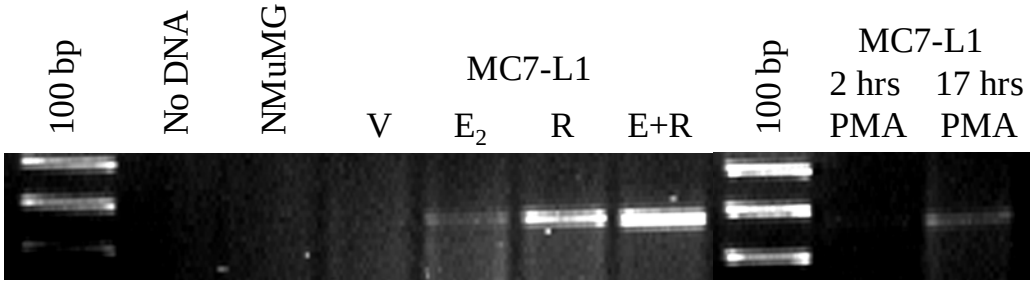

(e)

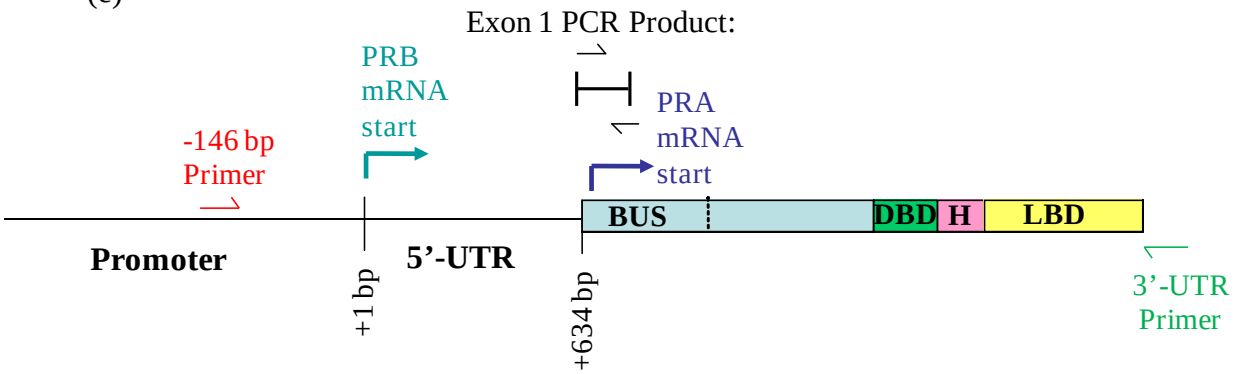

increased the level of $PR^{antisense}$ mRNA (Figure 4.4e). A shorter (2 hour) treatment with PMA had no observable effect on the $PR^{antisense}$ mRNA level (Figure 4.4e).

In order to obtain strand specific cDNAs, two different primers were used to prepare the sense and antisense cDNAs. Since these oligonucleotides may have different priming efficiencies, a quantitative difference between the transcript levels in the sense and antisense PCR reactions using the exon 1 ATG_B primer cannot be established. The general trend of transcript levels observed using semi-quantitative PCR was that the antisense transcript was more abundant in all of the samples tested with the exception of uterus from ovary-intact mice.

2. Characterization of the Antisense Promoter at the Pgr Locus

Since the antisense PR promoter is a novel promoter of unknown function and behavior, the next goal was to characterize the PR antisense promoter and its $PR^{antisense}$ transcript. *In vivo*, mouse PR is a hormone-responsive gene product with PRA being induced slightly by estradiol (E_2), but down regulated by progesterone (P) (Aupperlee MD 2007). PRB protein is differentially regulated than PRA, with PRB showing induction by P along with possible indirect regulation by E_2 (Aupperlee MD 2007). Because the $PR^{antisense}$ mRNA was found in ovarian hormone regulated tissues (uterus and mammary gland) it is important to determine if it is controlled by hormones as well and if so, if the regulation is similar to the control of PRA and PRB.

Based on *in silico* methods such as promoter prediction algorithms, transcription factor analysis, CAGE, EST, and RIKEN data plus direct primer extension mapping, a minimal $PR^{antisense}$ promoter was provisionally localized to a 332 bp region at the 3'-end of sense exon 1

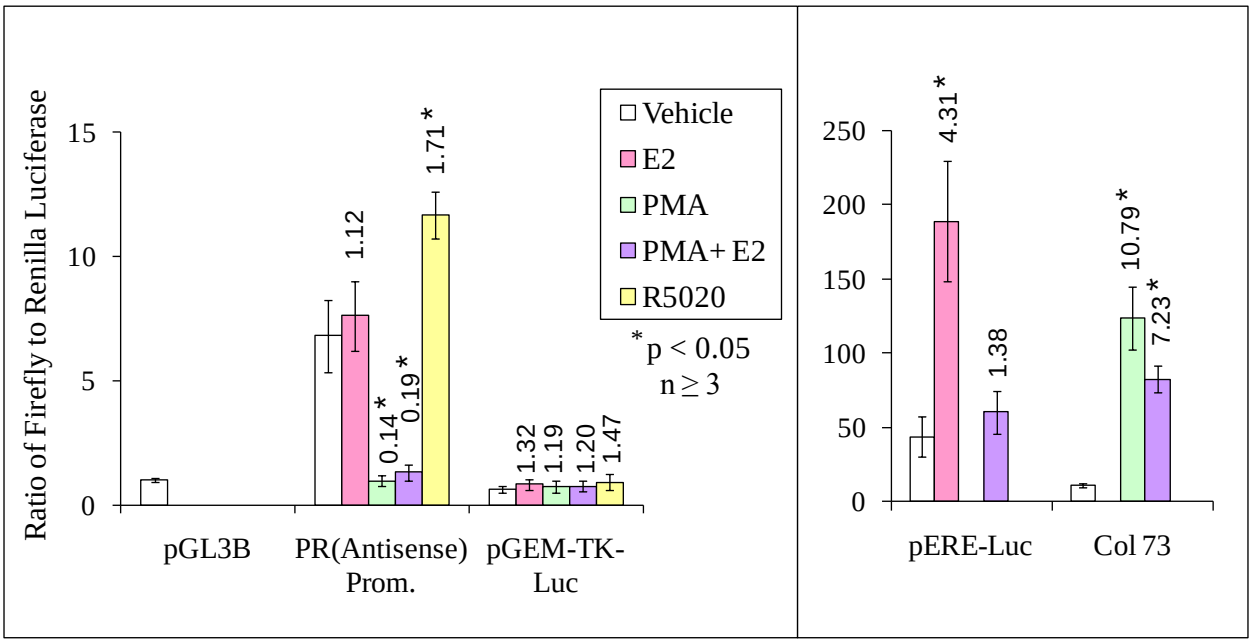

<u>Figure 4.5:</u> MCF-7 cell transfection of mouse antisense PR promoter constructs and controls. Left panel: Cells were transfected with pGL3Basic (pGL3B) empty vector control, PR antisense promoter and pGEM-TK-Luc (pGEM-thymidine kinase-luciferase vector).
Right panel: estrogen response element-TK-Luc (pERE-TK-Luc) and collagenase 73 (Col73) were used as estrogen and PMA positive control vectors, respectively. Note that the values of the ratio of firefly to renilla luciferase were dramatically higher for pERE-TK-Luc and Col73, requiring a different scale. Hormone treatments were as follows: estradiol (E_2), PMA, PMA+E_2 and R5020, and were administered for the final 24 hours prior to harvest. Fold changes are given as mean induction of treatment over vehicle control. Datapoints represent triplicate firefly luciferase values normalized to renilla luciferase in 4 replicate experiments. Statistical analysis utilized Student's *t* test and significance is denoted: *p< 0.05.

(Figure 4.6a). Transient transfection experiments were used to test various hormone (E_2, R5020, E_2+ R) and PMA treatments on the antisense promoter construct. These experiments established that the antisense promoter was not significantly induced by E_2 despite containing two consensus estrogen response elements (EREs) (Figure 4.5), but was weakly induced by R5020 (1.71 fold induction) (Figure 4.5). PMA or PMA+E_2 treatment repressed the antisense promoter 7.14 and 5.26 fold (Figure 4.5) suggesting possible AP-1 regulation.

Based on previous experiments analyzing regulation of the sense PR promoter constructs by AP-1, companion experiments were performed in MCF-7 cells comparing the PR promoter constructs with the antisense PR promoter (Figure 4.6a) following cotransfection with different AP-1 isoforms. The antisense PR promoter was weakly, but significantly induced by c-Jun (1.52 fold), 2.38 fold by c-Jun/Fra1 or 2.06 fold by c-Jun/Fra2 (Figure 4.6b). Induction by c-Jun plus c-Fos was not significant (1.25 fold). JunB induced the antisense PR promoter 2.51 fold, JunB/c-Fos 3.07 fold and JunB/Fra1 1.89 fold while JunB/Fra2 showed the greatest induction of antisense promoter activity (3.26 fold).

The antisense PR promoter was also up-regulated by JunD alone (2.37 fold), by JunD/Fra1 (2.66 fold) and by JunD/Fra2 (2.68 fold) (Figure 4.6b). As with c-Jun, cotransfection of c-Fos with JunD failed to reproducibly alter the level of transcription from the antisense PR promoter supporting only a non-significant 1.44 fold change. Based on these transient transfection results, the antisense promoter can be reproducibly activated by JunD, JunB, and c-Jun either alone or in combination with c-Fos, Fra1, or Fra2. Only a limited number of AP-1 combinations were ineffective, namely c-Jun/c-Fos and JunD/c-Fos. Therefore, it appears that any of the Jun isoforms can activate a basal level of antisense transcription in selected contexts.

However, only JunD can *uniquely* activate the antisense PR promoter above basal, without activating any of the sense PR promoters to the same extent. Overall, cotransfection with the different AP-1 isoforms showed that the antisense PR promoter is activated by JunD, JunB and c-Jun with or without Fra1/Fra2 as well as by JunB/c-Fos (Figure 4.6b).

3. Role of the $PR^{antisense}$ Transcript in Regulation of Mouse Pgr Gene Expression

a. In Situ Hybridization of Probes to Detect Sense and Antisense Transcripts at the Pgr Locus in Mouse Mammary Cells and Tissues

In silico and *in vitro* data suggested that the $PR^{antisense}$ mRNA may be co-expressed or co-regulated with sense PR mRNA. Since PRA and PRB proteins are regulated *in vivo* by hormones (Aupperlee MD 2007), it is probable that the $PR^{antisense}$ transcript is also hormonally regulated at either a transcriptional or post-transcriptional level. Analysis of the PR antisense promoter showed induction by R5020 and responsiveness to PMA (Figure 4.5). Therefore we assessed the effect of hormone treatment on endogenous $PR^{(A+B)}$ message and $PR^{antisense}$ transcript levels using *in situ* hybridization. Similar to the semi-quantitative PCR, *in situ* hybridization was chosen over other methods since it allows use of strand-specific probes and can differentiate between $PR^{(A+B)}$ and $PR^{(B)}$ transcripts. But *in situ* hybridization followed by immunofluorescence also allows simultaneous detection of the PR transcripts and protein on a cell by cell basis. In MC7-L1 mouse mammary tumor cells, an endogenous $PR^{(A+B)}$ transcript was detected in almost every cell (Figure 4.7(a-ii)). However, transcript levels were not noticeably altered with hormone treatments (data not shown). Similarly, endogenous $PR^{(B)}$

(a)

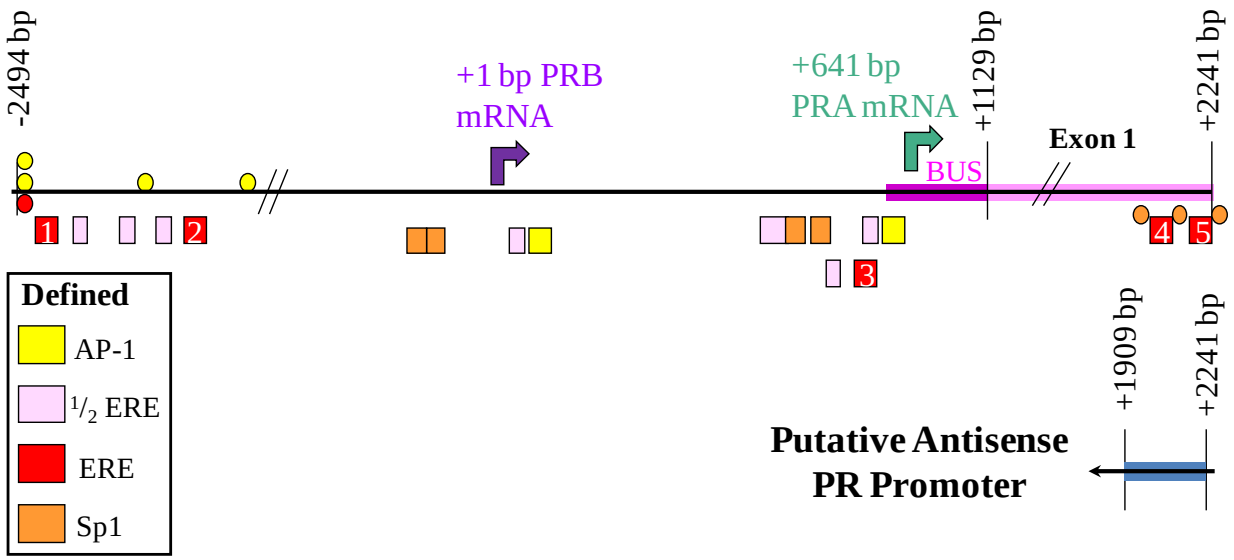

Figure 4.6: (a) The mouse Pgr locus showing the location of the antisense PR promoter in relation to the predicted PRB and PRA sense strand promoters. Defined sites are indicated as squares, while Genomatix MatInspector predicted sites are shown as circles (MatInspector 2005). Coordinates are relative to the predicted PRB mRNA start site (+1 bp) based on homology to human and rat sequences. The PRA mRNA start site is predicted at +641 bp.
(b) Cotransfection of the mouse PR antisense promoter construct with Jun/Fos.
The mouse antisense PR promoter construct was cotransfected with 50 ng of Jun (c-Jun, JunB or JunD) or 25 ng of Jun plus 25 ng of a Fos partner (c-Fos, Fra1 or Fra2) in MCF-7 cells. Fold changes are given as mean induction of cotransfected AP-1 over empty vector ± SE. Datapoints represent the average of triplicates in a minimum of 3 replicate experiments. Statistical analysis utilized Student's *t* test. Statistical significance is denoted: *p< 0.05.

Figure 4.6 (Cont'd.)

(b)

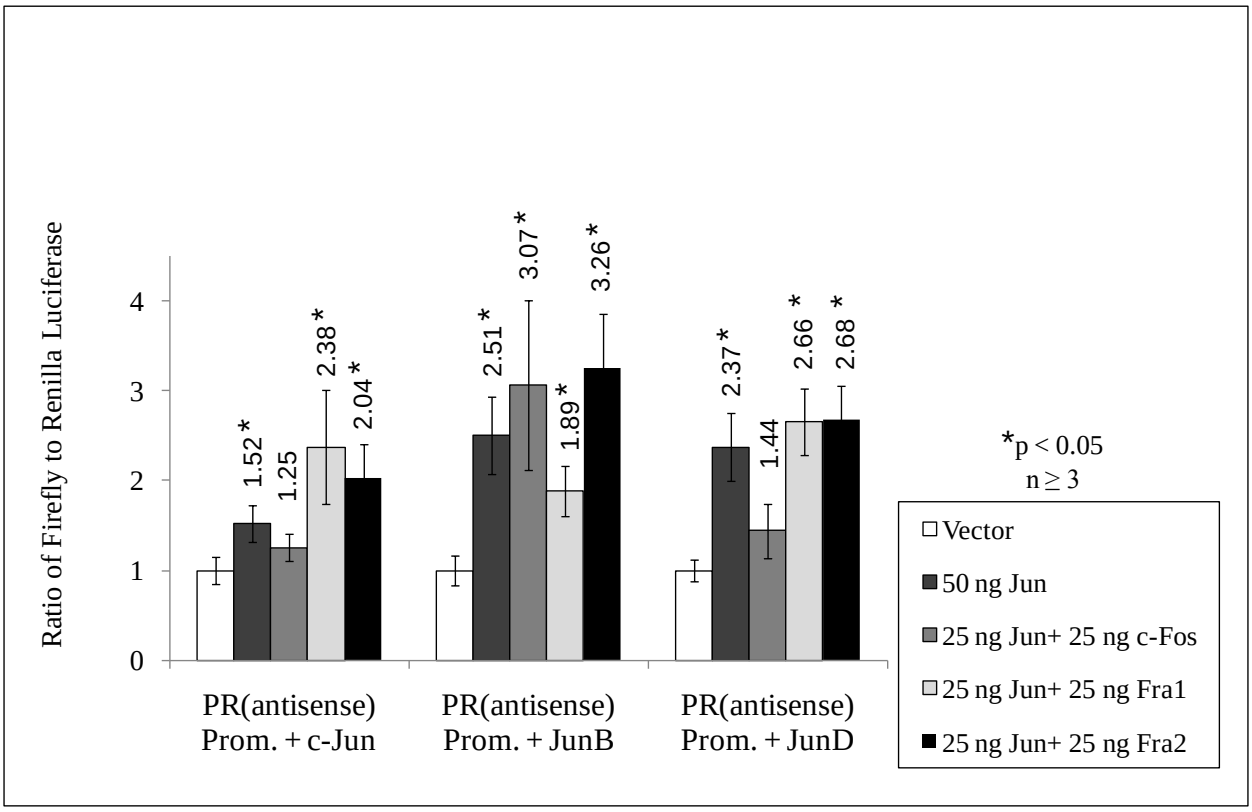

transcript was detected in almost every cell (Figure 4.7(a-iii)) and also did not noticeably change with hormone treatment (data not shown).

Endogenous $PR^{antisense}$ transcript was also detected in almost every cell (Figure 4.7(b-ii). There was a trend towards a slight increase in $PR^{antisense}$ message after R5020 and E_2+ R treatment, whereas E_2 treatment alone did not appreciably alter the level of $PR^{antisense}$ message in MC7-L1 cells (data not shown). Transiently over-expressing the $PR^{antisense}$ cDNA in MC7-L1 cells did not qualitatively change the amount of $PR^{(A+B)}$ or $PR^{(B)}$ message (data not shown). The reciprocal experiment was also examined, in which PR cDNA was transiently over-expressed in MC7-L1 cells, but this did not noticeably alter the level of $PR^{antisense}$ message (Figure 4.7(b-iii)). These transient transfection experiments suggest that the presence of PR^{sense} message may be compatible with $PR^{antisense}$ message in the same cell and that co-expression of either one does not appreciably alter the cellular concentration of the other, at least within the context of a transient transfection experiment.

For MC7-L1 cells (Figure 4.7) and UMD-208 cells (data not shown) there wasn't a qualitative difference between the expression of PR^{sense} or $PR^{antisense}$ message, or changes in their amounts following hormone treatments as observed using *in situ* hybridization with the colorimetric detection system. But, because $PR^{antisense}$ transcript was easily detectable in at least two mouse mammary cells lines (MC7-L1 and UMD-208 cells), this suggested that the $PR^{antisense}$ transcript would be present *in vivo* as well. Based on the *in vitro* experiments described above, we hypothesized that $PR^{antisense}$ mRNA would be co-expressed with PR protein

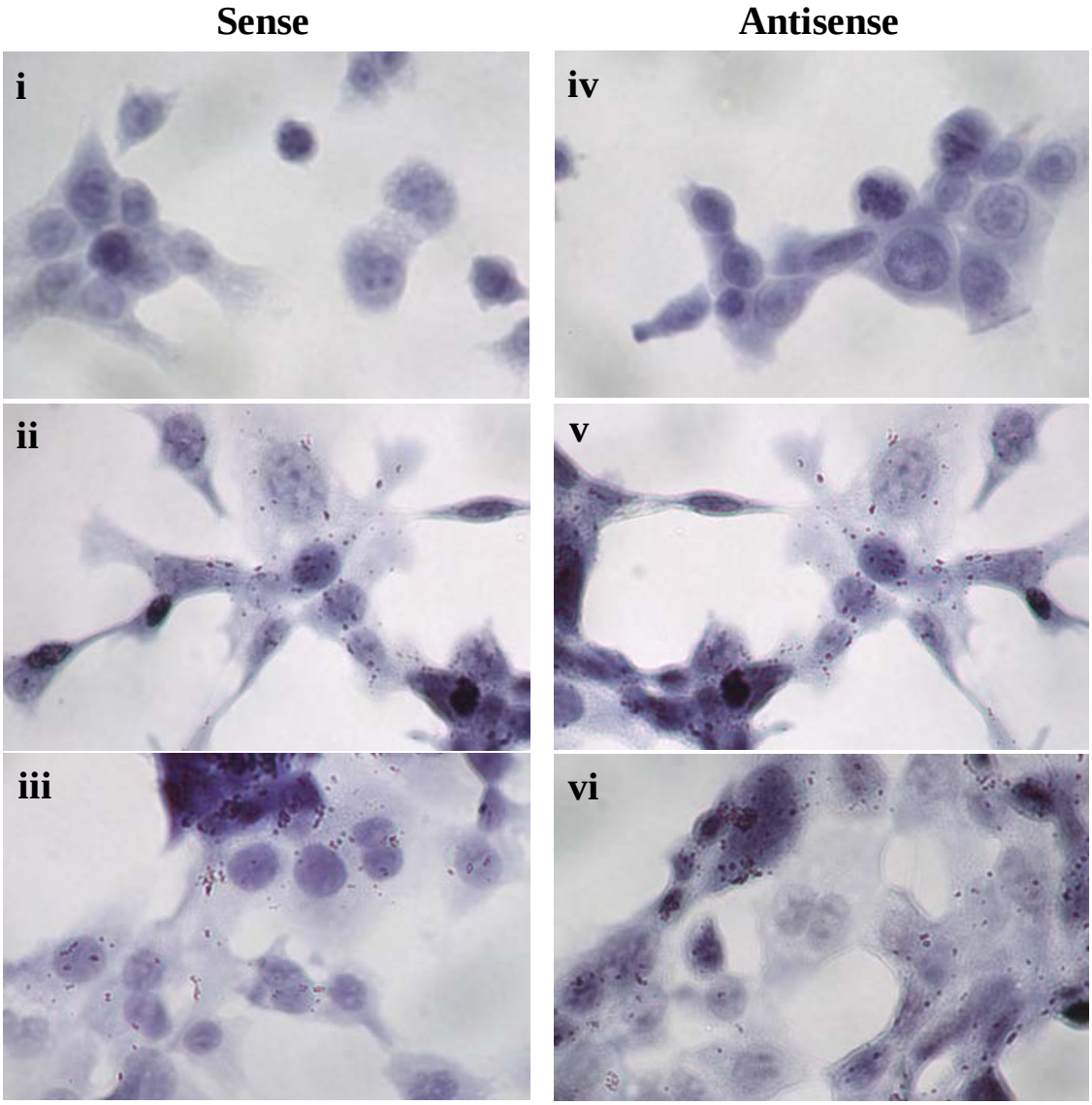

Figure 4.7: MC7-L1 cell *in situ* hybridization (ISH) of Pgr locus RNA. Digoxigenin labeled probes were visualized using nitroblue tetrazolium salt and 5-bromo-4-chloro-3-indolyl phosphate (NBT/BCIP). Cells were counterstained with hematoxylin and are shown at 40x magnification.
(i-iii) PR sense probes and control: (i) The no probe negative control shows no digoxigenin signal. (ii) The PRA+B probe detects total PR^{sense} message (i.e. PRA + PRB) in most cells (dark purple granules). (iii) The PRB probe detects $PR^{(B)}$ message in most cells.
(iv-vi) PR antisense probes and control: (iv) The no probe negative control shows no digoxigenin signal. (v) The PR antisense probe detects $PR^{antisense}$ message in most cells.
(vi) Over-expressing a PR cDNA expression vector did not noticeably alter the $PR^{antisense}$ message levels.

in many of the same cells and that the pattern of co-expression might differ among PR protein isoforms or developmental stages. To address this point, we sought to develop a more sensitive method to simultaneously detect the strand-specific RNAs and PR protein in cells and tissues.

In vivo analysis utilized mammary gland tissue obtained from the BALB/c mouse at the following stages: pubertal (6 weeks), virgin adult (19 weeks), and pregnancy-like (i.e. age-matched virgin adult mice treated for 14 days with E_2+P). *In situ* hybridization followed by immunofluorescence was used to determine the levels of endogenous $PR^{(A+B)}$, $PR^{(B)}$, and $PR^{antisense}$ mRNA in mammary gland tissue sections along with their level of co-expression with PRA and PRB proteins. An anti-human PR antibody (DAKO) was used that is specific for the PRA isoform (Figure 3.S3). To detect PRB, a custom generated anti-mouse PRB antibody (B15) directed against the first 15 amino acids in the mouse PRB sequence was generated (Kariagina A 2007); (Figure 3.S3).

Similar to *in situ* hybridization experiments in MC7-L1 cells, both $PR^{antisense}$ and $PR^{(A+B)}$ sense mRNA were detected in a majority of luminal epithelial cells of the mouse mammary gland (Figure 4.8). Both PR^{sense} and $PR^{antisense}$ message were co-expressed with PRA protein in the same cells across various stages of development (Figure 4.8; data not shown). Using serial sections, PR^{sense} and $PR^{antisense}$ mRNA were also co-expressed with PRB protein in a subset of 14 day E_2+P treated luminal epithelial cells. $PR^{antisense}$ RNA expression was ubiquitous across developmental stages and within all of the structures examined (terminal end buds, small ducts, large ducts and lobules) with no obvious qualitative difference in mRNA expression levels between structures (Figure 4.8; data not shown). In general, PRA

protein-positive cells had slightly higher levels of both $PR^{(A+B)}$ and $PR^{antisense}$ RNA (Figure 4.8) compared to cells that were PRA protein-negative.

b. Alternative Models of Antisense Transcription at the Progesterone Receptor Locus

One possible mechanism of $PR^{antisense}$ mRNA action is interference of PR protein expression at a post-transcriptional level. Alternatively, the $PR^{antisense}$ transcript may possess the activity of repression in *trans* of the sense strand promoters PRA, PRB or both. In this proposed mechanism, a previously transcribed single stranded $PR^{antisense}$ transcript would act in *trans* by forming a triplex structure with the PRA or PRB promoter region DNA, thereby preventing transcription initiation or elongation. This model differs from other types of transcriptional control in that the antisense transcript could be produced at a different time than the sense transcript, assuming an adequately long RNA half-life, yet it still requires expression to occur within the same cell. In order to test this mechanism, an increasing amount of $PR^{antisense}$ mRNA expression plasmid was co-expressed with a constant amount of PR promoter luciferase reporter in MCF-7 cells. MCF-7 cells were selected because of the known behavior of the PR promoter luciferase reporter plasmids, and the fact that these cells are known to lack the corresponding mouse $PR^{antisense}$ mRNA. The ratio of PR sense promoter reporter to $PR^{antisense}$ cDNA was varied from 20:1 (i.e. an excess of sense PR) up to 1:5 (i.e. an excess of $PR^{antisense}$ cDNA). The sense PR promoters tested included: proximal promoter A, distal promoter B and the long tandem PR promoter (LTP; consisting of both PRA+B) constructs. When $PR^{antisense}$ mRNA was co-transfected with these reporter constructs, it had no observable effect on sense PR

Figure 4.8: RNA Fluorescence *in situ* hybridization detection of PRA+B mRNA (i-iv), $PR^{antisense}$ mRNA (v-viii), and PRB mRNA (ix-xii) in 14 day E_2 +P treated virgin adult mouse mammary gland (RNA expression was evident as green perinuclear staining). PRA protein was detected using immunofluorescence on the same sections. (i, v, ix) mRNA (green), (ii, vi, x) PRA protein (red), (iii, vii,xi) overlay images of mRNA (green) and PRA protein (red), and (iv, viii, xii) merged images of mRNA (green), PRA protein (red) and DAPI counterstained nuclei (blue). White arrows show representative cells that have perinuclear PR message expression (green) in the absence of PR protein expression. Yellow arrows indicate cells that co-express PR message (green) and PRA protein (red). Note that both sense and antisense RNA are present in luminal epithelial cells and that PRA+ cells express both sense and antisense RNA. (xiii) No primary antibody control shows a background level of staining due to endogenous biotin (green) present primarily in stromal cells as determined by omitting the primary antibody (xiii), but is largely absent from luminal cells as seen when the no primary antibody control image is merged with DAPI stained nuclei (xiv).

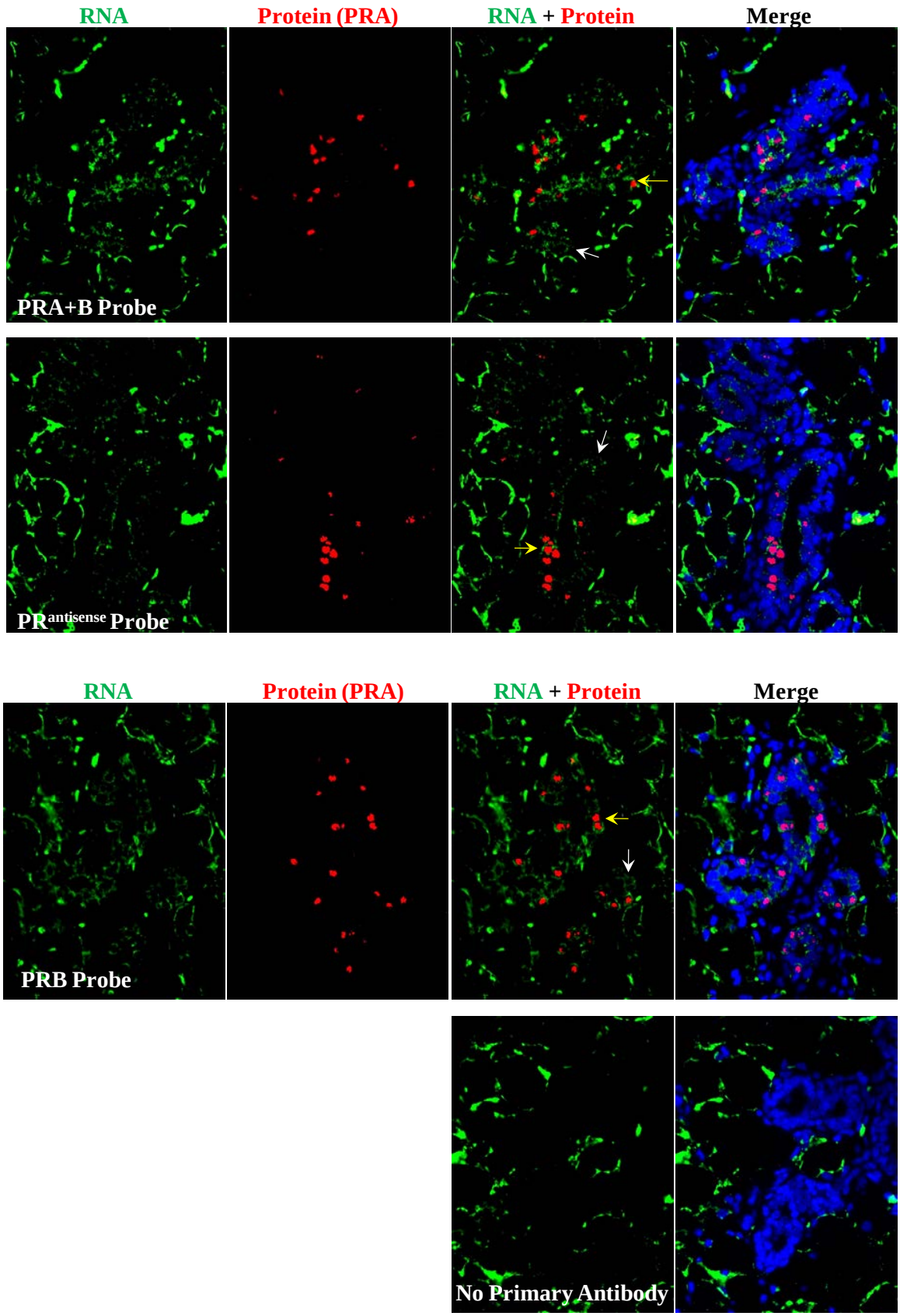
RNA
Protein (PRA)
RNA + Protein
Merge
PRA+B Probe
PR antisense Probe
RNA
Protein (PRA)
RNA + Protein
Merge
PRB Probe
No Primary Antibody

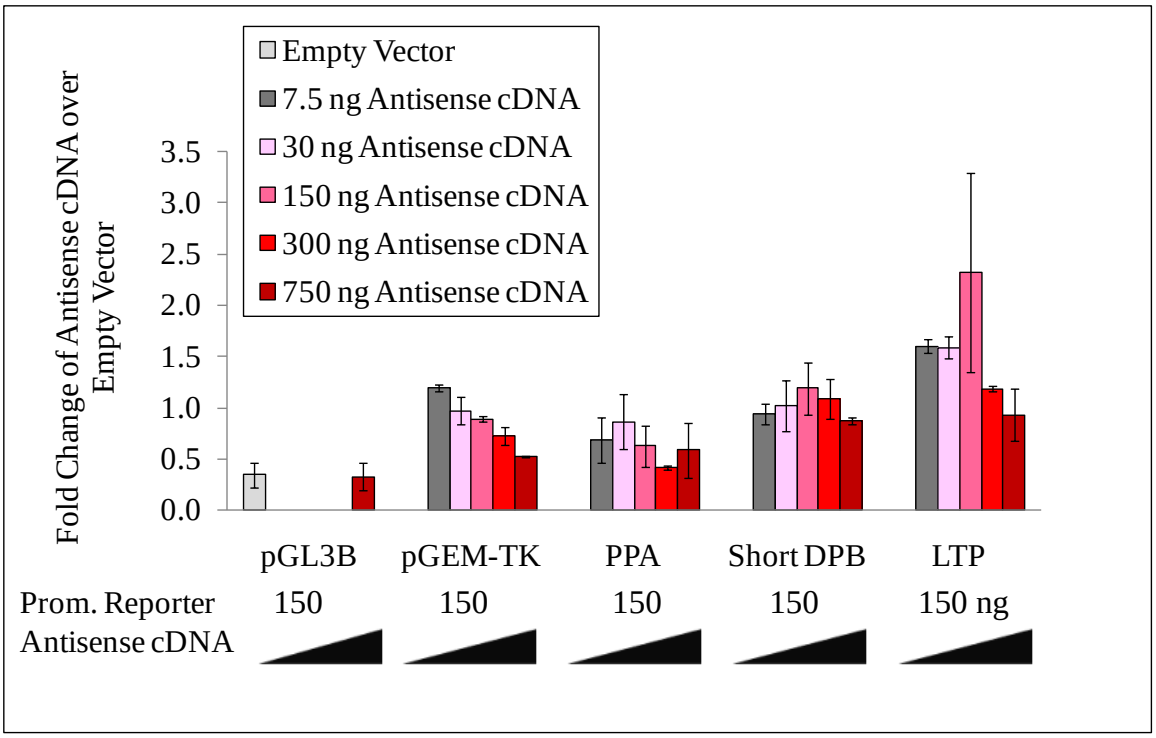

Figure 4.9: Cotransfection of MCF-7 cells with a constant amount of a sense PR promoter reporter and an increasing amount of PR^{antisense} cDNA. Fold changes are given as the average of the mean induction of cotransfected PR^{antisense} cDNA over empty vector ± SE. Sense PR promoter constructs used were: proximal promoter PRA (PPA), short distal promoter PRB (short DPB), and long tandem PR promoter (LTP). The ratio of sense PR to PR^{antisense} varied from: 20:1 to 1:5. Acting in t*rans*, cotransfection of the PR^{antisense} mRNA had no effect on the sense PR promoters as measured by luciferase assay. Data points represent triplicates in 2 experiments ±SEM.

promoter-reporter activity in *trans* as measured using the luciferase assay (Figure 4.9). Differences in the measured activities of these constructs were in all cases not significant.

DISCUSSION

In Silico Evidence of an Antisense Promoter and Transcript at the Pgr Locus

In the Natural Antisense Transcripts database (NATsDB), the BC059021 transcript is annotated as a naturally occurring *cis*-NAT with complementarity to the mouse PR mRNA (Zhang Y 2006a); (Zhang Y 2006b). This pairing of the PR message with the BC059021 transcript spans 1132 bp, most of which is contained within PR exon 1. The mouse PR sense/antisense pair therefore shows a divergent 5' overlapping arrangement in the head-to-head orientation with the antisense transcript overlapping the majority of PR sense exon 1 (Figure 4.1b). Based on *in silico* data, the mouse Pgr locus appears to have a single antisense transcriptional unit with a promoter most likely located at the 3'-end of sense PR exon 1. Furthermore, since the $PR^{antisense}$ transcript lacks significant homology to any known protein or protein domain it is most likely a non-coding RNA (ncRNA). The antisense transcript is an expressed, polyadenylated RNA which is therefore presumably transcribed by RNA Polymerase II. The presence of a Poly(A) tail predicts that the antisense transcript may be localized to the cytoplasm, however, *in situ* hybridization experiments showed that *in vivo* the $PR^{antisense}$ transcript was localized to the perinuclear region instead (Figure 4.8).

Studies have found that NATs are usually expressed in a spatially (cell or tissue specific) as well as temporally specific manner that is linked to the expression of their sense partner (Beiter T 2008). Since the mouse sense PRA and PRB proteins show differential spatial and temporal expression during development (Aupperlee M 2005a), it is possible that the antisense transcript is subject to either co-expression or inverse expression with respect to either one of the two sense messages, $PR^{(A)}$ or $PR^{(B)}$ mRNA. Bidirectional promoter activity which extends to the 5'-end of intron 1 in the sense gene is often associated with divergent sense/antisense pairs that are co-regulated (Beiter T 2008). The similarity of mouse PR with other coregulated sense/antisense pairs suggests that the coding strand mRNAs might also be coregulated or co-expressed with their antisense partner. Additional evidence from another promoter study also fits well with the organization of the mouse Pgr gene. The Pgr locus contains two CpG Islands stretching from +659 to +884 bp and +1572 bp to +2197 bp (Figure 4.1a) (Carninci P 2005); (Katayama S 2005). The overlap of transcripts from CpG-islands associated with bidirectional promoters may provide another layer of transcriptional control due to their potential for methylation (Beiter T 2008). This is thought to be important in promoters with widely spaced transcription start sites (Beiter T 2008), such as we observed for the mouse Pgr gene (Carninci P 2005); (Katayama S 2005).

Most large non-coding RNAs (ncRNAs) typically do not show sequence conservation across species, in particular between human and mouse (Yazgan O 2007). Large ncRNAs actually show less than 70% homology, which is similar to that seen for introns (Yazgan O 2007). Since there are several well studied examples of poorly conserved ncRNA sequences in mammals that nonetheless possess important regulatory functions (i.e. Xist/Tsix in X chromosome inactivation), this suggests that a lack of sequence conservation does not

necessarily mean a lack of function (Yazgan O 2007). The sequence homology for the mouse and human antisense PR transcript is 77%, which might seem low for an exonic region, but is actually high for a ncRNA. Considering that the antisense transcript encompasses the majority of sense PR exon 1, evolutionary selection for sequence conservation would be expected. Since large ncRNAs are expected to have <70% sequence conservation, having slightly more sequence conservation in a ncRNA complementary to an exonic region versus an intronic region seems reasonable and may be functionally significant. Transcriptional regulation of ncRNAs is often controlled by promoter elements which are frequently conserved between species such as human and mouse (Munroe SH 2006). The ncRNA for antisense PR is likely to be controlled by the Sp1 and ERE4/5 minimal promoter region due to both its location and the high degree of conservation of the ERE4/5 sites in particular. It is therefore not surprising that the mouse antisense PR transcripts appear to be both regulated and polyadenylated based on the PCR and primer extension experiments described herin.

Multiple models have been suggested to explain the function of antisense transcripts that are organized in sense/antisense pairs. In the first model, transcriptional interference (TI), RNA polymerase complexes on opposing strands collide, stalling transcriptional elongation (Osato N 2007); (Lapidot M 2006). Alternatively, transcription initiation is blocked due to competition between the transcription units (Lapidot M 2006). Since the actively transcribed antisense transcript (Figures 4.1a, b) overlaps entirely with sense PR exon 1 in the PR sense/antisense pair, it is quite possible that converging RNA polymerase complexes may collide in the PR 5'-UTR or the beginning of exon 1 during elongation, especially during conditions of high transcriptional activity. If collision and stalling occured downstream of the PRA start site, this could prevent successful transcription from the PRA promoter, while at the same time the upstream PRB

promoter could still initiate transcription. Once the colliding polymerases have dissociated from their DNA template, then the polymerase transcribing PRB could proceed through the site of interference to complete a functional PRB transcript. Alternatively, if collision and stalling occurs in the 5'-UTR region of PRB this would prevent successful transcription preferentially from the PRB promoter. If the downstream PRA start site was simultaneously not occluded, then transcription could initiate preferentially from the PRA promoter producing only PRA transcript and PRA protein. Therefore, it is conceivable that transcription initiation from the sense strand of mouse PR could be inhibited by the antisense transcript overlapping the 5'-end of either PRA alone or both the PRA and PRB messages. It has also been shown that alterations in local chromatin structure caused by transcriptional initiation from one strand may "open" the chromatin and activate transcription on the other strand, effectively bringing adjacent promoters into an active "transcription factory" (Munroe SH 2006).

A second model suggests that a nascent or mature antisense transcript could directly feed back to the overlapping gene or fold back to form a RNA/DNA complex (Munroe SH 2006). A few cases of non-imprinted *cis*-sense/antisense pairs been reported in mammals in which one strand spans the promoter region of the opposite strand have (Tufarelli C). In many of these cases the ncRNAs are relatively long (>600 bp), similar to the antisense transcript within the Pgr gene (Tufarelli C 2006). An interesting example showing a very similar organization to the PR *cis*-sense/antisense pair is the case of the haemochromatosis gene (*HFE*), in which a long polyadenylated antisense transcript overlaps *HFE* exon 1 and continues 1 kb into the promoter region of the sense gene (Tufarelli C 2006). The antisense HFE transcript has been shown to interfere *in vitro* with expression of the sense gene product, but it is unknown if regulation is exerted at a transcriptional or translation level (Tufarelli C 2006).

Alternatively, transcription of an antisense RNA through the CpG island of a non-imprinted autosomal gene, which is tissue specific, can also lead to methylation and silencing of the sense gene, consistent with the silencing model described above (Tufarelli C 2006). The mouse Pgr locus has two assigned CpG islands (Figure 4.1a), one located at the 5'-end of sense PR exon 1 (+659 to +884 bp) and a second island at the 3'-end of sense exon 1 (+1572 to +2197 bp) (Carninci P 2005); (Katayama S 2005). Interestingly, the second CpG island overlaps with the +1770 to +2020 bp cluster of antisense CAGE tags, ESTs and mRNAs (Figure 4.1a).

The third model, RNA masking, suggests that sites in the sense sequence which are required for expression (i.e. sites for RNA binding proteins or splicing factors) can be masked by the antisense transcript (Munroe SH 2006). This could occur during splicing, export, polyadenylation, stabilization, or control of translation, but the RNA interaction itself does not trigger downstream signaling events (Munroe SH 2006). This mechanism would show a pattern of expression in which the presence of the antisense transcript and the sense transcript that it regulates are positively correlated (Lapidot M 2006) as is the case for the mouse Pgr locus.

The fourth model, dsRNA-dependent regulation by RNA interference (RNAi), would involve the formation of a dsRNA duplex which subsequently recruits factors that alter expression (Munroe SH 2006). This model requires the simultaneous expression of both the sense and antisense transcripts, accounting for the co-expression of many sense/antisense pairs (Lapidot M 2006). Since the overlapping sequence in the sense/antisense pair at the mouse Pgr locus spans approximately 2.3 kb, this would provide plenty of dsRNA to degrade into the 21-24 nt siRNAs and incorporate in an RNAi mechanism necessary for recognition by the RNA-induced silencing complexes (RISC) which are involved in Dicer-mediated gene silencing (Hannon GJ 2002).

***In Vitro* Evidence: Primer Extension and Strand-Specific Semi-Quantitative PCR**

Semi-quantitative PCR was used to establish the existence of antisense transcription at the Pgr locus. This method was chosen so that strand-specific cDNAs could be synthesized for both the sense and antisense strands of PR. Overall, in any of the samples (except liver) both PR^{sense} and $PR^{antisense}$ transcript were readily detectable.

Using the exon 1 ATG_B primer set, there were moderate to high expression levels of $PR^{antisense}$ in all of the mouse tissues examined, in NMuMG cells and in UMD-208 cells. It is interesting to note that the NMuMG cells have high levels of $PR^{antisense}$ transcript (Figure 4.4b) but significantly less PR^{sense} transcript (Figure 4.4a). The abundance of $PR^{antisense}$ and PR^{sense} transcript are similar in the mouse liver, suggesting that the transcripts may be coregulated. Regulation in the mammary gland appears similar to liver since the $PR^{antisense}$ transcripts also show correlated expression with $PR^{(A+B)}$ or $PR^{(B)}$ transcript (Figure 3.12; data not shown).

In the liver, it appears that the location of the antisense start sites may differ between the ovariectomized animal and the ovary-intact mouse (Figure 4.2c). Since E_2 is no longer present after ovariectomy, this decrease in E_2 may be necessary to activate preferential transcription start sites within the antisense promoter. However, the overall abundance of $PR^{antisense}$ mRNA in liver in an ovariectomized mouse does not appear to differ from an ovary-intact mouse (Figure 4.2c). Furthermore, using PCR analysis, the effect of ovariectomy was not consistent across tissues examined (liver, uterus, mammary gland) (Figure 4.4a). Additionally, treatment of mouse mammary cell lines with E_2 yielded varying results for $PR^{antisense}$ transcript abundance (Figures 4.4c, d). Therefore, based on the primer extension, PCR analysis and transient

transfection experiments, consistent evidence for hormonal regulation of the $PR^{antisense}$ transcript is lacking and therefore is insufficient justification to conclude that ERE(4)/ERE(5) is able to serve as a functional E_2-responsive element in the context of the mouse PR antisense promoter.

The exon 1 ATG_B primer set was designed to detect only $PR^{(B)}$ mRNA. When used on a cDNA primed in the 3'-UTR, PCR analysis did not detect PR RNA in virgin adult mammary gland samples (Figure 4.4a). It has been established by immunohistochemical staining that PRB protein is not detected in the virgin adult mouse mammary gland and that PRA protein is the only isoform detected (Aupperlee M 2005a). Transcripts leading to the expression of both PRB and PRA proteins may be present, but only those transcripts initiating downstream of the PR ATG_B appear to produce functional protein in the virgin adult mammary gland. Since total PR^{sense} mRNA was detected with this same virgin adult mammary gland cDNA preparation using a common region exon 4/5 primer set (Figure 3.18c), this implies that PRB transcripts are either not being expressed in the virgin adult mammary gland or are not detected with the ATG_B primer set. Primer extension mapping of start sites in the vicinity of PR ATG_B revealed that the majority of start sites initiate in the region from +635 to +725 bp and are therefore capable of producing only PRA protein.

The third primer set used was the exon 1/2 primer set which straddles intron 1. Amplification of PR antisense with the exon 1/2 primer set did not yield any PCR products in any of the tissues (mammary gland, uterus, liver) or cell lines (NMuMG and UMD-208 cells) examined (data not shown). Additionally, the exon 4/5 primer set, which straddles intron 4, was tested on an antisense primed cDNA template for PCR analysis. Again, there were no PCR products detected, even after 36 cycles of amplification (data not shown). Combined with the

PCR analysis utilizing the exon 1 primer sets, this rules out the possibility that the $PR^{antisense}$ transcription unit includes the lower strand counterparts of exons 2, 4 or 5, making it likely that the transcription start sites for $PR^{antisense}$ RNA originate near the 3'-end of exon 1.

A TATA-less Antisense Promoter at the Pgr Locus Drives Expression of the $PR^{antisense}$ Transcript

Promoter, CpG island and transcription factor binding site prediction analysis of mouse PR exon 1 and intron 1 predicted an antisense PR promoter located at the 3'-end of sense exon 1. There are multiple putative antisense strand TATA boxes located with intron 1, but these lack any other recognizable characteristics of transcription start sites such as appropriately positioned CAAT or GC boxes. Additionally, TATA motifs present in intron 1 lack both *in silico* evidence (CAGE tags and ESTs) and *in vitro* evidence (primer extension and PCR) to support their location. Rather, all of the available data supports the conclusion that a TATA-less $PR^{antisense}$ promoter is located at the 3'-end of sense exon 1, overlapping the second CpG Island (Figures 4.1, 4.3, 4.6). Transcription factor binding site analysis predicted the presence of ERE(4) and ERE(5), previously defined in the rat (Kraus WL 1994), along with three putative Sp1 binding sites located adjacent to these EREs (MatInspector 2005).

The PR Antisense Promoter is regulated by R5020, PMA, and AP-1

Contrary to expectations, it is surprising that in transient transfection assays in MCF-7 cells (which are known to be E_2-responsive), the presence of two EREs did not appear to confer E_2-responsiveness to the antisense PR promoter (Figure 4.5). However, in light of our analysis of the sense PR promoter where the presence of multiple EREs and half EREs also failed to

achieve a significant level of PR promoter activation in MCF-7 cells these data are fitting (Figure 3.5). Additionally, when ERE(4) and ERE(5) were added as an enhancer cassette to the long tandem PR promoter (creating LTP-ERE), this once again failed to increase the transcriptional activity of the long tandem promoter in either the presence or absence of E_2 (Figure 3.6; data not shown). Therefore, regardless of the context of ERE(4/5), its presence failed to achieve E_2-inducibility.

When treated with R5020, the PR antisense promoter was weakly, but significantly induced in transient transfection assays (Figure 4.5). Transcription factor binding site analysis failed to predict a progesterone response element (PRE) in this region, but did find putative Sp1 sites to which PR has the ability to tether (Faivre EJ 2008). Conversely, PMA treatment alone or PMA combined with E_2 repressed the PR antisense promoter (Figure 4.5). This suggests possible AP-1 regulation of the PR antisense promoter. However, since PMA broadly targets many pathways downstream of protein kinase C (PKC) (Brose N 2002), this repression may be due to downstream targets and not directly including, or in addition to AP-1.

Cotransfections of the PR antisense promoter with various AP-1 isoforms established that c-Jun, JunB and JunD can all activate the antisense PR promoter in various combinations and to varying degrees (Figure 4.6b). Since the PR antisense promoter lacks a consensus AP-1 site, Jun activation of the antisense PR promoter may be through synergism of Jun tethering to estrogen receptor bound at the 2 predicted adjacent EREs (Figure 3.1). Since JunD is constitutively expressed in most tissues at a high level (Mechta-Grigoriou F 2001), up-regulation of the antisense PR promoter by JunD may lead to a basal level of antisense transcription throughout most stages of mouse mammary gland development. JunD protein was expressed in pubertal, virgin adult and pregnancy-like mouse mammary gland (Figure 3.18), suggesting that the PR

JunD may drive basal expression from the antisense promoter throughout development. The highest levels of JunD protein were expressed in the pubertal and virgin adult mammary gland, where there was a moderate degree of JunD/PRA colocalization (37-44% in ducts); (Figure 3.18). The total number of JunD expressing cells decreases in the 14 day E_2+P treated mouse, where 33-35% of the PRA+ cells in ducts were observed to be $JunD^+$ (Figure 3.18).

For c-Jun and JunD, transfection of the Jun subunit alone was sufficient to activate the antisense PR promoter while cotransfection of c-Jun/c-Fos or JunD/c-Fos was not significantly different than the empty vector control. This suggests that in the context of the endogenous AP-1 pool of MCF-7 cells, a c-Jun/c-Fos or JunD/c-Fos heterodimer is either less stable, has lower DNA binding capacity, or lower transactivation potential than the corresponding Jun homodimer. JunB/c-Fos was the only c-Fos heterodimer able to significantly activate the PR antisense promoter above control levels (Figure 4.6b). In the mouse mammary gland, c-Fos expression was low (1-4%) in pubertal and virgin adult mice, increasing to 5-8% of cells in the 14 day E_2+P treated mouse (Figures 3.20). Since c-Fos expression was so low and only colocalized in a random percentage of PRA^+ cells (Fischer's exact test), the consequence of c-Fos in regulation of the antisense PR promoter in the mouse mammary gland is unknown.

It is interesting to note, however, that c-Fos was dramatically up-regulated in the mammary glands of ovariectomized mice following 3 days of treatment with E_2 (Figure 3.23). In ovariectomized virgin adult mice, JunD was the predominant Jun isoform accounting for 53-63% of luminal epithelial cells (Figure 3.S6). JunB was expressed in a moderate number of cells, accounting for 36-38% of luminal epithelial cells (Figure 3.S5). The Jun isoform expressed in the lowest number of cells in adult ovariectomized mice was c-Jun, which was

found in 19-24% of luminal epithelial cells (Figure 3.17). If the *in vivo* PR antisense promoter behaves similarly to the way it behaves in MCF-7 cells, then an increase in c-Fos in the presence of c-Jun or JunB would fail to activate basal $PR^{antisense}$ message expression, whereas the presence of JunD would enable $PR^{antisense}$ induction. None of the AP-1 isoform combinations examined repressed the PR antisense promoter, rather all of them either were equivalent to empty vector (basal expression level) or showed significant induction above the basal level.

For the other Fos family members, Fra1 and Fra2, cotransfection with c-Jun, JunB, and JunD significantly activated the antisense PR promoter (Figure 4.6b). Fra1 colocalized with PRA in 19-23% of cells in the pubertal mouse, 17-19% in the virgin adult and 10-11% in the 14 day E_2+P treated mammary gland (Figure 3.21). Additionally, there is a high degree of Fra1/PRA and c-Jun/PRA colocalization at all three developmental stages (Figures 3.21, 3.17). Since the $PR^{antisense}$ transcript also colocalized with PRA protein expression in most cells across all developmental stages (Figure 4.8), this suggests that c-Jun, Fra1, PRA and PR^{anti} co-exist in a subpopulation of luminal epithelial cells, with the potential for important functional interactions.

In Situ Hybridization Readily Detected Sense and Antisense Transcripts at the Pgr Locus in Mouse Mammary Cells

In MC7-L1 mouse mammary tumor cells, endogenous $PR^{(A+B)}$, $PR^{(B)}$, and $PR^{antisense}$ message was detected in almost every cell (Figure 4.7a, b) using *in situ* hybridization. Levels of PR^{sense} transcript, which were present in a subset of luminal epithelial cells, were not noticeably altered by hormone treatment. $PR^{antisense}$ message levels did not appear to be altered by E_2 treatment, but showed a trend towards a slight increase in message levels after R5020 or

E_2 +R5020 treatment. This mirrors the observation that the antisense PR promoter was also weakly responsive to R5020 treatment, but not to E_2 treatment (Figure 4.5) suggesting that the slight increase in $PR^{antisense}$ message may be due to weak intrinsic progesterone-responsiveness of the antisense PR promoter. Similarly, $PR^{antisense}$ message levels were increased by R5020 or E_2+ R treatment when assayed by semi-quantitative PCR (Figure 4.4e).

When the $PR^{antisense}$ message was over-expressed in MC7-L1 cells there wasn't a noticeable change in the levels of endogenous $PR^{(A+B)}$ or $PR^{(B)}$ message. The same was true when the PR cDNA was over-expressed and the level of $PR^{antisense}$ message was measured. These *in situ* experiments were not quantitated due to the difficulty in measuring the level of or the percentage of mRNA positive cells using a colorimetric detection system. Therefore a subtle effect on mRNA levels due to over-expressing the sense or antisense transcript cannot be ruled out. These *in situ* hybridization experiments, however, suggest that sense and antisense message may exist in the same cell at the same time, at least within the time frame of a transient transfection experiment.

Based on these initial findings we hypothesized that *in vivo* $PR^{antisense}$ mRNA would be co-expressed with PR protein in the same cell. However, the pattern of co-expression of antisense RNA with protein could be different between the PRA and PRB protein isoforms or between the various developmental stages. Although most luminal epithelial cells in the mouse mammary gland expressed $PR^{antisense}$ message, the expression levels did not correlate with developmental stage or structure. The sense and antisense messages were co-expressed with PRA protein in the same cells at the same time across developmental stages (Figure 4.6b; data

not shown). Therefore expression of the PR^{sense} message does not prevent expression of the $PR^{antisense}$ message and vice versa. It has been reported that many genes that are co-expressed also show some degree of co-regulation, especially those that show bidirectional promoter activity (Beiter T 2008).

Co-expression of sense and antisense transcripts is not unique to the Pgr locus. One example is the sense and antisense transcript of the erythropoietin receptor (EPO-R) gene, both of which colocalize with EPO-R protein in the post-pneumonectomized lung (Zhang Q 2008). *In vitro*, the antisense EPO-R transcript was found to enhance EPO-R protein expression via regulation of the sense EPO-R transcript (Zhang Q 2008). This unique antisense transcript contains two putative ORFs that encode short regulatory proteins which control sense EPO-R transcription (Zhang Q 2008). This differs from the $PR^{antisense}$ transcript which does not appear to code for a protein. Therefore, potential regulatory mechanisms that involve $PR^{antisense}$ RNA clearly differ from EPO-R and would exclude an antisense polypeptide regulating transcription, processing, or stability of the sense PR mRNA or the PR protein.

Potential Roles of Antisense Transcription within the Progesterone Receptor Locus

Since co-expression of the $PR^{antisense}$ RNA had no effect upon sense PR promoter activity, this rules out a co-transcriptional model in which the $PR^{antisense}$ transcript acts in *trans* on the PR promoter. As discussed above, other possible regulatory mechanisms involving $PR^{antisense}$ include transcriptional interference where $PR^{antisense}$ acts in *cis* at either the initiation step of transcription or influences transcriptional elongation. Transcriptional interference at the

point of transcription initiation is due to the antisense transcript occluding necessary binding sites for the basal transcription apparatus or other critical transcription factor binding sites (Beiter T 2008); (Munroe SH 2006). TI at the transcription elongation step is due to steric constraints of the RNA polymerase complex moving down both strands concurrently or collision of opposing RNA polymerase molecules on the same molecule of DNA (Munroe SH 2006). The TI model differs from other models in its absolute requirement for transcription to occur on both strands of the DNA at the same time in the same cell or tissue type. However, since there was a subset of luminal epithelial cells that co-expressed PR sense and $PR^{antisense}$ transcripts with PRA protein this essentially rules out that transcriptional interference in *cis* operates within the context of the mouse Pgr gene. Additionally, since the sense and antisense transcripts were co-expressed this also rules out anti-expression of the Pgr locus transcripts.

A slight variation on the TI model is transcription factor binding site competition between the *cis*-antisense transcript and its sense transcript. In this model, the antisense transcription unit acts in *cis* to compete for or share transcription factor binding sites with the sense strand transcriptional unit (Munroe SH 2006). This model is more prevalent in transcripts with divergent promoters (i.e., in a head-to-head orientation) due to the proximity of transcription factor binding sites and enhancer elements (Munroe SH 2006). The $PR^{antisense}$ and PR^{sense} transcripts both contain the ERE(4)/ERE(5)/Sp1 enhancer element located near the 3'-end of exon 1 (Figure 4.1a), which therefore represents an obvious candidate control region for both the sense and antisense PR promoters. However, our evidence indicates that this element does not serve as a functional E_2-responsive enhancer either *in vivo*, in tissues, or in tissue culture.

Another transcriptional model postulates that a nascent or mature antisense transcript can physically feed-back on the overlapping gene or indirectly recruit factors (proteins or other RNAs) that will in turn promote or inhibit transcription of the overlapping gene in *cis*. In a double-stranded RNA (dsRNA)-dependent mechanism, formation of a dsRNA duplex would recruit factors that alter expression. This requires simultaneous spatial and temporal expression of the sense and antisense transcripts. Although possible, this mechanism is unlikely to lead to RNA degradation since the $PR^{antisense}$ transcripts are relatively easy to detect (i.e., by PCR, ISH) and therefore are likely to represent stable transcripts.

A possible post-transcriptional regulatory model is that the $PR^{antisense}$ RNA acts in *trans* to regulate $PR^{(A)}$ or $PR^{(B)}$ mRNA stability, export or translateability. This would occur without triggering any downstream signaling events. However, in the absence of compelling evidence that $PR^{antisense}$ RNA can interfere with the production of PR protein, this scenario also seems unlikely. Alternatively, a transcriptional or translational masking model would suggest that sites within the sense sequence that are required for RNA or protein expression can be masked by the antisense transcript. This could occur during splicing, export, polyadenylation, RNA transport, stability or control of translation. Again this mechanism wouldn't trigger downstream signaling events and it would show correlated levels of expression. Once again, however, the observed co-expression of PR^{sense} and $PR^{antisense}$ RNAs, together with the relative inability of $PR^{antisense}$ RNA to interfere with PR protein expression lends no support to such a model.

Future Directions

Technical limitations prevented a thorough examination of the effect of $PR^{antisense}$ on PRB protein. For example, immunofluorescence showed that PRA protein positive cells also express $PR^{antisense}$ mRNA. Likewise, cells expressing PRA protein in the 14 day E_2+P treated mammary gland always colocalized with PRB protein expression. Therefore, it is very likely that in PRA and PRB protein positive cells, $PR^{antisense}$ transcript is also co-expressed. Additionally, these experiments have not ruled out the possibility that the $PR^{antisense}$ transcript acts in *cis* at a transcriptional, post-transcriptional, or translational level. Technical limitations also prevented successful experiments to address the effect, if any, that the $PR^{antisense}$ transcript has in *cis* on the PR sense promoter, transcript, or protein. T47-D and Cos7 cells were transiently transfected with PRA-FLAG and PRB-HA expression vectors and expression levels measured using Western blotting. The goal was the develop stable cell lines expressing PRA and PRB which could then be transfected with the $PR^{antisense}$ cDNA expression vector to determine the effect of $PR^{antisense}$ on PRA and PRB protein levels. Unfortunately, detection of PR protein in the transient transfections was marginal at best and did not produce any useful data (data not shown).

Questions that remain to be addressed include the effect that $PR^{antisense}$ transcript has on PRB protein, effect on PR^{sense} mRNA stability, as well as the effect on PR protein stability, translateability, and degradation. What is clear is that understanding the role that the antisense transcript plays in PR-expressing tissues such as the mammary gland will require the development of improved cell culture models suitable for mechanistic studies, together with

methods for reliably manipulating the levels of $PR^{antisense}$ mRNA, or the activity of the PR antisense promoter, both in cells, *in vitro*, and in tissues, *in vivo*.

Conclusions

Overall, studies involving promoter analysis, *in vitro,* and *in vivo* characterization of the mouse Pgr locus bring us closer to ultimately unraveling exactly how the PRB and PRA promoters are differentially regulated during development, but many questions remain. Understanding how to differentially regulate the PRB and PRA promoters has important implications in the treatment of human breast cancer. Since the ratio of PR isoform abundance favors PRA in human mammary carcinomas (Bamberger AM 2000), reducing the expression of PRA through therapeutic means could lead to a restoration of the balance between PRB and PRA, which are typically expressed in approximately equal amounts in the normal human breast (Aupperlee M 2005b). Of note, the $PR^{antisense}$ transcript appears to be co-expressed at the cellular level and co-regulated with the PR^{sense} transcripts, so that it cannot be ruled out as a player in regulation of the Pgr locus. The role of the $PR^{antisense}$ transcript may also differ between the healthy breast and in breast cancer, where an imbalance between PR sense and $PR^{antisense}$ transcripts could have an effect on tumorigenesis.

REFERENCES

REFERENCES

Aupperlee M 2005a, Smith KT, Kariagina A, Haslam SZ. "Progesterone Receptor Isoforms A and B: Temporal and Spatial Differences in Expression during Murine Mammary Gland Development." Endocrinology 146.8 (2005): 3577-3588.

Aupperlee M 2005b, Kariagina A, Osuch J, Haslam SZ. "Progestins and Breast Cancer." Breast Disease 24 (2005): 37-57.

Aupperlee MD 2007, Haslam SZ. "Differential Hormonal Regulation and Function of Progesterone Receptor Isoforms in Normal Adult Mouse Mammary Gland." Endocrinology 148.5 (2007): 2290-2300.

Bamberger AM 2000, Milde-Langosch K, Schulte HM. "Progesterone Receptor Isoforms, PRB and PRA, in Breast Cancer: Correlations with Clinicopathologic Tumor Parameters and Expression of AP-1 factors." Hormone Research 54 (2000): 32-37.

Beiter T 2008, Reich E, Williams RW, Simon P. "Antisense Transcription: A Critical Look in Both Directions." Cellular and Molecular Life Sciences 66 (2008): 94-112.

Carninci P 2005, (The FANTOM Consortium and RIKEN Genome Exploration Research Group and Genome Science Group [Genome Network Project Core Group]). "The Transcriptional Landscape of the Mammalian Genome." Science 309 (2005): 1559-1563.

Faivre EJ 2008, Daniel AR, Hillard CJ, Lange CA. "Progesterone Receptor Rapid Signaling Mediates Ser345 Phosphorylation and Tethering to Sp1." Molecular Endocrinology 22.4 (2008): 823-828.

FANTOM3 S/AS 2005, (Functional Annotation of Mouse Consortium and the Riken Group). "FANTOM3 Sense/Antisense Pair Database." http://fantom31p.gsc.riken.jp/s_as/ (2005).

GenBank (NCBI) 2008. GenBank. <http://www.ncbi.nlm.nih.gov/Genbank/>.

Hannon GJ 2002. "RNA Interference." Nature 418 (2002): 244-251.

Kariagina A 2007, Aupperlee MD, Haslam SZ. "Progesterone Receptor Isoforms and Proliferation in the Rat Mammary Gland during Development." Endocrinology 148.6 (2007): 2723–2736.

Kastner P, Krust A, Turcotte B, Stropp U, Tora L, Gronemeyer H, Chambon P. "Two Distinct Estrogen-Regulated Promoters Generate Transcripts Encoding the Two Functionally Different Human Progesterone Receptor Forms A and B." The EMBO Journal 9.5 (1990): 1603-1614.

Katayama S 2005, Tomaru Y, Kasukawa T, Wak Ki, Nakanish M, Nakamura M, Nishida H, Yap CC, Suzuki M, Kawai J, Suzuki H (RIKEN Genome Exploration Research Group and Genome Science Group (Genome Network Project Core Group) and the FANTOM Consortium). "Antisense Transcription in the Mammalian Transcriptome." Science 309 (2005): 1564-1566.

Kawaji H 2006, Kasukawa T, Fukuda S, Katayama S, Kai C, Kawai J, Carninci P, Hayashizaki Y. "CAGE Basic/Analysis Databases: The CAGE Resourse for Comprehensive Promoter Analysis." Nucleic Acids Research 34 (2006): 632-636.

Kawaji H, Kasukawa T, Fukuda S, Katayama S, Kai C, Kawai J, Carninci P, Hayashizaki Y. "CAGE Basic/Analysis Databases: The CAGE Resourse for Comprehensive Promoter Analysis." Nucleic Acids Research 34 (2006): 632-636.

Kiyosawa H 2003, Yamanaka I, Osato N, Kondo S, RIKEN GER Group and GSL Members, Hayashizaki Y. "Antisense Transcripts With FANTOM2 Clone Set and Their Implications for Gene Regulation." Genome Research 13 (2003): 1324-1334.

Kraus WL 1994, Montano MM, Katzenellenbogen BS. " Identification of Multiple, Widely Spaced Estrogen-Responsive Regions in the Rat Progesterone Receptor Gene." Molecular Endocrinology 8 (1994): 952-969.

Lapidot M 2006, Pilpel Y. "Genome-wide Natural Antisense Transcription: Coupling its Regulation to its Different Regulatory Mechanisms." EMBO Reports (2006): 1216-1222.

MatInspector 2005. Genomatix MatInspector. 2005. <http://www.genomatix.de/cgi-bin/sessions/login.pl?s=5fea7747b00c3b1638b142a04b37e562>.

Mechta-Grigoriou F 2001, Gerald D, Yaniv M. "The Mammalian Jun Proteins: Redundancy and Specificity." Oncogene 20 (2001): 2378-2389.

Munroe SH 2006, Zhu J. "Review: Overlapping Transcripts, Double-stranded RNA and antisense Regulation: a Genomic Perspective." Cellular and Molecular Life Sciences 63 (2006): 2102-2118.

Osato N 2007, Suzuki Y, Ikeo K, Gojobori T. "Transcriptional Interferences in Cis Natural Antisense Transcripts of Humans and Mice." Genetics 176 (2007): 1299-1306.

Schott DR 1991, Shyamala G, Schneider W, Parry G. "Molecular Cloning, Sequence Analyses, and Expression of Complementary DNA Encoding Murine Progesterone Receptor." Biochemistry 30 (1991): 7014-7020.

Schwartz JC 2008, Younger ST, Nguyen NB, Hardy DB, Monia BP, Corey DR, Janowski BA. "Antisense Transcripts are Targets for Activating Small RNAs." Nature Structural & Molecular Biology 15.8 (2008): 842-848.

Su AI 2004, Wiltshire T, Batalov S, Lapp H, Ching KA, Block D, Zhang J, Soden R, Hayakawa M, Kreiman G, Cooke MP, Walker JR, Hogenesch JB. "A Gene Atlas of the Mouse and Human Protein-Encoding Transcriptomes." PNAS 101.16 (2004): 6062-6067.

Tabaska JE 1999, Zhang MQ. "Detection of Polyadenylation Signals in Human DNA Sequences." Gene 1999: 77 - 86.

Tufarelli C 2006. "The Silence RNA Keeps: Cis Mechanisms of RNA Mediated Epigenetic Silencing in Mammals." Philosophical Transactions of The Royal Society B 361 (2006): 67-79.

Yazgan O 2007, Krebs JE. "Noncoding But Nonexpendable: Transcriptional Regulation by Large Noncoding RNA in Eukaryotes." Biochemistry and Cell Biology 85 (2007): 484-494.

Zhang Q 2008, Zhang J, Moe OW, Hsia CCW. "Synergistic Upregulation of Erythropoietin Receptor (EPO-R) Expression by Sense and Antisense EPO-R Transcripts in the Canine Lung." PNAS 105.21 (2008): 7612-7617.

Zhang Y 2006a, Liu XS, Liu QR, Wei L. "Genome-wide in silico identification and analysis of cis-natural antisense transcripts (cis-NATs) in ten species." Nucleic Acids Research 34 (2006): 3465-3475.

Zhang Y 2006b, Li JT, Kong L, Gao G, Liu QR, Wei L. "NATsDB: Natural Antisense Transcripts DataBase." Nucleic Acids Research 00 (Database issue) (2006): D1-D6.

CHAPTER 5

The Correlation between PR and AP-1

Although both c-Jun and c-Fos were up-regulated in response to short term (3 day) estradiol (E_2) and progesterone (P) treatment in ovariectomized adult mice, the other AP-1 isoforms examined (JunB, JunD and Fra1) were not hormone-responsive (see Chapter 3). The AP-1 family members are regulated at the level of: transcription, mRNA stability, protein stability, and protein activation (Hess J 2004, AP-1 Subunits: Quarrel and Harmony Among Siblings). Because AP-1 acts as an extracellular signal responsive transcription factor complex located at the end of a vast array of signaling cascades, it has the potential to be regulated by growth factors and hormones through extensive cross-talk (Jochum W 2001, AP-1 in Mouse Development and Tumorigenesis). In the mouse mammary gland, regulation of AP-1 may differ from tissues that are not ovarian hormone-dependent, and is most likely controlled by growth factors (GFs) and hormones that are important for normal mammary gland development. Viewed in this light, regulation of PR expression may be a secondary consequence of a developmental program within the mammary gland that involves expansion and terminal differentiation of the luminal epithelial cell population in the context of an altered stromal environment. Additionally, many of these signaling pathways feed back to directly or indirectly regulate PR expression itself or to modulate the activity of other transcription factors that are important for mammary gland development.

It is established that PR up-regulates the prolactin receptor (PRLR) (Ormandy CJ 1992); (Ormandy CJ 1997) which subsequently acts through the Janus kinase 2 (Jak2)/signal transducer and activator of transcription 5a (Stat5a) pathway to exert the actions of prolactin (PRL) (Brockman JL 2002); (Grimm SL 2003). PRL stimulates P synthesis and secretion from the ovaries (Binart N 2000), and direct PRL action in the mammary gland is necessary for normal

alveolar proliferation and differentiation (Brisken C 1999). In addition to the role of PRL in Jak2/Stat5a signaling described above, PRL has also been shown to signal to AP-1 (Gutzman JH 2004). PRL signaling in MCF-7 cells that lack endogenous PRL was primarily through Jak2 and extracellular-signal-regulated kinase 1 and 2 (ERK 1/2) along with c-Src kinase, phosphatidylinositol 3-kinase (PIK3), protein kinase C (PKC), and other mitogen-activated protein kinase (MAPKs) to a lesser extent (Gutzman JH 2004). PRL activation of these pathways leads to increased levels of c-Jun and JunB protein as well as phosphorylation of c-Jun and c-Fos (Gutzman JH 2004). Therefore, PRL may act alone or together with steroid hormones to regulate c-Jun and c-Fos protein expression or phosphorylation. PRL could also act in an E_2- and P-independent manner to up-regulate JunB protein expression. PRL's action on JunB may also be through serum response element 1 (SRE1) transactivation, which is responsive to growth factors and recruits ternary complex factors (TCFs) (Mechta-Grigoriou F 2001). Additionally, liganded PRLR may signal back on PR (Grimm SL 2003) perhaps via the Jak2/Stat5a pathway since the mouse Pgr gene contains 4 putative Stat binding sites (MatInspector 2005) in the region upstream of the PRB promoter, ranging from -2017 to -665 bp.

It has also been shown that PRL can cooperate with E_2 to regulate AP-1 activity (Gutzman JH 2005). Using PRL deficient MCF-7 cells, PRL treatment led to an acute activation of ERK 1/2, while PRL and E_2 individually led to delayed increases in phosphorylated p38 MAPK and ERK 1/2 activity (Gutzman JH 2005). PRL+E_2 increased the level of phosphorylated c-Fos and also induced c-Fos promoter activity (Gutzman JH 2005). The synergistic activation of ERK 1/2 by PRL+E_2 treatment led to an increase of Elk-1, an Ets

transcription factor family member known to interact with the c-Fos promoter at the serum response element (SRE) (Gutzman JH 2005).

JunD is reported to be the least serum-responsive of the Jun family members (Mechta-Grigoriou F 2001), but phosphorylation still plays a role in JunD expression levels and/or activation (Hernandez JM 2008). There are binding sites for multiple transcription factors in the JunD promoter region that may themselves be phosphorylated, leading to JunD transactivation (Hernandez JM 2008). For example, the following transcription factors are known to bind the JunD promoter: Sp1, Krox-24, Oct1, AP-1 and cAMP response element binding protein/ activating transcription factor (CREB/ATF) (Mechta-Grigoriou F 2001). Additionally, JunD protein itself can be phosphorylated by JNK and ERK 1/2, both of which increase the transactivation potential of JunD (Hernandez JM 2008). Constitutive JunD expression is due to Octamer 1 occupancy of the Oct1 binding site adjacent to an AP-1 binding site located in the JunD promoter region, however, in the endogenous context this AP-1 site is not 12-O tetradecanoylphorbol 13-acetate (TPA)-responsive (Hernandez JM 2008). Two potential roles for the AP-1 binding site have been proposed, first, that binding of JunD homodimers creates a positive auto-regulatory loop (Hernandez JM 2008); (Berger I 1991). Second, c-Fos may be up-regulated by serum stimulation and that JunD/c-Fos heterodimers bind this AP-1 site to down-regulate JunD transcription (Berger I 1991); (Berger I 1994). Since JunD is highly expressed in the mouse mammary gland across development and in the ovariectomized adult mouse, it has the potential to play a role in mammary gland development, differentiation, and/or proliferation.

Similar to the other AP-1 family members, Fra1 is regulated at multiple levels, including: transcriptionally and post-translationally (Young MR 2006). Although Fra1 was not directly regulated by hormones in the ovariectomized adult mouse mammary gland (Figure 3.25), it may

be regulated *indirectly* by hormones. The Fra1 promoter contains a TRE that binds c-Jun/c-Fos (Verde P 2007) (or alternatively a dimer composed of a combination of c-Jun, JunD, or Fra2 (Young MR 2006)) depending on the cell line studied. Since c-Fos and c-Jun were up-regulated by both E_2 and P (Figures 3.23, 3.24), their induction may lead to an increase in c-Jun and c-Fos protein bound to the Fra1 promoter and a subsequent increase in Fra1 expression and consequently Fra1/AP-1 transcriptional activity. The Fra1 promoter and intron 1 regions are regulated transcriptionally by serum response factor (SRF)/Elk1, CREB/ATF1, MYC/myc associated factor X (MAX), Sp1, and c-Jun/Fra1 (Young MR 2006); (Verde P 2007); (Bergers G 1995), many of which can be subsequently phosphorylated. Fra1 itself is phosphorylated by ERK 1/2 in the C-terminal destabilizer region, preventing proteosome-dependent degradation (Gomard T 2008). Phosphorylated Fra1/c-Jun dimers also bind to the intron 1 TRE and activate a positive auto-regulatory loop, inducing Fra1 transcription (Bergers G 1995); (Young MR 2006). It is believed that high ERK activity leads to high levels of Fra1 protein that is heavily phosphorylated on multiple residues, while low ERK activity leads to reduced phosphorylation and a destabilization of Fra1 protein (Gomard T 2008); (Young MR 2006). This suggests that during normal mammary gland development, when ERK signaling is low (i.e. in the virgin adult gland), Fra1 transcription may be up-regulated but the majority of Fra1 protein present is not activated. Conversely, when ERK signaling is high (i.e. in TEBs during puberty and in lobules during pregnancy), then Fra1 transcription may be up-regulated, and Fra1 protein is likely to be hyper-phosphorylated, leading to its stabilization.

We showed that Jun/AP-1 is important for efficient PRA up-regulation across mouse mammary gland development and also in adult ovariectomized mice (see Chapter 3). However, this does not rule out the possibility that both AP-1 and PR are coregulated by an as yet

unidentified third factor or alternatively, that PR also regulates AP-1. It has been shown in the PR-negative HEC-1-B endometrial adenocarcinoma cell line that cotransfection of human PR increases the transcriptional activity of two AP-1-dependent promoters (Bamberger AM 1996). Cotransfection of human PR and an AP-1 reporter combined with TPA treatment lead to a dramatic synergistic induction of AP-1 reporter activity that was reversed by medroxyprogesterone acetate (MPA) treatment (Bamberger AM 1996). When Bamberger *et al*. tested other cell lines (Cos-7, SKUT-1-B, JEG-3) cotransfected human PR had no effect on either of the AP-1 reporter constructs (Bamberger AM 1996). It was further demonstrated that the effect was promoter-specific since it was reproducible in two additional TPA response element (TRE) containing promoters, but not control vectors or a progesterone response element (PRE) containing promoter (Bamberger AM 1996). Although the PR effect in HEC-1-B cells was cell-type specific in the study by Bamberger, *et al*., it may still be applicable to TRE containing promoters in other cell types not examined. Since this study shows that ligand-independent PR can activate a TRE containing promoter, it suggests that this regulation is via a non-classical (i.e. non-genomic) mechanism. If such a mechanism was functional in the mouse mammary gland, it would most likely be though PR activation of non-genomic signaling pathways leading to MAPK activation and subsequent phosphorylation of the AP-1 proteins themselves, their coregulators, and/or transcription factors that bind the AP-1 gene promoters, as discussed above.

Proliferation

The majority of proliferation in the adult mammary gland occurs in steroid receptor-negative epithelial cells, with a small percentage of ERα^+ cells incorporating 5'-bromo-2'-

deoxyuridine (BrdU) (Clarke RB 1997). Non-proliferative ER^+/PR^+ cells are thought to be growth arrested by high levels of inhibitors like p21 and p27 (Figure 3.29); (Lange C 2008). Based on the results of Chapter 3, it appears likely that P is more efficient than E_2 in promoting the expression of key cell cycle regulatory proteins as well as in priming the signaling pathways (i.e. MAPK) that are necessary for AP-1 activation. Cell cycle progression has been studied in breast cancer cells where the overall effect of progestin is to inhibit cell cycle progression, perhaps through the induction of differentiation (Sutherland RL 1998). However, this inhibition can be preceded by one round of replication as well as acute, but transient stimulation of growth (Sutherland RL 1998). More recently, studies in ovariectomized adult mice have shown that P induces proliferation via two different mechanisms (Beleut M 2010). First, within the initial 24 hours, a proportion of the PR^+ mammary epithelial cells (about 20%) proliferate in a cyclin D1-dependent manner (Beleut M 2010). Second, a larger proportion of mammary epithelial cells that are PR-negative proliferate in a cyclin D1-independent but receptor activator of NF-κB-ligand (RANKL)-dependent manner (Beleut M 2010). The RANKL-induced proliferation peaks at day 3 of E_2+P treatment and is controlled via a paracrine mechanism (Beleut M 2010).

In PR^+ mouse mammary gland cells, RANKL expression is up-regulated starting at mid-pregnancy by PRL, P, and parathyroid hormone related peptide (PTHrP) (Fata JE 2000). RANKL binds and activates its receptor, RANK, located at the cell membrane of neighboring PR-negative cells (Mulac-Jericevic B 2003). RANK is expressed constitutively in the mammary gland of both pregnant and non-pregnant mice (Tonko-Geymayer S 2002). RANK induces the IκB kinase (IKK) complex, which in turn phosphorylates IκB, leading to the degradation of IκB and activation of NF-κB, which translocates to the nucleus (Cao Y 2001). An important target

gene of NF-κB is cyclin D1, shown to be essential for mammary epithelial cell proliferation (Bakiri L 2000). The cyclin D1 gene is induced not only by NF-κB, but also by PRL (Brockman JL 2002), c-Jun (Schreiber M 1999), c-Fos (Jochum W 2001, AP-1 in Mouse Development and Tumorigenesis), Fra1 (Verde P 2007), and liganded PRB (Boonyaratanakornkit V 2008), all of which can interact at multiple different levels.

The role of NF-κB is not limited to proliferation, and NF-κB can interact physically with c-Jun/c-Fos AP-1 (Stein B 1993). Although it has only been studied in osteoclast differentiation, Fra1 is also induced by RANKL in a c-Fos-dependent mechanism (Matsuo K 2000). Since two of the Fos family members (c-Fos and Fra1) are both induced by RANKL during osteoclastogenesis (Matsuo K 2000), this raises the question of whether this regulation is cell type-specific, or if perhaps it's a common feature of other cell types during differentiation. Furthermore, the mechanism by which RANKL induces c-Fos and Fra1 is not well understood, but could be either through RANKL activation of the NF-κB pathway or via direct interaction of NF-κB with c-Jun/c-Fos (or c-Jun/Fra1), perhaps at a composite NF-κB/AP-1 site in the promoter region of the c-Fos or Fra1 genes.

Based on the mechanism of P-induced proliferation described by Beleut, *et al.* the second wave of proliferation, peaking after 3 days of P treatment, is cyclin D1-independent (RANKL-dependent) in PR-negative mammary epithelial cells (Beleut M 2010). In addition to its regulation of cyclin D1, RANKL signaling also increases nuclear translocation of inhibitor of DNA binding 2 (Id2), which down-regulates the cell cycle inhibitor p21 and leads to mammary cell proliferation (Kim NS 2006). Since cyclin D1 is not required for the second wave of proliferation in the context of studies performed by Beleut, *et al*, there must be other genes capable of allowing cell cycle progression. In addition to Id2, other genes known to be important

for cell cycle progression include c-Jun (Schreiber M 1999) and c-Fos (Jochum W 2001, AP-1 in Mouse Development and Tumorigenesis) mostly for their ability to up-regulate cyclin D1. c-Jun also inhibits p53, and therefore it's downstream effector p21, along with inhibiting p16 (Passegue E 2002) and up-regulating cyclin A (Verde P 2007). Additionally, c-Fos up-regulates cyclin E (Hess J 2004). One group addressed whether cyclin D1 expression could substitute for c-Jun in cell cycle progression using c-Jun$^{-/-}$ mammary epithelial cells transduced with cyclin D1 or c-Jun, and compared the ability of the two proteins to restore DNA synthesis (Wisdom R 1999). Compared to c-Jun transduction, cyclin D1 only restored 25-30% of DNA synthesis, thus there are c-Jun target genes in addition to cyclin D1 necessary for cell growth (Wisdom R 1999). This study from the Wisdom Lab suggests that up to 75% of the proliferative ability of c-Jun is not mediated by cyclin D1, fitting with the cyclin D1-independent second wave of proliferation in response to P (Beleut M 2010).

Although P was able to elicit two waves of proliferation in mammary epithelial cells, neither vehicle nor E_2 alone had any effect upon proliferation in the adult mouse (Beleut M 2010). This is contrasted by the pubertal mouse, where E_2 is strongly mitogenic (Daniel CW 1987). Thus, in the adult mouse mammary gland, E_2 is permissive for the proliferative effects of P, but by itself, E_2 is not mitogenic (Beleut M 2010). In our study on the correlation between AP-1 family members and proliferation in ovariectomized adult mice, we also found that 3 days of vehicle or E_2 treatment alone were not able to induce proliferation (Figures 3.26, 3.27, 3.29). Rather, 3 days of P (or E_2+P) was required for proliferation of luminal epithelial cells (Figures 3.26, 3.27, 3.29). Our results are consistent with a model in which a wave of increased

c-Jun and c-Fos expression is extremely transient in proliferating cells, where c-Jun and c-Fos proteins have a half-life of 1 and 2 hours, respectively (Jariel-Encontre I 1997); (Gomard T 2008). Of the $BrdU^+$ cells, 62% also co-expressed c-Jun and 35% c-Fos (Figures 3.26, 3.27), insufficient to account for all of the $BrdU^+$ cells. However, this represents cells that not only incorporated BrdU during the 2 hour labeling pulse, but also includes cells that are re-expressing c-Jun or c-Fos in preparation for another round of proliferation. Therefore, the remaining $BrdU^+$ cells that fail to co-express c-Jun (38%) or c-Fos (65%) may have previously expressed c-Jun or c-Fos, but c-Jun/c-Fos expression was rapidly lost (Figures 3.26, 3.27). Alternatively, these cells may express a different AP-1 family member (JunB, FosB, Fra1, etc). Since 3 days of treatment with P led to an increase in number of cells expressing both c-Jun and c-Fos (Figures 3.26, 3.27), this is perhaps due to an induction of MAPK signaling that both activates and stabilizes the AP-1 proteins.

REFERENCES

REFERENCES

Bakiri L 2000, Lallemand D, Bossy-Wetzel E, Yaniv M. "Cell Cycle-Dependent Variations in c-Jun and JunB Phosphorylation: A Role in the Control of Cyclin D1 Expression." The EMBO Journal 19.9 (2000): 2056-2068.

Bamberger AM 1996, Bamberger CM, Gellersen B, Schulte HM. "Modulation of AP-1 Activity by the Human Progesterone Receptor in Endometrial Adenocarcinoma Cells." Proceedings of the National Academy of Sciences U.S.A. 93 (1996): 6169-6174.

Beleut M 2010, Rajaram RD, Caikovski M, Ayyanan A, Germano D, Choi Y, Schneider P, Brisken C. "Two Distinct Mechanisms Underlie Progesterone-Induced Proliferation in the Mammary Gland." Proceedings of the National Academy of Sciences U.S.A. 107.4 (2010): 2989-2994.

Berger I 1991, Shaul Y. "Structure and Function of Human jun-D." Oncogene 6 (1991): 561-566.

Berger I 1994, Shaul Y. "The Human junD Gene is Positively and Selectively Autoregulated." DNA Cell Biology 13 (1994): 249-255.

Bergers G 1995, Graninger P, Braselmann S, Wrighton C, Busslinger M. "Transcriptional Activation of the Fra-1 Gene by AP-1 is Mediated by Regulatory Sequences in the First Intron." Mollecular and Cellular Biology 15 (1995): 3748-3758.

Binart N 2000, Helloco C, Ormandy CJ, Barra J, Clement-Lacroix P, Baran N, Kelly PA. "Rescue of Preimplantatory Egg Development and Embryo Implantation in Prolactin Receptor-Deficient Mice After Progesterone Administeration." Endocrinology 141 (2000): 2691-2697.

Boonyaratanakornkit V 2008, Bi Y, Rudd M, Edwards DP. "The Role and Mechanism of Progesterone Receptor Activation of Extra-Nuclear Signaling Pathways in Regulating Gene Transcription and Cell Cycle Progression." Steroids 73 (2008): 922-928.

Brisken C 1999, Kaur S, Chavarria TE, Binart N, Sutherland RL, Weinberg RA, Kelly PA, Ormandy CJ. "Prolactin Controls Mammary Gland Development via Direct and Indirect Mechanisms." Developmental Biology 210 (1999): 96-106.

Brockman JL 2002, Schroeder MD, Schuler LA. "PRL Activates the Cyclin D1 Promoter Via the Jak2/Stat Pathway ." Molecular Endocrinology 16.4 (2002): 774-784.

Cao Y 2001, Bonizzi G, Seagroves TN, Greten FR, Johnson R, Schmidt EV, Karin M. "IKKalpha Provides an Essential Link Between RANK Signaling and Cyclin D1 Expression During Mammary Gland Development." Cell 107.6 (n.d.): 763-775.

Clarke RB 1997, Howell A, Potten CS, Anderson E. "Dissociation between Steroid Receptor Expression and Cell Proliferation in the Human Breast." Cancer Research 57 (1997): 4987-4991.

Daniel CW 1987, Silbertstein GB, Strickland P. "Direct Action of 17 Beta-Estradiol on Mouse Mammary Ducts Analyzed by Sustained Release Implants and Steroid Autoradiography." Cancer Research 47 (1987): 6052-6057.

Fata JE 2000, Kong YY, Li J, Sasaki T, Irie-Sasaki J, Moorehead RA, Elliott R, Scully S, Voura EB, Lacey DL, Boyle WJ, Khokha R, Penninger JM. "The Osteoclast Differentiation Factor Osteoprotegerin-Ligand Is Essential for Mammary Gland Development." Cell 103.1 (2000): 41-50.

Gomard T 2008, Jariel-Encontre I, Basbous J, Bossis G, Mocquet-Torcy G, Piechaczyk M. "Fos Family Protein Degradation by the Proteasome." Biochmical Society Transactions 36.5 (2008): 858-863.

Grimm SL 2003, Rosen JM. "The Role of C/EBPBeta in Mammary Gland Development and Breast Cancer." Journal of Mammary Gland Biology and Neoplasia 8.2 (2003): 191-204.

Gutzman JH 2004, Rugowski DE, Schroeder MD, Watters JJ, Schuler LA. "Multiple Kinase Cascades Mediate Prolactin Signals to Activating Protein-1 in Breast Cancer Cells." Molecular Endocrinology 18.12 (2004): 3064-3075.

Gutzman JH 2005, Nikolai SE, Rugowski DE, Watters JJ, Schuler LA. "Prolactin and Estrogen Enhance the Activity of Activating Protein 1 in Breast Cancer Cells: Role of Extracellularly Regulated Kinase 1/2-Mediated Signals to c-fos ." Molecular Endocinology 19.7 (2005): 1765-1778.

Hernandez JM 2008, Floyd DH, Weilbaecher KN, Green PL, Boris-Lawrie K. "Multiple Facets of JunD Gene Expression are Atypical Among AP-1 Family Members." Oncogene 27 (2008): 4757-4767.

Hess J 2004, Angel P, Schorpp-Kistner M. "AP-1 Subunits: Quarrel and Harmony Among Siblings." Journal of Cell Science 117 (2004): 5965-5973.

Jariel-Encontre I 1997, Salvat C, Steff AM, Pariat M, Acquaviva C. "Complex Mechanisms for c-fos and c-jun Degradation." Molecular Biology Reports 24 (1997): 51-56.

Jochum W 2001, Passegue E, Wagner EF. "AP-1 in Mouse Development and Tumorigenesis." Oncogene 20 (2001): 2401-2412.

Kim NS 2006, Kim HJ, Koo BK, Kwon MC, Kim YW, Cho Y, Yokota Y, Penninger JM, Kong YY. "Receptor activator of NF-kappaB ligand regulates the proliferation of mammary epithelial cells via Id2." Molecular and Cellular Biology 26 (2006): 1002-1013.

Lange C 2008. "Challenges to Defining a Role for Progesterone Receptor in Breast Cancer." Steroids 73 (2008): 914-921.

MatInspector 2005. Genomatix MatInspector. 2005. <http://www.genomatix.de/cgi-bin/sessions/login.pl?s=5fea7747b00c3b1638b142a04b37e562>.

Matsuo K 2000, Owens JM, Tonko M, Elliott C, Chambers TJ, Wagner EF. "Fosl1 is a Transcriptional Target of c-Fos During Osteoclast Differentiation." Nature Genetics 24 (2000): 184-187.

Mechta-Grigoriou F 2001, Gerald D, Yaniv M. "The Mammalian Jun Proteins: Redundancy and Specificity." Oncogene 20 (2001): 2378-2389.

Mulac-Jericevic B 2003, Lydon JP, DeMayo FJ, Conneely OM. "Defective Mammary Gland Morphogenesis in Mice Lacking the Progesterone Receptor B Isoform." PNAS 100.17 (2003): 9744-9749.

Ormandy CJ 1992, Graham J, Kelly PA, Clarke CL, Sutherland RL. "The Effect Progestins on Prolactin Receptor Gene Transcription in Human Breast Cancer Cells." DNA Cell Biology 11 (1992): 721-726.

Ormandy CJ 1997, Hall RE, Manning DL, Robertson JF, Blamey RW, Kelly PA, Nicholson RI, Sutherland RL. "Coexpression and Cross-Regulation of the Prolactin Receptor and Sex Steroid Hormone Receptors in Breast Cancer." The Journal of Clinical Endocrinology and Metabolism 82 (1997): 3692-3699.

Passegue E 2002, Jochum W, Behrens A, Ricci R, Wagner EF. "JunB Can Substitute for Jun in Mouse Development and Cell Proliferation." Nature Genetics 30.2 (2002): 158-166.

Schreiber M 1999, Kolbus A, Piu F, Szabowski A, Mohle-Steinlein U, Tian J, Karin M, Angel P, Wagner EF. "Control of Cell Cycle Progression by c-Jun is p53 Dependent." Genes & Development 13 (1999): 607-619.

Stein B 1993, Baldwin Jr AS, Ballard DW, Greene WC, Angel P, Herrlich P. "Cross-Coupling of the NF-xB p65 and Fos/Jun Transcription Factors Produces Potentiated Biological Function." The EMBO Journal 12 (1993): 3897-3891.

Sutherland RL 1998, Prall OWJ, Watts CKW, Musgrove EA. "Estrogen and Progestin Regulation of Cell Cycle Progression." Journal of Mammary Gland Biology and Neoplasia 3.1 (1998): 63-72.

Tonko-Geymayer S 2002, Doppler W. "An Essential Link to Mammary Cancers?" Nature Medicine 8 (2002): 108-110.

Verde P 2007, Casalino L, Talotta F, Yaniv M, Weitzman JB. "Deciphering AP-1 Functions in Tumorigenesis: Fra-ternizing on Target Promoters." Cell Cycle 6.21 (2007): 2632-2639.

Wisdom R 1999. "AP-1: One Switch for Many Signals." Experimental Cell Research 253 (1999): 180-185.

Young MR 2006, Colburn NH. "Fra-1 a Target For Cancer Prevention or Intervention." Gene 379 (2006): 1-11.

CONCLUDING REMARKS

The mouse progesterone receptor exists in two isoforms, PRA and PRB that are encoded by the Pgr gene on chromosome 9. The human and rat progesterone receptor (PGR) genes contain a tandem arrangement of two promoters. These tandem promoters give rise to transcripts encoding the two major PR isoforms, PRA and PRB, which have different functions in the mammary gland. This was also believed to be true for the mouse Pgr gene however, evidence of two promoters and two classes of mRNA transcripts have not been previously defined. Herein we described the organization of the mouse Pgr locus, which is comprised of tandem distal and proximal promoters that give rise to $PR^{(B)}$ and $PR^{(A)}$ transcripts encoding PRB and PRA proteins, respectively. In comparison to the human and rat PGR genes, however, transcription initiation within the orthologous mouse gene is both more widely dispersed, and at least in the case of the distal promoter, closer to the PRB translation start site. Additionally, this locus also forms a *cis*-sense/antisense pair with a naturally occurring, non-coding antisense transcript ($PR^{antisense}$). The $PR^{antisense}$ transcript overlaps the majority of sense exon 1, with transcription initiating near the 3'-end of exon 1 driven by an antisense PR promoter. This novel antisense transcript was characterized in mouse mammary cell lines and *in vivo* in mouse mammary gland tissue. All three promoters (PRA, PRB and antisense PR) were AP-1 responsive, but the sense PRA and PRB promoters were up-regulated primarily in response to c-Jun while the antisense PR promoter was more responsive to JunD or JunB, and c-Jun to a lesser extent. All three promoters failed to show a significant response to E_2, but the antisense PR promoter was up-regulated by the synthetic progestin R5020 and down-regulated by the phorbol ester PMA. In

contrast, the sense promoter constructs were up-regulated by PMA to varying degrees, with the long tandem promoter being the most responsive. Both *in vitro* and *in vivo*, the $PR^{antisense}$ transcript was localized to the same cells that expressed PR^{sense} message and PRA protein. The PR sense and $PR^{antisense}$ transcripts showed co-regulation, rather than anti-regulation, and were co-expressed across mouse mammary gland development.

During the postnatal period of mammary gland development in the mouse, expression of the PRA and PRB proteins is temporally and spatially dissociated, allowing study of each isolated isoform. In both the immature and adult mammary gland of mice, PRA expression was restricted to a subset of luminal epithelial cells, followed by a reduction in the abundance and distribution of PRA and the appearance of PRB in developing lobules of pregnancy-like adults. The proximal promoter is responsible for supporting expression of the PRA isoform in the pubertal mammary gland, when the basic architecture of the ductal tree is established by a combination of steroid- and growth factor-driven ductal elongation and side-branching. A second set of transcripts gives rise to the full length PRB isoform, driven by the upstream (distal) promoter. PRB protein expression was restricted to luminal cells of lobules and ducts in mid- to late-pregnancy when the mammary gland is exposed to E_2, P, and other pregnancy hormones. Since PRA and PRB colocalized only in a subset of cells and responded differently to hormones, this supports our finding that the proximal and distal promoters are, at least to some extent, under independent transcriptional control. This pattern of hormonal and developmental regulation is most consistent with a scenario in which PR expression is primarily a secondary consequence of a program of lineage expansion and cellular differentiation that sequentially supports a transcriptional environment conducive initially to activation of the proximal promoter, leading

subsequently to activation of the pregnancy-specific PRB promoter. This contrasts with a simpler model in which transcription of the mouse Pgr gene is under direct regulation by ovarian steroids and their receptors.

Superimposed on these hormonal influences are important growth factor pathways, many of which ultimately converge on the AP-1 family, but AP-1 regulation of PR expression in the mouse has not been studied. Therefore, we examined the effect of steroid hormones and co-expression of Jun and Fos subunits on the activity of the mouse PR promoters and on their respective mRNA transcripts. The results reported herein show that the subunit composition of AP-1 and its expression pattern correlates more closely with expression of PRA compared to PRB. Specifically, the c-Jun subunit correlated highly with PRA expression, and PRA^+ cells invariably express one Jun isoform or another. In transient transfection assays, c-Jun was the only AP-1 subunit able to activate all of the PR promoter-reporter constructs. Interestingly, however, although c-Jun was able to induce the distal promoter B *in vitro*, none of the AP-1 isoforms correlated highly with PRB^+/PRA^- expressing cells *in vivo* by immunofluorescence. This suggests that other transcription factors alone or combined with AP-1 may be responsible for transcriptional regulation of the PRB promoter in the pregnant mammary gland *in vivo*. Two candidates include C/EBPβ and Stat5a, both of which are highly up-regulated during pregnancy and are capable of interactions or crosstalk with AP-1 and PR.

Expression of the various AP-1 isoforms was seen to vary across key stages of mouse mammary gland development as did the colocalization of AP-1 with PRA. In luminal epithelial cells, PRA colocalized highly with c-Jun and Fra1 across each of the developmental states examined, as well as with JunB and JunD to a lesser extent. This differs from PRB, which only colocalized with AP-1 isoforms in the small percentage of cells that co-expressed PRA.

Unexpectedly, c-Fos was expressed at very low levels across development, with a slight increase in c-Fos expressing cells in the pregnancy-like gland. Instead, Fra1 was the predominant Fos isoform detected and its expression colocalized highly with PRA at all developmental stages.

Since expression of certain members of the AP-1 family may also be regulated by steroid hormones, we examined the effect of E_2, P, or their combination on ovariectomized virgin adult mice. As expected, c-Fos was not expressed in control ovariectomized mice but was highly up-regulated following 3 days of E_2 and E_2+P treatment. Surprisingly, c-Fos was also modestly up-regulated by P treatment. c-Jun was expressed in a moderate number of cells in control ovariectomized mice and was slightly, but significantly, up-regulated by E_2, P, or E_2+P treatment. Colocalization of AP-1 with proliferating cells (i.e. those that incorporate BrdU) showed that in control ovariectomized mice, there is abundant c-Jun but no c-Fos expression, along with a complete lack of proliferation in luminal epithelial cells. Although there was sufficient c-Jun and c-Fos in E_2 treated mice, BrdU staining indicated that the mammary epithelium remains proliferatively quiescent under these conditions. The reason why short term (3 day) treatment with P or E_2+P, but not with E_2 alone, is able to stimulate proliferation remains unclear, however, AP-1 proteins must be phosphorylated in order to exert their transcriptional actions on target genes involved in cell cycle progression. It appears likely that P is therefore more efficient than E_2 in promoting the expression of key cell cycle regulatory proteins, or in priming the signaling pathways that are necessary for AP-1 activation.

This is the first report describing the correlation of AP-1 with PR in the mouse mammary gland, with a focus on normal development as well as the response to hormone treatment in the ovariectomized adult mammary gland. Since AP-1 acts as an extracellular signal responsive

transcription factor complex located at the end of a vast array of signaling cascades, it may indeed be the link between growth factor signaling and cell cycle control. Because both AP-1 and PR are known to be important in normal mammary gland development as well as in tumorigenesis, their regulation has important implications in the treatment of breast cancer. The ratio of PR isoform abundance favors PRA in human mammary carcinomas, therefore reducing the expression of PRA through therapeutic means could lead to a restoration of the balance between PRA and PRB. Since the $PR^{antisense}$ transcript is co-regulated and co-expressed with the sense PR transcripts, the role of $PR^{antisense}$ message may differ between the normal mammary gland and in breast cancer. Additionally, if the $PR^{antisense}$ transcript can alter the ratio of PRA to PRB protein, a hypothesis that remains to be tested pending the development of methods to effectively manipulate the levels of $PR^{antisense}$ mRNA *in vivo*, it may serve as a useful therapeutic tool in the treatment of breast cancer.